



Technical University of Crete

School of Chemical and Environmental Engineering

Aerosol exposure analysis using mechanistically based modules

Doctoral Thesis by

Mammi-Galani Eleni

Environmental Engineer, MSc

Supervisor: Dr. M. Lazaridis

Chania, 2024

The present doctoral thesis was supervised by Prof. Mihalis Lazaridis and was submitted within the postgraduate program “Environmental Engineering” at the School of Environmental Engineering in the Technical University of Crete.

The research was supported by the European Union 7th Framework program HEXACOMM (Human Exposure to Aerosol Contaminants in Modern Microenvironments) FP7/2007-2013 under grant agreement N° 315760

PhD. Dissertation Committee

Dr. M. Lazaridis, Professor, School of Chemical and Environmental Engineering, Technical University of Crete (supervisor)

Dr. K. Eleftheriadis, Researcher, Institute of Nuclear Technology-Radiation Protection, N.C.S.R. "Demokritos", Athens, Greece

Dr. D. Kolokotsa, Professor, School of Environmental Engineering, Technical University of Crete

Dr N. Kalogerakis, Emeritus Professor, School of Chemical and Environmental Engineering, Technical University of Crete

Dr T. Tsoutsos, Professor, School of Chemical and Environmental Engineering, Technical University of Crete

Dr A. Voulgarakis, Associate Professor, School of Chemical and Environmental Engineering, Technical University of Crete

Dr L. Diapouli, Researcher, Institute of Nuclear Technology-Radiation Protection, N.C.S.R. "Demokritos", Athens, Greece

Acknowledgements

I would like to express my sincere gratitude to the people I collaborated with, during this dissertation, since their help was crucial.

Mostly, I would like to thank my supervisor, Prof. Mihalis Lazaridis for giving me the opportunity to work in this PhD position and for his guidance throughout the course of my research. I am really grateful for his patience, support and encouragement during the last years that led to the realization of the present thesis.

I would like also to thank my colleagues from the Atmospheric Aerosol laboratory at Technical University of Crete, Dr. Theodoros Glytsos, Dr. Sofia-Irini Chatoutsidou and Dr. Ilias Kopanakis for their assistance whenever needed. Especially, I would like to thank Dr. Eleftheria Chalvatzaki, for her ongoing support.

I'm also very grateful to Prof. Roy Harrison, Professor of Environmental Health at the School of Geography, Earth and Environmental Sciences at Birmingham University, and his team for their assistance and guidance during my visit at Birmingham University at the 2nd semester of 2015. Specifically, I would like to thank Dr. Tuan Vu for the collaboration and all his help during my stay in Birmingham.

Abstract

The objective of the current thesis was to study the exposure to PM_{10} in personal and population scale, through a combination of case studies, measurements, dosimetry models and other computer-based tools like Geographical Information Systems.

In particular, the direct method of personal monitoring was chosen in order to estimate the daily personal dose. PM_{10} measurements were conducted in the city of Chania by residents and MSc students at the Technical University of Crete, with the use of a personal monitor and a diary of activities. The target was to examine the personal exposure and dose of the studied subjects in different microenvironments and to study the effect of different activities and indoor sources on human exposure. Additionally, an exposure and assessment model ExDoM2 was implemented and the received dose was estimated.

Furthermore, in order to investigate the exposure from indoor sources, the cooking activity was selected as one of the major indoor sources and the measurements were conducted in the University of Birmingham. Experiments of four different styles of cooking (Chinese, African, Indian and West) were carried out and the effect of the different styles of cooking on the particle number size distributions was analysed. Moreover, the dose after one hour exposure while cooking in the different styles and in background concentrations was estimated.

The personal exposure in Athens metro, as it is a microenvironment of public interest, was also investigated. With the target to study the exposure of both commuters and metro workers, two sampling campaigns were carried out both inside the trains and on several platforms. The time resolution used in the measurements was 1 sec and as a result it was feasible to study the effect of the train doors opening to the concentrations levels inside the train. The deposited dose of two types of metro workers and of the commuters was also estimated.

Additionally, the deposition of heavy metals in the human body from the inhalation of particle-bound metals was investigated for citizens of 5 European cities. ExDoM and a pharmacokinetic PBPK model were used to determine the particle-bound metals dose in the human body. PBPK model is a key factor in understanding the deposition of metals in human body, to estimate the dose and the potential health effects.

Finally, the exposure in population level was studied with the combination of available measurements from monitoring stations, census data and an interpolation method on a Geographical Information System. The proportion of population exposed in different PM_{10} concentrations in Attica was calculated for four years and the seasonal variation was also examined.

Table of Contents

ACKNOWLEDGEMENTS	II
ABSTRACT	III
TABLE OF CONTENTS.....	IV
TABLE OF FIGURES	VII
TABLE OF TABLES	XII
1. CHAPTER 1: INTRODUCTION TO AEROSOLS	1
1.1. INTRODUCTION.....	1
1.2. PARTICLE FUNDAMENTALS	2
1.3. PARTICLES SIZE AND SHAPE.....	2
1.4. PARTICLE SOURCES	4
2. CHAPTER 2: EXPOSURE, DEPOSITION AND DOSE A OF AEROSOL PARTICLES IN THE HUMAN RESPIRATORY TRACT.....	6
2.1. INTRODUCTION	6
2.2. HUMAN RESPIRATORY SYSTEM DESCRIPTION	6
2.3. MECHANISMS OF PARTICLE DEPOSITION IN THE RESPIRATORY SYSTEM	8
2.4. MECHANISMS OF PARTICLE CLEARANCE AND RETENTION IN THE RESPIRATORY TRACT.....	8
2.5. AEROSOL DEPOSITION MODELS	9
2.5.1. <i>ExDoM2</i>	9
2.5.2. <i>PBPK model</i>	10
2.5.3. <i>ExDoM2 interface and use</i>	11
3. CHAPTER 3: DISSERTATION OBJECTIVES AND OUTLINES	13
3.1. DISSERTATION OBJECTIVES	13
3.2. SCHEMATIC DISSERTATION OUTLINE	14
4. CHAPTER 4: DAILY PERSONAL EXPOSURE AND DOSE TO PARTICULATE MATTER OF CHANIA RESIDENTS	15
4.1. INTRODUCTION	15
4.2. EXPOSURE OF WORKERS LIVING IN CHANIA	16
4.2.1. <i>Study participants</i>	16
4.2.2. <i>Personal exposure monitoring</i>	16
4.2.3. <i>Instrumentation</i>	17
4.2.4. <i>Personal exposure of human subjects</i>	18
4.2.5. <i>Personal exposure</i>	19
4.2.6. <i>Personal exposure in different microenvironments and from different activities</i>	23

4.2.6.1. <i>Personal exposure in different microenvironments</i>	23
4.2.6.2. <i>Personal exposure during Cooking</i>	24
4.2.7. <i>Dose calculation</i>	26
4.2.7.1. <i>PN₁₀ human dose</i>	27
4.2.7.2. <i>PM₁₀ human dose</i>	28
4.3. EXPOSURE OF M.SC. STUDENTS IN THE TECHNICAL UNIVERSITY OF CRETE	31
4.4. CONCLUSIONS	34
5. CHAPTER 5: PM EXPOSURE FROM COOKING IN FOUR DIFFERENT STYLES.....	36
5.1. INTRODUCTION	36
5.2. EXPERIMENTS	36
5.3. MODEL INPUT DATA	37
5.4. RESULTS	38
5.4.1. <i>Particle number size distribution during four different styles of cooking</i>	38
5.4.2. <i>Lung dose after exposure to four different styles of cooking</i>	44
5.4.2.1. <i>Deposition efficiency</i>	44
5.4.2.2. <i>Respiratory tract dose after exposure to Chinese style cooking</i>	45
5.4.2.3. <i>Respiratory tract dose after exposure to Indian style cooking</i>	46
5.4.2.3. <i>Respiratory tract dose after exposure to African style cooking</i>	47
5.4.2.4. <i>Respiratory tract dose after exposure to West style cooking</i>	47
5.4.2.5. <i>Respiratory tract dose after exposure to four different styles of cooking and to background concentrations</i>	48
5.5. RESULTS.....	49
6. CHAPTER 6: PERSONAL EXPOSURE AND DOSE TO PARTICULATE MATTER INSIDE THE SUBWAY SYSTEM OF ATHENS	50
6.1. INTRODUCTION	50
6.2. SAMPLING SITE DESCRIPTION – ATHENS METRO.....	51
6.3. MEASUREMENT CAMPAIGNS.....	53
6.4. DOSE CALCULATION	54
6.5. RESULTS	56
6.5.1. <i>PM₁₀ concentrations inside trains</i>	56
6.5.2. <i>PM₁₀ concentrations on platforms</i>	61
6.5.3. <i>Dose calculation</i>	63
6.6. CONCLUSIONS	67
7. CHAPTER 7: PERSONAL EXPOSURE AND DOSE OF INHALED AMBIENT PARTICULATE MATTER BOUND METALS.....	69
7.1. INTRODUCTION	69

7.2. CITIES UNDER STUDY	69
7.3. EXPOSURE SCENARIO	70
7.4. EXPOSURE AND DOSE ASSESSMENT USING THE EXDOM MODEL.....	71
7.4.1. <i>Input Data</i>	71
7.5 RESULTS	75
7.5.1. <i>Calculation of the Dose of Particulate Matter-Bound Metals Using the ExDoM Model</i>	75
6. 8. CHAPTER 8: POPULATION EXPOSURE.....	83
8.1. INTRODUCTION	83
8.2. MONITORING STATIONS.....	83
8.3. POPULATION EXPOSURE IN ATTICA.....	86
8.4. SEASONAL POPULATION EXPOSURE IN ATTICA.	90
8.4. POPULATION DOSE CALCULATION	91
8.5. CONCLUSIONS	93
CHAPTER 9: CONCLUSIONS AND RECOMMENDATIONS.....	94
9.1. GENERAL CONCLUSIONS.....	94
9.2. RECOMMENDATIONS	96
REFERENCES.....	97
A. APPENDIX A.....	109
A1. SCIENTIFIC JOURNALS.....	109
A2. CONFERENCE PRESENTATIONS.....	109
B. APPENDIX B.....	110

Table of Figures

Figure 1.1: Particle size ranges (adapted from Lazaridis and Colbeck, 2013).	3
Figure 1.2: Scanning electron microscope images (not at the same scale) of aerosols (volcanic ash, pollen, sea salt, and soot. [Micrographs courtesy USGS, UMBC (Chere Petty), and Arizona State University (Peter Buseck) (NASA, 2010).	4
Figure 1.3: Sources of aerosols and particulate matter in the environment Source: Kemp, (2004).	5
Figure 2.1: Human Respiratory Tract model.	7
Figure 2.2: ExDoM2 interface.	12
Figure 2.3: ExDoM2 interface (PBPK module).	12
Figure 4.1: Subject 4 daily exposure (number concentration) (day 3).	20
Figure 4.2: Subject 4 daily exposure (mass concentration) (day 3).	21
Figure 4.3: Subject 1 daily exposure (number concentration) (day 3).	22
Figure 4.4: Subject 6 daily exposure (number concentration) (day 2).	22
Figure 4.5: Subject 6 daily exposure (number concentration) (day 1).	23
Figure 4.6: Average PN ₁₀ and PM ₁₀ exposure in different microenvironments (in the parenthesis is stated the number of times the subjects visited each microenvironment or activity).	24
Figure 4.7: Subject 7 daily exposure (number concentration) (day 2).	25
Figure 4.8: Average PN ₁₀ and PM ₁₀ exposure to different types of cooking (in the parenthesis is stated the number of times the subjects visited each microenvironment or activity).	26
Figure 4.9: Hourly deposited dose in the human respiratory tract of the studied subjects (cross symbol depicts the outliers).	27
Figure 4.10: Particulate matter dose in the different regions of the human respiratory tract during a working day of S4 (day 3).	28
Figure 4.11: Particulate matter dose in the human respiratory tract of the 8 studied subjects (very high outliers have been removed from S7).	29
Figure 4.12: Particulate matter 72h total dose (48h in the case of S5) in the different regions of the human respiratory tract for the 8 studied subjects.	30
Figure 4.13: M6 daily exposure (day 1).	32
Figure 4.14: M5 daily exposure (day 1).	33
Figure 5.1: Particle number concentration in the size range between 14.6 and 615.3 nm, as measured by an SMPS system during three Chinese stir frying cooking activities.	38
Figure 5.2: Particle number concentration in the size range between 14.6 and 615.3 nm at different times during a Chinese stir frying cooking event (2 nd experiment).	39
Figure 5.3: Particle number concentration in the size range between 14.6 and 615.3 nm, as measured by an SMPS system during three Indian cuisine cooking activities.	40

Figure 5.4: Particle number concentration in the size range between 14.6 and 615.3 nm at different times during an Indian style (frying and boiling) cooking event (3 rd experiment). ..	41
Figure 5.5: Particle number concentration in the size range between 14.6 and 615.3 nm, as measured by an SMPS system during three African cuisine cooking activities.....	41
Figure 5.6: Particle number concentration in the size range between 14.6 and 615.3 nm at different times during an African style (frying and boiling) cooking event (2 nd experiment). ..	42
Figure 5.7: Particle number concentration in the size range between 14.6 and 615.3 nm, as measured by an SMPS system during two West cuisine cooking activities.....	43
Figure 5.8: Particle number concentration in the size range between 14.6 and 615.3 nm at different times during a West style (deep frying) cooking event (2 nd experiment).....	44
Figure 5.9: Ultrafine particles (up to 98.2nm) deposition efficiency in the ET, TB, AL and in the total respiratory tract during 4 different cooking styles.....	44
Figure 5.10: Accumulation mode (up to 615.3nm) deposition efficiency in the ET, TB, AL and in the total respiratory tract during 4 different cooking styles.....	45
Figure 5.11: Particulate matter dose in the different regions of the human respiratory tract for an adult male, after 45min exposure to Chinese cooking, calculated by the EXDOM dose model. Error bars represent the standard deviation of the three experiments.	46
Figure 5.12: Particulate matter dose in the different regions of the human respiratory tract for an adult male, after 65min exposure in Indian cooking, calculated by the EXDOM dose model. Error bars represent the standard deviation of the three experiments.	46
Figure 5.13: Particulate matter dose in the different regions of the human respiratory tract for an adult male, after 95min exposure to African cooking, calculated by the EXDOM dose model. Error bars represent the standard deviation of the three experiments	47
Figure 5.14: Particulate matter dose in the different regions of the human respiratory tract for an adult male, after 45min exposure to West cooking, calculated by the EXDOM dose model. Error bars represent the standard deviation of the three experiments.	48
Figure 5.15: Particulate matter dose in the different regions of the human respiratory tract for an adult male, after 1h exposure to four different styles of cooking, calculated by ExDoM2 . Error bars represent the standard deviation of the three experiments.	48
Figure 6.1: Athens metro map.....	53
Figure 6.2: Average PM ₁₀ concentrations in the red and blue lines during the campaigns in May 2014 and November 2015 and average weekend concentration.	57
Figure 6.3: PM ₁₀ concentrations inside the trains in the stations of red line. The central box presents the values between the 25th (lower part) and the 75th (upper part) percentiles. The <i>whiskers</i> show the maximum and minimum values, the horizontal line in the box constitutes the median value, and the cross symbols the average value.....	58

Figure 6.4: PM ₁₀ concentrations inside the trains in the stations of blue line. The central box presents the values between the 25th (lower part) and the 75th (upper part) percentiles. The whiskers show the maximum and minimum values, the horizontal line in the box constitutes the median value, and the cross symbols the average value.....	59
Figure 6.5: Real-time PM ₁₀ concentration during an eastbound journey of blue line (time resolution 1 s); grey bars depict the period of the doors opening.....	60
Figure 6.6: Comparison of PM concentrations inside metro carriages between the current study and other studies conducted in metro systems around the world.	61
Figure 6.7: Comparison of PM concentrations on platforms between the current study and other studies conducted in metro systems around the world.	63
Figure 6.8: Particulate matter 24-h dose in the different regions of the human respiratory tract for a commuter, a metro worker with sedentary occupation, and a metro worker with light exercise occupation.	65
Figure 6.9: Retention of particles in the RT, the amount of material transferred to the GI tract and absorbed in blood after 24-h exposure of a commuter, a metro worker with sedentary occupation, and a metro worker with light exercise occupation.	66
Figure 7.1: PM ₁₀ , PM _{Pb} and PM _{Cd} size distribution in (a) Athens (adapted from Karanasiou et al. 2007) (b) Rome (adapted from Canepari et al., 2008), (c) Zabrze (adapted from Rogula-Kozłowska et al., 2013) (d) Seville (adapted from Álvarez et al., 2004) and (e) Frankfurt (adapted from Zereini et al., 2005).....	75
Figure 7.2: Internal Dose in human tissues provided by the PBPK model in conjunction with the ExDoM for adult males (nose breather) of five European countries (after an 24 h exposure scenario) of (a) Arsenic (As) (b) Lead (Pb).....	81
Figure 7.3: Lead Dose provided by the PBPK model in conjunction with the ExDoM for adult males of four European countries after a 24h exposure scenario, in (a) Lungs and intestines (b) Blood, liver, kidney and other tissues.	81
Figure 8.1: Air pollution monitoring stations across Greece (created in ArcGIS Pro).	84
Figure 8.2: Air pollution measurements stations in Attica (created in ArcGIS Pro).....	84
Figure 8.3: PM ₁₀ measurement stations in Attica (created in ArcGIS Pro).....	85
Figure 8.4: Population in Attica's municipalities (created in ArcGIS Pro).....	86
Figure 8.5: PM ₁₀ annual average concentration in Attica in 2017 (created in ArcGIS Pro), (values in µg/m ³).	87
Figure 8.6: PM ₁₀ annual average concentration in Attica in 2018 (created in ArcGIS Pro) (values in µg/m ³).	88
Figure 8.7: PM ₁₀ annual average concentration in Attica in 2019 (created in ArcGIS Pro), (values in µg/m ³).	89

Figure 8.8: PM ₁₀ annual average concentration in Attica in 2020 (created in ArcGIS Pro), (values in µg/m ³).	89
Figure B.1: Subject 1 daily exposure (number concentration) (day 1).....	110
Figure B.2: Subject 1 daily exposure (mass concentration) (day 1).....	110
Figure B.3: Subject 1 daily exposure (number concentration) (day 2).....	111
Figure B.4: Subject 1 daily exposure (mass concentration) (day 2).....	111
Figure B.5: Subject 1 daily exposure (number concentration) (day 3).....	112
Figure B.6: Subject 1 daily exposure (mass concentration) (day 3).....	112
Figure B.7: Subject 2 daily exposure (number concentration) (day 1).....	113
Figure B.8: Subject 2 daily exposure (mass concentration) (day 1).....	113
Figure B.9: Subject 2 daily exposure (number concentration) (day 2).....	114
Figure B.10: Subject 2 daily exposure (mass concentration) (day 2).....	114
Figure B.11: Subject 2 daily exposure (number concentration) (day 3).....	115
Figure B.12: Subject 2 daily exposure (mass concentration) (day 3).....	115
Figure B.13: Subject 3 daily exposure (number concentration) (day 1).....	116
Figure B.14: Subject 3 daily exposure (mass concentration) (day 1).....	116
Figure B.15: Subject 3 daily exposure (number concentration) (day 2).....	117
Figure B.16: Subject 3 daily exposure (mass concentration) (day 2).....	117
Figure B.17: Subject 3 daily exposure (number concentration) (day 3).....	118
Figure B.18: Subject 3 daily exposure (mass concentration) (day 3).....	118
Figure B.19: Subject 4 daily exposure (number concentration) (day 1).....	119
Figure B.20: Subject 4 daily exposure (mass concentration) (day 1).....	119
Figure B.21: Subject 4 daily exposure (number concentration) (day 2).....	120
Figure B.22: Subject 4 daily exposure (mass concentration) (day 2).....	120
Figure B.23: Subject 4 daily exposure (number concentration) (day 3).....	121
Figure B.24: Subject 4 daily exposure (mass concentration) (day 3).....	121
Figure B.25: Subject 5 daily exposure (number concentration) (day 1).....	122
Figure B.26: Subject 5 daily exposure (mass concentration) (day 1).....	122
Figure B.27: Subject 5 daily exposure (number concentration) (day 2).....	123
Figure B.28: Subject 5 daily exposure (mass concentration) (day 2).....	123
Figure B.29: Subject 6 daily exposure (number concentration) (day 1).....	124
Figure B.30: Subject 6 daily exposure (mass concentration) (day 1).....	124
Figure B.31: Subject 6 daily exposure (number concentration) (day 2).....	125
Figure B.32: Subject 6 daily exposure (mass concentration) (day 2).....	125
Figure B.33: Subject 6 daily exposure (number concentration) (day 3).....	126
Figure B.34: Subject 6 daily exposure (mass concentration) (day 3).....	126
Figure B.35: Subject 7 daily exposure (number concentration) (day 1).....	127

Figure B.36: Subject 7 daily exposure (mass concentration) (day 1).....	127
Figure B.37: Subject 7 daily exposure (number concentration) (day 2).....	128
Figure B.38: Subject 7 daily exposure (mass concentration) (day 2).....	128
Figure B.39: Subject 7 daily exposure (number concentration) (day 3).....	129
Figure B.40: Subject 7 daily exposure (mass concentration) (day 3).....	129
Figure B.41: Subject 8 daily exposure (number concentration) (day 1).....	130
Figure B.42: Subject 8 daily exposure (mass concentration) (day 1).....	130
Figure B.43: Subject 8 daily exposure (number concentration) (day 2).....	131
Figure B.44: Subject 8 daily exposure (mass concentration) (day 2).....	131
Figure B.45: Subject 8 daily exposure (number concentration) (day 3).....	132
Figure B.46: Subject 8 daily exposure (mass concentration) (day 3).....	132
Figure B.47 : M1 daily exposure (day 1).....	133
Figure B.48: M1 daily exposure (day 2)	133
Figure B.49: M1 daily exposure (day 3)	134
Figure B.50: M2 daily exposure (day 1)	134
Figure B.51: M2 daily exposure (day 2)	135
Figure B.52: M2 daily exposure (day 3)	135
Figure B.53: M3 daily exposure (day 1)	136
Figure B.54: M3 daily exposure (day 2)	136
Figure B.55: M3 daily exposure (day 3)	137
Figure B.56 : M4 daily exposure (day 1)	137
Figure B.57: M4 daily exposure (day 2)	138
Figure B.58: M4 daily exposure (day 3)	138
Figure B.59: M5 daily exposure (day 1).	139
Figure B.60: M5 daily exposure (day 2).	139
Figure B.61: M5 daily exposure (day 3).	140
Figure B.62: M6 daily exposure (day 1).	140
Figure B.63: M6 daily exposure (day 2).	141

Table of tables

Table 4.1: Subjects household type, working environment and days of measurements.	16
Table 4.2: Average PN ₁₀ and PM ₁₀ exposure of the studied population.....	18
Table 4.3: Mass retained in the RT, transferred to the GI tract and absorbed by the lymph nodes and the blood	31
Table 4.4: Study participants characteristics and average PM ₁₀ mass concentration of the 3-day measurements.	32
Table 4.5: Microenvironments the students visited and average PM ₁₀ mass concentration in each microenvironment	34
Table 5.1: Description of the cooking experiments.....	36
Table 5.2: Number mean Diameter, Peak diameter and total number of particles during three experiments of Chinese cuisine cooking.	38
Table 5.3: Number mean Diameter, Peak diameter and total number of particles during three experiments of Indian cuisine cooking.....	40
Table 5.4: Number mean Diameter, Peak diameter and total number of particles during three experiments of African cuisine cooking.....	42
Table 5.5: Number mean Diameter, Peak diameter and total number of particles during two experiments of West cuisine cooking.....	43
Table 5.6: Particulate matter dose (#) in the five regions of human respiratory tract the ET1, the ET2, the BB, the bb and the AL	45
Table 5.7: Particulate matter dose (#) in the five regions of human respiratory tract the ET1, the ET2, the BB, the bb and the AL after 65min of Indian style cooking.....	46
Table 5.8: Particulate matter dose (#) in the five regions of human respiratory tract after 95min of African style cooking	47
Table 5.9: Particulate matter dose (#) in the five regions of human respiratory after 45min of West style cooking	47
Table 5.10: Particulate matter dose in the different regions of the human respiratory tract after 1h exposure to four different styles of cooking and 1h to background concentrations.	49
Table 6.1: Summary of PM ₁₀ concentrations inside the trains, average, standard deviation, and maximum and minimum values	56
Table 6.2: Summary of PM ₁₀ concentrations at stations (platforms), average, standard deviation, and maximum and minimum values.....	62
Table 6.3: Daily time-activity pattern, PM ₁₀ exposure concentrations, microenvironment, and activity level [resting (rest.), sedentary activity (sed. act.), light exercise (light ex.)]	64

Table 6.4: Dose in the respiratory tract after 1-h exposure in different microenvironments, total daily dose, time fraction, and dose fraction in each microenvironment for the three different subjects.	66
Table 7.1: Table 1 Concentrations of PM ₁₀ , PM _{PB} , PM _{As} and PM _{Cd} in Athens (Karanasiou et al. 2007), Rome (Canepari et al., 2008), Seville (Álvarez et al., 2004), Frankfurt (Zereini et al., 2005) and Zabrze (Rogula-Kozłowska et al., 2013).....	72
Table 7.2: Percentages of PM ₁₀ being in the fine and coarse fraction in the five European countries.	76
Table 7.3: Particulate matter dose in human respiratory tract, blood and GI tract for adult males in five European countries after 24h exposure scenario, calculated by the ExDoM model. ..	77
Table 7.4: Lead particulate matter dose in human respiratory tract, blood and GI tract for adult males in five European countries after 24h exposure scenario, calculated by the ExDoM model.	77
Table 7.5 Arsenic particulate matter dose in human respiratory tract, blood and GI tract for adult males in five European countries after 24h exposure scenario, calculated by the ExDoM model.	78
Table 8.1: PM ₁₀ monitoring stations in Attica.....	85

Chapter 1: Introduction to Aerosols

1.1. Introduction

Urbanization and population growth have led to densely populated cities with high elevated anthropogenic gaseous and particulate matter emissions. As a result, the levels of particulate matter are elevated in big cities with adverse health effects for citizens. Many epidemiological studies (Pope, 2000; Brunekreef, 2005; Davidson, 2005) studied the risk of health impacts of particulate matter to human health.

Dizziness, Cardiovascular disease, asthma, chronic obstructive pulmonary disease (COPD), central nervous system damage and cancer are some of the diseases linked with elevated particulate matter (PM) concentrations. It is estimated that around 300 million people are affected by asthma worldwide. According to the World Health Organization (WHO), every year, 250,000 asthma related deaths are reported worldwide. In industrialized countries, like Canada, United Kingdom and Australia, the prevalence rate of asthma ranges from 2 to 10% of the total population (Morris and Pearson, 2020). In 2016, according to the Global Burden of Disease Study, 251 million cases of COPD were reported worldwide, while in 2015, 5% of the total annual deaths were caused by COPD (WHO, 2020). Furthermore, in 2016, 58% of air pollution related premature deaths were due to ischaemic heart disease. Many studies (Barnett et al., 2005, McGowan et al., 2002, Moolgavkar, 2000) have linked the increase of PM_{2.5} levels with increased admission rates in hospitals. Pope and Dockery stated that an increase of 10 µg/m³ in PM_{2.5} concentration is associated with 1% increase in mortality.

The majority of the anthropogenic emissions outdoors, cannot be decreased with individuals' actions. Governments need to do investments and make policies related to low carbon design houses, cleaner transportation, power generation and industry. WHO Air Quality Guidelines (AQG) recommend threshold limits for important air pollutants and provide a reference for countries for setting air pollution targets. It is worth mentioning, that in 2016, 91% of the world population, mainly in low- and middle-income countries, was living in areas where the WHO AQG were not met.

Since people are spending around 90% of their day in indoor environments, the last decades, studies related to aerosols exposure, focus on the determination of indoor sources and their impact on indoor air quality. According to WHO, around 3 billion people worldwide, cook and heat their houses with kerosene, biomass fuels and coal and as a result, indoor sources are a serious health risk for them. Many studies focus also on workplace and commuting exposure,

since in those microenvironments people spend a big fraction of their day and can be exposed in high PM concentrations.

1.2. Particle fundamentals

The various types of suspended microscopic particles in the air, like smoke from combustion processes, dust from wind erosion, fog formed by suspension of liquid droplets, resulted from condensation of a liquid or from a spray, are known as aerosols. The term aerosol is used to describe solid or liquid particles suspended in gas and it includes both the particles and the gas in which they are suspended, as aerosols are two-phase systems. Monodisperse aerosols, which are produced on the laboratory for aerosol test purposes, have identical particles of the same size, whereas polydisperse aerosols are more common in the atmosphere and have a wide range of particle sizes (Hinds, 1999).

Particles vary considerably in size and shape. Particle size is the main parameter that determines the chemical composition, the optical properties (ability of aerosols to scatter and absorb radiation in different wavelengths) and the deposition mechanisms (e.g. in the human respiratory tract) of particles (Lazaridis, 2008). Other factors that determine the physical and chemical characteristics of an aerosol are the origin and method of generation.

1.3. Particles size and shape

Particles can be classified in different categories regarding their diameter (d_p) based on their modal distribution, or the 50% cut-off diameter of the measurement instrument or on the exposure and dosimetry variables, usually in $PM_{2.5}$ and PM_{10} (Lazaridis, 2008).

Based on their modal distribution, particles are classified as:

- Nucleation mode: particles with $d_p < 10$ nm newly formed through nucleation processes. Particles in the nucleation category soon become part of the Aitken category by condensational growth.
- Aitken mode: particles with diameter $10 \text{ nm} < d_p < 100$ nm.
- Accumulation mode: $0.1 \text{ }\mu\text{m} < d_p < 1 \text{ }\mu\text{m}$, formed from the aggregation of smaller particles or from the condensation of air particles.
- Ultrafine particles: includes particles in the Aitken and nucleation modes.
- Fine particles: includes the nucleation, Aitken and accumulation modes.
- Coarse particles: $d_p > 1\text{-}3 \text{ }\mu\text{m}$ diameter are typically generated mechanically rather than through nucleation and condensation processes.

On Fig. 1, the size fractions of atmospheric, typical and health related particles are illustrated.

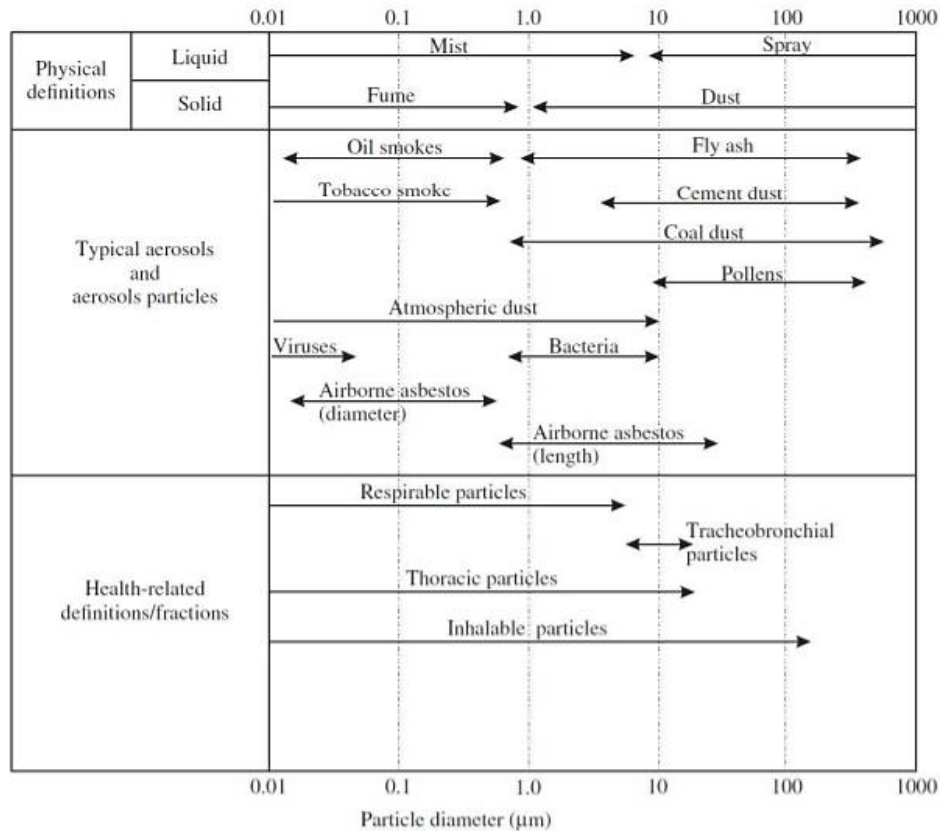


Figure 1.1: Particle size ranges (adapted from Lazaridis and Colbeck, 2013).

As it can be observed on Fig. 1.2 aerosol particles have different and complex shapes, that vary from spherical, through irregular, to fibres and plates. For this reason, correction factors in the form of an equivalent diameter are used for non-spherical particles. As equivalent diameter is defined the sphere that has the same value of a physical property as that of the irregular particle of interest (Hinds, 1999). The most commonly used equivalent diameter, is the aerodynamic equivalent diameter and it is the diameter of a sphere, with standard density equal to 1g/cm^3 , that has the same gravitational settling velocity as the particle of interest. This equivalent diameter is useful for particles bigger than $1\mu\text{m}$. Particles, smaller than $0.5\mu\text{m}$ can be better described by the thermodynamic equivalent diameter, which is the diameter of a unit-density sphere having the same diffusion coefficient as the particle under investigation. Other commonly used equivalent diameters are the mobility equivalent diameter, the mass equivalent diameter and the volume equivalent diameter.

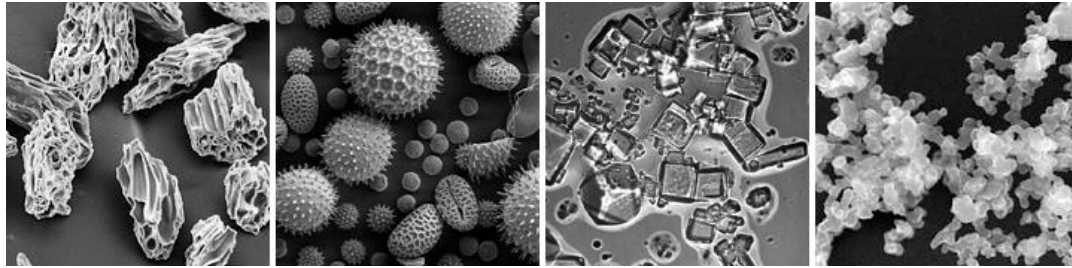


Figure 1.2: Scanning electron microscope images (not at the same scale) of aerosols (volcanic ash, pollen, sea salt, and soot). [Micrographs courtesy USGS, UMBC (Chere Petty), and Arizona State University (Peter Buseck) (NASA, 2010).

1.4. Particle sources

Particle sources are both natural and anthropogenic as can be seen on Fig.3. The natural sources represent the biggest part of aerosol emissions and they elevate the aerosol concentrations worldwide, but locally the main sources are from anthropogenic activities.

Natural particle sources include:

- Dust particles: suspended soil by wind erosion, mainly above deserts, dried lakes and regions with low vegetation. In Europe main dust source is Sahara desert and the wind-blown particles have a strong impact on aerosols composition and concentration levels (EEA, 2012).
- Volcanic dust particles from volcanos eruptions and earthquakes activities.
- Ocean spray particles: suspension of liquid droplets, containing sea salt, due to the activity of the winds.
- Particles from wild-land fires: the particles from fires of natural cause (e.g. lightning).
- Primary biological aerosols: include spores (includes in PM_{10}), pollen grains (usually bigger than PM_{10}), bacteria and viruses.

Except from the particles primary natural sources, there are also secondary sources, formed in the atmosphere by chemical reactions and not emitted directly, like primary emissions. The particles origin, in relation with the formation process and the environmental conditions, determine the chemical composition of aerosols. Physical and chemical processes, condensation, evaporation, coagulation, and chemical reactions change the chemical composition of particles. An example of secondary natural aerosols are the secondary organic biogenic aerosols, which are formed in the atmosphere via reaction of volatile organic compounds that plants and the soil are emitting (EEA, 2012). Elevated concentrations of secondary organic biogenic aerosols are common in the summer in areas with high vegetation coverage. Other secondary pollutants include SO_x (formed from volcanos emissions) and NO_x .

The anthropogenic sources that elevate PM concentration, especially in cities are fossil fuels combustion, including power plants for energy production, biomass combustion (like wood burning), industrial activities (e.g. cement industry), waste management, traffic (including road dust, break and tyre emissions), loading/unloading of bulk goods, mining activities, residential and non-industrial combustion, human driven fires and agriculture.

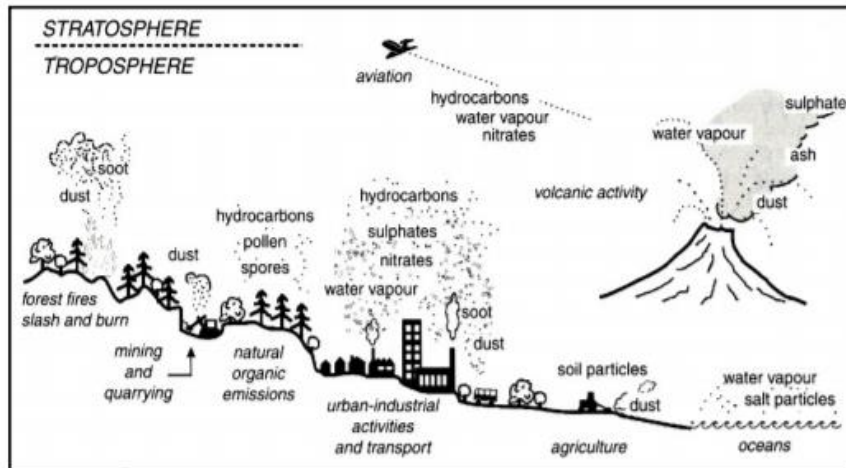


Figure 1.3: Sources of aerosols and particulate matter in the environment Source: Kemp, (2004).

Chapter 2: Exposure, deposition and dose of aerosol particles in the human respiratory tract.

2.1. Introduction

The personal exposure in particulate matters varies from person to person and depends on many factors. The main factors, which influence PM exposure, are the place of living (urban, suburban, rural), the occupation, time-activity patterns, mode of transport and the indoor activities taking place (cooking, painting etc.).

Pollutants enter the human body through inhalation (breathing), swallowing (ingestion or eating) and skin (or eye), however aerosols enter the body mainly through inhalation. Knowledge of the deposition patterns of inhaled aerosols in the human respiratory tract is particularly important for risk evaluation of occupational and environmental exposure in aerosols, for respiratory tract diseases diagnosis and for inhalers' drug delivery technologies. The precise knowledge of the lung deposited fraction of inhaled particles is necessary, in order to connect measured particulate matter exposure concentration with tissue-delivered dose, which is major determinant of the particle-induced biological response (Löndahl et al., 2014).

The wide range of particles sizes and their complex chemical composition and morphology makes the relation between them and health impacts a complex process (Solomon, 2011). How dangerous atmospheric particulate matter are for human health depends both on the amount of mass deposited and on the absorbed substances on the different regions of the respiratory tract. The airway dimensions and the breathing pattern of the individuals also play an important role on how deep particles penetrate in the human lungs and where they deposit. Soluble particles, dissolve and their components are transferred via blood to other human tissues (WHO, 1999).

Consequently, the aerosol deposition in the respiratory tract, the absorption into the blood and the removal of particles from the body by the mechanisms of clearance and excretion are the main processes to evaluate harmful effects of aerosol exposure (Majid and Madl, 2011).

2.2. Human respiratory system description

According to the International Radiological Protection Commission (ICRP) the human respiratory tract consists of the extra thoracic region (ET), the tracheobronchial region (TB) and the alveolar interstitial region (AI). The model of the respiratory tract and the five regions can be seen on Fig. 2.1.

The upper respiratory tract, ET region, contains the ET1, anterior nose, and the ET2 region, posterior nasal passages. The nasal cavity (ET1) and then the mucous membrane lining the larynx (ET2) control the temperature and the humidity of the inhalable air and clean the

incoming air from big particles. The inhaled air from the nose moves to the pharynx and not the larynx. Both nasal and oral cavity are considered the first filter of the inhaled particles

The tracheobronchial region consists of the bronchial (BB) region and the bronchiolar (bb) region. The BB region includes the trachea the main bronchi, and the intrapulmonary bronchi. The trachea connects the larynx with the two main bronchi and protects the respiratory surface from foreign particles. The mucous membrane of the trachea consists of cells with hair like projections, called cilia, that trap particles. In addition, there are also blood vessels, which control cellular maintenance and lymphatic vessels, which remove the particles accumulated on the trachea walls surfaces (Britannica, 2014). The particles are moved back to the larynx and they are removed through coughing (either expelled or ingested). The bb region is consisted of the bronchioles. The bronchioles have ciliated that clean the secretory fluid towards the BB region (Majid and Madl, 2011).

The Alveolar-interstitial region is the last part of the respiratory tract, and it is consisted of the respiratory bronchioles, the alveolar ducts and sacs with their alveoli, and the interstitial connective tissue (ICRP, 2015).

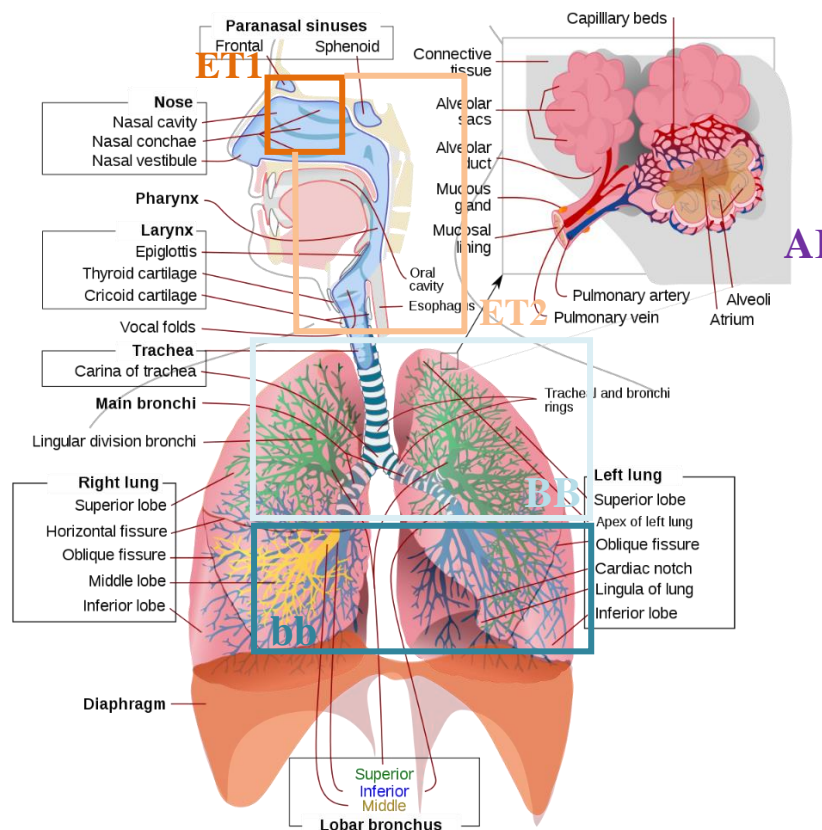


Figure 2.1: Human Respiratory Tract model.

2.3. Mechanisms of particle deposition in the respiratory system

The wide range of particles sizes and their complex chemical composition and morphology makes the relation between them and health impacts a complex process (Solomon, 2011). The airway dimensions and the breathing pattern of the individuals also play an important role on how deep particles penetrate in the human lungs and where they deposit. Soluble particles, dissolve and their components are transferred via blood to other human tissues (WHO, 1999).

A particle is deposited when it sticks to a surface. The main particle deposition mechanisms are the following:

Impaction: Due to inertia, large particles (bigger than 1 μm), are not able to follow the air stream and they deposit on the airway walls. This type of deposition is more common in the naso-pharyngeal and TB regions. Deposition by impaction increases when the particles' size and the flow rates increase (Majid and Madl, 2011).

Sedimentation: Particles sedimentation is caused by gravity when the gravity force is higher than the drag force of air. Deposition by sedimentation is more common in the bronchiolar and alveolar regions for particles greater than 0.5 μm . The increase of particles size and decrease of flow rates makes sedimentation of the particles more common.

Diffusion: Diffusion of particles occurs due to the collision of small particles (smaller than 0.5 μm) with the air molecules. This is caused by Brownian motion and it is more common at the alveolar region. The decrease of particles' size and flow rate increases the deposition by diffusion.

Except the already mentioned types of deposition, two other mechanisms that play minor role in the particles' deposition are electrostatic charge and particle interception (when particles deposit on the walls of the respiratory tract because they are not large enough to have inertia and not small enough to diffuse within the flow stream).

2.4. Mechanisms of particle clearance and retention in the respiratory tract

Clearance is the particles removal from the respiratory tract either by particle transport or by absorption into blood. At each region of the respiratory tract different clearance mechanisms take place. The main clear mechanisms are the following:

- **Mechanical clearance:** mechanical clearance mechanisms are the coughing sneezing and swallowing. Mainly particles bigger than 5 μm are being removed this way and this type of clearance takes place at the nasal and oral cavity, where the particles are removed directly after their entering.

- **Mucociliary clearance** is the main mechanism of insoluble particles removal from the TB region. The removal is achieved by the mucous that transports the aerosols to the larynx where are either being swallowed or removed as sputum.

- **Macrophage-mediated clearance:** main clearance mechanism in the alveolar region. The macrophages relocate the particles to the bronchiolar region. Macrophage-mediated clearance is a slow type of clearance and it can take years the aerosols to be removed from the alveolar region.

- **Blood absorption:** is a clearance mechanism which occurs at all the respiratory tract regions except from the ET1 region. Absorption into blood occurs in two stages. Firstly, the particles are dissolved into substances that can be absorbed into blood and the second stage is the uptake of the dissolved particles. The absorption speed depends on the dissolution rate of the materials that can be fast, medium, or slow.

2.5. Aerosol Deposition Models

2.5.1. ExDoM2

Exposure Dose Model (ExDoM2) is a revised model of ExDoM (Alexandropoulou and Lazaridis, 2013), which was based on the Human Respiratory Tract Model (HRTM) of the ICRP (1994a). Into ExDoM2 (Chalvatzaki and Lazaridis, 2015) new data from the revised HRTM (ICRP, 2015) and a Physiologically Based Pharmacokinetic (PBPK) module for specific metals (As, Cd, Cr, Mn and Pb), were integrated.

ExDoM2 simulates the dynamics of inhaled particulate matter in human airways and estimates the dose in the five regions of the RT; which are the ET1 (anterior nose) and ET2 (posterior nasal passages), the thoracic BB (trachea and bronchial), bb (bronchiolar) and the AI (alveolar interstitial). Parameters that influence the dose deposition and are input parameters for ExDoM2 are the characteristics of particles (particles concentration, size distribution, shape factor and density) and of the exposed subject (gender, breathing type, activity pattern and activity level). Within each region of the lung, exposure is influenced by the inhalability, and the deposition is calculated after accounting for the filtering effect of the preceding airways.

The individual's dose rate (H ; $\mu\text{g}/\text{h}$) is estimated by the equation:

$$H = \sum BC_i n_{i,j} \quad (2.1)$$

where C_i : exposure concentration ($\mu\text{g}/\text{m}^3$) of particles in the size fraction i , B : the ventilation rate of the exposed individual (m^3/h) that is related to the activity level of the subject and $n_{i,j}$: the deposition fraction in region j of the respiratory tract for particles in the size fraction i . The Σ is the sum of dose rate of all the size fractions in a specific region of the respiratory tract.

The ventilation rate B (m^3/h) of the exposed subject is estimated by the equation:

$$B = f_R \times V_T \times 0.06 \quad (2.2)$$

where f_R : breathing frequency (min^{-1}), number of total breaths per minute (Lazaridis, 2011), V_T : tidal volume, the total volume of air inhaled and exhaled during a breathing. The factors f_R , B , V_T depend on the exertion level of the exposed subject.

The mass of particles from each region of the RT, during and after exposure to PM, is transferred to the GI tract, lymph nodes and absorbed in blood. The mass transferred and absorbed to the blood is estimated by the expression:

$$\frac{dR_j}{dt} = \sum_i [m_{k,j} R_k - (m_{k,j} + s) \times R_j] + H_j ()$$

where m : mechanical movement rate of particles between the compartments k and j , R : retained mass in the compartment j at time t , s : the rate of absorption into blood and H : the instantaneous dose applied to the compartment j at time t .

The absorption to the blood depends on the chemical composition of the particles and can be characterized as fast, moderate, or slow.

Dose is a function of ventilation rate that depends on physical activity effort. The ventilation rates that are used as input data for resting, sedentary activity and light exercise are 0.45, 0.54 and 1.5 m^3/h (reference values for adult males; ICRP, 1994a), respectively.

2.5.2. PBPK model

A physiologically based pharmacokinetic (PBPK) model for inhaled PM-bound metals in humans is a module of ExDoM2. The PBPK model was developed to describe the movement of metals from the blood into the tissues as a blood-flow limited model. The model is applicable for the prediction of the kinetics and metabolism of As, Pb, Cd, Mn and Cr in the human body. The PBPK model is based on the studies of Chou et al. (2009) and Sharma et al. (2005) for As and Pb, respectively. The Cd pharmacokinetics were modelled using the formulation proposed in Kjellstrom and Nordberg model (Kjellstrom and Nordberg, 1978). The PBPK model structure contains compartments for the lung, liver, kidney, GI tract, skin, muscle, fat tissues, heart, brain, and remaining body tissues. Model parameters were obtained from the scientific literature. To implement the model, the following parameters are required: Tissue/Blood partition coefficients for the various tissue groups (adopted from Liao et al. (2008) for As and from Sharma et al. (2005) for Pb), elimination rate constants (adopted from Liao et al. (2008)), whereas biochemical constants for first-order rate constants for inorganic As were derived from Chou et al. (2009). The physiological constants (blood flow rates and tissue volumes) were

obtained from ICRP (2003) and Lenz (2010). A thorough description of the model parameters are given in Chalvatzaki et al. (2014).

2.5.3. ExDoM2 interface and use

In order to use ExDoM2, the user needs to import important data both for the studied subject and the PM characteristics. On Fig. 2.2 the user-friendly model interface designed by Papagiannakis E., TUC, can be seen. The following data should be imported by the user in order to calculate the dose, the deposition and the clearance:

- Exposure duration expressed in days and hours.
- The gender and the age of the studied person. The user can choose between male/female adult, male/female 15 years old, male/female 10 years old male /female 5 years old and a baby 1 years old.
- The breathing type of the studied subject (nose or mouth).
- The particle density in g/cm^3 .
- The shape factor of the particles (for spherical particles the value 1 should be used).
- Time after initial intake for calculation of the retention in the respiratory tract in days and hours. It should be taken into consideration, that for the clearance procedure the time period used should be greater or equal to the exposure period.
- At the next step, the user chooses if the model for PM or $\text{PM}_{\text{Bound-metal}}$ will be used. In the second case the Pharmacokinetic module PBPK of ExDoM2 will be used. If it is chosen to proceed with the PBPK model for $\text{PM}_{\text{Bound-metal}}$ the user has to select the metal studied (As, Cd, Cr, Mn and Pb).
- In case the user has available size distribution data from a cascade impactor, the number of the impactor's stages should be defined and an excel file with the size distribution data should be imported.
- Giving to the type of experimental data that the user has available (total concentration or different concentrations for fine and coarse particles) the Input.xls file has to be filled accordingly. In case there are available exposure data from different microenvironments, the user can specify it and import the data accordingly.
- The user can select to proceed or not to the application of the clearance model. In case the user proceeds with clearance the absorption behaviour of the particles during clearance has to be specified.

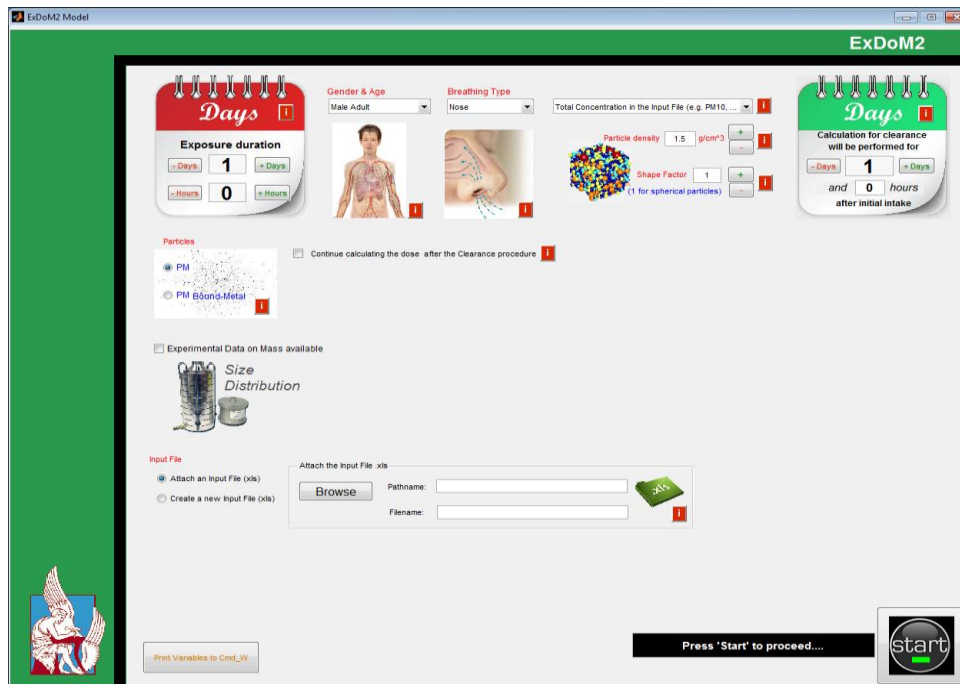


Figure 2.2: ExDoM2 interface.

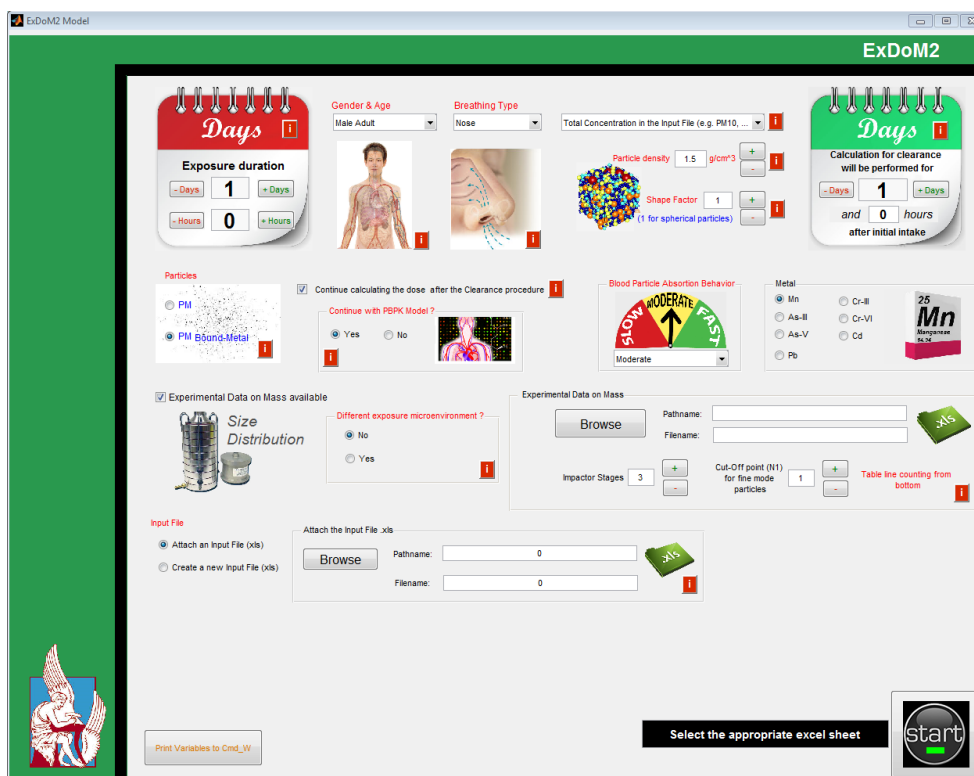


Figure 2.3: ExDoM2 interface (PBPK module).

Chapter 3: Dissertation objectives and outlines

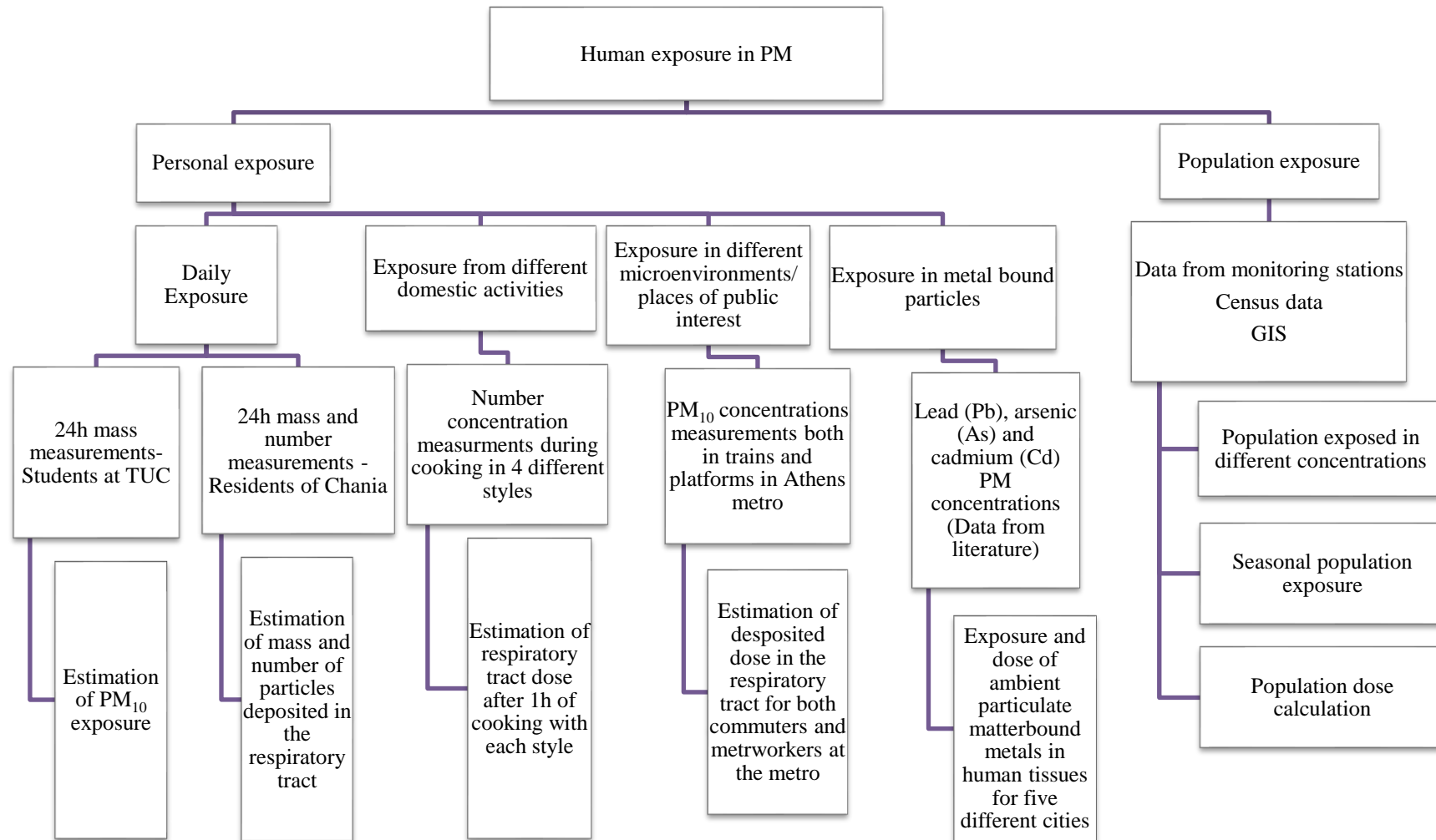
3.1. Dissertation objectives

The present study has been part of the HEXACOMM (Human Exposure to Aerosol Contaminants in Modern Microenvironments) research project. The main aim of HEXACOMM was to utilize modelling and experimental data to link indoor PM to its sources and to the impact on human exposure, at both individual and population level in modern microenvironments, considering contributions from outdoor air.

The focus area of this thesis is to contribute to the understanding of aerosol exposure of humans in different microenvironments, through the use of experimental methods and to estimate the personal dose in PM with the use of a dosimetry model. Specifically, different exposure types were investigated in homes, cars and public transportation, as well as work environments.

The research was carried out in five parts, in which the human exposure was measured and the PM dose deposited was calculated. In the first part, presented in chapter 4, the objective was to estimate the personal exposure of residents of Chania, working and studying, using a personal monitor that recorded their exposure in PM₁₀ (mass) and PN₁₀ (number) for 72h. Chapter 5 presents the third part of the study, which investigated the human exposure and dose from cooking in four different styles. The third study, outlined in chapter 6, investigated the personal exposure of people working and commuting in the metro of Athens by conducting measurements both in platforms and inside the trains. In the fourth part (chapter 7), using data from literature for metal bound particles concentrations (lead, arsenic and cadmium) in European cities, the exposure and dose in human tissues was calculated. The fifth part, is different in that it estimates exposure and dose at population level. The study was carried out in Attica using data from monitoring stations and population spatial distribution in order to estimate the population exposure at the studied area with the use of an interpolation method at a geographical information system.

3.2. Schematic dissertation outline



Chapter 4: Daily personal exposure and dose to particulate matter of Chania residents

4.1. Introduction

Exposure to ambient particulate matter is a topic of global concern and an important factor for developing air pollution control policies. Many epidemiological studies (IARC, 2023, Delfino et al., 2005, Ruckerl et al., 2011, Pope et al., 2002) have pointed out the adverse health effects of exposure in elevated PM concentrations, with children, elderly, and people with pre-existing health issues to be more vulnerable. The level of human exposure to PM can vary significantly depending on several factors such as location, time, indoor sources, and weather conditions, among others.

Using ambient measurements for estimating personal exposure is more economical, easier, on the terms that there is no need to recruit volunteers, and more feasible (Boomhower et al., 2022). Nevertheless, underestimates (Mosqueron et al., 2002, Nerrier et al., 2005) have shown that the use of ambient PM concentrations underestimates personal exposure.

Personal monitoring enables the capturing of real-time data on PM levels and is the most relevant exposure method for assessing individual exposure. By combining personal monitoring with a diary of activities, it is possible to gain insight into the factors that elevate PM concentrations and into the contribution of each microenvironment in the daily exposure. In the case that ambient measurements are used to estimate personal exposure, factors like indoor sources, personal cloud, and filtration of pollutants by the building envelopes are not being taken into consideration (Hänninen et al., 2009).

The purpose of this study was to estimate the personal exposure of citizens of Chania and to calculate the potential inhaled dose both for mass and number PM concentrations. The direct method of personal monitoring was selected, and key selection criterion for the participants was that they dwelled and worked in the city of Chania. The volunteers had to keep a detailed diary of activities and microenvironments, while performing their usual activities along a 72-h period. This method enables the collection of real time data on PM levels in the different microenvironments and in combination with the 1 min time resolution that was used, the effect of different activities in the PM concentrations could be determined.

4.2. Exposure of workers living in Chania

4.2.1. Study participants

A group of people were asked to participate in the study. All the volunteers were females and their age varied from 30 to 35 years old, all living and working in the city of Chania, Greece. Chania is a small coastal city located in the island of Crete in Greece with 54,000 inhabitants.

In total, eight subjects took part in the study and there were five different types of households: 3 households with two adults, 1 household with two adults and two kids, 1 household with two adults, two kids and one pet (dog), 2 households with two adults and one pet (dog) and one household with one adult. At Table 1 can be seen the 8 different subjects and their working environment. Subjects 6 and 7 are working at the same nut bars workshop, Subjects 1 and 4 are primary school teachers in different schools and Subject 5 is working at the office of a logistics company. The rest of the subjects are working remotely from their home environment.

Table 4.1: Subjects household type, working environment and days of measurements.

Subjects	Household	Days of measurements	Working microenvironment
Subject 1 (S1)	2 adults	3	School (Teacher)
Subject 2 (S2)	2 adults 2 kids	3	Home -Office
Subject 3 (S3)	2 adults one pet	3	Home -Office
Subject 4 (S4)	2 adults	3	School (Teacher)
Subject 5 (S5)	2 adults	2	Logistics Company
Subject 6 (S6)	1 adult	2	Nut bars workshop
Subject 7 (S7)	2 adults, 2 kids, one pet	3	Nut bars workshop
Subject 8 (S8)	2 adults, one pet	3	Home Office

4.2.2. Personal exposure monitoring

The target was a three-day period (72h) of personal monitoring, however one subject managed to collect data only for 48h, due to incorrect use of the instrument. Since microenvironment contributions to the daily exposure vary significantly with time activity patterns, it is crucial for the participants to keep a diary of activities to get a comprehensive understanding of the PM levels in each microenvironment. Study subjects should record time-activity patterns keeping a diary of time, location, and activities, including cooking, household activities, training, driving, and sleeping. A short description of the area where their home is located should also be given, with data like the density of the traffic on the closest streets and the occurrence of any construction site in the area. Participants should also record the ventilation patterns, the use of air purifiers or extractor fans and the use of heating or cooling devices. This diary should include information about where the monitor was placed, the time of the day, and what activities were taking place during the monitoring period. The aforementioned data can help identify

sources of PM pollution and determine how activities impact PM levels. The participants were advised to perform their routine both in occupational and private life and there were no restrictions on daily habits, including smoking.

A variety of different methods of estimating personal exposure are available, including direct and indirect methods. The indirect methods include the use of data from fixed site monitoring stations, microenvironmental monitoring (instruments fixed at the different microenvironments) and survey instruments and exposure models (Lioy, 1995). In the current study, the direct method of personal monitoring was selected as more appropriate for the estimation of the actual human exposure. Since exposure varies a lot spatially and temporally, personal monitoring is the best way to estimate personal exposure for small or specific groups, in comparison with using data from fixed monitoring stations that can result to inaccurate assumptions regarding the individual exposure (Cattaneo et al, 2021). As it is stated also in Kousa et al. (2002), PM data from fixed stations are not good predictors for the estimation of the personal exposure, due to the movement of the subjects in different microenvironments, but in the case of no indoor sources, outdoors and indoors PM concentrations have good correlation (Chalvatzaki, et al. 2023).

4.2.3. Instrumentation

The instrument used for this study was an optical particle sizer, the TSI OPS 3330, although is not a personal monitor. Since the objective of this study is the estimation of the personal exposure in PM and the determination of the deposited dose, the availability of particle size distribution data was necessary. OPS TSI 3330 measures particles in the size range of 0.3 to 10 μm in up to 16 channels and it is a light portable instrument, which can be used both plugged and with batteries. The study participants were supplied with OPS batteries, so they didn't need to turn off the instrument while changing microenvironments, being outdoors or driving. All the participants were trained to use the instrument correctly, but by reducing the interaction with the instrument, more errors can be avoided. Additionally, volunteers were advised to put the instrument as close as possible to the breathing height when they were changing microenvironment.

The time resolution used was 1 min, as can be seen also at the figures at section 4.3. The objective of the study was to determine how the different activities affect the PM concentration, so the time resolution of 1 min was appropriate to be used. OPS measures fast and accurately particle concentration and particle size distribution using single particle counting technology in a wide concentration range from 0 to 3000 particles/ cm^3 . During the current study this threshold was exceeded in the cases of frying meat at home and during the use of a professional oven baking nuts.

4.2.4. Personal exposure of human subjects

On Table 4.2 can be seen the 3-day measurements average PN₁₀¹ concentration for each of the nine subjects. S5 due to an error at the use of the instrument, had sufficient measurements for 2 days instead of three. The personal mean exposure in PN₁₀ ranged from 32 to 80 particles/cm³ with average daily exposure 50 ± 17 particles/cm³. The PN₁₀ measurements with OPS were converted from number to mass concentrations.

The conversion from number to mass is done by the following equation:

$$m = \rho \frac{\pi D_p^3 n}{6},$$

Where,

m = mass concentration

ρ = particle density

D_p = particle diameter

n = number weighted concentration per channel

Table 4.2: Average PN₁₀ and PM₁₀ exposure of the studied population.

Subjects	Average PN ₁₀ number concentration of the 3-day measurements	Average PM ₁₀ mass concentration of the 3-day measurements μg/m ³
Subject 1	36	12.5
Subject 2	33	17.8
Subject 3	69	11.0
Subject 4	79	23.7
Subject 5	49	15.7
Subject 6	80	18.6
Subject 7	55	36.1
Subject 8	36	14.2

On Table 4.2 the mean exposure in PM₁₀ is shown. The personal average exposure in PM₁₀ ranged from 11.0 μg/m³ for S3 to 36.1 μg/m³ for S7. The average PM₁₀ exposure concentration of the 9 subjects was 18.7 ± 8.07 μg/m³.

The PM₁₀ concentrations were lower than at other sites, for instance, Nerriera et al. (2005) estimated the personal exposure in Paris 43.7 ± 9.8, 67.6 ± 32.0 in Rauen and 73.7 ± 20.5 in Strasbourg.

Regarding PM₁₀ exposure, none of the subjects was exposed to concentrations higher from the daily limit set by European Air Quality Directive (2008/50/EC) for outdoor environments,

¹ PN₁₀ refers to number concentration of particles in the range of 0.3 to 10 μm

which even though is not applied indoors, can serve as guideline for studying the human health risk from exposure in PM particles.

S6 displays relatively higher average personal exposure in PN_{10} , due to her working environment, where there is in use an industrial oven and the ventilation is not working well, while S4 was exposed to the highest number of PM_{10} concentrations among the nine subjects, as it is shown on table 4.2. S4, was exposed to higher concentrations in the home environment and as would be described later in detailed graphs, the opening of the windows was elevating the indoor concentration due to construction works in close proximity to her building.

4.2.5. Personal exposure

Graphs with all the 24h measurements and activities of the 8 subjects can be found on Appendix A, nevertheless at this section several daily exposure cases of different subjects are presented.

Figure 4.1 illustrates the daily exposure time series of S4 during a typical working day, and the activity data annotated on the graph were gathered from the activity diary. S4 and S1 are the two primary school teachers among the study population and they spend a big proportion of their day at school. As is shown on Table 2, S4 had the second highest number and mass exposure among the subjects. Contrary to other subjects, S4 was exposed to high PN_{10} concentrations in the home environment, even when no indoor sources were active. All the subjects were encouraged to describe the close outdoor environment of their home and as S4 mentioned there were daily construction works at a building nearby. As it can be seen on Fig. 4.2. the opening of the windows for ventilation elevated sharply the indoor PN_{10} concentration, which reached the high value of 232 particles per cm^3 , while PM_{10} concentration reached also the very high value of 320 $\mu g/m^3$. Significant elevation from the opening of the windows were also observed on S8 measurements during the morning hours, also due to a construction site in very close proximity to the studied apartment. The selection of 1 min time resolution has the advantage of understanding better how the different activities, like for example cooking, windows opening, household activities influence the indoor PM concentrations.

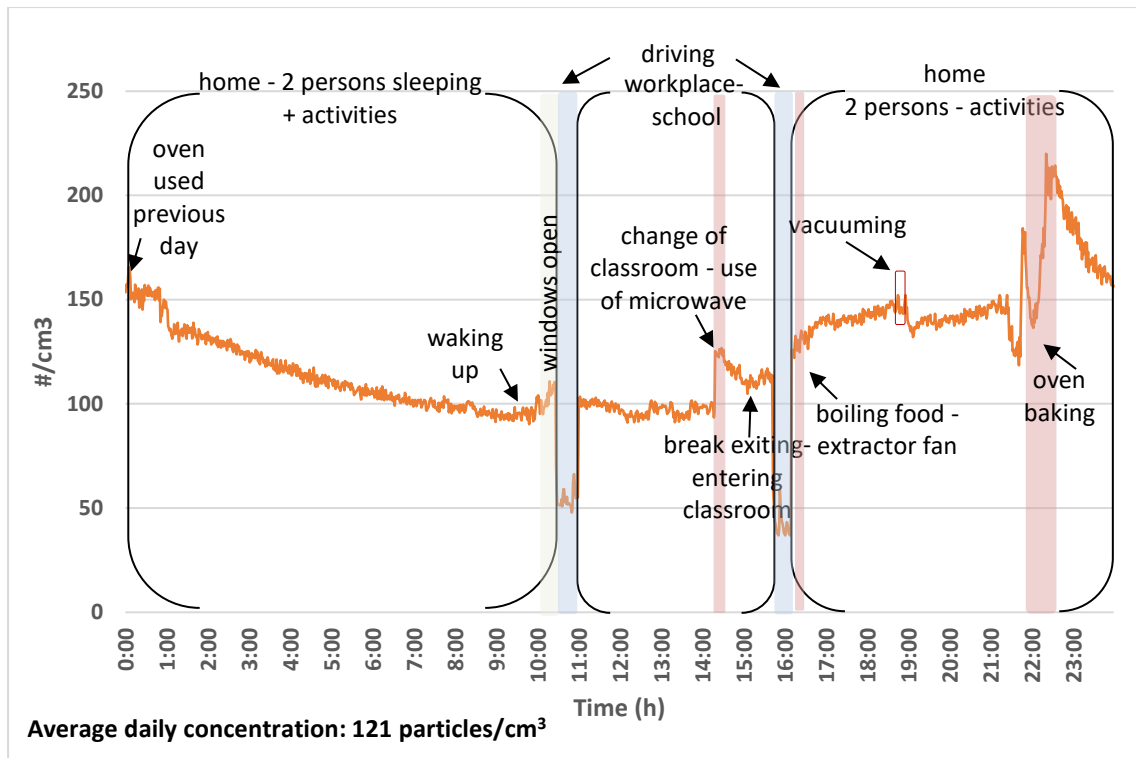


Figure 4.1: Subject 4 daily exposure (number concentration) (day 3).

As it can be seen in Fig. 4.1 and 4.2 and 4.3 indoor sources like cooking, vacuuming and hair dryer use are depicted both in PN and PM concentration by increasing the indoor concentration. Cooking is considered the main PM indoor source and, in all exposure, time series the indoor concentrations were increased. Both PM₁₀ and PN₁₀ concentrations varied a lot during cooking and this variation depended mainly on the style of cooking, the length and type of ventilation used (extractor fan, windows opening). Among figures 4.1, 4.2 and 4.3 oven baking elevated the indoor PN₁₀ concentrations more with the oven door opening causing a considerable increase that reached the level of 220 particles/cm³. However, the highest PM₁₀ concentration (196 µg/m³) during a cooking event was recorded during the use of a microwave in the school environment.

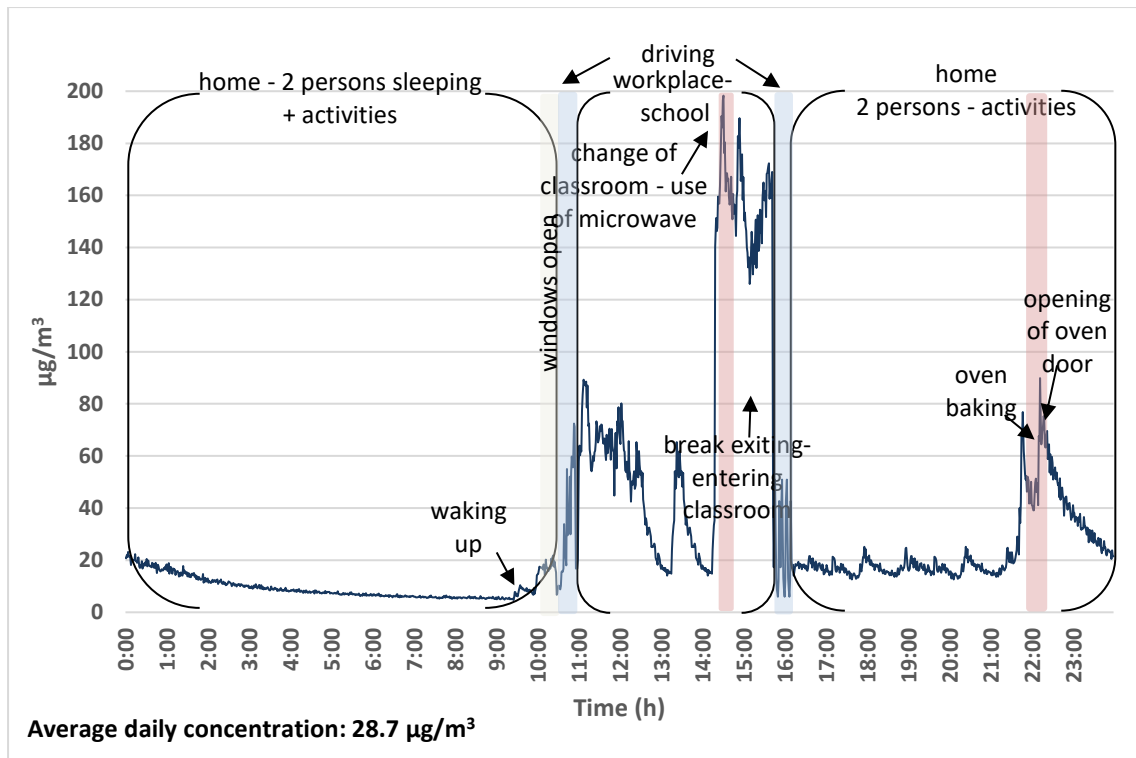


Figure 4.2: Subject 4 daily exposure (mass concentration) (day 3).

At the school environment, both in the case of S1 and S4, big fluctuations at the indoor PM₁₀ concentrations were observed due to the many students and the continuous moving in and out of the classroom, while the classroom used for the students to have lunch had the highest PM levels due to the use of a microwave.

S6 was the subject with the higher average daily exposure, due to her working environment, where an industrial oven is in use and the ventilation system was not working efficiently during the period of the measurements. As it can be seen on Figure 4.4 the PN₁₀ concentration reached the high levels of 1700 particles/cm³ and during another measurement's day in the same workshop the OPS threshold of 3000 particles/cm³ was exceeded due to the industrial oven. It should be mentioned that on day 3 of S6, when the oven was used again the door close to the oven was open for ventilation and the PN₁₀ levels were considerably lower, 530 particles/cm³.

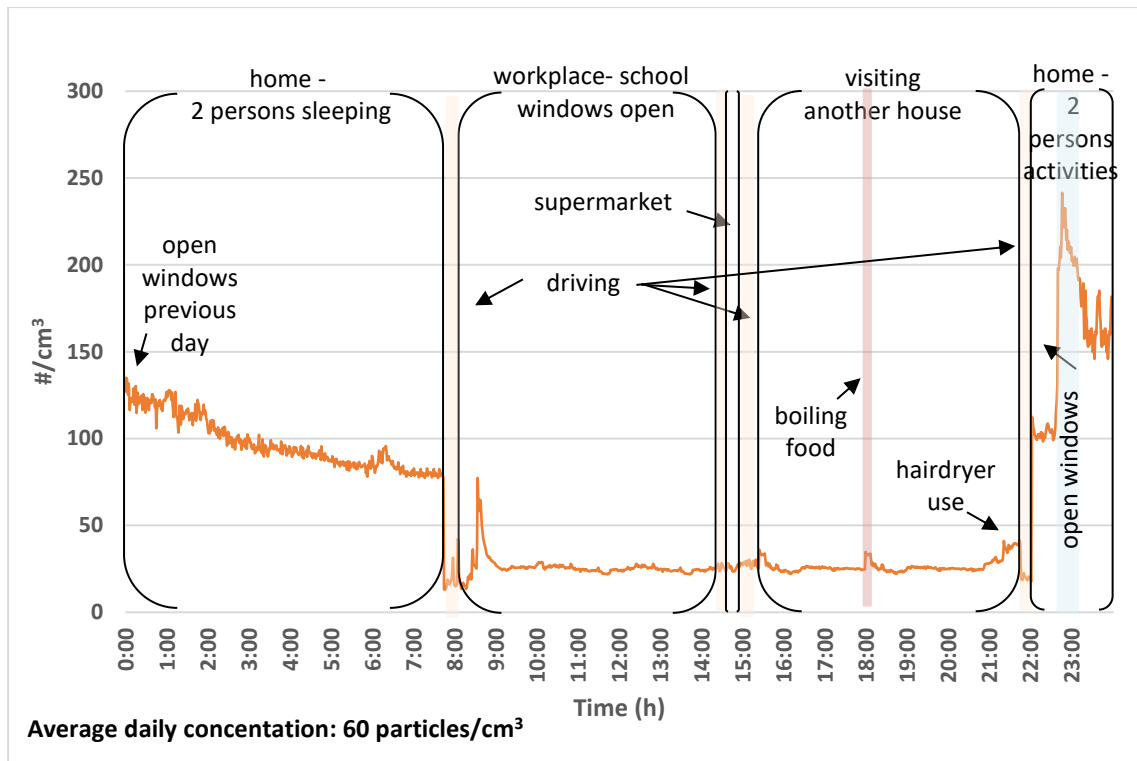


Figure 4.3: Subject 1 daily exposure (number concentration) (day 3).

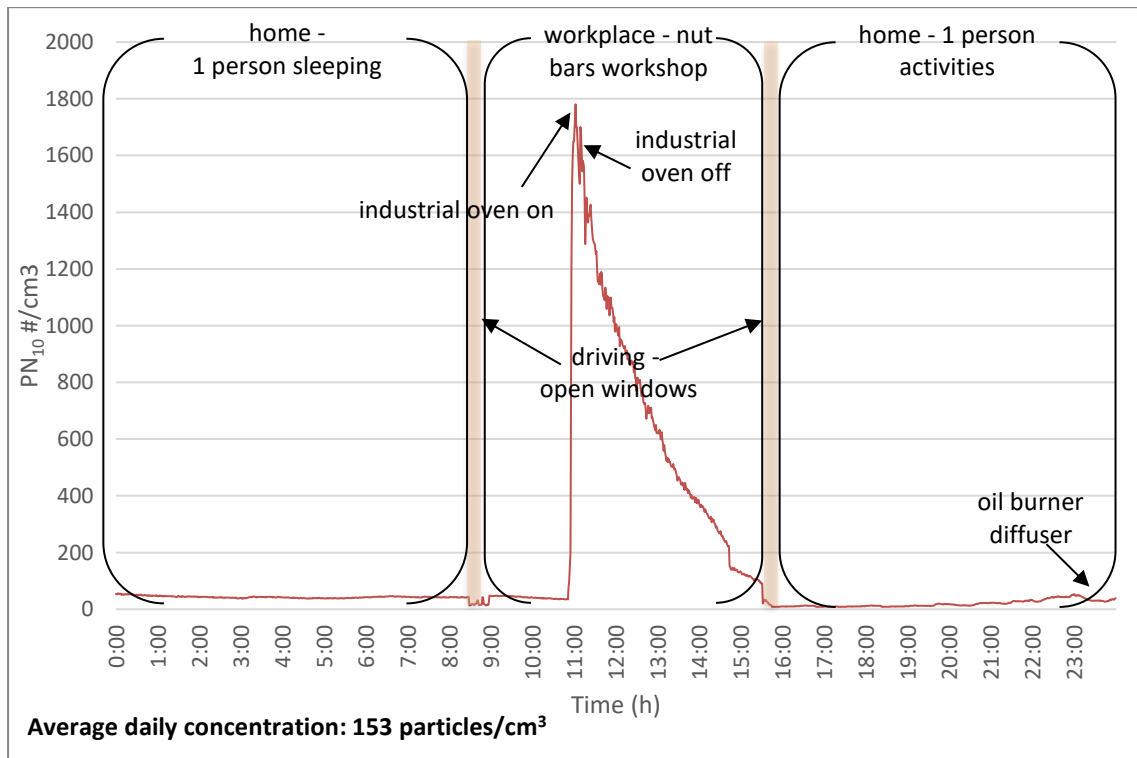


Figure 4.4: Subject 6 daily exposure (number concentration) (day 2).

All the studied subjects were nonsmokers and since smoking is not allowed indoors, their personal exposure was not affected by cigarette smoke. The only exception is S6, who is a

smoker, but doesn't smoke indoors. On Fig. 5 the subject is smoking at the balcony with open balcony doors while keeping the instrument indoors and as it can be seen there is a sharp rise on PN_{10} concentrations.

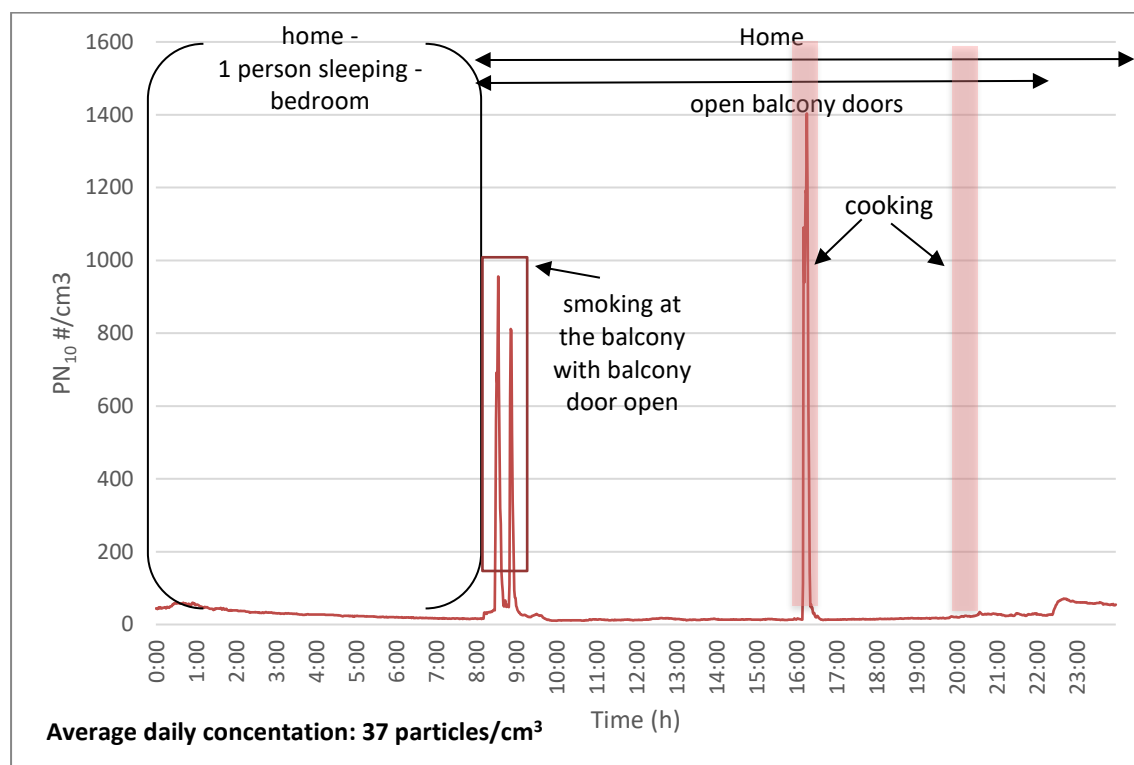


Figure 4.5: Subject 6 daily exposure (number concentration) (day 1).

As is shown in all the 24h exposure examples presented at the current section, all the subjects spent most of the day indoors, with the only exception the time they were driving from the one microenvironment to the other. All the measurements were conducted on working days so this can be a reason subjects didn't spend any time in leisure activities outdoors. It should also be taken into consideration that the instrument used, even though is portable, is relatively big and this fact might have discouraged the subjects from participating in outdoor activities, where they should carry the instrument.

4.2.6. Personal exposure in different microenvironments and from different activities

4.2.6.1. Personal exposure in different microenvironments

Exposure in the workplace and at home were the most important microenvironments in total uptake of particulate matter since the studied subjects spent the majority of the time indoors. Among the participants, only 4 of them had a working place and were not working remotely from home. S1 and S4, primary school teachers, were exposed to average PN_{10} concentration 36 particles/cm³, while the average PM_{10} concentration was 27.1 $\mu\text{g}/\text{m}^3$. Relatively close to the

teachers' exposure, was the exposure of S5, who is working at the office of a logistics company, to PN₁₀ (34 particles/cm³) and PM₁₀ concentration (21.2 µg/m³). However, S6, who is working at a nut bar workshop, had the highest exposure at the workplace environment with PN₁₀ average concentration 377 particles/cm³. Since not all the subjects were working the same hours, the average values were calculated for 5 hours of work.

On Fig.4.6 is illustrated the exposure in the main different microenvironments, that most of them were common between all the subjects. The average PN₁₀ 6-hour concentration of no activities in the home environment (while subjects were sleeping) was 48±27 particles/cm³, while the PM₁₀ concentration was 8.9±4.6µg/m³. Higher concentrations were observed during household activities like vacuuming, cleaning, hairdryer use etc., as it is presented on Fig.6. According to the subjects' diaries the in-vehicle measurements were 24 in total, with average PN₁₀ concentration 37±15 particles/cm³, while the average PM₁₀ concentration was 28.9 ±16.0 µg/m³. The means of transport of all the subjects was private car with all of them being alone in the car while commuting or going to other microenvironments. In most cases, Subjects stated that were driving with open windows.

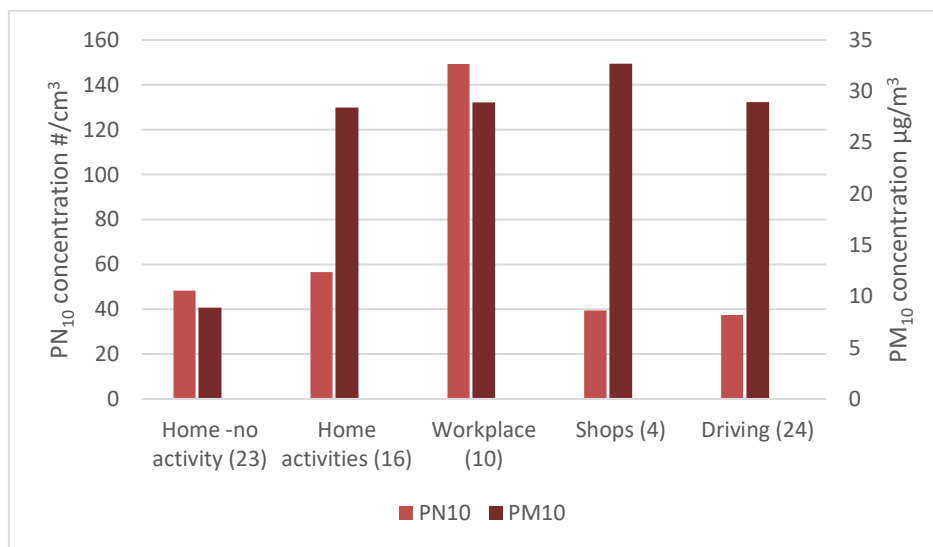


Figure 4.6: Average PN₁₀ and PM₁₀ exposure in different microenvironments (in the parenthesis is stated the number of times the subjects visited each microenvironment or activity).

4.2.6.2. Personal exposure during Cooking

PM emissions from cooking can be a significant source of indoor air pollution, since during cooking a variety of pollutants are emitted, including PM, CO, NO₂ and VOCs. The PM emission levels depend on many factors like the type of fuel, the cooking method (frying, boiling, grilling) and the ventilation system of the kitchen. As it is stated in many studies (Wenlu et al., 2022, Williams et al., 2012, Hongmei Xu et al., 2018) cooking in the traditional

way with solid fuels like wood, coal or charcoal elevates massively the PM levels with adverse health effects for the people exposed to these emissions. In all the households in the current study, electric stoves were used, and the ventilation pattern was extractor fans and, in some cases, participants also chose to open the windows during cooking.

On Fig. 7 can be seen a cooking event that took place on measurements day 3 of S7, during which both the oven and the cooktop plate were being used simultaneously. As it was stated at the time activity diary of the subject, the subject was frying pork and due to the fat frying a great number of particles were produced and the threshold of 3000 particles/cm³ of OPS was exceeded. The frying of meat products with fat produces more particles than vegetables frying as was found in other studies than vegetables (Buonanno et al., 2009). The instrument started working again after the decreasing of the indoor PN₁₀ concentrations.

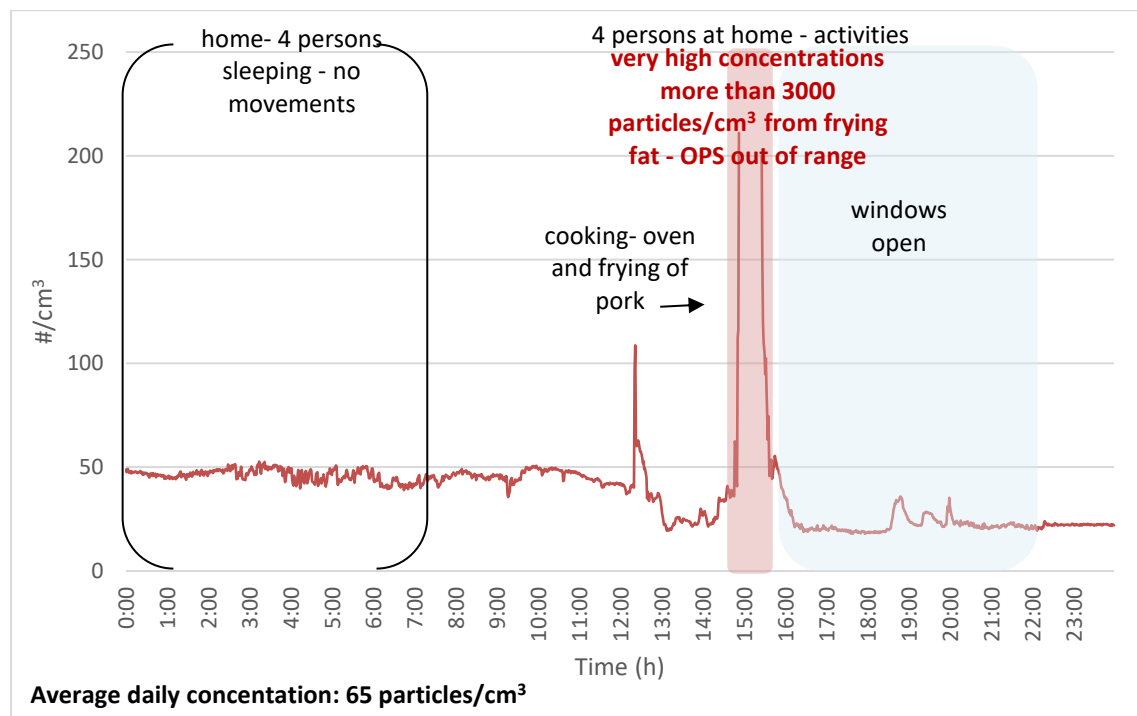


Figure 4.7: Subject 7 daily exposure (number concentration) (day 2).

On Fig.8 can be seen all the cooking events that took place during the measurements divided by style of cooking. In total 20 cooking events occurred, and in order to calculate the average concentration the measurements of the main 20 min of the cooking were used, since each style of cooking has different length, for comparison reasons. The average PN₁₀ concentration was 154 ± 259 particles/cm³, with standard deviation being high due to the frying events, while the average PM₁₀ concentration was 42.7 ± 35.2 µg/m³.

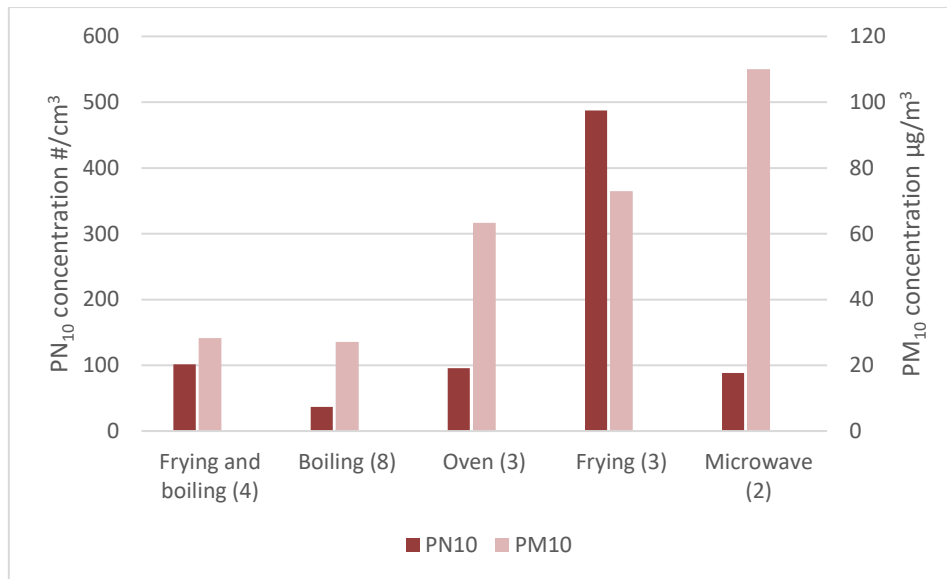


Figure 4.8: Average PN₁₀ and PM₁₀ exposure to different types of cooking (in the parenthesis is stated the number of times the subjects visited each microenvironment or activity).

4.2.7. Dose calculation

Since many epidemiological studies (Dockery et al. 1993; Schwartz et al. 1999; Pope et al. 2002) have highlighted the correlation between PM concentrations and increased human mortality and morbidity, it is important to estimate the individual dose.

The dosimetry model ExDoM2 (Chalvatzaki and Lazaridis, 2015), was used in order to determine the dose of particles in the regions of the respiratory tract, for the 8 subjects, who took part in the current study. A detailed description of ExDoM2 is available at the section 2.5. Required input data, in order to estimate the human dose, are the subjects' characteristics, the activity pattern of the studied subjects and the physical characteristics and the size distribution data of the particles.

At the current study, there are available detailed activity pattern data, since the participants were keeping track of all their activities during the day. In comparison with other studies, that use daily size distribution data usually from gravimetric methods, in the current study there is the advantage of having size distribution data per minute due to the use of OPS instrument. The subjects are adult females, nose breathers and their activity pattern is depicted on their diaries. The activity pattern and the breathing parameters of the subject studied, influence the personal exposure and dose, and as a result are important parameters.

4.2.7.1. PN₁₀ human dose

ExDoM2 model was applied for the 8 subjects for all the three days of measurements and on Fig. 9 can be seen the hourly deposited dose in the respiratory tract of the studied subjects. The central mark on each box shows the median deposited dose and the edges of the box indicate the 25th and 75th percentiles. The + marker symbol indicates the outliers.

As it can be seen S4 has the higher deposition, since this subject was exposed in higher PN₁₀ concentrations during more hours relative to the rest of the studied subjects, and additionally was exposed to higher concentrations at the home environment. S6 has the higher outlier, 401,372 particles/h, due to the exposure in high concentrations at the work environment, because of the industrial oven use. The average hourly deposited dose, among the studied subjects, was $44,421 \pm 43,305$ particles/h.

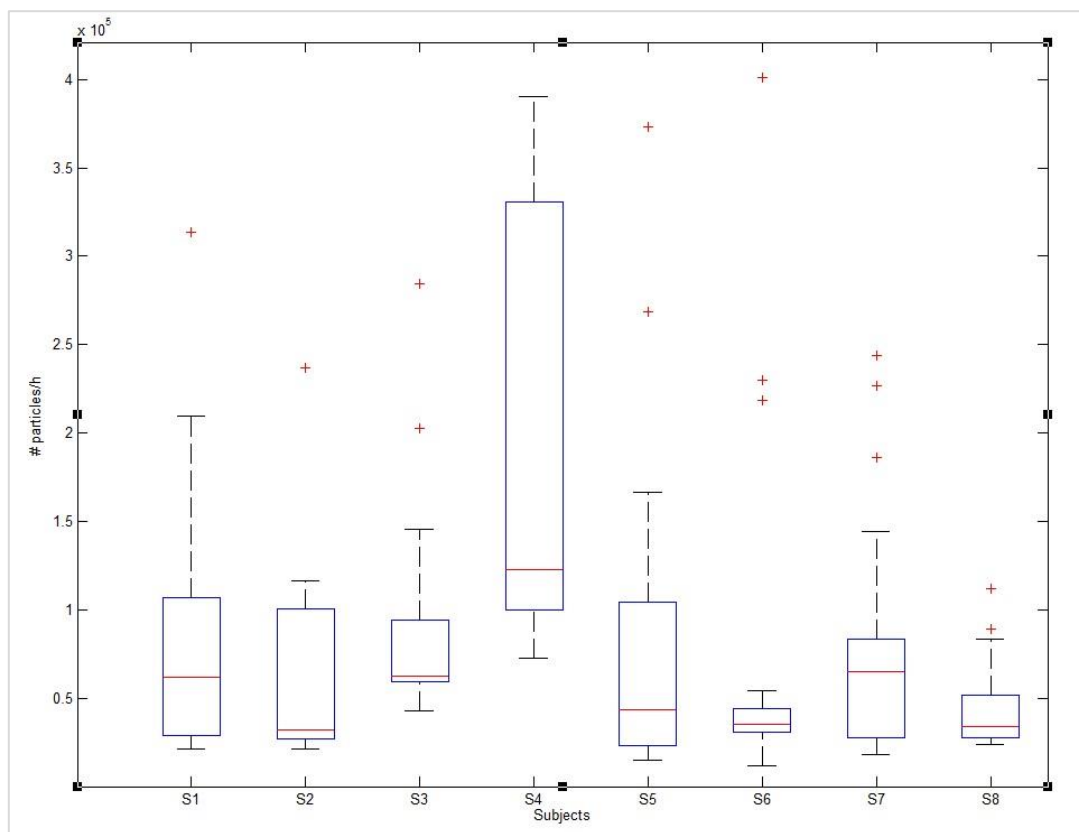


Figure 4.9: Hourly deposited dose in the human respiratory tract of the studied subjects (cross symbol depicts the outliers).

On Fig. 4.10 is shown the particles deposition in the three different regions of the human respiratory tract; the extrathoracic region (ET), the tracheobronchial region (TB) and the alveolar interstitial region (AI) during a typical working day of Subject 4. On Fig. 4.2 can be seen the exposure of S4 during the same day. The main activities are annotated on Fig. 4.10 and can be seen how they impact the dose in the different regions of RT. Additionally, the difference in dose between the different microenvironments the subject changes during the day

is also depicted. Fig. 4.10 shows that the highest deposition in the respiratory tract occurs at the ET region, while the subject is at her workplace, school, that the activity level is light exercise whereas in the rest of the day the highest deposition occurs at the AI, while the activity level is either sitting or sleeping. The higher dose was received during the use of a microwave in a classroom full of students, since it was the part of the day with the higher PN_{10} concentrations. It should be taken into consideration that the instrument used doesn't count ultrafine particles and this is a limitation of the study. In the case of counting also the ultrafine particles the highest deposition would have been in the AI region.

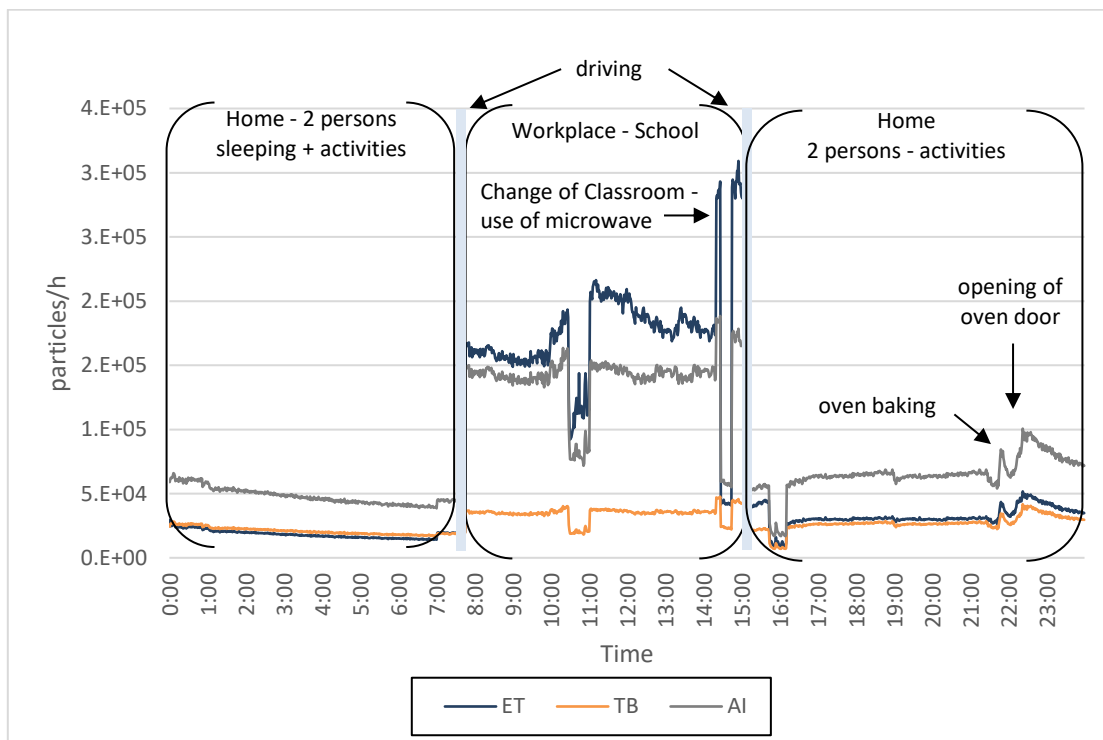


Figure 4.10: Particulate matter dose in the different regions of the human respiratory tract during a working day of S4 (day 3).

4.2.7.2. PM_{10} human dose

ExDoM2 was also applied for the calculation of the mass deposited in the human RT for the 8 studied subjects. On Fig. 4.11 is depicted the hourly deposited dose. The central mark on each box shows the median deposited dose and for better results' display 2 extreme outliers were removed from S7. The values removed are the mass deposition during the hours 15 and 16 on the second measurement day, when the cooking had elevated the mass concentration extremely and the deposited dose was 805 and 372 $\mu\text{g}/\text{h}$, respectively, with most of the mass deposited in the ET region.

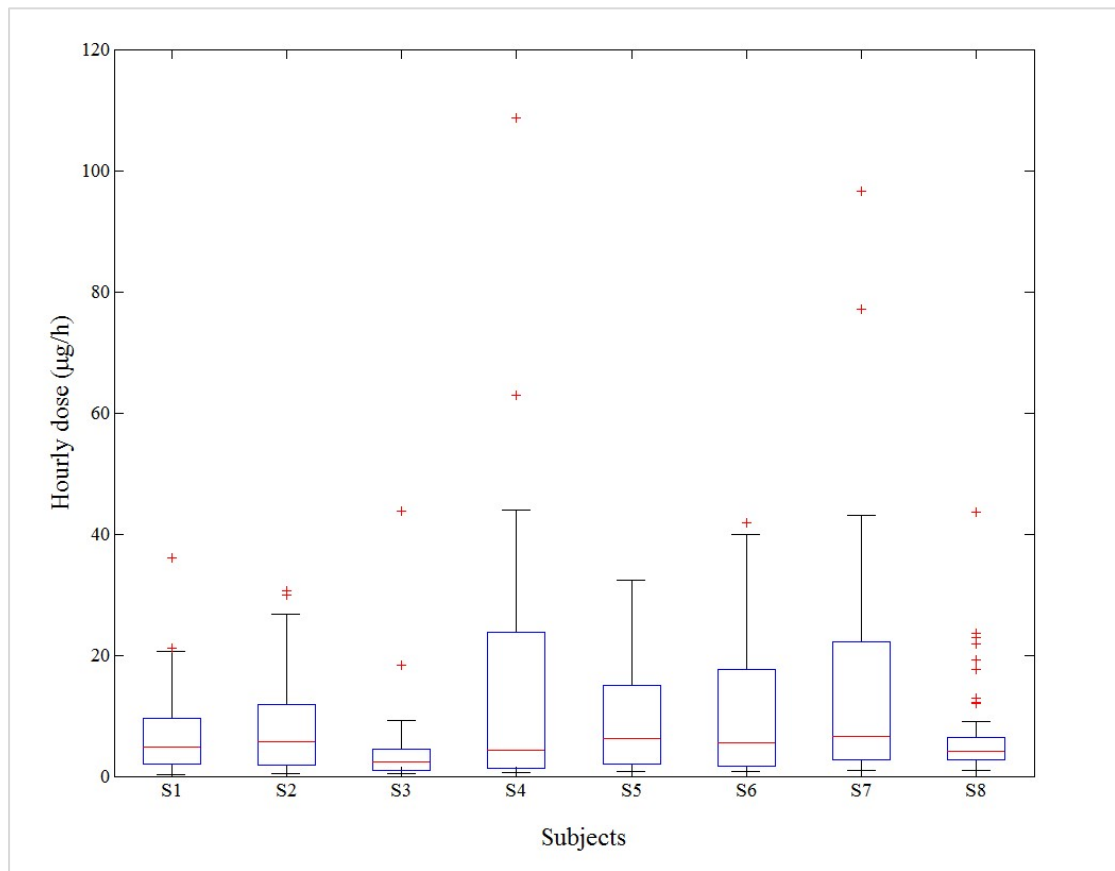


Figure 4.11: Particulate matter dose in the human respiratory tract of the 8 studied subjects (very high outliers have been removed from S7).

On Fig. 4.12 can be seen the deposited dose for the available 72 h exposure data (48 h for S5). The highest dose among the studied subjects was deposited in the RT of S7, due to high exposure concentrations during cooking events, especially a cooking event that took place on the 2nd measurement day, when the subject was frying pork, that elevated enormously the PM₁₀ concentration (Fig. 4.7), as it was aforementioned. The lowest dose was deposited in S3 RT, who has the lower exposure in mass concentration.

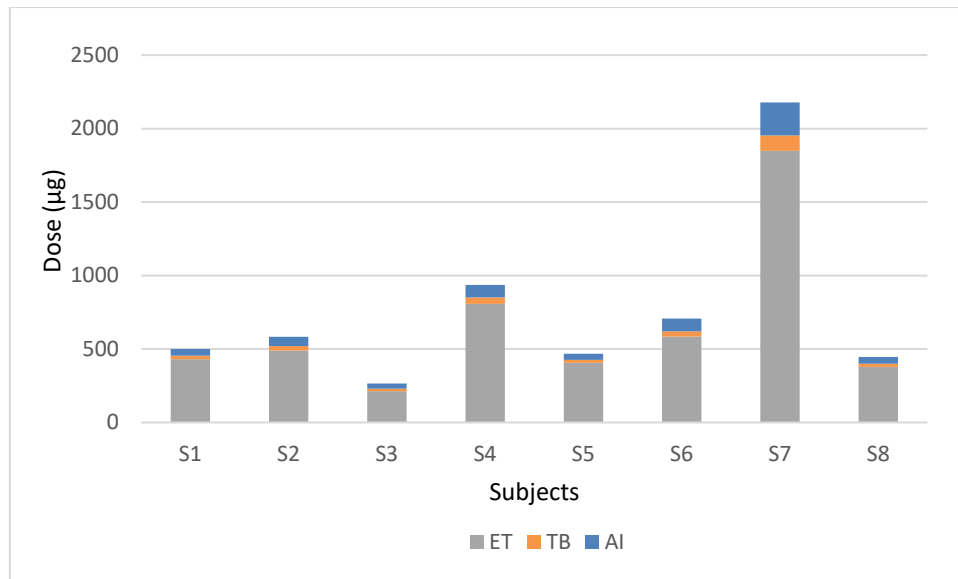


Figure 4.12: Particulate matter 72h total dose (48h in the case of S5) in the different regions of the human respiratory tract for the 8 studied subjects.

The cumulative dose for the 3 days measurement period for the studied subjects ranged from 445 µg for S8 to 2178 µg for S7 with average deposited dose 802 µg, as can be seen also in Fig.4.12. The majority of the particles were in the coarse mode, and as a result they deposited in the ET region. The particle absorption in blood was considered moderate and the coarse particles are transferred to the trachea, swallowed and end up in the GI tract.

In the case of S4, of the 936.25 µg of particles deposited in the RT, 153 µg were retained in the RT (16%), 628 µg were transferred to the GI tract (67%), 8×10^{-4} µg was absorbed by the lymph nodes and 23.6 µg were absorbed to blood (3%), as it can be seen on Table 4.3. The average deposition in the RT among the studied subjects was 20%, the average transfer to the GI tract 59% and the average absorption to blood 3%. In the study of Alexandropoulou and Lazaridis (2013) for the calculation of human dose in Finokalia, Greece, the corresponding values for the deposition in RT, GI tract and blood are 24%, 67.4% and 7.7% respectively. In both studies the highest dose is transferred to the oesophagus since coarse particles are mostly moved to the trachea by the mucociliary escalator and swallowed.

Table 4.3: Mass retained in the RT, transferred to the GI tract and absorbed by the lymph nodes and the blood

Subjects	RT (μg)	GI tract(μg)	Lymph nodes (μg)	Blood (μg)
S1	9.47E+01	3.25E+02	3.85E-04	1.27E+01
S2	1.11E+02	3.76E+02	4.83E-04	1.73E+01
S3	5.81E+01	1.63E+02	2.02E-04	9.33E+00
S4	1.53E+02	6.28E+02	8.33E-04	2.36E+01
S5*	1.01E+02	2.97E+02	2.59E-04	1.12E+01
S6	1.49E+02	4.44E+02	5.70E-04	2.29E+01
S7	5.23E+02	9.67E+02	5.66E-04	3.61E+01
S8	6.72E+01	1.92E+02	1.76E-04	7.76E+00

*48^h measurements

4.3. Exposure of M.Sc. students in the Technical University of Crete

Six M.Sc. students, four males and 2 females, were asked to participate in the current study. The students had to carry for a 72h period the instrument TSI Sidepak A510 and to keep a diary of all their activities. For this study a small portable monitor was chosen, as the students spend their time in many different microenvironments including cafes and outdoor activities, in comparison with the working adults of the study on 4.2. The limitation of using this instrument is that data only for the mass PM_{10} concentration are obtained and that no size distribution data are calculated.

All students live in the city of Chania and are studying for their master's degree at Technical University of Crete, while three of them are also working. The students were encouraged to follow their schedule, following all their activities including smoking if they are smokers. On table 4.4., can be seen the gender of the students if they are smokers and their average exposure in PM_{10} mass concentration during the 3 days of measurements. The personal highest mean daily PM_{10} exposure was $130.1 \mu\text{g}/\text{m}^3$ with average daily exposure for all the participants $50.2 \pm 16.7 \mu\text{g}/\text{m}^3$. For M1 and M4 the daily limit set by European Air Quality Directive (2008/50/EC) for outdoor environments, is exceeded. Both students are smokers, and they are smoking indoors so their exposure in PM_{10} is relatively high. The lowest average PM_{10} exposure have the two students, M3 and M6, who are non-smokers.

Table 4.4: Study participants characteristics and average PM₁₀ mass concentration of the 3-day measurements.

M.Sc. Students	Gender	Smoker	Average PM ₁₀ mass concentration of the 3-day measurements $\mu\text{g}/\text{m}^3$
M1	Male	Yes	75.9
M2	Male	Yes	33.4
M3	Female	No	29.4
M4	Male	Yes	60.9
M5	Male	Yes	45.9
M6	Female	No	16.3

Figures with the detailed daily PM₁₀ exposure of the students that participated in the current study and the different microenvironments they visited can be found at the Appendix B. On Fig. 4.13 can be seen the detailed activities of M6 during her first day of measurements. The participant spent her day at many different microenvironments as can be seen. The PM₁₀ concentrations were relatively low at the home environment, especially during the sleeping hours, when there was no indoor activity. The blowing out of a candle elevated extremely the indoor concentration but only for the time smoke was present, while the concentrations elevated also during the cooking, especially when the oven door opened. M6 also visited an outdoor market, where she mentioned that meat was being grilled that elevated the particle concentration, while the concentrations were lower when she visited different retail shops.

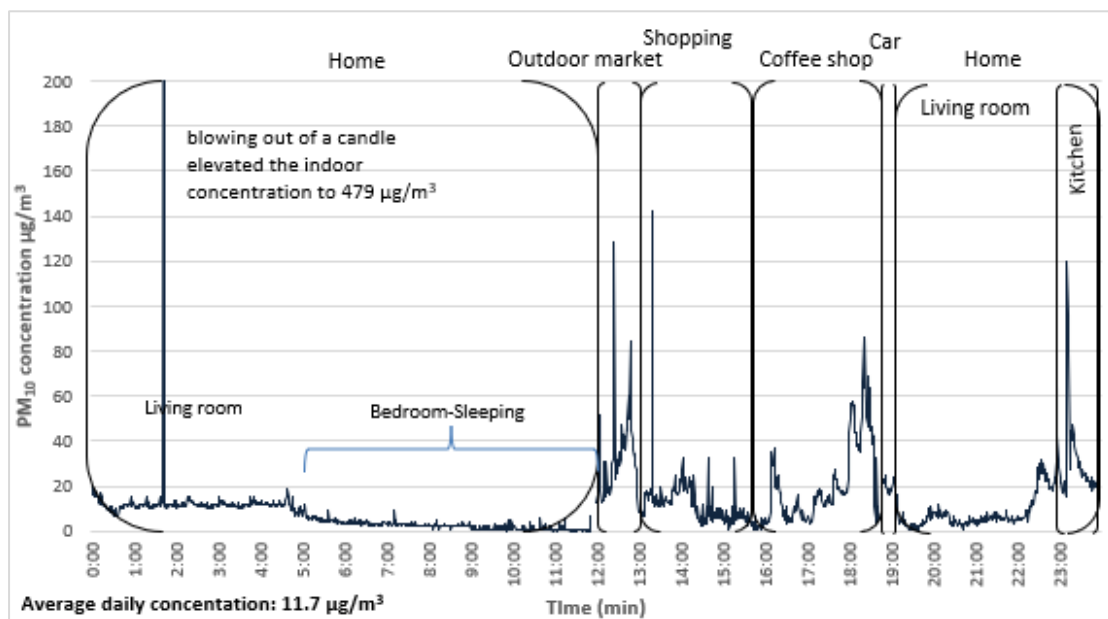


Figure 4.13: M6 daily exposure (day 1).

Another example of a detailed daily exposure of participant M5 can be seen on Fig. 4.14. Student M5 is a smoker and the impact of this can be seen both in the home and car environment when there is presence of cigar smoke. During the day 1 of measurements, M5 visited many different microenvironments including the work office, the university and a dance party were the presence of 25 persons elevated the indoor concentration up to 190 $\mu\text{g}/\text{m}^3$

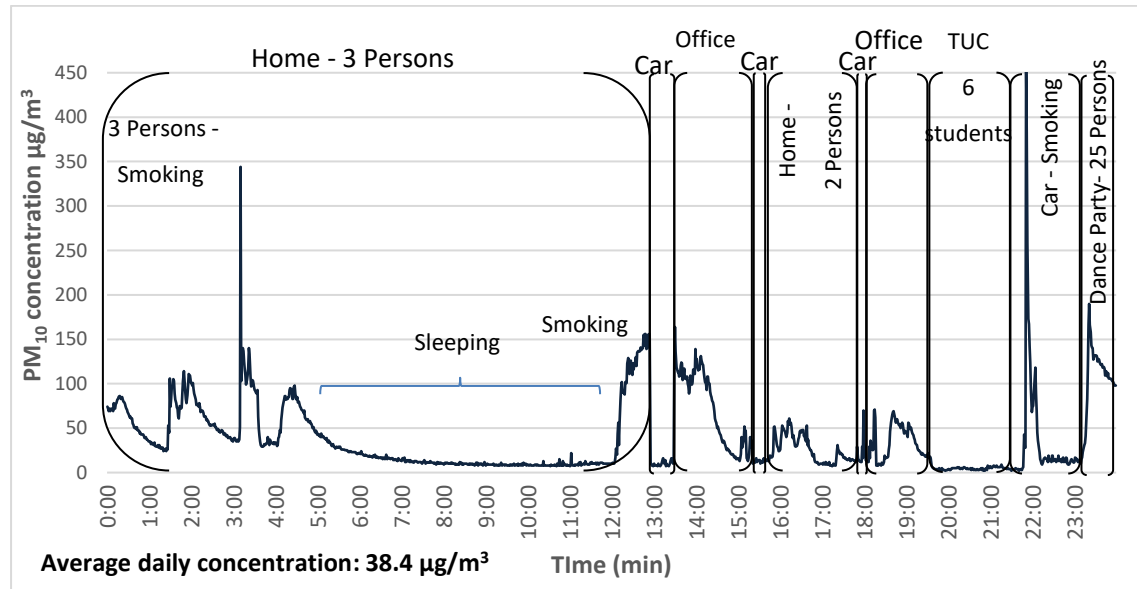


Figure 4.14: M5 daily exposure (day 1).

On Table 4.5 can be seen the different microenvironments, the students changed and additionally the number of people present in them and the presence or not of indoor sources. With the help of the diaries kept by the participants, this information was available and their day could be divided in the following microenvironments: home with or without indoor sources with one two or more than 3 people present, Café and restaurants, retail shops, outdoors and in offices with or without indoor sources. On the table 4.5, the times the students visited each microenvironment are stated and the average PM₁₀ mass concentration.

The average highest PM₁₀ mass concentration, $145.0 \pm 82.2 \mu\text{g}/\text{m}^3$ was observed in the office microenvironment due to the people smoking inside a small space. Similarly, high average PM₁₀ concentrations, $100.3 \pm 115.7 \mu\text{g}/\text{m}^3$, were observed in the home environment, when 3 or more people were present and there were indoor sources. The most common indoor source in the home environment was cigar smoke, but other activities like cooking and burning of incense stick or candles elevated the indoor concentrations sharply.

Table 4.5: Microenvironments the students visited and average PM₁₀ mass concentration in each microenvironment.

Microenvironment and characteristics	Average PM ₁₀ mass concentration μg/m ³	Standard Deviation (σ) μg/m ³	Number of times of occurrence
Home without indoor sources 1 person	20.0	25.1	34
Home without indoor sources 2 persons	38.9	35.1	16
Home without indoor sources 3 or more persons	60.3	80.7	14
Home with indoor sources 1 person	58.1	41.6	5
Home with indoor sources 2 persons	91.0	113.1	10
Home with indoor sources 3 or more persons	100.3	115.7	15
Café and Restaurants	59.8	42.6	10
Retail shops	20.6	9.3	4
Car	21.3	16.6	19
Outdoors city center	39.54	28.1	5
Outdoors suburbs	15.9	8.8	12
Office without indoor sources	54.0	38.2	12
Office with indoor sources	145.0	82.2	12

4.4. Conclusions

Daily measurements were conducted in the city of Chania, where 8 subjects were measuring for 3 days their exposure with the use of an optical particle sizer, the TSI OPS 3330 and 6 M.Sc. students with the use of TSI Sidepak AM510. The subjects were keeping a diary of their activities and the microenvironments they visited. The objective of this study was to estimate the exposure and the consequent dose of citizens of Chania using the data provided by the studied subjects. Additionally, a time resolution of 1min was selected in order to study the impact of various activities and indoor sources in human exposure and consequently in the human dose.

The personal highest mean exposure in PN₁₀ was 80.5 particles/cm³ with average daily exposure 50.2 ± 16.7 particles/cm³, while the highest PM₁₀ exposure was 36.1 μg/m³ with average PM₁₀ exposure concentration 18.7 ± 8.07 μg/m³ in the case of the working subjects. The subjects with higher exposure, were the ones that their work microenvironment had elevated concentrations,

due to the use of an industrial oven, and this also shows the importance of occupational exposure, since people spend a big proportion of their day at work. At the daily concentration figures is depicted the impact of the various activities in the indoor concentrations, with cooking causing sharp elevations, while other household activities also impact the particles levels. A limitation of the current study is that the instrument selected TSI 3330 measures particles in the size range of 0.3 to 10 μm , so we have no data on how the different activities impact the ultrafine particle concentrations. However, it was important to also estimate the daily dose, and as a result size distribution data of the different microenvironments were necessary. This feature of the instrument and additionally its relatively small size led to its selection.

The exposure and dose assessment model, ExDoM2, was used in order to calculate the deposition and dose for both PN_{10} and PM_{10} . Additionally, the retention of PM_{10} in the RT, the GI tract, and their absorption to blood was also estimated. The highest PM_{10} deposition occurred in the ET region of the RT and after the 3 days of exposure, the highest amount of particles was transferred to the GI tract. The rest of the particles deposited in the TB and AI region are remaining to the RT or/and absorbed to the blood.

The daily personal exposure among the M.Sc. students ranged from 11.7 to 130.1 $\mu\text{g}/\text{m}^3$ with average daily exposure for all the participants $50.2 \pm 16.7 \mu\text{g}/\text{m}^3$. Most of the participants were smokers, who were smoking also indoors and their daily exposure was relatively higher than the non-smokers ones, reaching daily average values higher than the EU limit which although is not applied indoors, can serve as a guideline for studying the human health risk from PM exposure.

The results of the current study show the importance of studying the personal exposure since it can vary significantly between people dwelled in the same city. The direct method of personal monitoring is considered the most appropriate since it gives real time data and can help identify the health risks in different microenvironments.

Chapter 5: PM exposure from cooking in four different styles

5.1. Introduction

Cooking is one of the most important indoor sources, as during cooking activities particle concentrations can increase excessively in comparison with background concentrations. Cooking activities increase the particle number concentration indoor, especially the concentration of ultrafine particles, which are the most dangerous for the human health. In this chapter, the effects of four different styles of cooking on the particles number concentrations are investigated. Furthermore, the dose from the inhalation of ultrafine particles (up to 615nm) produced during cooking in four different styles (Chinese, Indian, African, West) activities is estimated.

The measurements were conducted by the team of Professor Roy Harrison, Professor of Environmental Health at the School of Geography, Earth and Environmental Sciences at Birmingham University during my visit at Birmingham University at the 2nd semester of 2015.

5.2. Experiments

In order to determine the personal exposure and dose of particles during cooking activities, 11 cooking experiments were conducted in the same domestic kitchen. During the experiments, no way of ventilation was used (windows closed, no extractor fan). In order to measure the number concentration of ultrafine particles during the cooking activities a Scanning Mobility Particle Sizer (SMPS) instrument was used, measuring particles up to 615nm. Experiments were conducted for four different cuisines and a detailed description of them can be seen on Table 5.1.

Table 5.1: Description of the cooking experiments.

Cuisine (cooking style)	Number of experiments	Cooking activity	Min time of each style of cooking	Cooking activity in details
Chinese	3	Stir frying and rice boiling	45	1. 34min stir frying, 11min rice boiling
				2. 30min stir frying, 25min rice boiling
				3. 25min stir frying, 20min rice boiling
Indian	3	Stew frying -boiling	65	1. 54min frying and boiling stew, 11min rice boiling

		and rice boiling		2. 50min frying and boiling stew, 15min rice boiling
				3. 43min frying and boiling stew, 22min rice boiling
African	3	Chicken and stew frying - boiling, rice boiling and plantain frying	95	1. 20min chicken boiling and frying, 18min both chicken and stew boiling and frying, 11min both stew boiling and frying and rice boiling, 40min rice boiling, 15min both rice boiling and plantain frying
				2. 8min chicken boiling and frying, 30min both chicken and stew boiling and frying, 23min both stew boiling and frying and rice boiling, 10min rice boiling, 8min both rice boiling and plantain frying
				3. 11min chicken boiling and frying, 33min both chicken and stew boiling and frying, 40min both stew boiling and frying and rice boiling, 10min rice boiling, 2min both rice boiling and plantain frying
West	2	Deep frying	45	1. 32min chicken frying, 12min both chicken and chips frying
				2. 12min chicken frying, 23min both chicken and chips frying, 11min chips frying

5.3. Model Input data

The dose of particles in the five regions of the human respiratory tract ET1, ET2, BB, bb and AI was calculated using the exposure and dose assessment model, ExDoM (Alexandropoulou and Lazaridis 2013), that was analyzed in Chapter 2 of the current thesis.

The subject was considered a male, adult, nose breather and non-smoker. Cooking is considered light exercise and for this reason the ventilation rate used as input data was 1.5m³/h (reference values for adult males; ICRP 1994a). The density was considered equal to 1g/cm³ and the shape factor equal to 1.

5.4. Results

5.4.1. Particle number size distribution during four different styles of cooking

5.4.1.1. Chinese cuisine

Three Chinese style cooking experiments were conducted, during which the two main cooking activities were stir frying and boiling. During these cooking activities the particle number concentrations showed an 8 to 91-fold increase, with concentrations increasing to $4.22 \times 10^5 \text{ cm}^{-3}$ compared to $4.6 \times 10^3 \text{ cm}^{-3}$ background concentrations. The highest increase was observed during stir-frying. On Figure 5.1, the total size distributions (particles up to 615.3nm) of the three experiments can be seen. The mode was found between 33.40 and 55.20nm. The number mean diameters, the diameters that the distribution peaks and the total number of particles during 45min of Chinese style cooking can be seen on Table 5.2.

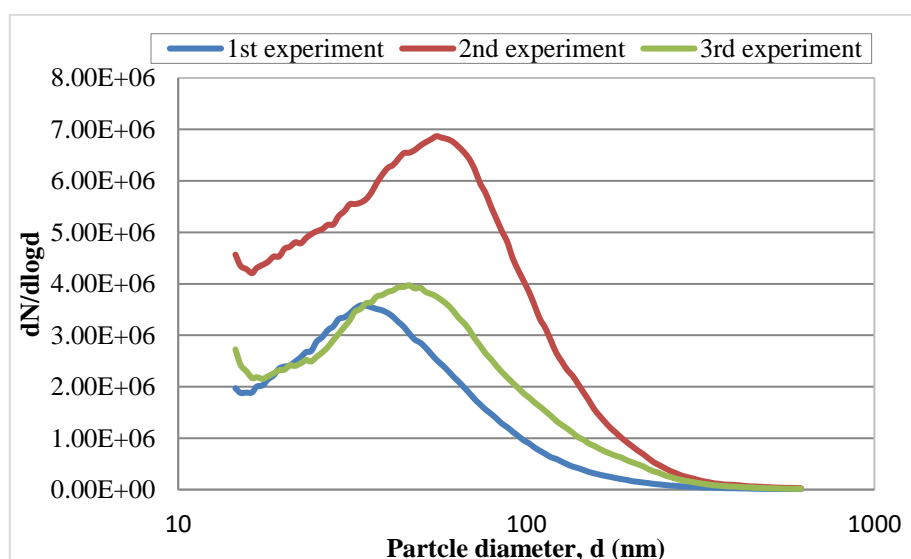


Figure 5.1: Particle number concentration in the size range between 14.6 and 615.3 nm, as measured by an SMPS system during three Chinese stir frying cooking activities.

Table 5.2: Number mean Diameter, Peak diameter and total number of particles during three experiments of Chinese cuisine cooking.

	Experiment 1	Experiment 2	Experiment 3
Number mean Diameter (nm)	45.87	84.81	55.27
Peak diameter (nm)	33.40	55.20	46.10
Total number of particles	2.51E+05	4.51E+05	3.18E+05

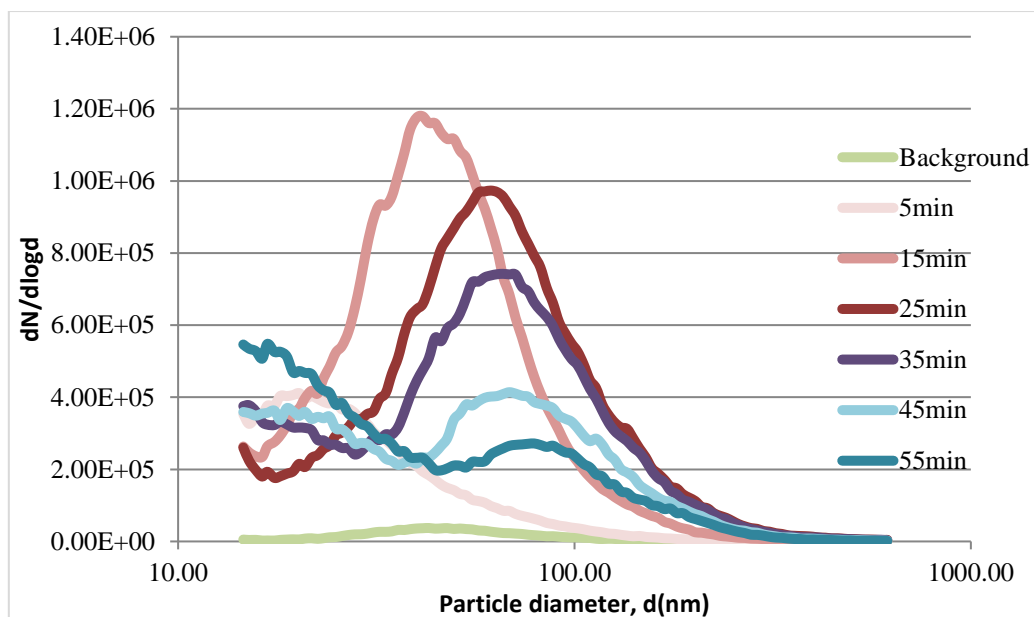


Figure 5.2: Particle number concentration in the size range between 14.6 and 615.3 nm at different times during a Chinese stir frying cooking event (2nd experiment).

The particles number size distributions in different times during the activity can be seen on Figure 5.2. It is observed that the first five minutes there is a major increase in the ultrafine particles, especially in the particles below 23nm and that during the first 35min (stir frying) the mode is between 40 and 61.5nm. After 33 minutes of the experiment the boiling starts and for this reason the size distribution on the 35th, 45th and 55th minute have 2 peaks. When the only activity is boiling (45th min and afterwards) the one mode is on 14.6nm because of the boiling and the second between 50 to 80nm as the particles of the stir-frying procedure are still present. The outcome that boiling presents a peak in the number concentration of particles close to 10nm comes in agreement with the study of Seea et al. (2008).

5.4.1.2. Indian cuisine

The main cooking activities during the three experiments of Indian style cooking were boiling and frying. On Fig. 5.3 the total size distributions (particles up to 615.3nm) of the three experiments are depicted. During Indian style cooking the particle number concentration increased up to 97-fold with comparison to background concentrations (from $3.45 \times 10^3 \text{ cm}^{-3}$ background to $3.36 \times 10^5 \text{ cm}^{-3}$ after 15min of cooking). Due to the fact that the main activity is boiling there is a peak on the number concentration at the size of 14.6nm. The number mean diameter, peak diameter and the total number of particles during 65min of Indian style cooking can be seen on Table 5.3. There is also a mode close to 30nm due to the frying activity.

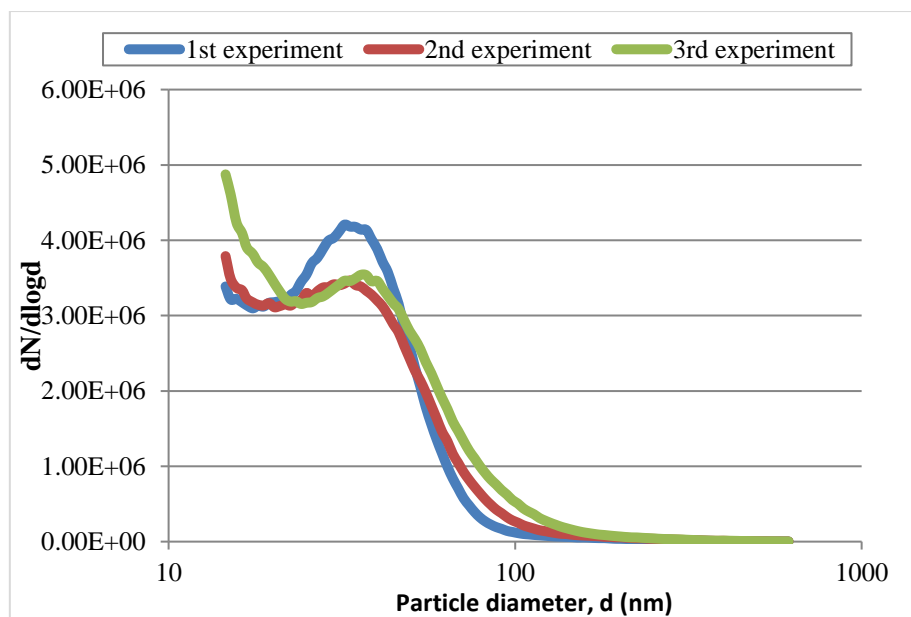


Figure 5.3: Particle number concentration in the size range between 14.6 and 615.3 nm, as measured by an SMPS system during three Indian cuisine cooking activities.

Table 5.3: Number mean Diameter, Peak diameter and total number of particles during three experiments of Indian cuisine cooking.

	Experiment 1	Experiment 2	Experiment 3
Number mean Diameter (nm)	28.13	28.55	26.70
Peak diameter (nm)	32.20	14.6	14.6
Total number of particles	1.64E+05	3.76E+03	1.67E+05

The particle number size distributions in different times during the 3rd Indian cooking experiment can be seen on Figure 4. Similarly, with the Chinese style cooking experiment during the last 15 minutes (50th minute and afterwards) the rice boiling produces a peak close to 14.6nm. From the 15th – 45th minutes is obvious the effect of the frying on the distribution that creates a mode from 34 to 40nm. Ten minutes after the cooking experiment the number concentrations are close to the background values, as after each experiment the kitchen was ventilated.

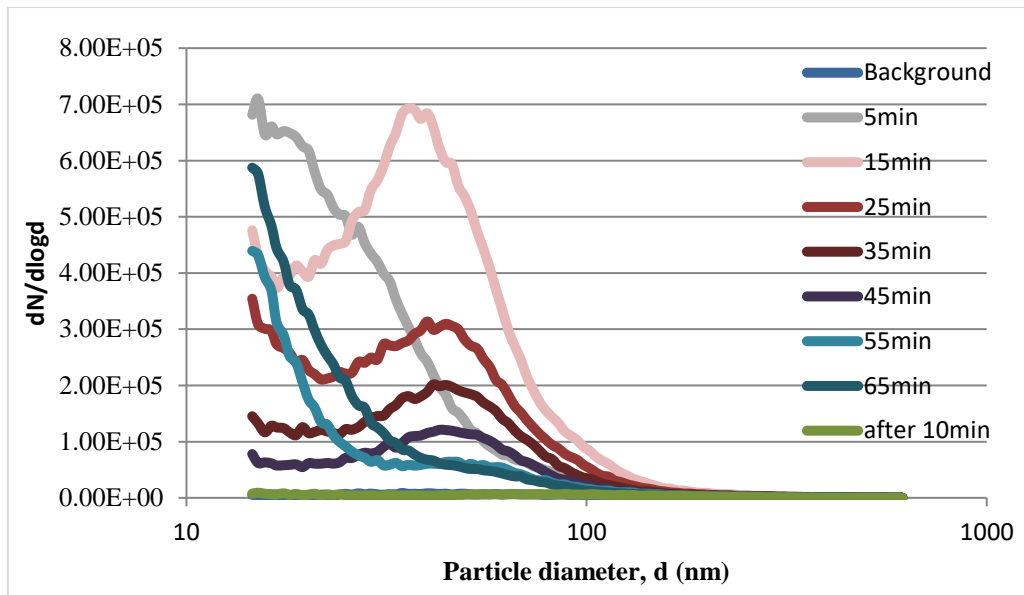


Figure 5.4: Particle number concentration in the size range between 14.6 and 615.3 nm at different times during an Indian style (frying and boiling) cooking event (3rd experiment).

5.4.1.3. African cuisine

During the African style cooking both frying and boiling procedures were used. The total size distributions of the three experiments can be seen on Figure 5. The peak on experiments 1 and 3 is close to 35nm. The number mean diameter, peak diameter and the total number of particles during 95min of African style cooking can be seen on Table 5.4.

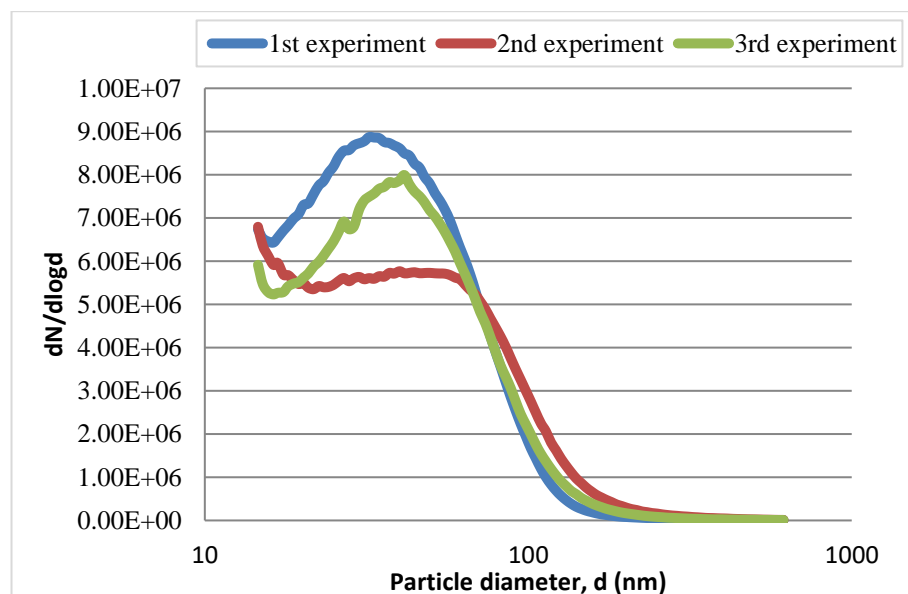


Figure 5.5: Particle number concentration in the size range between 14.6 and 615.3 nm, as measured by an SMPS system during three African cuisine cooking activities.

Table 5.4: Number mean Diameter, Peak diameter and total number of particles during three experiments of African cuisine cooking

	Experiment 1	Experiment 2	Experiment 3
Number mean Diameter (nm)	46.38	40.81	42.57
Peak diameter (nm)	32.20	14.60	38.50
Total number of particles	5.84E+06	4.82E+06	5.20E+06

The particle number size distributions in different times during the 2nd Indian cooking experiment is illustrated on Fig 5.6. As it was observed in all the styles of cooking examined in the current study the first 5min the concentration of ultrafine particles increases. During this African style experiment, the first 35min minutes the cooking procedure followed was frying and boiling of chicken and the next 30min frying and boiling of stew. The differences on the concentrations can be seen on Fig. 5.6. During the frying and boiling of chicken the mode was between 24 and 41.4nm, measurement that comes in agreement with the study of Li et al., (1993) stating that the mode during frying chicken is between 30-60nm. Chicken frying produces more particles than vegetables frying as it is also stated in other studies due to the fact that chicken is more fatty than vegetables (Buonanno et al., 2009). On the 75th minute the only procedure is rice boiling and the size distribution is similar to the other styles of cooking during rice boiling.

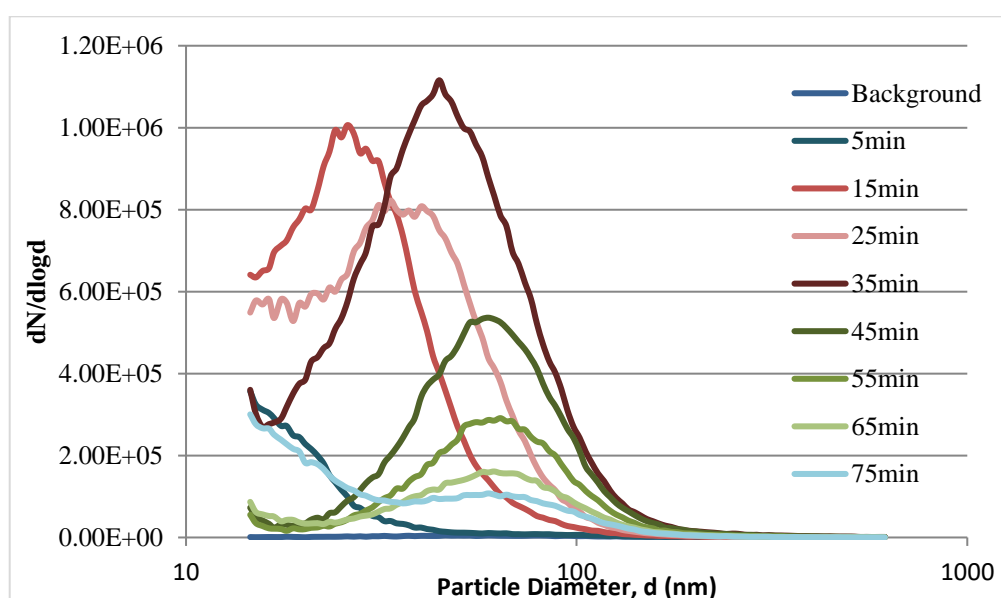


Figure 5.6: Particle number concentration in the size range between 14.6 and 615.3 nm at different times during an African style (frying and boiling) cooking event (2nd experiment).

5.4.1.4. West cuisine

The procedure of deep-frying was used in both the experiments of west style cooking. As it can be seen on Figure 7 both size distributions peak close to 30nm. The number mean diameter, peak diameter, and the total number of particles during 45min of West style cooking can be seen on Table 5.5.

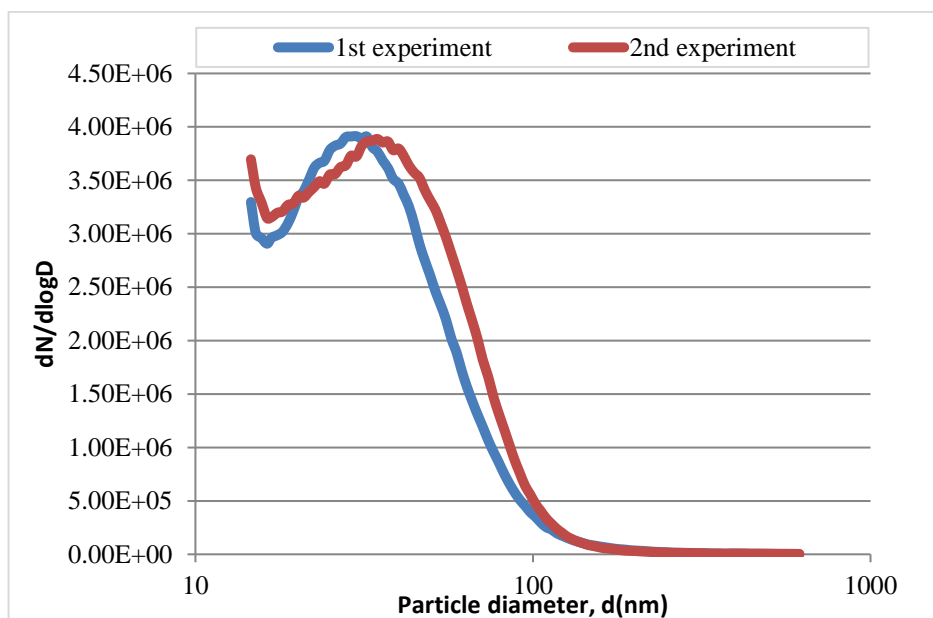


Figure 5.7: Particle number concentration in the size range between 14.6 and 615.3 nm, as measured by an SMPS system during two West cuisine cooking activities

Table 5.5: Number mean Diameter, Peak diameter and total number of particles during two experiments of West cuisine cooking.

	Experiment 1	Experiment 2
Number mean Diameter (nm)	41.09	28.64
Peak diameter (nm)	30.00	34.60
Total number of particles	1.90E+05	6.81E+03

During the West style cooking experiment shown on Fig. 5.8, the first 25 minutes the main cooking procedure was chicken deep-frying and the next 20 minutes both chicken and chips frying. The different procedures can be observed on Fig. 5.8, as on the 35th minutes the simultaneous deep frying of two ingredients causes higher concentrations. On the 45th minute that the only procedure is chips frying the mode is close to 50nm like in the study of Buonanno et al. (2009).

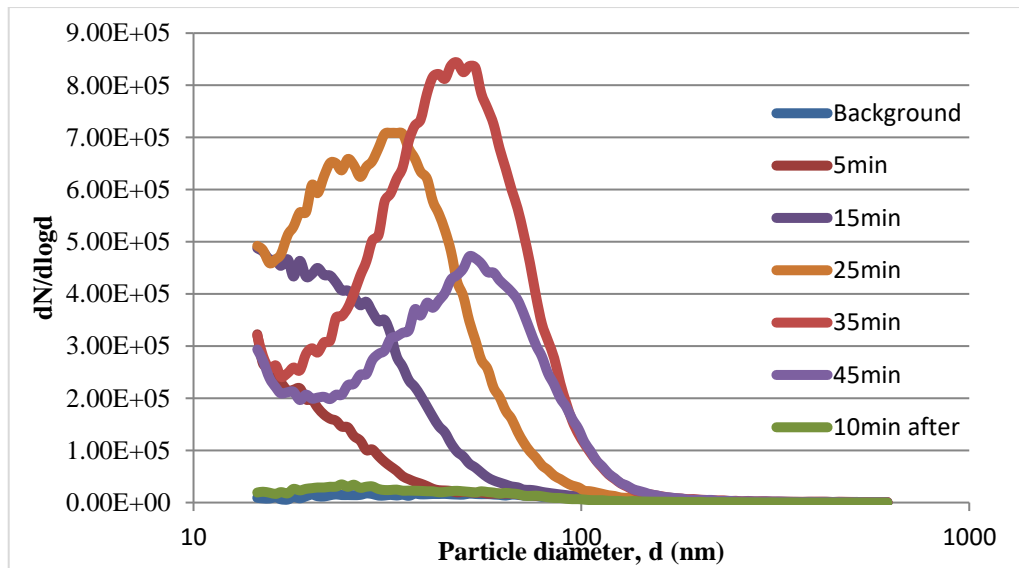


Figure 5.8: Particle number concentration in the size range between 14.6 and 615.3 nm at different times during a West style (deep frying) cooking event (2nd experiment).

5.4.2. Lung dose after exposure to four different styles of cooking

5.4.2.1. Deposition efficiency

The calculated deposition efficiencies for the three main regions of the RT for the ultrafine mode can be seen on Fig. 5.9 and on Fig. 5.10 for the accumulation mode. From the figures can be observed that the particles in the ultrafine mode penetrated deeper in the human lung, as it was presumed. On figure 5.12, the average of the 4 different cooking styles regional lung deposition is presented.

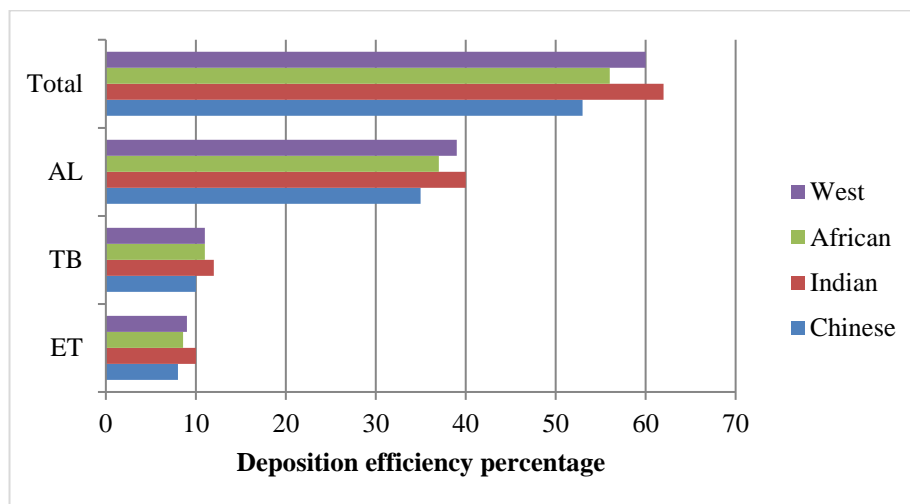


Figure 5.9: Ultrafine particles (up to 98.2nm) deposition efficiency in the ET, TB, AL and in the total respiratory tract during 4 different cooking styles.

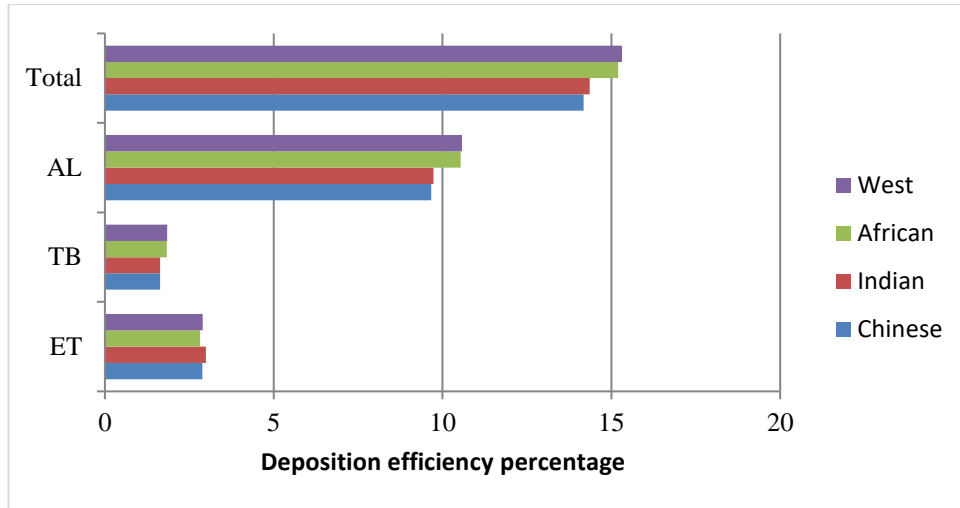


Figure 5.10: Accumulation mode (up to 615.3nm) deposition efficiency in the ET, TB, AL and in the total respiratory tract during 4 different cooking styles.

5.4.2.2. Respiratory tract dose after exposure to Chinese style cooking

The exposure and dose model ExDoM, was used in order to determine the dose of particles in the regions of the respiratory tract after 45min of Chinese style cooking. The results of the three experiments can be seen on Table 5.6 and the average dose of the three experiments on Fig.5.11. As it was expected the highest dose occurs in the AI region due to the fact that the majority of the particles are at the ultrafine mode.

Table 5.6: Particulate matter dose (#) in the five regions of human respiratory tract the ET1, the ET2, the BB, the bb and the AL

	ET1	ET2	BB	bb	AL	TOTAL
1st Experiment	9.83E+09	1.06E+10	2.97E+09	2.19E+10	1.00E+11	1.45E+11
2nd Experiment	1.59E+10	1.69E+10	4.79E+09	3.48E+10	1.60E+11	2.32E+11
3rd Experiment	1.16E+10	1.24E+10	3.50E+09	2.55E+10	1.17E+11	1.70E+11

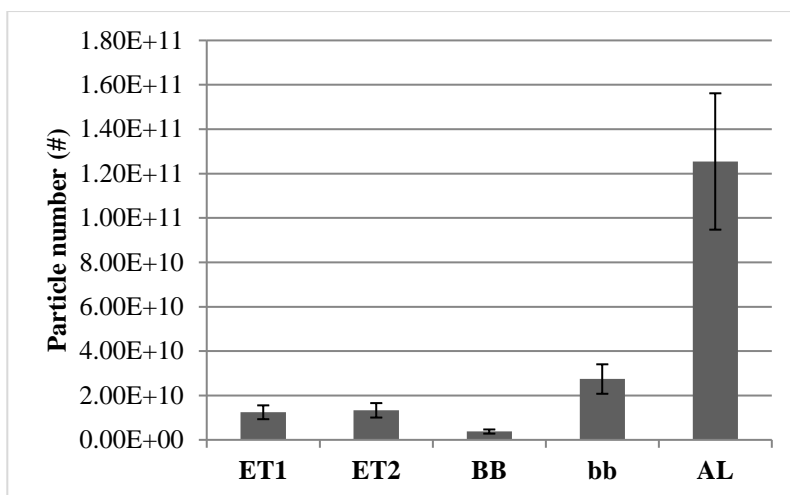


Figure 5.11: Particulate matter dose in the different regions of the human respiratory tract for an adult male, after 45min exposure to Chinese cooking, calculated by the EXDOM dose model. Error bars represent the standard deviation of the three experiments.

5.4.2.3. Respiratory tract dose after exposure to Indian style cooking

On Table 5.7, the total dose and the dose in the five different regions of the respiratory tract are presented. The average dose can be seen on Fig. 5.12.

Table 5.7: Particulate matter dose (#) in the five regions of human respiratory tract the ET1, the ET2, the BB, the bb and the AL after 65min of Indian style cooking.

	ET1	ET2	BB	bb	AL	TOTAL
1st Experiment	1.09E+10	1.18E+10	3.30E+09	2.46E+10	1.11E+11	1.61E+11
2nd Experiment	1.03E+10	1.13E+10	3.14E+09	2.33E+10	1.05E+11	1.53E+11
3rd Experiment	1.07E+10	1.17E+10	3.26E+09	2.42E+10	1.08E+11	1.58E+11

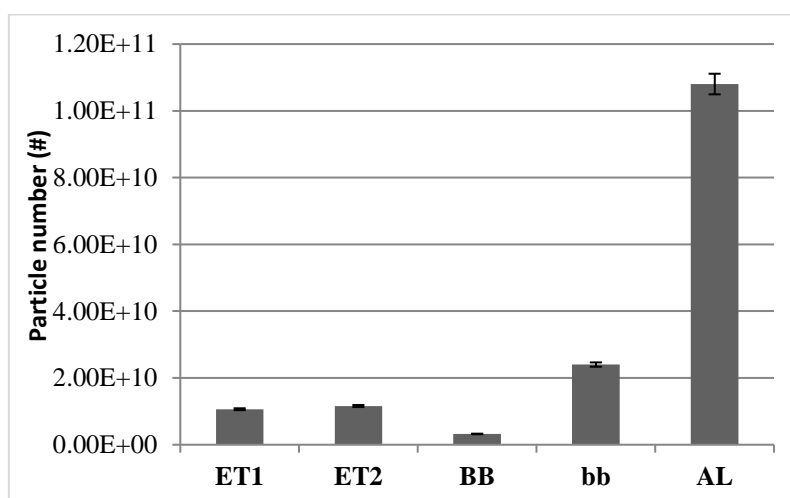


Figure 5.12: Particulate matter dose in the different regions of the human respiratory tract for an adult male, after 65min exposure in Indian cooking, calculated by the EXDOM dose model. Error bars represent the standard deviation of the three experiments.

5.4.2.3. Respiratory tract dose after exposure to African style cooking

Similarly, ExDoM was used to estimate the dose from African style cooking and the dose deposited in the different regions of the RT is presented on Table 5.8 and Fig. 5.13.

Table 5.8: Particulate matter dose (#) in the five regions of human respiratory tract after 95min of African style cooking

	ET1	ET2	BB	bb	AL	TOTAL
1 st Experiment	2.71E+10	2.94E+10	8.23E+09	6.09E+10	2.77E+11	4.02E+11
2 nd Experiment	2.12E+10	2.29E+10	6.45E+09	4.73E+10	2.14E+11	3.12E+11
3 rd Experiment	2.33E+10	2.52E+10	7.06E+09	5.21E+10	2.37E+11	3.45E+11

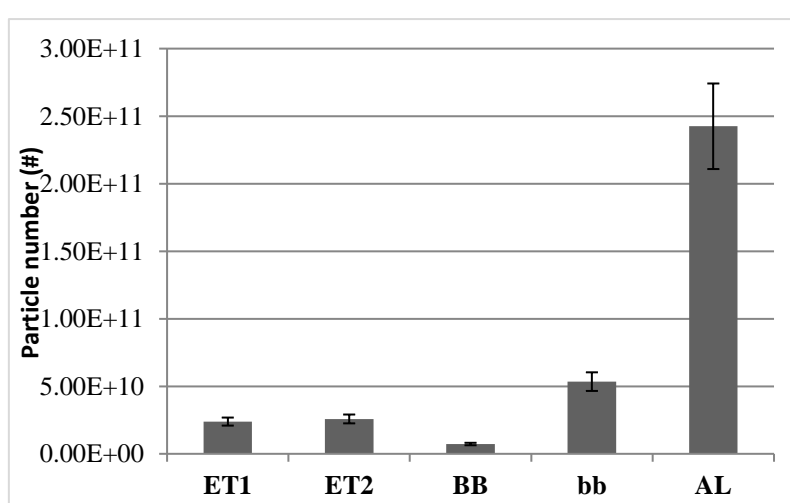


Figure 5.13: Particulate matter dose in the different regions of the human respiratory tract for an adult male, after 95min exposure to African cooking, calculated by the EXDOM dose model. Error bars represent the standard deviation of the three experiments

5.4.2.4. Respiratory tract dose after exposure to West style cooking

The results for the estimated dose after the 1h exposure in West style cooking are showed on Table 5.9 and Fig. 5.16.

Table 5.9: Particulate matter dose (#) in the five regions of human respiratory after 45min of West style cooking

	ET1	ET2	BB	bb	AL	TOTAL
1 st Experiment	1.09E+10	1.18E+10	3.30E+09	2.45E+10	1.11E+11	1.61E+11
2 nd Experiment	1.18E+10	1.29E+10	3.60E+09	2.67E+10	1.21E+11	1.76E+11

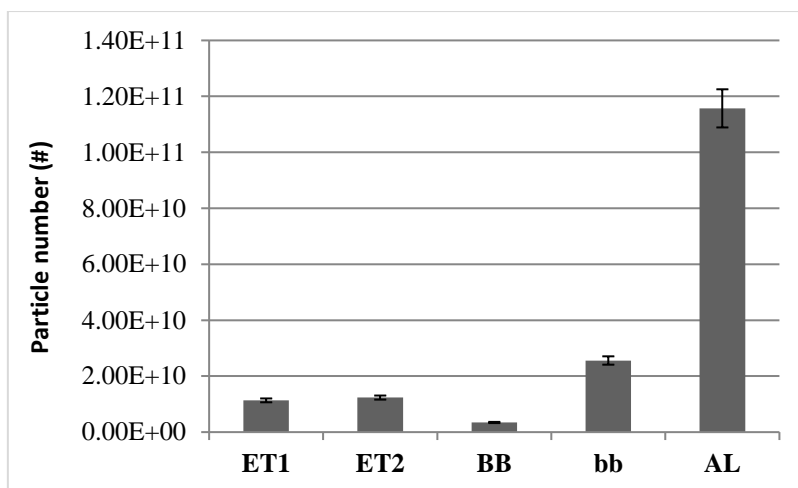


Figure 5.14: Particulate matter dose in the different regions of the human respiratory tract for an adult male, after 45min exposure to West cooking, calculated by the EXDOM dose model. Error bars represent the standard deviation of the three experiments.

5.4.2.5. Respiratory tract dose after exposure to four different styles of cooking and to background concentrations

The dose after 1hour exposure to the four different styles of cooking can be seen on Fig. 5.15. The dose depends on the initial concentration of particles and as the concentration was higher during Chinese stir-frying; the subject receives the highest dose after 1h of cooking Chinese style food. The subject receives the lower dose after 1h of cooking Indian style food and this occurs because the main activity in this cuisine was boiling, which does not increase the particles number concentration as frying does.

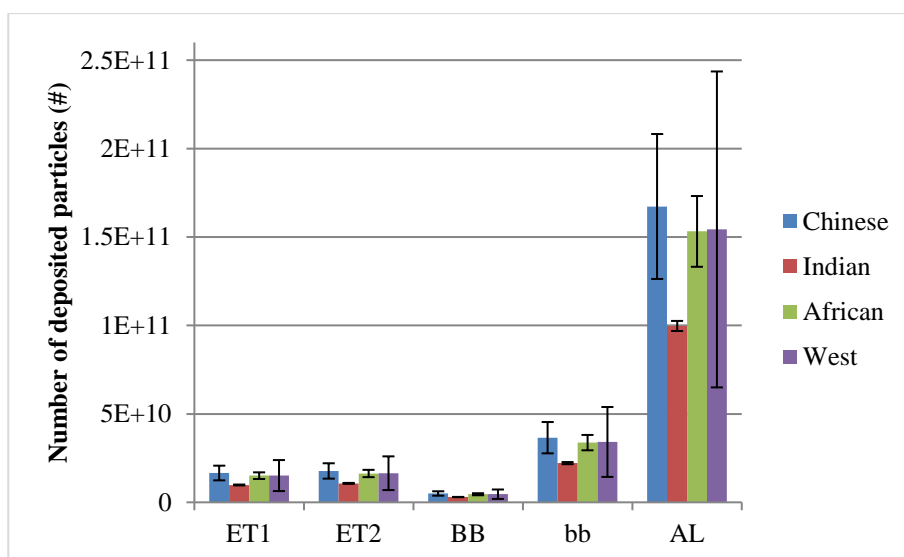


Figure 5.15: Particulate matter dose in the different regions of the human respiratory tract for an adult male, after 1h exposure to four different styles of cooking, calculated by ExDoM2 . Error bars represent the standard deviation of the three experiments.

In order to show the difference between exposure to cooking activities indoors and to background concentrations indoors, ExDoM2 was used to estimate the dose after 1h exposure to background concentrations. As it can be seen on Table 5.10 the total dose after 1h exposure in background concentrations is 2.51×10^3 , much lower compared to 1h exposure in a microenvironment that cooking activity takes place, where the estimated dose ranges from 1.45×10^{11} - 2.43×10^{11} .

Table 5.10: Particulate matter dose in the different regions of the human respiratory tract after 1h exposure to four different styles of cooking and 1h to background concentrations.

	ET1	ET2	BB	bb	AL	TOTAL
Chinese	1.66E+10	1.77E+10	5.00E+09	3.65E+10	1.67E+11	2.43E+11
Indian	9.82E+09	1.07E+10	2.98E+09	2.22E+10	9.97E+10	1.45E+11
African	1.51E+10	1.63E+10	4.58E+09	3.38E+10	1.53E+11	2.23E+11
West	1.51E+10	1.65E+10	4.60E+09	3.41E+10	1.54E+11	2.25E+11
Background	1.78E+08	1.85E+08	5.27E+07	3.74E+08	1.72E+09	2.51E+09

5.5. Results

The personal exposure from cooking in four different styles was examined in Chapter 5, as cooking is one of the most important indoor sources in residences. The effect of the different styles of cooking on the ultrafine particles was analyzed and also the dose after 1h exposure was estimated and compared to 1h exposure in background concentration. The different procedures (boiling, frying, deep frying) affected the overall concentration and the particle number size distributions. During boiling the peak mode of the particles size distribution was at 14.6 nm, while during the frying activity the peak mode was at 30-60 nm. In cases where the frying and the boiling activity were taking place simultaneously the particles size distribution was bimodal. From the application of the dosimetry model ExDoM, it was concluded that the highest concentrations and consequently the highest dose was received during the Chinese style of cooking due to the fact that the main activity was frying in contrast with Indian style of cooking that the main cooking activity was boiling.

6. Chapter 6: Personal exposure and dose to particulate matter inside the subway system of Athens

6.1. Introduction

In big cities, residents spend 4–8% (1–2 h) of their day commuting and as has been pointed out in several studies, during this time they are exposed to high PM concentrations (Nieuwenhuijsen et al. 2007). For this reason, Athens metro was chosen as a microenvironment of interest regarding daily exposure in particles.

In recent years, considerable attention has been paid to the study of air quality in transportation microenvironments and mainly in the underground subway microenvironment, since it is a unique microenvironment. The metro microenvironment is a confined underground space, poorly ventilated, with indoor emission sources, characterized by high PM concentrations rich in chemical elements, which can have implications in human health (Gali et al. 2017), like iron (Fe), total carbon (TC), barium (Ba), copper (Cu), manganese (Mn), chromium (Cr), and zinc (Zn) (Moreno et al. 2017; Martins et al. 2016a). The main sources of particles are the wheels, the rail tracks, and the brake pads (Johansson and Johansson 2003). Moreno et al. (2015) concluded that the majority of the particles in Barcelona metro system were Fe-oxide, mostly hematite (Fe_2O_3) formed from the rapid oxidation of magnetite (Fe_3O_4), and after investigating the oxidative potential of the Fe particles Chillrud et al. (2004, 2005) indicated that the metro microenvironment is the main source of people exposure to Fe, Cr, and Mn particles during non-occupational exposure, with the concentration of these elements to be 100 times higher in subway microenvironments than outdoors (Chillrud et al. 2004). Furthermore, Karlsson et al. (2005) exposed human lung cells to metro particles and concluded that particles in metro microenvironment are eight times more genotoxic and four times more likely to cause oxidative stress in lung cells than outdoor particles.

Athens, like most big cities, is facing an important air pollution problem, characterized by high concentrations of particles, nitrogen dioxide, and tropospheric ozone. The PM_{10} limit values defined by the European Air Quality Directive (2008/50/EC) have been frequently exceeded (Grivas et al. 2008) the last decades, with road transport to be a major source of air pollution in Athens (Fameli and Assimakopoulos 2015; Karanasiou et al. 2007). A high variability is observed across the central and suburban areas of the metropolitan area (Eleftheriadis et al. 2014; Aleksandropoulou and Lazaridis 2016). In order to control air pollution, two main investments were implemented, the metro system in 2000 and traffic control improvements. It is estimated that due to the operation of the two lines of Athens metro, the number of cars entering the city center daily was reduced by 71,000 that corresponds to less 335,000 vehicle-kilometers traveled per day (STASY 2017). The last two decades before the construction of

Athens metro, the percentage of citizens of Athens using public transportation was declining due to the increase of the percentage of private car ownership. A study (Ypeka 2006) which compared pollutant concentration, related with on-road traffic, before (2000) and after 1 year (2001) of the metro operation, concluded that the concentration of carbon monoxide and nitrogen dioxide was reduced by 7% while the concentration of smoke by 5% due to the construction of Athens metro.

Since the annual ridership of Athens metro is 136 million (STASY 2017), the study and the characterization of passengers' exposure in Athens metro microenvironment is essential. The current study is part of an extensive and intensive study for assessing exposure of passengers to aerosols in the metro systems of Athens (Martins et al. 2016b), Barcelona (Martins et al. 2015b, 2016a, b), Prague (Cusack et al. 2015), and Oporto (Martins et al. 2016b). The extensive study includes physical and chemical characterization of the particles (covering sizes from 10 nm to 10 μ m), present in the Athens metro, and employs diverse methods. The current work examines PM₁₀ concentrations in carriages at the two lines of Athens metro and in the platforms of several stations. The objective of this study is to evaluate PM₁₀ concentration levels in the metro and to estimate the exposure and related dose of commuters and metro workers in the Athens metro system.

6.2. Sampling site description – Athens metro

Athens metro started operating in 2000 and it is consisted of two lines, the red and the blue line. It is connected with the partially over ground electric railway (green line) that started operating in 1869. Red line connects the north suburbs of Athens with the city center and the south suburbs of the city. When the operation of this line started in 2000, the line consisted of 7 stations, but nowadays, it is consisted of 20 stations and spans 19.4 km. The line is fully underground. Blue line connects the northeast part of greater Athens with the city center, the northwest part of the city, and the Athens International Airport. When metro started operating, this line consisted of 7 stations, but at the present time, the line consists of 21 stations and spans 39.1 km, the 20.7 km of which are over ground connecting Doukissis Plakentias station with the Athens International Airport. Trains pass every 3–5 min during rush hour and every 5–10 min during non-rush hour and weekends. The one-way trip of both lines is approximately 30 min.

Three generations of trains are being used by both lines of Athens metro (Attiko metro 2017). The first-generation trains have air-forced ventilation. The second-generation trains started operating in 2003 and are equipped with air-conditioning systems. The third-generation trains started operating in 2014 and are fully air-conditioned. All the trains have windows that can be opened by the passengers.

Measurements were performed inside the trains of both lines of Athens metro and on the platforms of several stations. The overground section of the blue line was not sampled during this study since the focus was on the underground part of the metro. During the sampling campaigns, it was noticed that most of the times the windows were open, especially during sampling in first-generation trains that are naturally ventilated, whereas they were mainly closed on the third generation trains that offer better thermal comfort due to the good air-conditioning system. Complementary to the measurements conducted inside the trains, PM_{10} concentrations were measured also on the platforms of several stations.

The stations selected were the terminal stations of both lines, Anthoupoli and Helliniko stations of red line and Aghia Marina and Doukissis Plakentias of the blue line. Sintagma and Omonia stations of the red line were also selected because they are central stations that connect the lines; Sintagma station connects the red with the blue line and Omonia station connects the red line with the electrical railway. According to statistical data, these two stations display the highest passenger numbers; 9.7% of the passengers start their journey from Sintagma station and 5.9% of the passengers from Omonia station (Attiko metro 2017). Two additional stations of the blue line were selected, Ethniki Amina and Katehaki, because these stations are located under heavily trafficked streets and because during the sampling campaigns in the trains, it was noticed that PM_{10} concentrations were increasing significantly at this section of the journey. At the metro stations, there is no heating or cooling system since the platforms and tunnels are located in great depth and the thermal comfort of the passengers is achieved without the use of any mechanical system. Figure 6.1 shows the Greater Athens Area, the two lines of the metro, and the stations where PM_{10} measurements were conducted.



Figure 6.1: Athens metro map.

6.3. Measurement campaigns

PM₁₀ mass concentrations were monitored inside the trains of the Athens metro red and blue line and in several platforms during two campaigns, a 2-week campaign in May 2014 and an intensive 1-week campaign in November 2015. The instruments used in order to measure PM particles during the campaigns were a light-scattering laser photometer TSI DustTrak II Aerosol Monitor 8532 inside the trains and a laser photometer TSI Sidepak Personal Aerosol Monitor AM510 on the platforms. PM₁₀ inlet was used in both instruments, which give real-time aerosol mass concentrations and are designed for the estimation of personal exposure since they are portable. PM₁₀ concentrations were measured along the entire route of both lines and each line was measured 12 times (6 in each campaign). Measurements were carried out at weekdays during rush hours, 08:00–17:30, and especially during the hours that commuters use the metro (8:30, 14:30, and 17:00), except two measurements that were carried out during weekend. The measurements were conducted in the central carriage; the trains consist of six carriages and either carriage 3 or 4 was being selected. Zero calibration of the instruments was performed before each measurement. During the measurements, a timer and a voice recorder were used in order to record the exact location (station) of the train and when the doors of the train were opening, with the aim to study how the opening of the doors influences PM₁₀ concentrations. Furthermore, the time resolution used was 1 s. Fluctuations of PM₁₀ concentrations observed on the instruments' screen, the number of passengers, if the windows were open in the carriage,

and any other important factor that could influence particle concentration were recorded. On the platforms, the measurements were conducted in the middle of the platform but not close to the stairs, and the duration of each measurement was 15 min.

Furthermore, measurements of PM₁, PM_{2.5}, and PM₁₀ were conducted with a TSI DustTrak DRX during the campaign in May 2014 on a fixed site on a subway platform of blue line (Nomismatokopio) for variable measurement periods. This station is located at a high trafficked street. The TSI DustTrak DRX used on the fixed site at Nomismatokopio station was calibrated against gravimetric measurements conducted on the platform during the sampling campaign on May 2014 by NCSR Demokritos. PM₁₀ samples were collected on Teflon filters using a low-volume sampler (LVS, model SEQ 47/50, Leckel). In total, 18 filter samples were collected, one per day, with variable measurement periods that ranged from 5 to 19 h (total of metro working hours) each.

That resulted in a calibration curve of :

$$[\text{Corrected PM}_{10} \text{ concentration}] = 0.47 \times [\text{DustTrak DRX PM}_{10} \text{ measurement}] + 14.27, \\ R^2=0.69.$$

The calibration factors for TSI Sidepak and TSI DustTrak II were adjusted for the underground aerosol type by calibrating both instruments with the DustTrack DRX.

6.4. Dose calculation

A main objective of this study is to determine the deposited dose and the retention of particles deposited in the respiratory tract of people exposed to the Athens metro microenvironment. In order to calculate the deposition, dose, and retention of aerosol particles in the RT, the GI tract, and their absorption to blood, the exposure and assessment model, ExDoM2, was implemented. An analytical description of ExDoM2 is reported at Chapter 2 and at Chalvatzaki and Lazaridis (2015) and Aleksandropoulou and Lazaridis (2013).

The present work focus on the calculation of dose of three different subjects, one person commuting to work by metro and exposed to the metro microenvironment for 1 h per day, one person working in the metro having a sedentary employment (e.g., metro driver) and exposed 9 h per day in the metro microenvironment (8-h working and 1-h commuting), and one metro worker with light exercise activity (e.g., metro track maintenance workers). An individual's exposure depends mainly on the air quality of the microenvironments visited per day (Woodrow et al. 2016). All subjects selected were considered to be adult males, non-smokers, nose breathers, and citizens of Athens who commute to work by metro. With the purpose of estimating the daily dose, a realistic exposure scenario was chosen for the subjects. In order to

choose a realistic scenario, the USEPA Exposure Factors Book (2011) that suggests an activity pattern for people spending their day in three main microenvironments (indoors, outdoors, and in transportation) was consulted. It was assumed that all the subjects selected (commuter and metro workers) spend 10-h indoors resting, 8-h indoors doing sedentary work (or light exercise in the case of the one metro worker subject), 3-h indoors doing light exercise (personal care and household activities are considered light exercise), 2-h outdoors doing light exercise, and 1-h commuting (50 min in trains and 10 min in platforms). Detailed timetable of the subjects and the type of activity in each microenvironment can be seen in Table 3. Commuting by metro was considered a light exercise activity. According to USEPA Exposure Factors Book (2011), activities like driving a car are defined as sedentary activities; thus, metro drivers were considered to have a sedentary occupation.

The focus of this study is on the dose received in the metro microenvironment, and thus, it was assumed that the rest of the day the subject is exposed to indoor environments without indoor sources. The average annual PM₁₀ concentration of the urban traffic and background stations (YPEKA 2015) in Athens in 2015 was used as outdoor concentration. In order to calculate the indoor particle concentration, an average indoor/outdoor ratio for naturally ventilated buildings in the absence of indoor sources was used. Morawska and Salthammer (2003) concluded that, for naturally ventilated buildings in the absence of indoor sources, I/O ratios for PM₁₀ ranged from 0.5 to 0.98, and in the current study, an average ratio 0.75 was adopted. The mass median aerodynamic diameter (MMAD) of the fine particles in the metro microenvironment was considered 1.7 µm with a geometric standard deviation (GSD) of 2.1 (Martins et al. 2015a), and the MMAD of the coarse particles was considered 5 µm with a GSD of 2.5. Taking into consideration the measurements of the DustTrak DRX conducted on the platform of Nomismatokopio station, 86% of the particles were on the fine fraction. The density of the particles inside the metro microenvironment was considered 2.2 g/cm³ (Martins et al. 2015a). The size distribution characteristics used in the calculations in the rest of the microenvironments were based on the measurements conducted by Karanasiou et al. (2007) in Athens. The MMAD of the fine particles was considered 0.39 µm with a geometric GSD of 2.02 and the MMAD of the coarse particles was considered 2.77 µm with GSD of 1.73, with 62% of the particles being on the fine fraction. The density of the particles outdoors and in the other microenvironments was considered 1.5 g/cm³. The particles were considered spherical (shape factor 1) in all the microenvironments (Martins et al. 2015a; Sánchez-Soberón et al. 2015).

6.5. Results

6.5.1. PM₁₀ concentrations inside trains

PM₁₀ concentration measurements were conducted inside the trains of both lines. Particle concentration was measured for six entire routes in each direction. The overall measurements results are summarized in Table 6.1. Observed PM₁₀ concentration ranged from 97.2 to 181.3 µg/m³ in the red line with average journey concentration 132.2 ± 34.0 µg/m³. Similar concentrations were observed in the blue line and the average journey PM₁₀ concentration was 138.0 ± 35.6 µg/m³.

Table 6.1: Summary of PM₁₀ concentrations inside the trains, average, standard deviation, and maximum and minimum values

Metro line	PM ₁₀ concentration (µg/m ³)			
	Average	Standard deviation	Maximum	Minimum
Red line (10 journeys) ^a	132.2	34.0	181.3	97.2
Blue line (12 journeys)	138.0	35.6	212.5	95.6

^aThe two weekend measurements are excluded

During the journeys, PM₁₀ concentrations displayed on the instrument's screen were carefully observed and all the significant variations were recorded. The average PM₁₀ concentrations observed in the red and blue lines during the campaigns in May 2014 and November 2015 and the average weekend concentration can be seen in Fig.6.2. Higher concentrations were detected during the measurements conducted in May 2014. The main difference between the two different campaigns, where the average PM₁₀ concentration of the May 2014 campaign was higher by a factor of 1.5, is that at the campaign of November 2015, measurements were conducted only on third-generation trains, which are fully air-conditioned and most of the windows are kept closed. Air-conditioning system can attribute to the decrease of particle concentration in the metro cabins (Martins et al. 2015b). Higher PM concentrations on trains with open windows show that a major source of particles inside the trains is the air exchange between the tunnels and the carriages. Two journeys of red line were monitored during the weekend in order to examine potential differences in PM concentrations, in relationship with the weekdays. During the weekend measurements, the trains' ridership and the trains' frequency were lower than weekdays. It was observed that the concentrations were significantly lower and that there were not many fluctuations along the journey. This fact indicates that passengers' movement inside the carriages that causes resuspension of the settled dust and train frequency are major factors affecting the PM concentration inside the trains. Furthermore,

during the weekend, the outdoor traffic within the city is lower, fact that may affect the urban background PM₁₀ levels and as a result the PM₁₀ levels in the metro. It should be taken into consideration that the weekend measurements took place in the fully air-conditioned, third-generation trains.

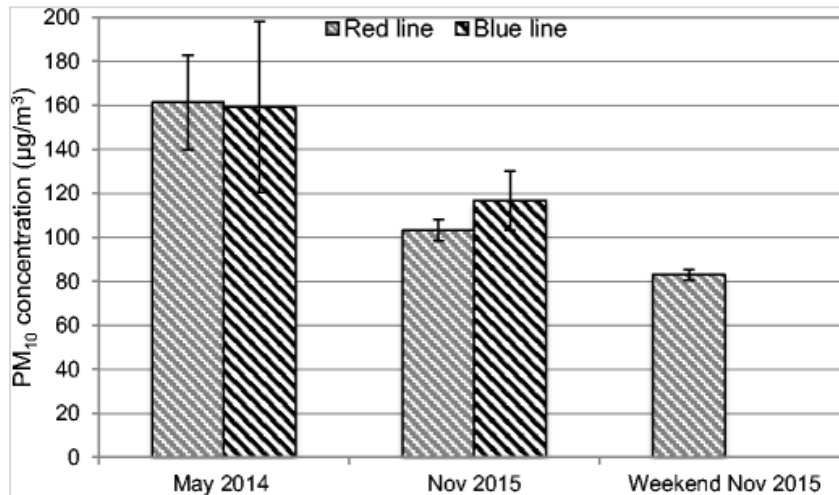


Figure 6.2: Average PM₁₀ concentrations in the red and blue lines during the campaigns in May 2014 and November 2015 and average weekend concentration.

Figure 6.3 shows the range of PM₁₀ concentrations, the average, median, maximum, and minimum values, inside the trains on the stations (stops) along the journey of red line. The weekend measurements were not taken into account. The maximum average value, 166.3 µg/m³, was recorded when the train approached Sigrou-Fix station and the lower, 92.2 µg/m³, at Helliniko station. Sigrou-Fix station is located under a densely trafficked street in the center of Athens, and as result, the background levels in the metro are elevated. In addition, the stronger curvature in the railway causes more friction and enhances the wear of the rails and the wheels, Higher PM₁₀ concentrations were observed in the sections of the line with higher curvature, like Attiki station and the section Neos Kosmos–Sigrou-Fix. The fresh air is supplied in the tunnels from blast shafts, and the majority of these blast shafts are located close to the stations. As a result, PM concentrations in the metro areas are affected by the outdoor PM concentrations. At the beginning of the journey, PM₁₀ concentrations were low and were increasing gradually and reach the maximum values when the train was located at the central stations, where the train is more crowded with passengers. In the section of the red line (Fig. 6.3) that started operating in 2000, Dafni-Sepolia, concentrations were higher with Aghios Antonios and Aghios Dimitrios stations that started operating in 2004, following. The rest of the stations started operating in 2013, and the concentrations were significantly lower in these sections of the journey.

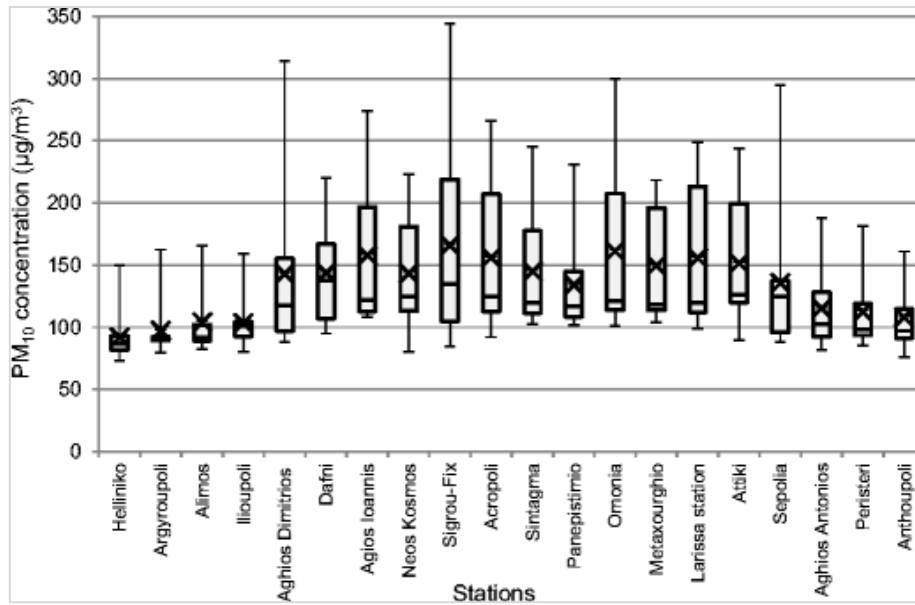


Figure 6.3: PM₁₀ concentrations inside the trains in the stations of red line. The central box presents the values between the 25th (lower part) and the 75th (upper part) percentiles. The *whiskers* show the maximum and minimum values, the horizontal line in the box constitutes the median value, and the cross symbols the average value.

The range of PM₁₀ concentrations, the average, median, maximum, and minimum values, inside the trains on the stations along the journey of blue line are depicted on Fig. 6.4. In the blue line, all the real-time measurements in the carriages were conducted in first- and second-generation trains, in which the windows are mostly kept open (on first-generation trains always open), and as a result, the internal concentrations were affected by the concentration of particles in the tunnels. At the older section of blue line Ethniki Amaryna–Monastiraki (started operating in 2000), PM₁₀ concentrations were higher compared to the section passing from the newer stations like Aghia Marina (started operating 2013). Guo et al. (2014) also reported higher concentrations in the older metro lines of Shanghai. This observation shows that inside the trains, when the windows are open, the particle concentration is affected mainly by the exchange of air between the train and the tunnels, which are areas poorly ventilated. Furthermore, elevated concentrations were also observed at the section Katehaki-Panormou-Ampelokipi, where the curvature of the railway is higher. The enhanced wearing of the wheels, the brake pads, and the rails increases the PM₁₀ concentrations in the tunnels and as a result in the trains due to the penetration of particles through the open windows. It was observed that when the trains accelerate in the tunnels, after leaving a station, PM₁₀ concentrations were increasing significantly. In some cases, concentrations increased by 50 µg between two stations. The acceleration of the train causes intense airflow in the tunnels that lead to resuspension of the dust settled. The increase continues, while the train is braking in order to stop at a station and starts decreasing when the train doors open. Braking of the trains is a source of particles in the metro microenvironment. Particles are generated from the friction of the wheels on the train

tracks and the wear of brakes (Nieuwenhuijsen et al. 2007). After the arrival at a station and the opening of the doors, PM₁₀ concentrations decreased in the majority of cases. In Fig.6.4 , the real-time PM₁₀ concentrations (time resolution 1 s) during an eastbound journey of blue line are demonstrated. The grey shaded bars depict the seconds that the metro doors were open. In the majority of the stops, the opening of the doors led to a decrease on PM₁₀ concentrations, with the decrease to be proportional to the seconds the doors remained open. The contrary phenomenon was observed at stations where the platforms were crowded, and many people left and entered the train. The movement of the passengers in the train, causing resuspension and dispersion of the settled particles, led to an increase of the concentrations in these cases. Furthermore, increase of the particle concentration because of the opening of the doors was observed at stations that PM₁₀ concentrations are high on the platforms, like Katehaki station (Fig. 6.4 and Table 6.2).

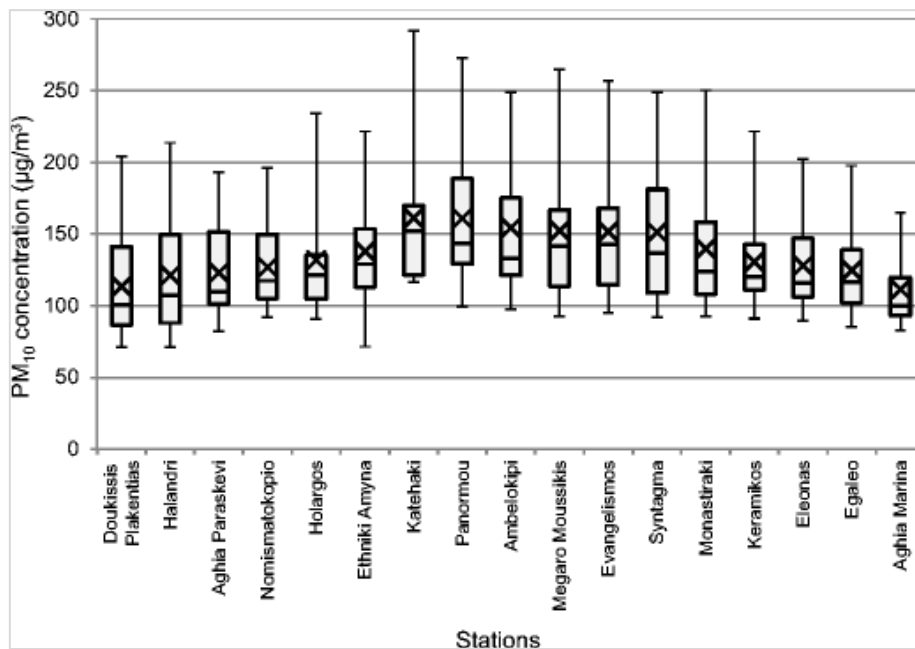


Figure 6.4: PM₁₀ concentrations inside the trains in the stations of blue line. The central box presents the values between the 25th (lower part) and the 75th (upper part) percentiles. The whiskers show the maximum and minimum values, the horizontal line in the box constitutes the median value, and the cross symbols the average value.

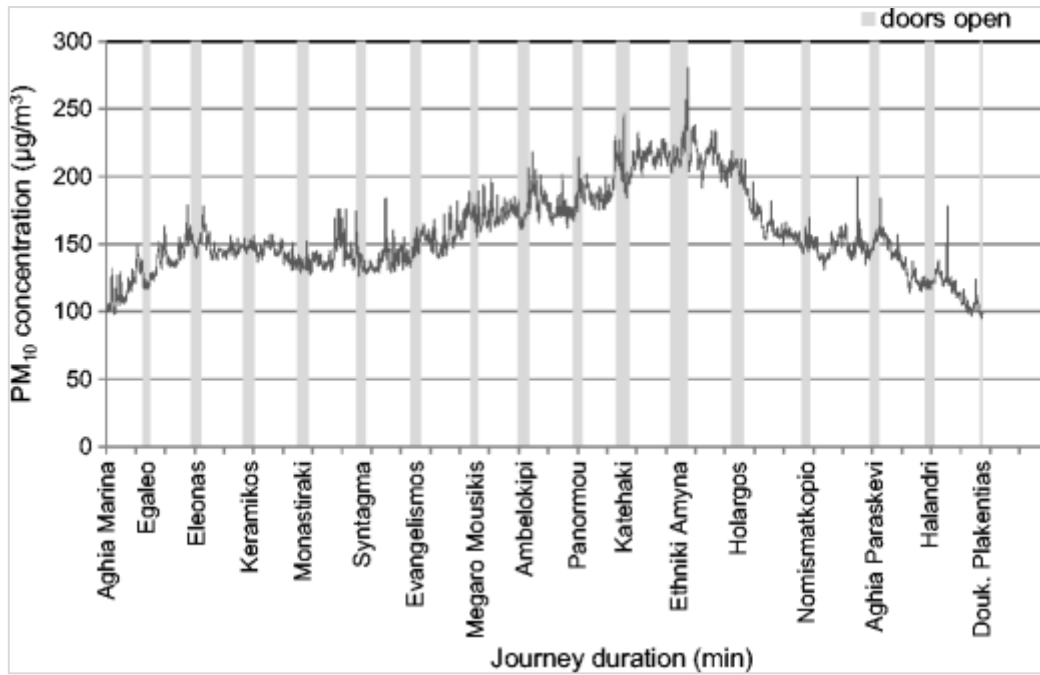


Figure 6.5: Real-time PM₁₀ concentration during an eastbound journey of blue line (time resolution 1 s); grey bars depict the period of the doors opening.

High particle concentrations have been reported by several studies around the world, that conducted measurements both inside metro carriages and platforms, including those in Athens (Barnarparesos et al. 2016), Barcelona (Martins et al. 2015b), Budapest (Salma et al. 2007), Helsinki (Aarnio et al. 2005), London (Adams et al. 2001), Los Angeles (Kam et al. 2011), Lisbon (Ramos et al. 2016), Naples (Carteni et al. 2015), New York (Wang and Gao 2011), Rome (Perrino et al. 2015), Prague (Cusack et al. 2015), Shanghai (Guo et al. 2014), Seoul (Kim et al. 2008), Taipei (Cheng et al. 2012), and Tehran (Kamani et al. 2014). Among these studies, higher concentrations inside the trains were observed in the metro of Seoul (Kim et al. 2008) and London (Adams et al. 2001), with average PM₁₀ concentration equal to 312 and 247 µg/m³, respectively.

Figure 6.6 presents a comparison of the average particle concentration inside metro carriages between the current study and other studies conducted in metro systems around the world. Average PM₁₀ concentration measured in Athens metro (135 µg/m³) is close to Naples' (Carteni et al. 2015) and Rome metro (Perrino et al. 2015) results where the average concentrations were 128 and 158 µg/m³, respectively. Athens average PM₁₀ concentration was significantly lower by a factor more than 2 compared to Seoul (Kim et al. 2008), where the average PM₁₀ concentration was 186 µg/m³. Among the studies in metro systems around the world, there are significant variations in the particle concentrations reported due to many factors, like the age of the metro system, the depth, the type of ventilation, the material of the wheels, the braking system, the measuring period (season and time), the measurement

equipment, and the correction or not of the values taken from the online instruments against gravimetric measurements. Athens metro is a relatively newer system and this can be a main factor of having lower PM concentrations. In the London subway system (Adams et al. 2001), which is one of the oldest metro systems, the higher PM_{2.5} concentrations were observed, 247 µg/m³.

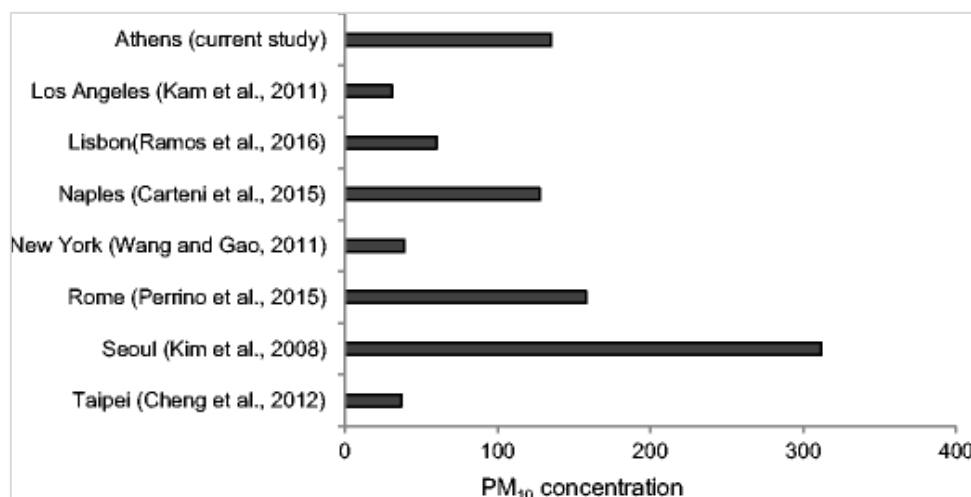


Figure 6.6: Comparison of PM concentrations inside metro carriages between the current study and other studies conducted in metro systems around the world.

6.5.2. PM₁₀ concentrations on platforms

The overall results from the 15-min PM₁₀ concentration measurements conducted on the platforms are summarized in Table 6.2. The average PM₁₀ concentrations ranged from 85.1 ± 12.3 µg/m³ at Helliniko platform in red line to 230.2 ± 102.0 µg/m³ at Sintagma platform in the blue line. The maximum concentrations were observed at Ethniki Amynta and Sintagma stations, 347.7 and 298.4 µg/m³, respectively. The lower PM₁₀ concentrations were detected at Anthoupoli and Helliniko stations, 100.4 and 110.1 µg/m³, respectively, which are the terminal stations of red line.

Lower PM₁₀ concentrations were observed at the terminal stations of both lines, and this can be attributed to the lower ridership in these stations in relationship with stations located in the center of Athens. According to statistical data (STASY 2017), 9.7% of the metro users start their journey from Sintagma station and 5.9% from Omonoia station, while 3.6% from Douk. Plakentias station (terminal station of blue line). Furthermore, the terminal stations are in the suburbs of Athens where the outdoor PM concentration is lower than in the city center. Higher concentrations were detected in the stations located in the center of Athens, where the stations are more crowded, older, and the outdoor PM concentrations are higher, like in Sintagma and Omonia stations and at stations located under densely trafficked streets like Katehaki station.

At the sections of the journey that observed higher concentrations in the trains, the concentrations on the platforms were higher.

Table 6.2: Summary of PM₁₀ concentrations at stations (platforms), average, standard deviation, and maximum and minimum values.

PM ₁₀ concentration (µg/m ³)					
Station	Line	Average	Standard deviation	Maximum	Minimum
Sintagma	Blue	230.2	102.0	298.4	217.5
Ethniki Amyna	Blue	175.3	72.5	347.7	108.1
Katehaki	Blue	133.8	13.1	175.1	106.5
Doukissis Plakentias	Blue	129.4	57.9	204.0	87.9
Aghia Marina	Blue	95.3	8.0	116.3	84.8
Omonia	Red	179.6	51.6	248.7	89.9
Anthoupoli	Red	90.9	10.5	100.4	77.4
Helliniko	Red	85.1	12.3	110.1	75.7

Among the studies that have been conducted in metro stations around the world, the highest PM₁₀ concentrations in metro platforms were reported in the study of Perrino et al. (2015) on the metro of Rome, where average PM₁₀ concentration was equal to 409 µg/m³ and in the study of Kim et al. (2008) on the metro of Seoul, where the average PM₁₀ concentration measured was equal to 359 µg/m³. In the majority of the studies conducted in metros, particle concentration was significantly higher in the metro microenvironment than outdoors. Salma et al. (2007) reported concentrations 5 to 20 times higher in the metro of Budapest compared to outdoors.

Particle concentrations measured in metro systems around the world are presented in Fig. 7. Current study's PM₁₀ concentrations on platforms are close to the Budapest's study (Salma et

al. 2007). Among the studies compared, higher PM10 concentrations on platforms were observed in Rome $409 \pm 22 \mu\text{g}/\text{m}^3$ (Perrino et al. 2015), and in Seoul, $359 \mu\text{g}/\text{m}^3$ with values range from 238 to $450 \mu\text{g}/\text{m}^3$ (Kim et al. 2008). Important aspect in the comparison of particle concentrations on platforms between different metro systems, except the aspects mentioned already in the comparison of concentrations in trains, is the station selected. In many studies, measurements were conducted only in central stations with high ridership, like Sintagma station (average PM10 concentration $230.2 \mu\text{g}/\text{m}^3$). In this study, particle concentrations were measured both in central and suburban stations. As a result, the overall average concentration is lower. The average PM10 concentration on the platforms of Athens metro with high ridership was $169.7 \mu\text{g}/\text{m}^3$.

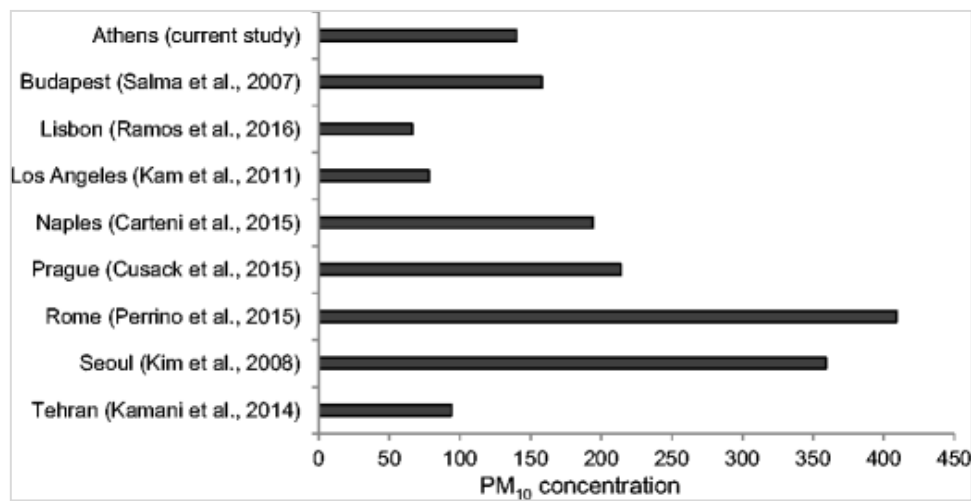


Figure 6.7: Comparison of PM concentrations on platforms between the current study and other studies conducted in metro systems around the world.

6.5.3. Dose calculation

The influence of metro microenvironment in the daily exposure of people using metro to commute and metro workers is examined in the current study. Table 3 presents the activity pattern, the hourly average PM10 concentration, the microenvironments, and the type of activities of the studied subjects. The yearly average PM10 concentration of the Athens' urban traffic and background stations in 2015 was used as PM10 exposure concentration for outdoor microenvironments and multiplied by 0.75 (I/O ratio; Morawska and Salthammer (2003)) for indoor microenvironments. It was considered that the subjects commute by metro 1 h per day, spending 10 min waiting in platforms and 50 min traveling in the trains. The average entire journey PM10 concentration of the two lines was $135.1 \mu\text{g}/\text{m}^3$, and the average PM10 concentration on platforms (taking into account only the stations with the high ridership) was $169.7 \mu\text{g}/\text{m}^3$. Depending on the time spent in each microenvironment, the calculated exposure concentration for commuting was $140.9 \mu\text{g}/\text{m}^3$. The average entire journey PM₁₀ concentration $135.1 \mu\text{g}/\text{m}^3$ was used as exposure concentration for the employees during

working hours. This exposure concentration could be considered worst-case scenario, in the case of metro workers like train drivers since the drivers spend most of the time in the concourses, where there is no resuspension from passenger's movement. Based on the measurements performed using the TSI DustTrak DRX at Nomismatokopio platform, the PM_{2.5}-to-PM₁₀ ratio was 0.86. This value was used as fine fraction in order to estimate the dose with ExDoM2. Similar PM_{2.5}-to-PM₁₀ ratios were found by Ramos et al. (2016) (0.82 Lisbon metro), Park and Ha (2008) (0.80 Seoul metro), Kam et al. (2011) (0.79 Los Angeles metro), and Cheng et al. (2012) (0.77 Taipei metro).

Table 6.3: Daily time-activity pattern, PM₁₀ exposure concentrations, microenvironment, and activity level [resting (rest.), sedentary activity (sed. act.), light exercise (light ex.)].

	PM ₁₀ exposure concentration (µg/m ³)		Microenvironment		Type of activity	
	Commuters	Metro workers	Commuters	Metro workers	Commuters	Metro workers
00:00–07:00	27.5		Home		Rest.	
07:00–08:00	27.5		Home		Light ex.	
08:00–8:30	36.6		Outdoors		Light ex.	
08:30–09:00	137.5		Metro (train & platform)		Light ex.	
09:00–17:00	27.5	135.1	Office	Metro	Sed. act.	Sed.act//light ex.
17:00–17:30	137.5		Metro (train & platform)		Light ex.	
17:30–20:00	36.6		Outdoors		Light ex.	
20:00–22:00	27.5		Home		Light ex.	
22:00–00:00	27.5		Home		Rest.	

The exposure and assessment model ExDoM2 was used in order to evaluate the dose from the exposure in the metro microenvironment for a commuter, a metro worker with sedentary occupation, and a metro worker with light exercise activity. Among the three different subjects, the highest dose is deposited in the respiratory tract of the metro worker with light exercise occupation, since the dose is proportional to the exposure concentrations and depends also on the inhalation rate. Comparing the total daily dose of commuter and metro workers, the daily dose of a metro worker with sedentary occupation is higher by a factor of 1.7 and of a metro worker with light exercise occupation by a factor of 3.6. The results obtained by Grass et al.

(2010), who examined the particle dose of metro workers, suggested that train operators/drivers and platform cleaners are exposed in lower concentrations than metro track maintenance or construction workers. Metro drivers' work can be characterized as sedentary work, whereas other occupations in the metro microenvironment can be characterized as light exercise activities. Kim et al. (2008), who studied the exposure of metro workers by measuring particle concentrations both in workers' activity areas and in passengers' activity areas, concluded that the drivers' PM₁₀ exposure is lower by a ratio 0.87 from the passengers' exposure, while the exposure in PM_{2.5} is almost equal. The higher PM₁₀ concentration in the passenger carriages probably is result of the resuspension occurring due to the movement of the passengers.

In Fig.6.8 , it is shown that the highest deposition in the respiratory tract occurs at the ET1 (46.3% for the commuter, 44.2% for the metro worker, and 50.8% for the metro worker with light exercise occupation) with ET2 (24.9% for the commuter, 23.8% for the metro worker, and 27.4% for the metro worker with light exercise occupation) and AI (22.1% for the commuter, 24.9% for the metro worker, and 16.7% for the metro worker with light exercise occupation) following, while the lowest dose is received by the tracheobronchial (BB and bb) region. Retention of particles in the RT and the amount of material transferred to the GI tract and absorbed into blood are presented in Fig.6.9 From the particles deposited on the RT, 46.4% in the case of commuter, 44.5% in the case of worker with sedentary occupation, and 36.9% in the case of metro worker with light exercise occupation remained in the RT. Due to the high deposition of particles in the extrathoracic region of the RT, the greatest amount of particles is transferred to the GI tract (41.6% for a commuter, 40.4% for a metro worker with sedentary occupation, and 51.0% for a metro worker with light exercise occupation).

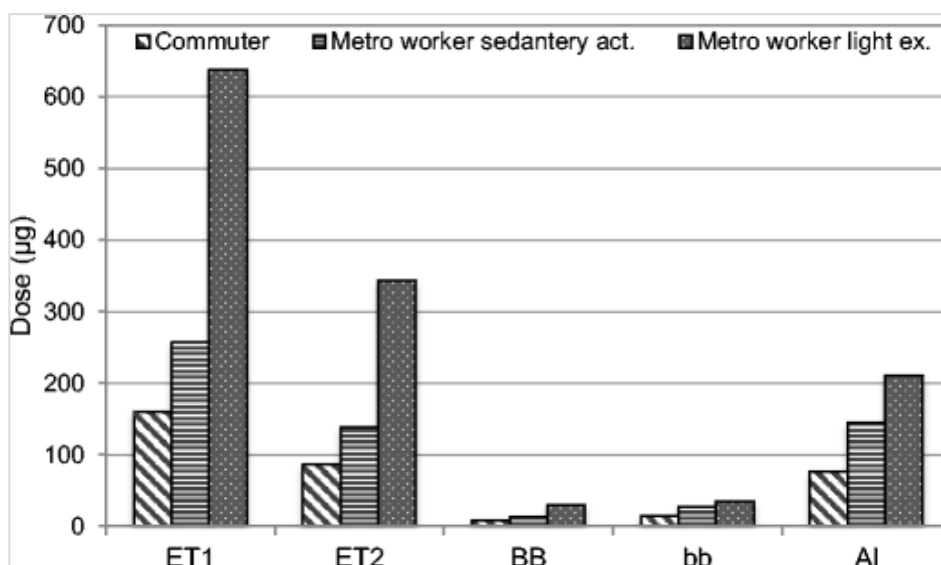


Figure 6.8: Particulate matter 24-h dose in the different regions of the human respiratory tract for a commuter, a metro worker with sedentary occupation, and a metro worker with light exercise occupation.

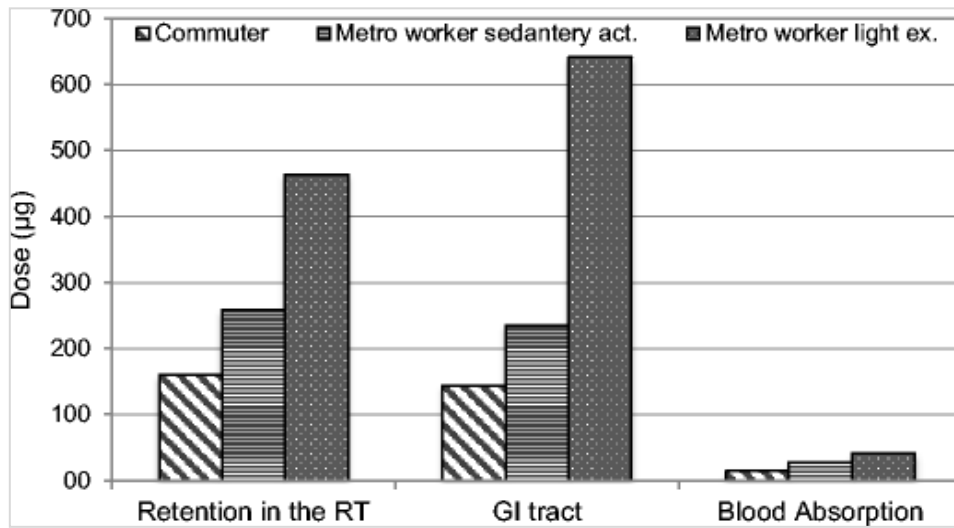


Figure 6.9: Retention of particles in the RT, the amount of material transferred to the GI tract and absorbed in blood after 24-h exposure of a commuter, a metro worker with sedantery occupation, and a metro worker with light exercise occupation.

In Table 6.3 , the dose in the respiratory tract after 1-h exposure in different microenvironments, the total dose, and the dose fraction in each microenvironment are presented. The dose in the RT after 1-h commuting by metro (light exercise activity level) is 125.4 µg, dose that corresponds to 36.3% of the total daily dose of a commuter that has sedentary occupation in indoor environment. This result is the worst-case scenario as it was considered that there were no indoor sources in the office and home microenvironment. However, it shows the important contribution of 1-h exposure in high concentrations to the daily dose. Martins et al. (2015a) concluded that commuting by metro contributes 47% in the total daily dose, corresponding to 36 µg per day.

Table 6.4: Dose in the respiratory tract after 1-h exposure in different microenvironments, total daily dose, time fraction, and dose fraction in each microenvironment for the three different subjects.

Micro-environment	Dose after 1-h exposure (µg)	Total daily dose (µg)	Time exposure fraction	Dose fraction for commuter	Dose fraction for metro worker (sedentary activity)	Dose fraction for metro worker (light exercise)
Home	8.8	114.75	55.0%	33.2%	19.8%	9.1%
Outdoor	27	54	8.0%	15.6%	9.3%	4.3%
Metro	125.4	125.4	4.0%	36.3%	21.6%	10.0%

Workplace (sedentary activity)	6.4	51.2	33.0%	14.8%	–	–
Metro as workplace (sedentary activity)	35.8	286.4		–	49.3%	–
Metro as workplace (light exercise)	120.23	961.8		–	–	76.6%

6.6. Conclusions

Two sampling campaigns were conducted, in May 2014 and November 2015, inside the trains and in several platforms of Athens' metro. The objective of this study was to estimate the exposure and consequent dose of commuters and metro workers. PM₁₀ concentrations were relatively high both in trains and in platforms, compared to the daily limit set by European Air Quality Directive (2008/50/EC) for outdoor environments. The PM₁₀ EU limit is not applied indoors but can serve as guideline for studying the human health risk from air pollution. Taking into consideration that during measurements in the fully air-conditioned, third-generation trains, the concentrations were lower, compared to trains where the windows were open, it was concluded that major source of particles inside the trains is the air exchange between the trains and the tunnels. Therefore, in order to reduce passengers' PM₁₀ exposure inside the trains, the windows should be kept closed on the second- and third-generation trains, which are equipped with air-conditioning system. In this way, the penetration of PM from the tunnels will be avoided and the air-conditioning system, which is equipped with filters, will work efficiently and filter the air in the carriages. In measurements conducted during the weekends, when the train frequency is lower, the trains are not crowded, and the outdoor particle concentration is lower, PM₁₀ concentrations were significantly lower than weekdays. The opening of the train doors at the stations, in the majority of cases, decreased the internal concentrations. The opposite phenomenon was observed only in stations with high particle concentration and when many passengers were leaving/entering the carriage. Higher concentrations were observed in the section of the journeys and platforms that are located in the center of Athens, under heavily trafficked streets and in curved railway sections. The air supplied to the tunnels through the ventilation shafts will have higher PM concentration in highly polluted areas in comparison

with the air supplied to the tunnels located in the suburbs. An exposure and dose assessment model, ExDoM2, was used in order to calculate the deposition, dose, and retention of aerosol particles in the RT, the GI tract, and their absorption to blood for a commuter, a metro worker with sedentary occupation, and a metro worker with light exercise occupation. Highest dose was deposited in the RT of the metro worker with light exercise occupation due to the fact that dose depends on the exposure concentrations and inhalation rate. The highest deposition occurred in the extrathoracic region of the RT. After 1 day of exposure, the highest amount of particles was transferred to the GI tract. Even though commuters spend a short fraction of the day in the metro, the metro microenvironment contributes highly in the total dose. In the current study, the contribution of 1-h metro exposure in the total daily dose of a subject exposed to indoor microenvironments without indoor sources was 36.3%.

The results of the current study show the importance of studying the air quality in microenvironments, like metros where a big proportion of the population is exposed daily. Air quality studies in combination with dosimetry models assist to calculate the human exposure and dose and to identify the health risks in order to protect the public health. This kind of studies can be used as a tool in order to take effective policy measures with the aim to reduce human exposure in aerosols.

Chapter 7: Personal Exposure and Dose of Inhaled Ambient Particulate Matter Bound Metals

7.1. Introduction

Air pollution is increasing as urbanization and industrialization processes expand worldwide. As a result, the levels of particulate matter are elevated in big cities and due to human activity they are enriched with heavy metals. Many epidemiological studies (Pope, 2000; Brunekreef, 2005; Davidson, 2005) studied the risk of health impacts of particulate matter to human health.

Accumulation of particulate matter compounds, like heavy metals, to human organs is related with the cause of serious diseases (Jarup, 2003). In the urban atmosphere many heavy metals bound with particulate matter are present. The current study focus on toxic metals associated with ambient particulate matter such as lead (Pb), cadmium (Cd) and arsenic (As). Many studies focus on these metals because Pb, Cd and As are in the list of the ten chemicals of major public health concern (WHO, 2010), Pb is characterized as possibly carcinogenic to humans (WHO, 2006), Cd is characterized as carcinogenic to humans (WHO, 2006) and As associated with an increased risk of cancer (Chiou et al., 1995). These three heavy metals can be characterized as being road-specific, so high concentrations of them are found in big cities (Hildemann et al., 1991). Moreover, the major part of these metals is in the fine mode (Espinosa et al., 2001; Samara et al., 2005; Pérez et al., 2008).

The objective of this study is to determine the deposition of heavy metals in the human body from the inhalation of particle-bound metals, which are present in the atmosphere. The exposure model Exposure Dose Model (ExDoM; Aleksandropoulou and Lazaridis, 2013) is used for the estimation of the deposited dose and retention of aerosol particles-bound metals (Pb, Cd, As) in the respiratory tract (RT) of human body and a pharmacokinetic PBPK model (Chalvatzaki et al., 2014; Chalvatzaki et al., 2015) is also applied to estimate the movement of metals from the blood into the tissues as a blood-flow-limited model.

7.2. Cities under study

In order to estimate the exposure of residents of different European cities to atmospheric particle-bound metals, data from five different studies were evaluated. The studies selected from the literature meet the following criteria: (1) the studies had to be performed at big European cities and in different geographical parts of Europe; (2) The studies had to include not only the chemical composition of particulate matter, but also the size distribution of the heavy metals analyzed, in order to determine their deposition fraction in different parts of the human respiratory tract. The studies that were selected took place in Athens (Karanasiou et al.,

2007), Rome (Canepari et al., 2008), Seville (Álvarez et al., 2004), Frankfurt (Zereini et al., 2005) and Zabrze (Rogula- Kozłowska et al., 2013).

Athens, the capital of Greece, is a densely populated city of about 4 million residents with some industries in its greater metropolitan area. The measurements (Karanasiou et al., 2007) were performed from June to July 2001, at a central avenue of Athens, Patission, at 21m height above street. The site is affected by the heavy traffic of the avenue (37,000 cars day⁻¹, Thomaidis et al., 2003).

Rome, capital of Italy with population about 2.7 million, has not heavy industrial activity (Perrino et al., 2008). The sampling in Rome (Canepari et al., 2008), took place, in April 2006, at an urban background site, which is influenced by the traffic of a near located urban street and a parking lot. The site is at the area of the University of Rome «La Sapienza» and the duration of the measurements was 15 days.

Seville, the fourth largest city of Spain, is one of the most populated cities of Spain with some industrial activity concentrated in industrial parks. In Seville (Álvarez et al., 2004), samples were collected, in duration of 18 months, in 24 different sites, including urban, traffic, suburban and industrial sites. The data provided by the authors are average values of all sites.

Frankfurt, the fifth largest city in Germany, is characterized by heavy traffic. Zereini et al. (2005) selected a street with heavy traffic (32,500 vehicles day⁻¹) to collect samples for analyzing the chemical composition of ambient particulate matter. Three different samples were taken during the period of August 2001–July 2002.

Zabrze, a city in Silesia in southern Poland, is smaller than the rest of the selected cities in the current work with population about 200,000 but is a city with big interest in terms of air pollution. In this area there is high concentration of particulate matter due to the presence of old steel works, cokeries and coal mines. The measurements (Rogula- Kozłowska et al., 2013) were done at an urban background site during the period of January to March 2008.

There are a limited number of studies in the scientific literature including size distribution data of ambient particulate matter and bound metals simultaneously. Therefore, the data used in the current study were obtained at different time periods and from different sites in urban areas in Europe. The main objective was to calculate the human exposure and dose of PM₁₀ and bound metals in different urban areas in Europe.

7.3. Exposure Scenario

The activity pattern and the breathing parameters of the subject studied, influence the personal exposure and dose. The subject is considered to be a male, adult, resident of the cities under

study who works 8h outdoors. The daily timetable of the person is the following: Resting (indoors) 12 p.m. to 8 a.m., light exercise (outdoors - urban environment) 8 a.m. to 4 p.m., sitting awake (indoors) 4 p.m. to 12 p.m. It is considered that the subject is nose breather and no smoker. The ventilation rates that were used as input data for resting, light exercise and sitting awake are 0.45, 1.5 and 0.54 m³ h⁻¹ (reference values for adult males; ICRP, 1994a), respectively.

7.4. Exposure and Dose Assessment Using the ExDoM Model

7.4.1. Input Data

Available data in the scientific literature, on ambient metal concentrations of PM₁₀ levels including Pb (all five cities), Cd (Athens, Rome, Seville and Zabrze) and As (Seville, Rome, Zabrze) were used.

The calculation of the deposition of heavy metals in different human body organs was accomplished with the use of ExDoM and PBPK models. ExDoM needs specific input data in order to calculate the deposition of particles in the RT, the GI tract and their absorption to blood. Input data for ExDoM are: particles concentration, size distribution, density, shape factor and exposed subject's characteristics like breathing type and pattern. Furthermore, the results of ExDoM model are input data for the PBPK model. In the case of Cd it is not necessary to use the ExDoM model, as the applied PBPK model for Cd calculates the deposition of particles in the lung, the GI tract and their absorption to blood.

An important factor that influences the inhalability of PM₁₀ and is input parameter for the ExDoM model is the wind speed. For each city, the yearly average wind speed was used in the calculations.

Data for the concentrations of PM₁₀ and particulate matter bound metals were used from the studies selected (Table 7.1). The highest PM₁₀ levels were occurred in Zabrze followed by Frankfurt, Seville, Rome and Athens. In this classification it must be taken into consideration that PM_{8.8} were measured in Athens and not PM₁₀ as in the rest of the cities. Cadmium particles concentration was more elevated in Zabrze (1.2 ng/m³) and Athens (0.8 ng/m³) in relation with Seville (0.5 ng/m³) and Rome (0.3 ng/m³). In Zabrze this occurs due to the intense industrial activity in the city. Lead particles concentration was higher in Athens (77.1 ng/m³) and Zabrze (40.6 ng/m³), respectively, with Frankfurt (33.0 ng/m³), Seville (14.0 ng/m³) and Rome (9.6 ng/m³) following. The elevated levels of Pb in Athens are result of the vehicular traffic which is the main emission source of Pb in Athens (Thomaidis et al., 2003). In the increased Pb levels in Athens contributes the presence of vehicles which used still leaded gasoline at the period of the sampling, while in the other four cities the measurements were done after the ban of leaded

gasoline. Arsenic particles concentration was notably higher in Seville (3.4 ng/m³) and Zabrze (3.0 ng/m³) with large difference from Rome (0.3 ng/m³), where the concentration is almost eight times lower. The emission sources of Pb and As are mainly vehicle emissions and re-suspended road dust, whereas the emission sources of Cd and a part of As are industrial activity (Thomaidis et al., 2003). Main sources of As particles are combustion processes, iron and steel industry, timber industry, waste treatment and disposal facilities (Maggs, 2000). For these reasons, As and Cd levels are elevated in Zabrze that has industrial activity and are lower in Rome, where the industries are far from the city centre.

Table 7.1: Table 1 Concentrations of PM₁₀, PM_{Pb}, PM_{As} and PM_{Cd} in Athens (Karanasiou et al. 2007), Rome (Canepari et al., 2008), Seville (Álvarez et al., 2004), Frankfurt (Zereini et al., 2005) and Zabrze (Rogula-Kozłowska et al., 2013)

City	PM ₁₀ (µg/m ³)	PM _{Pb} (µg/m ³)	PM _{As} (µg/m ³)	PM _{Cd} (µg/m ³)
Athens ¹	19.11	0.0771	-	0.0008
Rome	27.98	0.0096	0.0004	0.0003
Seville	41.8	0.0140	0.0034	0.0005
Frankfurt	36.43	0.0330	-	-
Zabrze	38.52	0.0406	0.0030	0.0012

¹ PM_{8,8}

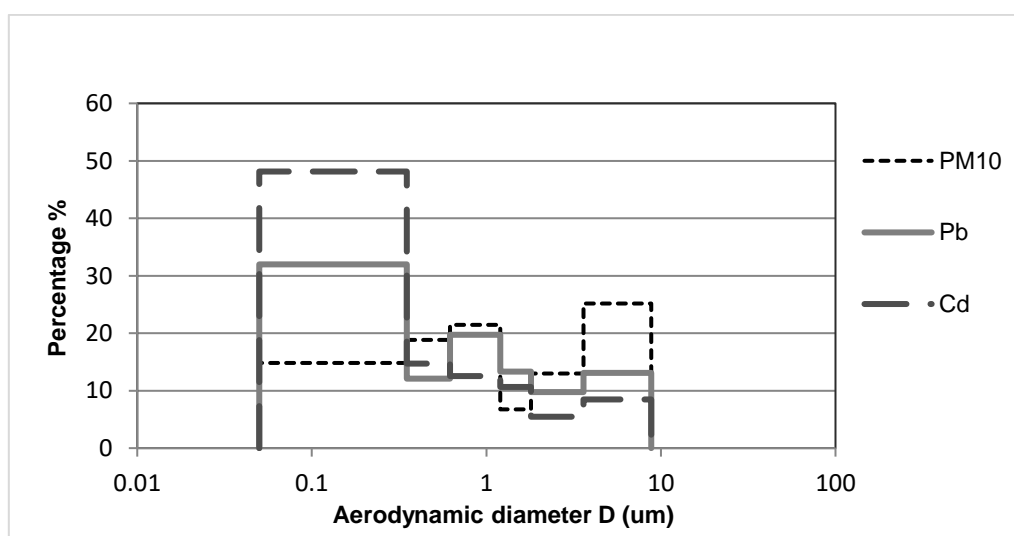
The European Union thresholds of particle-bound Pb, Cd and As inhalation were not reached by the mean values for the sampling period in none of the cities under study. Threshold value for Pb concentration averaged over a calendar year, in the PM₁₀ fraction, is 500 ng/m³ according First Daughter Directive (1999/30/EC). Target values for Cd and As concentrations averaged over a calendar year, in the PM₁₀ fraction, are 5 ng/m³ and 6 ng/m³ respectively. US-EPA has created the Integrated Risk Information System (IRIS), a program that evaluates information on health effects that may result from exposure to environmental contaminants. For the inhalation of heavy metals, such as As and Cd, exist specified risk levels. Risk is presented as the probability of formation of cancer of 1 in 10,000 (E-4 risk level), 1 in 100,000 (E-5 risk level) or 1 in 1,000,000 (E-6 risk level), (U.S. EPA., 1986). For exposure in As particles, concentration close to 2×10^{-3} µg/m³ is E-5 risk level and close to 2×10^{-4} µg/m³ is E-6 risk level.

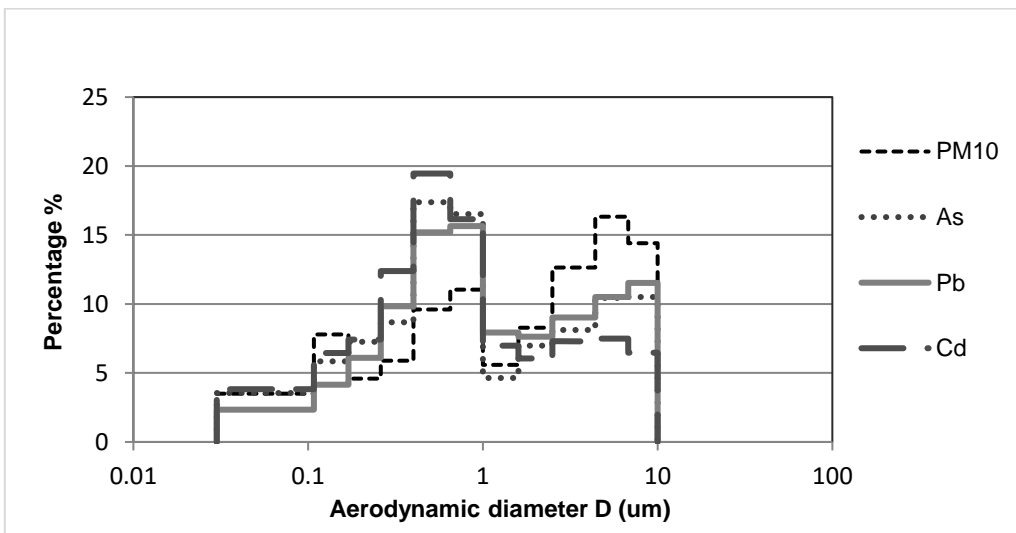
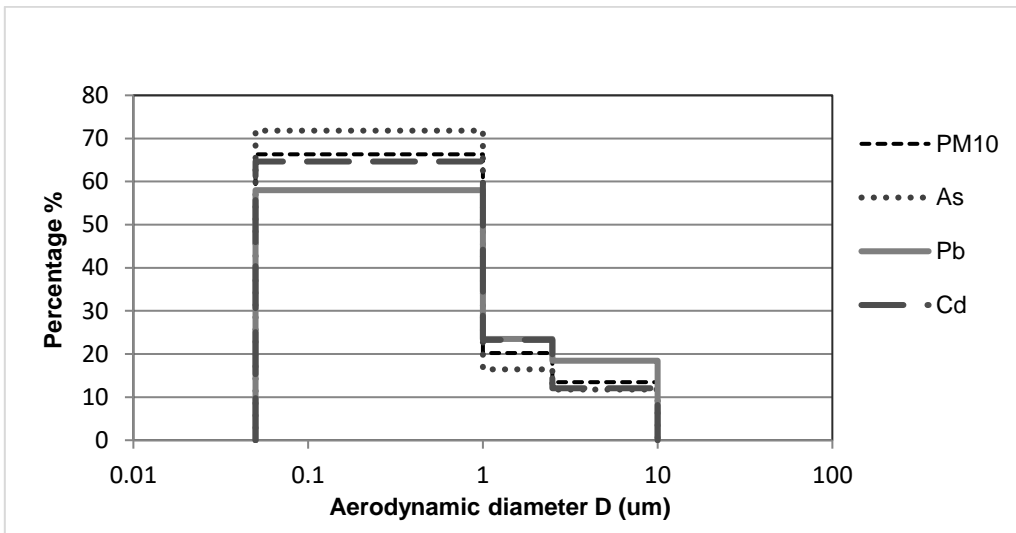
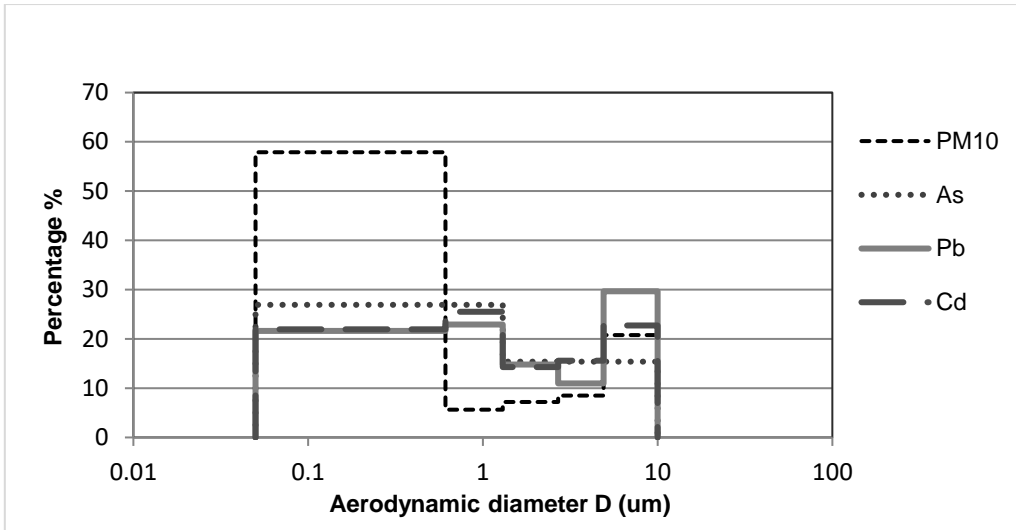
Taking into consideration the mean concentrations of arsenic particles for the sampling periods, shown on Table, the probability of cancer formation due to inhalation of As is 1 in 100,000 in Seville and Zabrze and 1 in 1,000,000 in Rome. Regarding Cd, the mean exposure

concentrations for the sampling periods in all the cities studied, is below or close to $6 \times 10^{-4} \mu\text{g}/\text{m}^3$ that is E-6 risk level.

The indoor particle concentration (for fine and coarse modes) was calculated using the indoor/outdoor ratio for naturally ventilated buildings in the absence of indoor sources. Morawska and Salthammer (2003) concluded that, for naturally ventilated buildings in the absence of indoor sources, I/O ratios for PM_{10} and $\text{PM}_{2.5}$ ranged from 0.5 to 0.98 and 0.54 to 1.08, respectively. Therefore, for fine ($\text{PM}_{2.5}$) and coarse ($\text{PM}_{10-2.5}$) indoor/outdoor ratio an average ratio equal to 0.8 and 0.5, respectively, was adopted.

One of the most important factors, determining the deposition of particulate matter in the human respiratory tract is their size. In the ExDoM model, it is necessary to use the size distribution of the particulate matter as an input parameter. The determination of concentrations and size distribution of heavy metals in the PM_{10} fraction was performed using data obtained from gravimetric measurements. In Athens (Karanasiou et al., 2007), the samples were collected with a six stage Andersen cascade impactor, with cut-off diameters (at 50% efficiency collection) $0.35 \mu\text{m}$, $0.62 \mu\text{m}$, $1.2 \mu\text{m}$, $1.8 \mu\text{m}$, $3.6 \mu\text{m}$ and $8.8 \mu\text{m}$ (Fig. 7.2(a)). In Rome (Canepari et al., 2008) (Fig. 7.2(b)) and Zabrze (Rogula-Kozłowska et al., 2013) (Fig. 7.2(c)), a 13-stage impactor (DLPI DEKATI Ltd) was used with cut-off diameters (at 50% efficiency collection) $0.030 \mu\text{m}$, $0.060 \mu\text{m}$, $0.108 \mu\text{m}$, $0.17 \mu\text{m}$, $0.26 \mu\text{m}$, $0.40 \mu\text{m}$, $0.65 \mu\text{m}$, $1 \mu\text{m}$, $1.6 \mu\text{m}$, $2.5 \mu\text{m}$, $4.4 \mu\text{m}$, $6.8 \mu\text{m}$ and $10 \mu\text{m}$. A cascade impactor with cut-off diameters (at 50% efficiency collection) $0.6 \mu\text{m}$, $1.3 \mu\text{m}$, $2.7 \mu\text{m}$, $4.9 \mu\text{m}$ and $10 \mu\text{m}$ was used to collect samples in Seville (Álvarez et al., 2004) (Fig. 7.2(d)). An eight-stage Andersen impactor was selected for the sampling in Frankfurt (Zereini et al., 2005) (Fig. 7.2(e)) with cut-off diameters (at 50% efficiency collection) $0.43 \mu\text{m}$, $0.63 \mu\text{m}$, $1.1 \mu\text{m}$, $2.1 \mu\text{m}$, $3.3 \mu\text{m}$, $4.7 \mu\text{m}$, $5.8 \mu\text{m}$, $9 \mu\text{m}$ and $10 \mu\text{m}$.





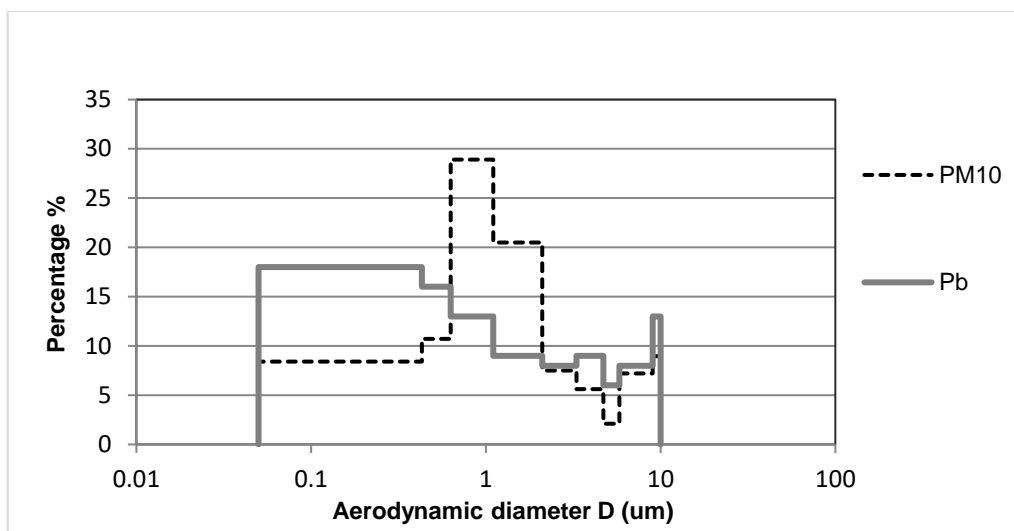


Figure 7.1: PM₁₀, PM_{Pb} and PM_{Cd} size distribution in (a) Athens (adapted from Karanasiou et al. 2007) (b) Rome (adapted from Canepari et al., 2008), (c) Zabrze (adapted from Rogula-Kozłowska et al., 2013) (d) Seville (adapted from Álvarez et al., 2004) and (e) Frankfurt (adapted from Zereini et al., 2005).

Table 7.2 shows the percentage of particle mass and metals that are in the fine and coarse modes. From the measurement campaigns the majority of the particle mass and metal mass are in the fine fraction. Specifically, in Seville (Fig. 7.2(d)) 84% of arsenic particles, 75% of lead particles and 67% of cadmium particles are in the PM_{1.3} fraction and in Zabrze (Fig. 7.2(c)) 72% of arsenic particles, 58% of lead particles and 65% of cadmium particles are in the PM₁ fraction. These data agree with other studies in the literature (Espinosa *et al.*, 2001; Samara *et al.*, 2005; Pérez *et al.*, 2008) which studied the size distribution of Pb, As and Cd and concluded that most particle-bound metals are in PM1 fraction.

7.5 Results

7.5.1. Calculation of the Dose of Particulate Matter-Bound Metals Using the ExDoM Model

The exposure and dose assessment model, ExDoM, was used to evaluate the dose from the inhalation of particulate matter and particle-bound metals. In Table 7.3 the deposition of PM₁₀ in the RT, GI tract and blood is shown. Between the European cities studied in the current study, the highest dose in the respiratory tract has a resident in Seville ($3.56 \times 10^2 \mu\text{g}$), Frankfurt ($3.22 \times 10^2 \mu\text{g}$), Zabrze ($2.74 \times 10^2 \mu\text{g}$), Rome ($2.81 \times 10^2 \mu\text{g}$) and Athens ($1.73 \times 10^2 \mu\text{g}$), respectively for the pre-described 24 h exposure scenario.

Similar classification follows the PM₁₀ deposit in blood with $2.14 \times 10^1 \mu\text{g}$ in Seville, $1.62 \times 10^1 \mu\text{g}$ in Zabrze, $1.57 \times 10^1 \mu\text{g}$ in Frankfurt, $1.31 \times 10^1 \mu\text{g}$ Rome and $8.42 \times 10^1 \mu\text{g}$ in Athens. These classifications are in agreement with the concentration of PM₁₀ in the different European cities as the internal PM₁₀ dose is proportional to the ambient PM₁₀ concentration. A proportion

of the particles deposited, remain in the RT. Specifically 50% of the particles in Seville, 48% in Zabrze, 35% in Frankfurt, 32% in Rome and 34% in Athens deposited in the RT. It is observed that the percentage of deposition in blood is similar in the different cities (7–8%). Regarding GI tract the highest dose receives a citizen of Frankfurt $1.26 \times 10^2 \mu\text{g}$, with Rome ($1.15 \times 10^2 \mu\text{g}$), Seville ($1.11 \times 10^2 \mu\text{g}$), Zabrze ($8.98 \times 10^1 \mu\text{g}$) and Athens ($6.93 \times 10^1 \mu\text{g}$) following. The deposition in the GI tract is related with the ambient concentration of coarse particles (Table 2) because coarse particles are mainly deposited in the upper respiratory tract regions and transferred to the trachea by the mucociliary escalator and swallowed to the GI tract (Aleksandropoulou and Lazaridis,2013). The greater the percentage of coarse particles the greater the transport of particles from the respiratory tract to GI tract and more specifically the percentage of particles transported to the GI tract correspond to: 61% in Rome; 59% in Athens; 57% in Frankfurt; 44% in Zabrze and 42% in Seville.

Table 7.2: Percentages of PM₁₀ being in the fine and coarse fraction in the five European countries.

City	PM ₁₀		PM _{Cd}		PM _{As}		PM _{Pb}	
	Fine	Coarse	Fine	Coarse	Fine	Coarse	Fine	Coarse
Athens ¹	62%	38%	86%	14%	-	-	77%	23%
Rome ²	57%	43%	79%	21%	71%	29%	69%	31%
Seville ³	71%	29%	83%	17%	88%	12%	87%	13%
Frankfurt ⁴	69%	31%	-	-	-	-	56%	44%
Zabrze ²	87%	13%	88%	12%	88%	12%	82%	18%

¹ Fine: PM_{1.8}, Coarse:PM_{8.8-1.8}, ² Fine: PM_{2.5}, Coarse:PM_{10-2.5}, ³ Fine: PM_{2.7}, Coarse:PM_{10-2.7},
⁴ Fine: PM_{2.1}, Coarse:PM_{10-2.1}

Table 7.3: Particulate matter dose in human respiratory tract, blood and GI tract for adult males in five European countries after 24h exposure scenario, calculated by the ExDoM model.

PM					
City	Cumulative deposited dose to respiratory tract (μg)	Cumulative deposited dose in 4 regions of the respiratory tract (μg)	Retention in respiratory tract (μg)	Blood (μg)	GI Tract (μg)
Athens	1.73E+02	1.18E+02	4.05E+01	8.42E+00	6.93E+01
Rome	2.81E+02	1.88E+02	5.98E+01	1.31E+01	1.15E+02
Seville	3.56E+02	2.66E+02	1.33E+02	2.14E+01	1.11E+02
Frankfurt	3.22E+02	2.19E+02	7.75E+01	1.57E+01	1.26E+02
Zabrze	2.74E+02	2.04E+02	9.79E+01	1.62E+01	8.98E+01

Table 7.4: Lead particulate matter dose in human respiratory tract, blood and GI tract for adult males in five European countries after 24h exposure scenario, calculated by the ExDoM model.

PM_{Pb}					
City	Cumulative deposited dose to respiratory tract (μg)	Cumulative deposited dose in 4 regions of the respiratory tract (μg)	Retention in respiratory tract (μg)	Blood (μg)	GI Tract (μg)
Athens	5.87E-01	4.48E-01	2.04E-03	3.60E-01	8.51E-02
Rome	7.88E-02	5.37E-02	2.12E-04	3.82E-02	1.51E-02
Seville	1.14E-01	9.41E-02	4.96E-04	8.18E-02	1.15E-02
Frankfurt	3.27E-01	2.26E-01	8.95E-04	1.64E-01	6.05E-02
Zabrze	3.23E-01	2.33E-01	1.02E-03	1.75E-01	5.59E-02

The deposition of PM_{Pb} in the lungs, GI tract and blood is shown in Table 7.4. Due to the fast absorption behaviour of Pb (ICRP, 1994a) only a very low percentage, below 0.5% in all the cities, remains in the respiratory tract. The majority of particles deposited to RT are transferred to blood: with 87%, 80%, 75%, 73% and 71% of the deposited particles to RT transferred to blood for residents of Seville, Athens, Zabrze, Frankfurt and Rome, respectively. The

deposition in the RT follows the same classification in respect to the ambient concentrations. Therefore, in the city with the higher concentration of Pb, Athens, there is calculated also the higher deposition in blood. In the GI tract, the deposition classification from the higher dose to the lower is Athens ($8.51 \times 10^{-2} \mu\text{g}$), Frankfurt ($6.05 \times 10^{-2} \mu\text{g}$), Zabrze ($5.59 \times 10^{-2} \mu\text{g}$), Rome ($1.51 \times 10^{-2} \mu\text{g}$) and Seville ($1.15 \times 10^{-2} \mu\text{g}$).

Table 7.5 presents the deposition of PMAs in the RT, GI tract and blood. Only for Rome, Seville and Zabrze were found data for PMAs concentration and their corresponding size distribution. The highest deposition in the RT and blood occurs for a resident of Seville where there is the highest As ambient concentration in respect to the cities studied, and follows Zabrze and Rome. Rome has very low As ambient concentration due to the absence of industrial activity. For a resident in Rome 34% of the As particles deposited in the respiratory tract retained there after one day, whereas the percentage of deposited As particles in the respiratory tract that retained there after one day for a resident of Seville is 65% and 51% for a resident in Zabrze. This difference occurs because the percentage of particles being in the coarse mode is higher in Seville, compared with the other two cities. The percentage of the deposition in blood is similar in the three cities and ranges from 7–9% of the initial deposited particles in the RT.

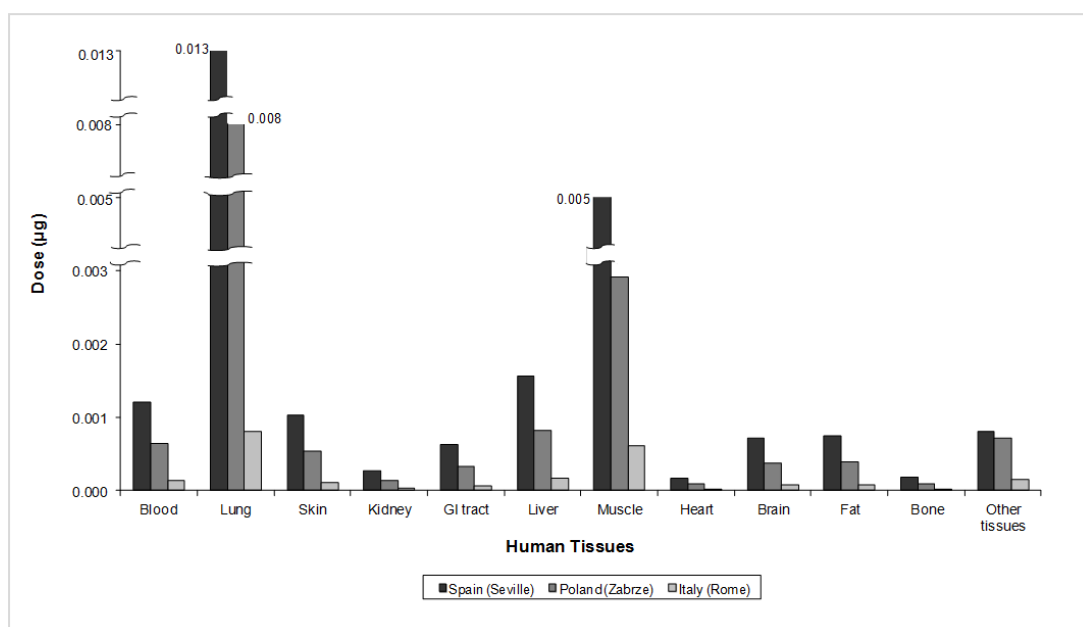
Table 7.5 Arsenic particulate matter dose in human respiratory tract, blood and GI tract for adult males in five European countries after 24h exposure scenario, calculated by the ExDoM model.

PM _{As}					
City	Cumulative deposited dose to respiratory tract (μg)	Cumulative deposited dose in 4 regions of the respiratory tract (μg)	Retention in respiratory tract (μg)	Blood (μg)	GI Tract (μg)
Athens	-	-	-	-	-
Rome	3.54E-03	2.34E-03	7.86E-04	1.66E-04	1.38E-03
Seville	2.79E-02	2.34E-02	1.52E-02	2.09E-03	6.09E-03
Frankfurt	-	-	-	-	-
Zabrze	1.97E-02	1.50E-02	7.74E-03	1.23E-03	6.07E-03

7.5.2. Application of a PBPK Model for Calculating the Dose of Metals in the Human Body

A physiologically-based pharmacokinetic (PBPK) model is used for the determination of internal dose in several pre-selected anatomical compartments. The body is subdivided into various compartments representing specific organs or homogeneous groups of tissues linked and irrigated by blood vessels (Yang et al., 2010). The output (lung dose, blood dose and GI tract dose) from the ExDoM model was used as input for PBPK model. In particular, PBPK model was developed to describe the movement of metals from the blood (ExDoM results) into the tissues. Estimations of particle-bound metals dose in the human body were performed for arsenic (As), lead (Pb) and cadmium (Cd) of an adult male. Among the European cities studied, the highest dose in the human body for As, Pb and Cd was found in Seville (Spain), Athens (Greece) and Zabrze (Poland), respectively due to higher ambient concentration in these countries (see Figs. 7.2a, 7.2b, 7.3a and 7.3b). In particular, during the period of PMPb measurements in Athens (Greece), by Karanasiou et al. (2007), leaded gasoline for older vehicles lacking catalytic converters was still available. Therefore, emissions from those vehicles are responsible for high concentrations of PM_{Pb} in Athens (Greece). In addition, PM_{Cd} measurements in Zabrze (Poland) by Rogula- Kozłowska et al. (2013) were done in a winter heating season, when the emissions from combustion of fossil fuels for energy production (especially municipal) result to high PM_{10} concentrations ($38.52 \mu\text{g m}^{-3}$). Rogula-Kozłowska et al. (2013) reported that the combustion of low-quality coal in domestic furnaces (municipal emission) is the source of Cd in Zabrze in winter. It is observed in Fig. 7.2a that after one day of exposure to PM_{AsIII} (particle-bound arsenite), the major accumulation occurs in the lung, muscles and liver ($1.53 \times 10^{-2} \mu\text{g}$ in the lung, $3.27 \times 10^{-3} \mu\text{g}$ in the muscles and $3.27 \times 10^{-3} \mu\text{g}$ in the liver for a resident of Seville, where there is the highest ambient measured As concentration). This result is in agreement with the study by Chou *et al.* (2009), where it was found that the highest dose is present in lungs and liver tissues after chronic exposure to Arsenic. For PMPb, it is observed in Fig. 2b that the major accumulation occurs in the bone, blood and muscles whereas as regard PM_{Cd} (see Fig. 7.3) the highest dose is present in the lungs ($3.07 \times 10^{-3} \mu\text{g}$ in Zabrze), due to the slow absorption to the blood and intestines ($6.89 \times 10^{-4} \mu\text{g}$ in Zabrze) at the end of first day. In Athens the Pb accumulation in bones is $2.19 \times 10^{-1} \mu\text{g}$, in blood $7.05 \times 10^{-2} \mu\text{g}$ and in the muscles $4.56 \times 10^{-2} \mu\text{g}$. According to WHO (2007) inhalation of cadmium can cause chronic obstructive airway disease. For Pb, the major accumulations occur in bone due to the high tissue/blood partition coefficient, in blood due to fast absorption and in muscle due to high blood flow. For Cd, because of its slow absorption from the human body, in addition to the calculation of its deposition after 24 h, the deposition of Cd after 800 h was also calculated. It was observed that after 800 h the major accumulation

occurs in the other tissues, kidney and liver. This estimation comes in agreement with WHO (2007) that states that the majority of Cd inhaled is retained in the kidneys and liver with half-life in these organs about 10–20 years. The conclusions are also in agreement with the study by Kjellstrom and Nordberg (1978). Furthermore, the WHO has recommended a provisional tolerable intake at 7 $\mu\text{g}/\text{kg Cd}/\text{kg (body weight)}/\text{week}$ (WHO, 1993) from all types of exposure (inhalation, ingestion). The body weight of an adult male was considered to be 73 kg in the current study and therefore the weekly allowable intake was 511 μg . In the European cities weekly intake for Cd ranged from 0.05 to 0.10 μg which are considerably lower than the recommended value. Likewise, the weekly allowable intake for Pb was calculated, from the provisional tolerable weekly intake of 25 $\mu\text{g}/\text{kg body weight}$, recommended by FAO/WHO (1999), to be 1.825 μg per week. In the current study, weekly intake for Pb ranged from 1.18 to 9.61 μg which is lower than the recommended value.



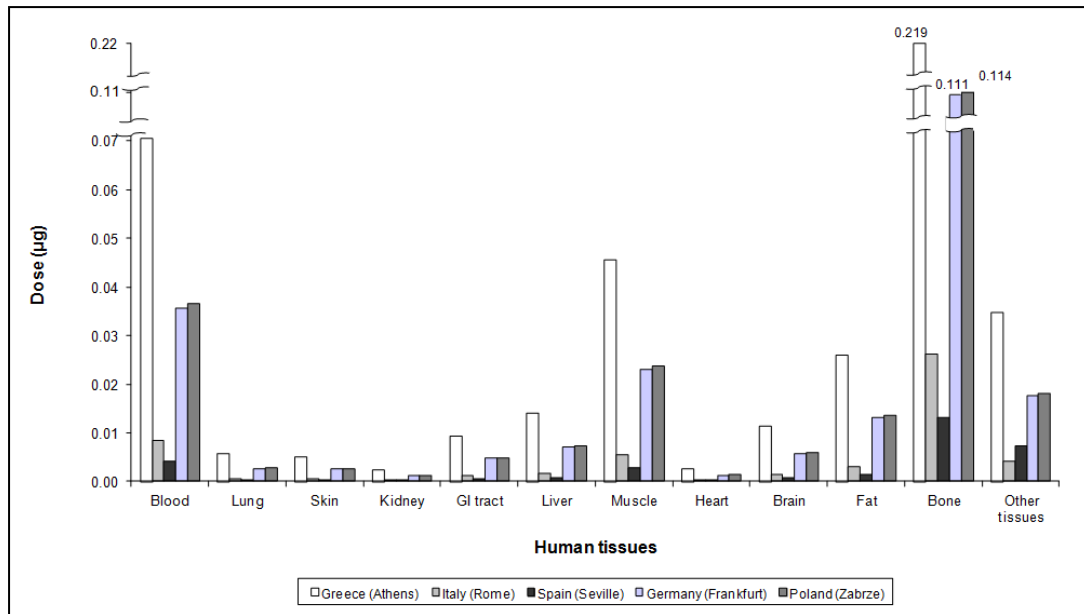


Figure 7.2: Internal Dose in human tissues provided by the PBPK model in conjunction with the ExDoM for adult males (nose breather) of five European countries (after an 24 h exposure scenario) of (a) Arsenic (As) (b) Lead (Pb).

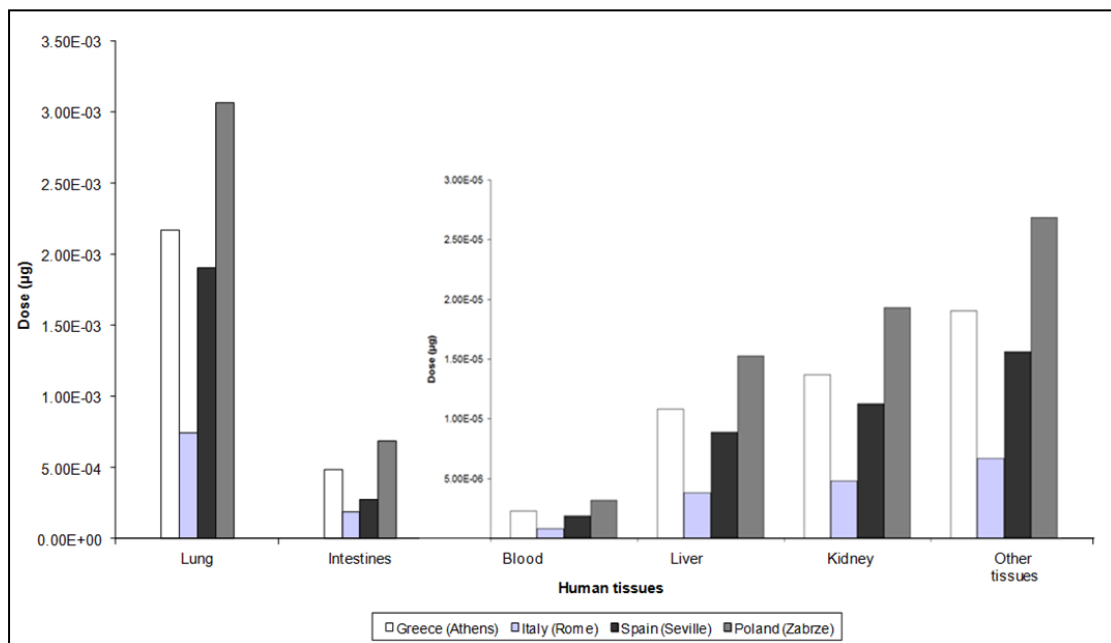


Figure 7.3: Lead Dose provided by the PBPK model in conjunction with the ExDoM for adult males of four European countries after a 24h exposure scenario, in (a) Lungs and intestines (b) Blood, liver, kidney and other tissues.

7.6. Conclusions

In the current study, the dose of particles-bound metals in human body of an adult male in five European countries during 24-h exposure scenario was calculated. The ExDoM in conjunction with a PBPK model was applied to determine the dose in the human body. The models are capable of studying human exposure under variant exposure conditions and for particles bound

metals. The models have been implemented using a typical exposure scenario and real measurement data. The model results showed that the highest dose in the human tissues for As and Cd was found for Italian (resident in Rome) and Polish (resident in Zabrze) male, respectively, whereas as regard Pb the highest dose was found for Greek (resident in Athens) male because ambient particles-bound metal concentrations at these cities were more elevated during the measurement periods. Therefore, elevated particulate matter-bound metals concentrations result in elevated dose in human tissues. Nowadays, with the removal of lead from gasoline and the use of new technologies, there have been some changes in vehicle emissions which will result to lower exposure and dose. Finally, the use of PBPK model can become a key component of human health effect of particulate matter-bound metals. With the use of the PBPK modelling it is possible to estimate the contaminant burden (dose) of organs and thereby potential health effects from human exposure to particulate matter-bound metals.

In the cities studied, the heavy metals concentrations were below the EU thresholds and as a result the inhaled intake of Pb and Cd (not available for As) were both lower than the recommended WHO values for heavy metals intake from all sources.

Chapter 8: Population Exposure

8.1. Introduction

Air pollution is a major health threat that causes a multifaceted challenge to public health. Since population and urbanization is growing, despite various pollution reduction measurements taken, air pollution is still correlated with many annual deaths. It is considered that in the cities of the EU-28 countries the major treat compared to other air pollutants, at the present time, is $PM_{2.5}$ levels, with ozone levels following. It is concerning, that while in the EU-28, the $PM_{2.5}$ concentrations have been decreased and as a result the annual deaths have been reduced by on average 4.85 per 1,000,000 inhabitants annually between 2000 and 2017, in Greece it was observed an increase to annual deaths correlated with $PM_{2.5}$ concentrations (+1.22 per 1,000,000) (Sicard et al., 2021).

PM_{10} and $PM_{2.5}$ pollution poses a considerable threat to human health, and the first step in quantifying health impacts of human exposure to PM_{10} pollution is exposure assessment. The aim of this study was to predict the exposure and dose of population in Attica using available data from monitoring stations and population spatial distribution data in order to estimate the population exposure at the studied area with the use of an interpolation method at a geographical information system. The dose was calculated with the help of the exposure dose model ExDoM2 (Chalvatzaki and Lazaridis, 2015), considering that the studied subjects are exposed to ambient PM_{10} for the whole day.

8.2. Monitoring stations

There are several monitoring stations across Greece that are under the supervision of the Greek Ministry of Environment and Energy (YPEKA). The focus of this study is on the stations that are measuring PM_{10} . On Figure 8.1 can be seen the monitoring stations across the whole country. As it can be seen most of the stations are in Attica and Thessaloniki, the two biggest cities, where a significant proportion of the population lives.

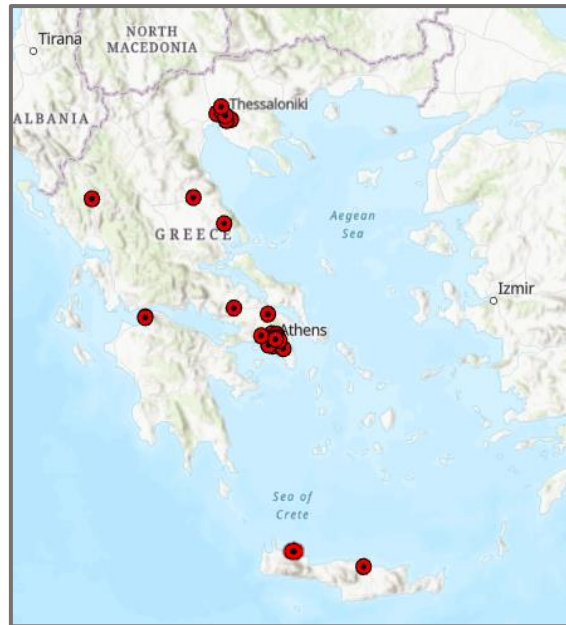


Figure 8.1: Air pollution monitoring stations across Greece (created in ArcGIS Pro).

Attica has 14 monitoring stations, as can be seen on Figure 8.2, from which 11 of them are measuring PM₁₀ (Figure 8.3).

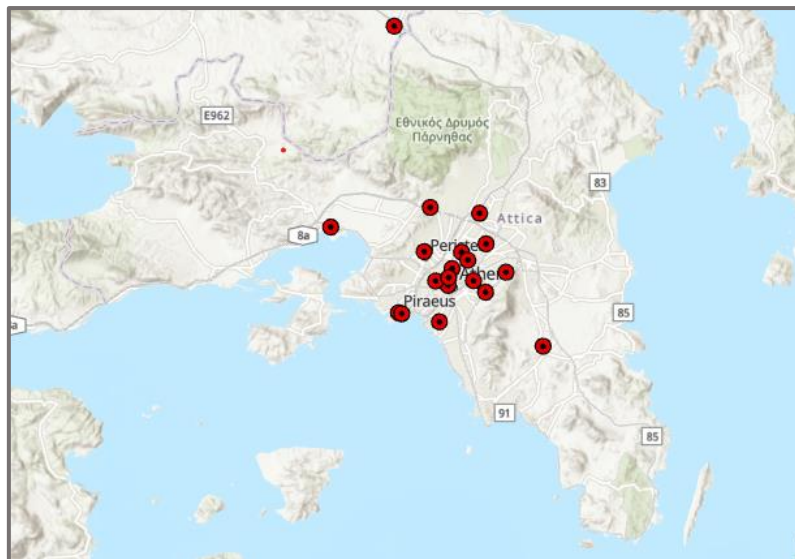


Figure 8.2: Air pollution measurements stations in Attica (created in ArcGIS Pro).

The monitoring air pollution stations are classified according to how dense is the built-up area that surrounds the station and according to the predominant emission sources in the area. Regarding the surrounding built-up area, they are classified as: urban; for continuously built-up area, suburban; for largely built-up area and rural; for the rest of areas. Considering the main emission source, they are characterized as: traffic monitoring stations; close to busy street, industrial stations: for stations located in industrial areas and background stations; when the concentrations are representative of the average population exposure. On Table 8.1, can be seen

the name, the coordinates, and the type of the monitoring stations, taken into consideration in the current study. Most of the stations used are background stations, two are traffic stations and one is an industrial station located in Eleusina, which is the industrial area of Attica. PM₁₀ concentrations are measured online with an automatic beta attenuation monitor (FH 62 I-R, Thermo Electron Corporation, Erlangen) placed in each monitoring station.

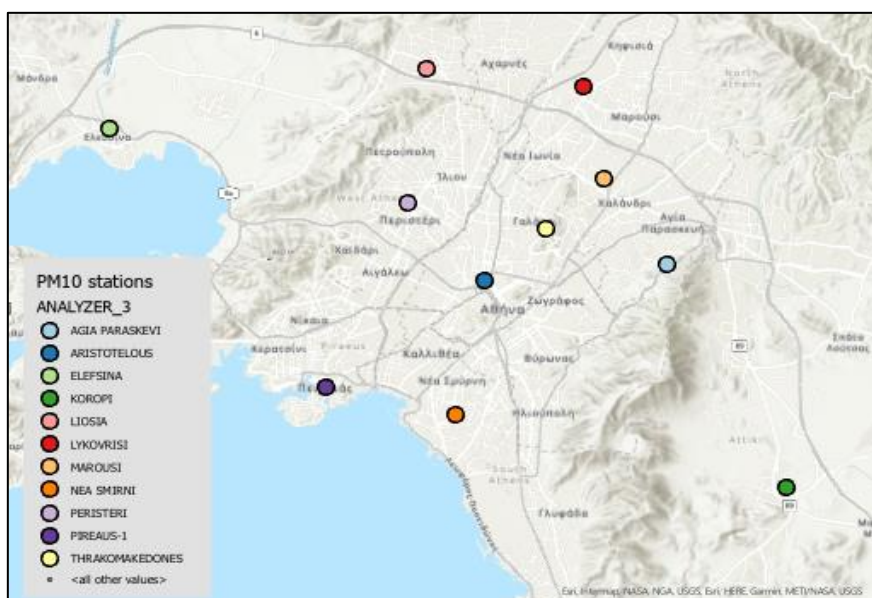


Figure 8.3: PM₁₀ measurement stations in Attica (created in ArcGIS Pro).

Table 8.1: PM₁₀ monitoring stations in Attica.

Name of monitoring stations	Longitude (WGS84)	Latitude (WGS84)	Classification of monitoring stations
Ag. Paraskevi	23.819421	37.995110	Suburban - Background
Aristotelous	23.727617	37.988066	Urban-Traffic
Elefsina	23.538432	38.051322	Suburban - Industrial
Koropi	23.879026	37.901308	Suburban - Background
Liosia	23.697781	38.076741	Suburban - Background
Lykovrissi	23.788986	38.067793	Suburban - Background
Marousi	23.787372	38.030837	Urban - Background
Nea Smirni	23.713020	37.931998	Urban - Background
Peristeri	38.020811	38,020811	Urban - Background
Pireaus-1	23.645230	37.944656	Urban-Traffic
Thrakomakedones	23.758195	38.143521	Suburban - Background

In order to estimate the number of residents of Attica that are exposed to elevated concentrations the population map in Figure 8.4 was created. Data from geodata.gov.gr were used for the municipal boundaries. Attica has 59 municipalities, some very densely populated, like municipality of Athens that has 664,046 residents, and other less. The population data were taken from the Hellenic statistical authority, and they are the results of the census that took

place in 2011. The color graduation in the map depicts the number of residents in each municipality and darker colors represent the ones with the larger population.

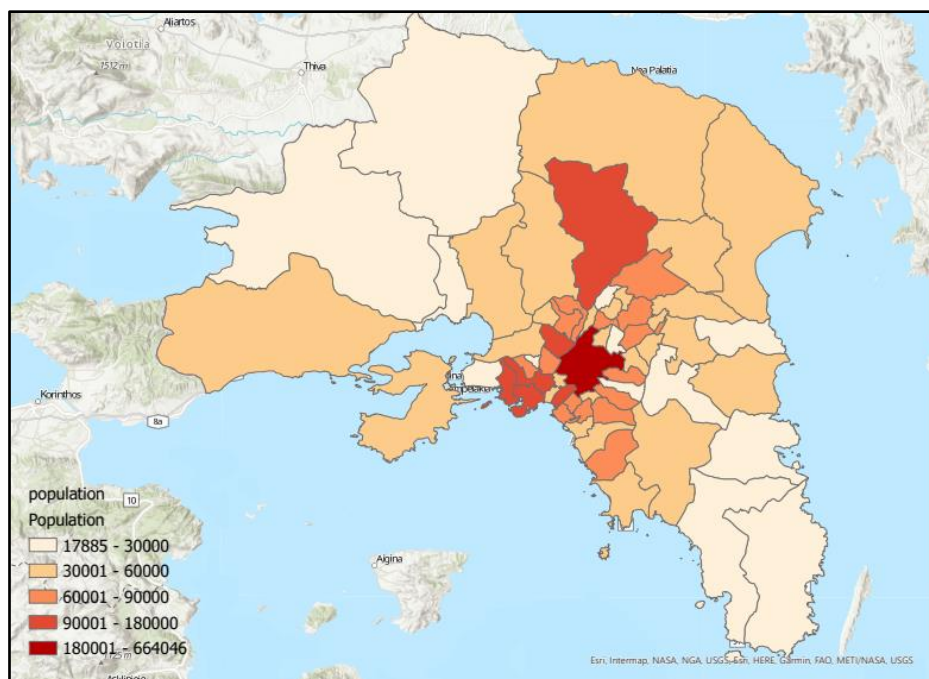


Figure 8.4: Population in Attica's municipalities (created in ArcGIS Pro).

8.3. Population exposure in Attica

Attica has around 3.7 million residents according to the last published census (ELSTAT, 2011). In order to estimate the exposure of the residents in particulate matter, PM_{10} concentration data from the aforementioned monitoring stations were used in relation with spatial distribution data of the population. The software used was ArcGIS Pro and with the help of an interpolation method, the population exposure was estimated. The interpolation method used is Kriging and is a feature of the Spatial Analyst ArcGIS extension.

Kriging is a statistical method which is commonly used in pollution, health science and in geochemistry modeling and it uses complex mathematical formulas to predict values of a variable over a continuous spatial field based on known values in different points. The predicted values are derived from the measure of relationship in samples using sophisticated weighted average technique. The generated cell values can exceed the value range of samples. The most common method of kriging is the ordinary kriging, which assumes that there is no trend, that means not constant mean for the data over an area mean (Childs, 2004).

It is important to have enough known points distributed across the study area. As it was already mentioned in Greece most of the stations are in Attica and Thessaloniki (Fig. 8.1). Since the stations are not distributed around the country, and are mainly in two areas, it was not possible to apply the kriging method for the whole country, thus the study focused on Attica.

According to WHO the annual mean concentration is the best indicator for PM-related health effects. The annual means given by Ypeka (2021) for the years 2017-2020, were used. On Figures 8.5-8.8 can be seen the predicted PM₁₀ values across the study area for the years 2017-2020. Due to the limitation that there are not enough monitoring stations across the whole study area, in this case Attica, it was not possible to calculate the concentrations for the whole area. The area covered is inhabited by 3.06 million people, so the estimations are for the 83% of the population in Attica.

As it is depicted at the map on Fig. 8.5 the PM₁₀ concentrations in 2017 ranged from 20 to 38 µg/m³ in 2018 (Fig. 8.6) from 15 to 39 µg/m³ and in 2019 (Fig. 8.7) from 22 to 32 µg/m³. Lower concentrations were observed in 2020 (Fig. 8.7), where the PM₁₀ values ranged from 15 to 32 µg/m³. The air pollution levels were affected by the economic crisis that started in Greece in 2010 in two ways. On the one hand, there was a reduction of air pollution since the vehicle traffic and the industrial activity were reduced but on the other hand PM levels were elevated mainly during the winter due to the biomass burning for heating (Gerasopoulos, et al 2017).

Higher values were observed in 2018, which is the year among the studied years with the highest contribution of Sahara dust, 7-9 µg/m³ to all the stations, while the rest of the three years the contribution was varying from 3-5 µg/m³ (YPEKA, 2021). Sahara dust is a natural source that affects significantly PM₁₀ levels in Greece and in south European region in general (Kopanakis et al. 2018) and it is related to the weather conditions.

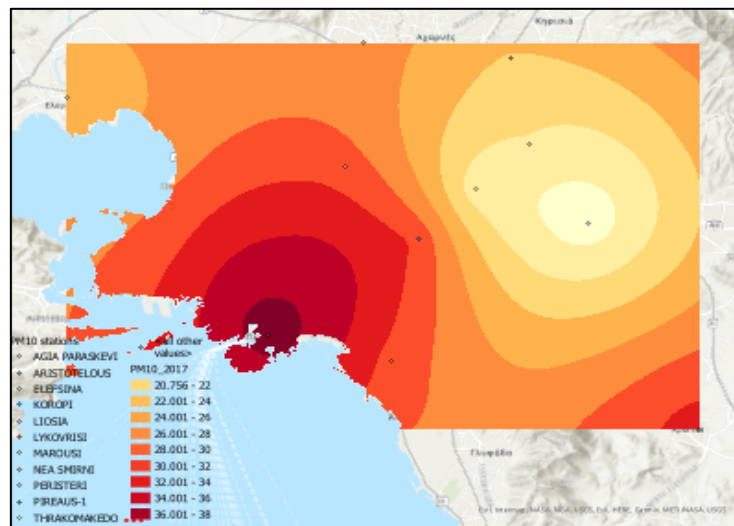


Figure 8.5: PM₁₀ annual average concentration in Attica in 2017 (created in ArcGIS Pro), (values in µg/m³).

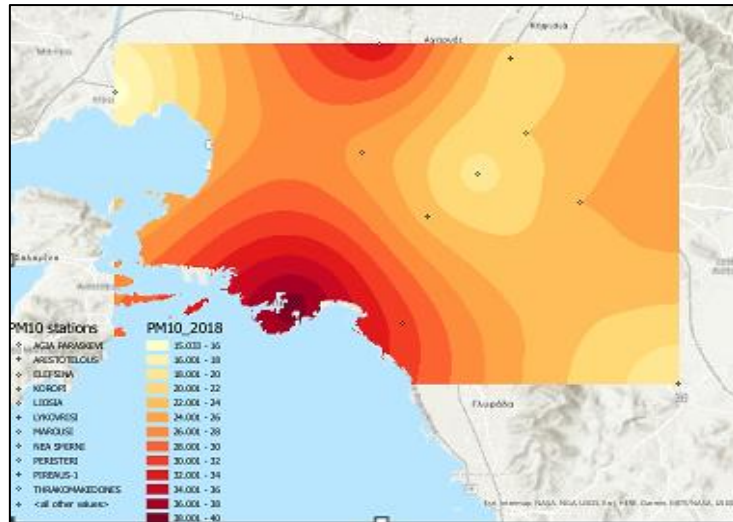


Figure 8.6: PM₁₀ annual average concentration in Attica in 2018 (created in ArcGIS Pro) (values in µg/m³).

The lowest concentrations were observed in 2020 and this can be correlated with the pandemic Covid-19 that due to the lockdown and restrictions most of the people were working remotely so the commuting was reduced significantly. It is worth mentioning that all the eleven monitoring stations recorded the lowest annual average values from all the years they have been operating. According to Kalantzi et al (2021) there was a 13-38% decrease in PM₁₀ levels due to the lockdown while Varotsos et al (2021) supports that there was no statistically significant change in PM₁₀ levels due to the lockdown and that the lower values are related to the meteorological conditions that contributed significantly to the long-range transport of the pollutants.

In all the years studied, higher concentrations were recorded from the urban traffic stations, Piraeus 1 which is located close to the port of Athens and Aristotelous monitoring station which is a traffic station in the center of Athens. Traffic is a major contributor to particulate concentrations, so it is expected these types of stations to have more elevated concentrations. The monthly variation to PM₁₀ levels differs from station to station and it is related to the type of the station (type of sources) and varies from year to year mainly due to the natural sources (dust transportation from deserts, bioaerosols and marine aerosols).

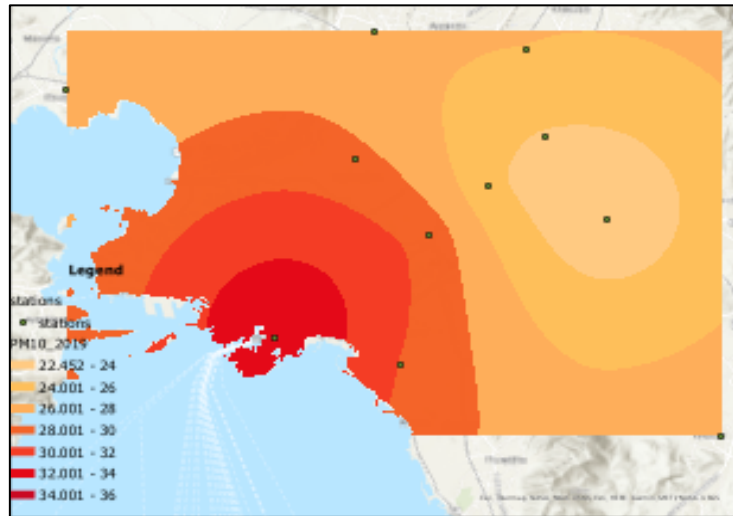


Figure 8.7: PM₁₀ annual average concentration in Attica in 2019 (created in ArcGIS Pro), (values in $\mu\text{g}/\text{m}^3$).

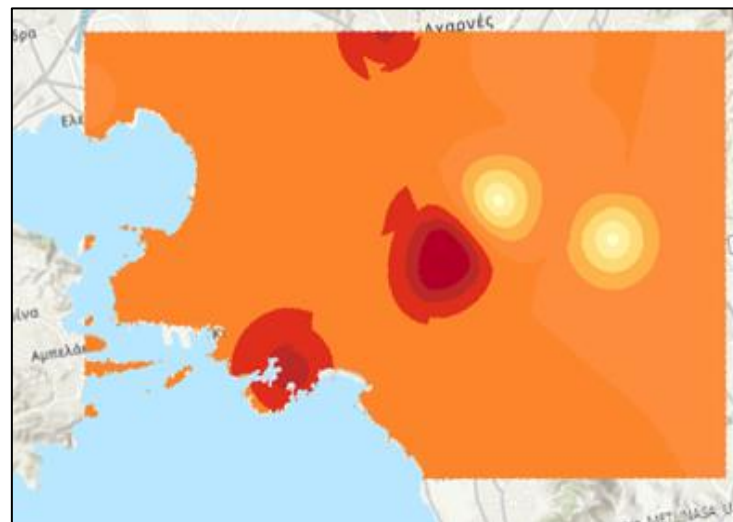


Figure 8.8: PM₁₀ annual average concentration in Attica in 2020 (created in ArcGIS Pro), (values in $\mu\text{g}/\text{m}^3$).

As it was already mentioned, due to the limited number of monitoring stations, kriging could not be applied to the whole area of Attica and the population under study is 3.06 million people, instead of 3.7 million. It can be seen on Table 8.2 that in 2020 the majority (91.7%) of the population studied, had average annual PM₁₀ exposure less than $26 \mu\text{g}/\text{m}^3$. On the other hand, in 2019, 79.8% of the population studied, were exposed to annual average concentrations higher than $26 \mu\text{g}/\text{m}^3$. Although the highest concentrations were observed in 2018, in 2019 larger proportion of the population was exposed to higher concentrations. People living closer to the main port of Athens, Piraeus, were exposed in higher concentrations. According to the European Ambient Air Quality Directive (Directive 2008/50/EC) the annual mean PM₁₀ concentration shouldn't be higher than $40 \mu\text{g}/\text{m}^3$ and this limit was not exceeded for any Attica

resident. Oppositely, WHO states that the annual value should not be higher than $20 \mu\text{g}/\text{m}^3$ and according to our study only 2% in 2018 and 3% in 2020 are exposed in concentrations under this limit, with the rest of population exposed in higher concentrations.

Table 8.2: Percentage of population exposed in different PM_{10} concentrations in the studied area.

Year	Percentage of population exposed in PM_{10} concentration:				
	under $26 \mu\text{g}/\text{m}^3$	between 26 and $30 \mu\text{g}/\text{m}^3$	between 31 and $34 \mu\text{g}/\text{m}^3$	between 35 and $38 \mu\text{g}/\text{m}^3$	greater than $38 \mu\text{g}/\text{m}^3$
2017	10.3%	39.8%	48.6%	0.0%	0.0%
2018	57.0%	22.5%	13.7%	6.0%	0.8%
2019	20.2%	36.6%	43.0%	0.1%	0.0%
2020	91.7%	7.8%	0.5%	0.0%	0.0%

8.4. Seasonal population exposure in Attica.

PM concentrations vary highly both spatially and seasonally. In order to investigate the seasonal variations in PM_{10} concentrations in Athens, the kriging method was applied for the warm period (June – September) and the cold period (December – March) for the year 2018. As it can be seen on Fig. 8.9 and 8.10 the average concentration was higher during the cold period.

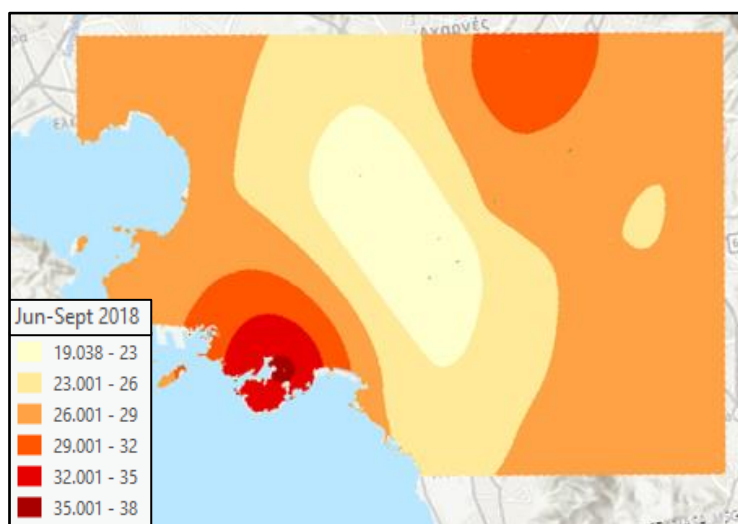


Figure 8.9: Average PM_{10} concentration during the warm period (June- September) in Attica in 2018 (created in ArcGIS Pro), (values in $\mu\text{g}/\text{m}^3$).

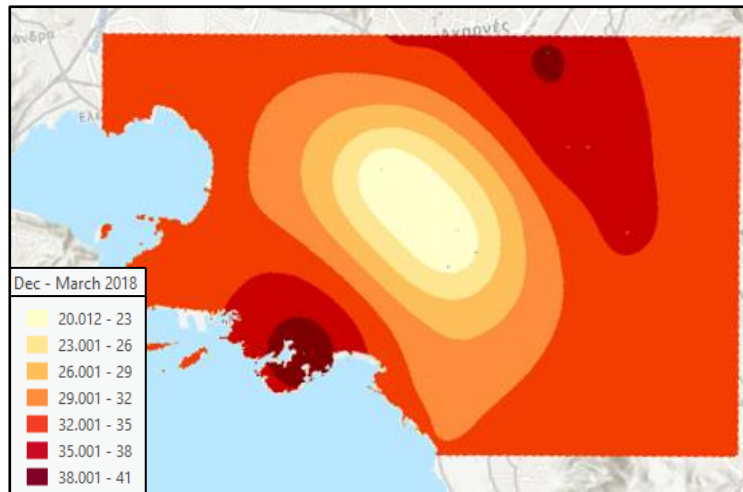


Figure 8.10: Average PM₁₀ concentration during the cold period (December- March) in Attica in 2018 (created in ArcGIS Pro) (values in µg/m³).

More than half (56%) of the population were exposed to concentration under 26 µg/m³ during the warm period while this percentage dropped to 9.8% during the cold period. On Table 8.3 can be seen that almost half of the population studied, was exposed to PM₁₀ concentration higher than 35 µg/m³, with 100,000 residents of Attica exposed in concentration over the 40 µg/m³ annual EU limit, during the cold period in 2018. Seasonal variations depend on many factors, including natural sources, but since 2012 that the biomass burning was increased for heating purposes, PM levels elevated during the cold period.

Table 8.3: Percentage of population exposed in different PM₁₀ concentrations in the studied area during the warm and cold period in 2018.

Season	Percentage of population exposed in PM ₁₀ concentration:				
	under 26 µg/m ³	between 26 and 30 µg/m ³	between 31 and 34 µg/m ³	between 35 and 38 µg/m ³	greater than 38 µg/m ³
Warm period (June- Sep)	56.0%	22.3%	14.0%	6.1%	0.8%
Cold period (Dec- March)	9.8%	22.4%	19.5%	43.2%	3.6%

8.4. Population dose calculation

The aim of this study was also to calculate the deposited dose caused by inhalation of airborne PM₁₀ in the respiratory system of the residents of Attica. The dose was estimated with the use of the exposure and dose model ExDoM₂. An analytical description of ExDoM₂ is reported at Chapter 2 and at Chalvatzaki and Lazaridis (2015) and Aleksandropoulou and Lazaridis (2013).

Important input data for the calculation of the human dose is the size distribution of the particles. Since there was not available mass size distribution data for all the studied monitoring stations available literature data were used. A mass size distribution measured in Agia Paraskevi monitoring station, during 2014–2015, using a low pressure Berner cascade impactor that collects particles into 9 size fractions (0.0255–0.062 μm , 0.062–0.11 μm , 0.11–0.173 μm , 0.173–0.262 μm , 0.262–0.46 μm , 0.46–0.89 μm , 0.89–1.77 μm , 1.77–3.4 μm , and 3.4–6.8 μm) was used (Chalvatzaki et al. 2018). Wind speed is another parameter that is important for the calculation of the personal dose. In this study the annual mean wind speed values for all the monitoring stations were used for both 2018 and 2020 (METEO).

The model was applied for 2018 where the higher concentrations, among the 4 years investigated, were recorded and for 2020 where the lowest concentrations were recorded. As it can be observed in Fig. 8.9 the personal dose in 2018 varies from 267-691 μg and in 2020 (Fig 8.10) from 267-569 μg . These results were expected as the dose is mainly correlated to the PM concentrations.

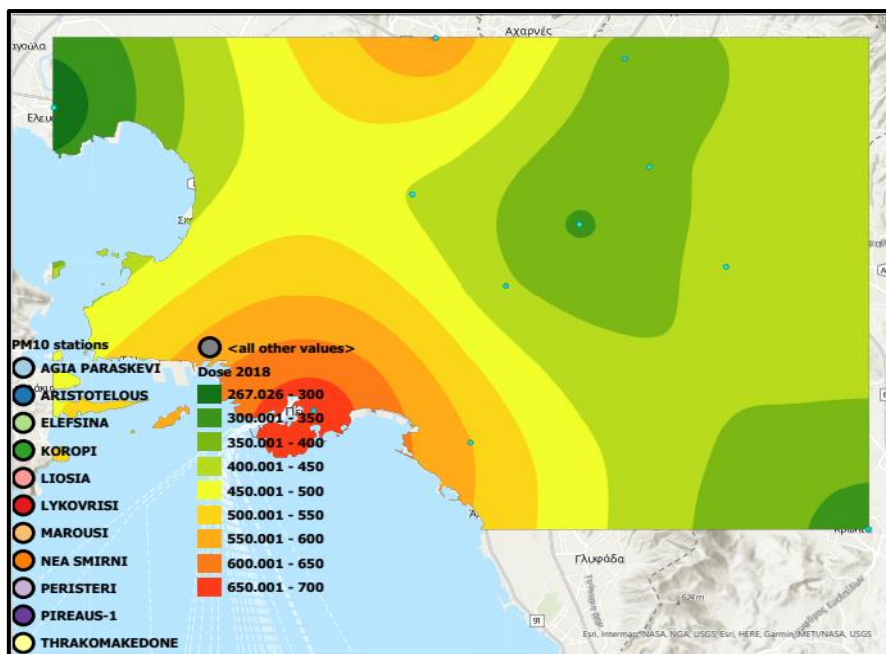


Figure 8.9: Personal dose for the population of Attica in 2018 (created in ArcPro GIS), (values in μg).

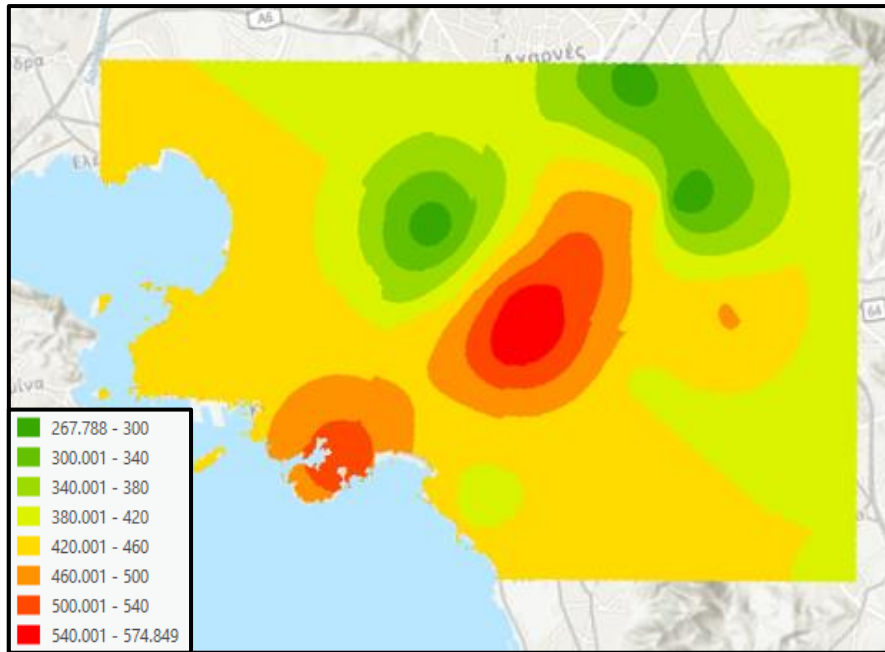


Figure 8.10: Personal dose for the population of Attica in 2020 (created in ArcPro GIS) (Values in μg).

The estimated personal dose is close with the dose estimated by Alexandropoulou and Lazaridis (2013) in Finokalia (Crete, Greece), where the daily dose ranged from 345 to 761 μg and is significantly higher from the dose calculated for Oslo, which ranged from 133 to 212 μg . Greece and the rest of southern countries are highly affected by the Sahara dust and as a result the PM levels are higher from northern cities and as a consequence also the personal dose.

8.5. Conclusions

The target of the current study was to assess the human exposure in PM_{10} with the use of a statistical method at a geographical information system. GIS systems can be very useful in visualizing and predict pollution levels if there are enough available input data. With the use of the data from the monitoring stations in Attica, population data from the census and the interpolation method of kriging, the number of people exposed in different concentration in the studied area was predicted. Moreover, spatial, yearly, and seasonal variations of PM_{10} concentrations were investigated. Finally, the dosimetry model ExDoM2 was used in combination with ArcGIS Pro to visualize and predict the human dose in the different areas of Attica. Spatial interpolation allows more efficient monitoring of air pollution and is considered an important tool in pollution prediction and environmental protection policies decision-making.

Chapter 9: Conclusions and Recommendations

9.1. General conclusions

The objective of this thesis was to study the personal and population exposure to PM₁₀ through a combination of measurement campaigns, dose models, data analysis and other computer-based systems like GIS.

The personal exposure of residents of Chania to both mass and number concentration of PM₁₀ was examined in Chapter 4 of the current thesis by conducting 24h measurements with the use of a personal monitor and a diary of activities. The aim of the study was the estimation of the exposure and dose of the studied subjects. Furthermore, the use of 1min resolution made possible to study the effect of different activities and indoor sources on human exposure. Higher concentrations among the indoor activities were observed during cooking with results varying according to the type of cooking. Between the studied subjects, higher exposure had the subjects working in a workshop, where an industrial oven was in use, highlighting the importance of occupational exposure in the daily exposure. It should be mentioned that the use of TSI OPS 3330 had the advantage of having real time size distribution data for the whole day of the measurements, but the limitation of this instrument is that particles in the size range of 0.3 to 10 µm were not measured. As a result, it was not possible to study the effect of the different activities in ultrafine particles. Furthermore, the dose model ExDoM2, was used in order to estimate the personal dose and the particles deposition in the different areas of the respiratory tract. It was concluded that most of the particles deposited in the ET region are later transferred to the GI tract, while the particles deposited to the other region of the RT are remaining to the RT or/and absorbed to the blood. Additionally, the PM₁₀ exposure of 6 M.Sc. students, the majority of them smokers, was studied showing that the smokers had daily average exposure higher than the EU limit of 50 µg/m³. Even though the limit is not applied for indoor exposure, can serve as a guideline for studying the human health risk from PM. The findings of this study highlight the importance of studying personal exposure, as it can vary significantly among individuals residing in the same city. Personal monitoring is a direct method of estimating personal dose and is considered the most appropriate, as it provides real-time data and aids in identifying health risks in diverse microenvironments.

The personal exposure from cooking in four different styles was examined in Chapter 5, as cooking is one of the most important indoor sources in residences. The effect of the different styles of cooking on the ultrafine particles was analyzed and also the dose after 1h exposure was estimated and compared to 1h exposure in background concentration. The different procedures (boiling, frying, deep frying) affected the overall concentration and the particle number size distributions. Highest concentrations and consequently highest dose was received

during the Chinese style of cooking due to the fact that the main activity was frying in contrast with Indian style of cooking that the main cooking activity was boiling.

In Chapter 6, the target of interest was the Athens metro, as it is a microenvironment of public interest since thousands of people are using it daily. Two sampling campaigns were carried out both inside the trains and on several platforms. The target was to study the exposure both of the commuters and the metro workers. Elevated concentrations were observed both inside the trains and on the platforms. Measurements were conducted mutually in the fully air-conditioned, third-generation trains and in older ones with open windows, with higher concentrations being observed at the older ones, showing the influence of the air exchange between the trains and the tunnels in the inside the trains air quality. Since the major source of particles is the air penetrating from the tunnels, the closing of the windows and the filtration of the air on the third-generation trains, which are equipped with a ventilation system, can reduce the inside the trains concentration. Lower concentrations were detected during the measurements carried out in the weekends, since the train frequency is lower, and the wagons are not crowded. Moreover, it was concluded that in the majority of the cases the opening of the train doors at the stations, decreases the internal concentration, except the cases that the train stops in popular stations, which have elevated concentrations. Regarding the measurements conducted on the platforms, higher concentrations were measured at the ones located in the center of Athens or/and under heavily trafficked streets. Additionally, the deposition and dose of particles was estimated with the use of ExDoM2 for a commuter, a metro worker with sedentary occupation, and a metro worker with light exercise occupation. Metro worker with light exercise received the highest dose among the studied subjects since dose depends on the exposure concentration and on the inhalation rates. It is worth mentioning, that it was concluded that even though commuters spend a short fraction of the day in the metro, the metro microenvironment contributes highly to their daily dose.

Moreover, the deposition of heavy metals in the human body from the inhalation of particle-bound metals, is the studied subject in Chapter 7. Available concentration data from five different European cities, along with ExDoM and a pharmacokinetic PBPK model (Chalvatzaki et al., 2014; Chalvatzaki et al., 2015) were used to determine the particle-bound metals dose in the human body. Higher metals deposition was observed in the residents of the cities with the more elevated particulate matter-bound metals concentrations. In all the cities under study, heavy metal concentrations were below the EU thresholds for intake of Lead and Cadmium. The measuring of particle-bound metals is very important so as to identify the potential sources of contamination and take measurements in order to maintain low concentrations. PBPK model is a key factor in understanding the deposition of metals in human body, to estimate the dose and the potential health effects.

Finally, in Chapter 8, unlike with the rest of the chapters, the focus is on the population exposure. The aim was to estimate the population exposure in PM by employing available data from monitoring stations, census data and statistical techniques within a GIS. Available PM data along with kriging interpolation, predicted the number of individuals exposed to different concentrations of PM₁₀ across the studied area. During the 4 studied years, the average annual PM₁₀ concentration didn't exceed the EU limit, but almost the whole population is exposed in average annual concentration higher than 20 µg/m³, that is the limit suggested by WHO. Furthermore, the seasonal variation was also studied for the year with the higher concentration among the studied years, that showed that almost half of the population studied, was exposed to PM₁₀ concentration higher than 35 µg/m³, with 100,000 residents of Attica exposed in concentration over the 40 µg/m³ annual EU limit, during the cold period. Air quality studies in combination with dosimetry models and spatial interpolation can assist to calculate and visualize the human exposure and dose and to identify the health risks in order to protect the public health.

9.2. Recommendations

The enhanced understanding of personal exposure to PM, leads to better indoor air quality and helps in decision making of strategies aiming to reduce human exposure.

Future studies can focus on personal monitoring campaigns in larger scale or in a specific group of people, or on more vulnerable people like people with respiratory issues (COPD patients). Alterations could be made to the dosimetry model in order to apply also to patients with COPD.

Furthermore, in the current study the GIS tool was used with the available data of the YPEKA monitoring stations. In the future, for more accurate estimations, data from many microsensors placed in the studied area, subsequently with the data available from the monitoring stations can lead to a more accurate estimation of the personal dose.

References

- Aarnio P., Yli-Tuomi T., Kousa A., Mäkelä T., Hirsikko A., Hämeri K., Räsänen M., Hillamoc R., Koskentalo T., Jantunen M. (2005) The concentrations and composition of and exposure to fine particles (PM 2.5) in the Helsinki subway system. *Atmospheric Environment* 39:5059-5066. doi:10.1016/j.atmosenv.2005.05.012.
- Adams H., Nieuwenhuijsen M., Colvile R., McMullen M., Khandelwal P. (2001) Fine particle (PM 2.5) personal exposure levels in transport microenvironments, London, UK. *Science of the Total Environment* 279:29-44. doi:10.1016/S0048-9697(01)00723-9.
- Aleksandropoulou V., Lazaridis M. (2013) Development and application of a model (ExDoM) for calculating the respiratory tract dose and retention of particles under variable exposure conditions. *Air Quality Atmosphere & Health* 6:13–26. doi: 10.1007/s11869-010-0126-z.
- Álvarez F., Rodríguez T., Espinosa F., Dabán G. (2004) Physical speciation of arsenic, mercury, lead, cadmium and nickel in inhalable atmospheric particles. *Analytica Chimica Acta* 524: 33–40. doi: 10.1016/j.aca.2004.02.004.
- Canepari S., Perrino C., Olivieri F., Astolfi M.L. (2008) Characterization of the traffic sources of PM through size-segregated sampling, sequential leaching and ICP analysis. *Atmospheric Environment* 42: 8161–8175. doi: 10.1016/j.atmosenv.2008.07.052.
- Attiko metro (2016) <http://www.ametro.gr>. Accessed 15 January 2016
- Barmpareos N., Assimakopoulos V., Assimakopoulos M., Tsairidi E. (2016) Particulate matter levels and comfort conditions in the trains and platforms of the Athens underground metro. *AIMS Environ Sci* 3(2):199–219. doi:10.3934/environsci.2016.2.199.
- Barnett A., Williams G., Schwartz J, Neller A., Best T., Petroeschevsky A., Simpson R. (2005). Air pollution and child respiratory health: a case-crossover study in Australia and New Zealand. *Am J Respir Crit Care Med*. 2005 Jun 1;171(11):1272-8. doi: 10.1164/rccm.200411-1586OC. Epub 2005 Mar 11.
- Boomhower S.R., Long C.M., Li W., Manidis T.D., Bhatia A, Goodman J.E. (2022) A review and analysis of personal and ambient PM_{2.5} measurements: Implications for epidemiology studies. *Environ Res*. 2022 Mar;204(Pt B):112019. doi: 10.1016/j.envres.2021.112019.
- Brunekreef B, Forsberg B. Epidemiological evidence of effects of coarse airborne particles on health. *Eur Respir J*. 2005 Aug;26(2):309-18. doi: 10.1183/09031936.05.00001805.

Buonanno G., Morawska L., Stabile L., (2009) Particle emission factors during cooking activities. *Atmospheric Environment*, Volume 43, Issue 20, 2009, Pages 3235-3242, doi:10.1016/j.atmosenv.2009.03.044.

Carteni A., Cascetta F., Campana S. (2015) Underground and ground-level particulate matter concentrations in an Italian metro system. *Atmos Environ* 101:328-337. doi:10.1016/j.atmosenv.2014.11.030.

Cattaneo A., Campo L., Iodice S., Spinazzè A., Olgiati L., Borghi F., Polledri E., Angelici L., Cavallo DM., Fustinoni S., Bollati V.. (2021) Environmental and biological monitoring of personal exposure to air pollutants of adult people living in a metropolitan area. *Sci Total Environ*. 2021 May 1;767:144916. doi: 10.1016/j.scitotenv.2020.144916.

Chalvatzaki E., Aleksandropoulou V. and Lazaridis M. (2014) A Case Study of Landfill Workers Exposure and Dose to Particulate Matter-Bound Metals. *Water, Air, & Soil Pollution* 225:1782. doi :10.1007/s11270-013-1782-z.

Chalvatzaki E., Lazaridis M.. (2015) Development and application of a dosimetry model (ExDoM2) for calculating internal dose of specific particle-bound metals in the human body. *Inhal Toxicol* 27:308-320. doi: 10.3109/08958378.2015.1046201.

Chalvatzaki E., Chatoutsidou S.E, Mammi-Galani E., Almeida S.M., Gini M.I., Eleftheriadis K., Diapouli E., Lazaridis M. (2018). Estimation of the Personal Deposited Dose of Particulate Matter and Particle-Bound Metals Using Data from Selected European Cities. *Atmosphere* 9 (7), 248. doi:10.3390/atmos9070248.

Chalvatzaki E., Chatoutsidou S.E., Almeida, S.M., Morawska, L., Lazaridis, M. (2023) The Representativeness of Outdoor Particulate Matter Concentrations for Estimating Personal Dose and Health Risk Assessment of School Children in Lisbon. *Int. J. Environ. Res. Public Health* 2023, 20, 5564. doi:10.3390/ijerph20085564.

Cheng Y., Liu Z., Yan J. (2012) Comparisons of PM₁₀, PM_{2.5}, particle number, and CO₂ levels inside metro trains travelling in underground tunnels and on elevated tracks. *Aerosol Air Qual. Res* 12:879-891. doi: 10.4209/aaqr.2012.05.0127.

Childs C. (2004). Interpolating SURFACES IN ArcGIS spatial analyst (pp. 32–35). ArcUser, July–September. Internet version available at <http://www.esri.com>.

Chillrud S., Epstein D., Ross J., Sax S., Pederson D., Spengler J., Kinney P. (2004) Elevated airborne exposures of teenagers to manganese, chromium, and iron from steel dust and New York City's subway system. *Environ Sci Technol* 38:732–737. doi:10.1021/es034734y.

Chillrud S., Grass M., Ross M., Coulibaly D., Slavkovich M., Epstein M., Sax S., Pederson D., Johnson D., Spengler J., Kinney P. (2005) Steel dust in the New York City subway system as a source of manganese, chromium, and iron exposures for transit workers. *J Urban Health* 82:33-42. doi: 10.1093/jurban/jti006

Chiou H.Y., Hsueh Y.M., Liaw K.F., Horng S.F., Chiang M.H., Pu Y.S., Lin J.S., Huang C.H., Chen C.J. (1995) Incidence of internal cancers and ingested inorganic arsenic: a seven-year follow-up study in Taiwan. *Cancer Research* 55: 1296–1300.

Chou WC., Chio CP., Liao CM. (2009) Assessing airborne PM-bound arsenic exposure risk in semiconductor manufacturing facilities. *Journal of Hazardous Materials*, Volume 167, Issues 1–3, P 976-986. doi: 10.1016/j.jhazmat.2009.01.079.

Chung A, Chang D, Kleeman M, Perry K, Cahill T, Dutcher D, McDougall E, Stroud K (2001) Comparison of Real-Time Instruments Used To Monitor Airborne Particulate Matter. *J Air Waste Manage* 51:109-120. doi: 10.1080/10473289.2001.10464254.

Colbeck I., Lazaridis M. (2013) *Aerosol Science: Technology and Applications*. John Wiley & Sons, Ltd. ISBN:9781118682555. doi:10.1002/9781118682555.

Cusack M, Talbot N, Ondráček J, Minguillón M, Martins V, Klouda K, Scwarz J, Ždímal V (2015) Variability of aerosols and chemical composition of PM 10, PM 2.5 and PM 1 on a platform of the Prague underground metro. *Atmos Environ* 118: 176-183. doi:10.1016/j.atmosenv.2015.08.013. doi:10.1080/02786820500191348.

Davidson C., Phalen R., Solomon P. (2005). Airborne Particulate Matter and Human Health: A Review. *Aerosol Science and Technology*. 39. 737-749. doi:10.1080/02786820500191348.

Delfino, R.J., Sioutas, C., Malik, S. (2005) Potential role of ultrafine particles in associations between airborne particle mass and cardiovascular health. *Environ Health Perspect*. 2005 Aug;113(8):934-46. doi: 10.1289/ehp.7938.

Dockery DW, Pope CA 3rd, Xu X, Spengler JD, Ware JH, Fay ME, Ferris BG Jr, Speizer FE. (1993) An association between air pollution and mortality in six U.S. cities. *N Engl J Med*. 1993 Dec 9;329(24):1753-9. doi: 10.1056/NEJM199312093292401.

Eleftheriadis K., Ochsenkuhn K.M., Lympelopoulou T., Karanasiou A., Razos P., Ochsenkuhn-Petropoulou M. (2014) Influence of local and regional sources on the observed spatial and temporal variability of size resolved atmospheric aerosol mass concentrations and water-soluble species in Athens metropolitan area. *Atmos Environ* 97:252–261. doi:10.1016/j.atmosenv.2014.08.013.

ELSTAT (2011) Census 2011. Available online :
<https://geodata.gov.gr/dataset?groups=society>

Espinosa A.F., Rodriguez T., Barragan F., Sánchez J. (2001) Size distribution of metals in urban aerosols in Seville (Spain). *Atmospheric Environment* 35: 2595-2601. doi:10.1016/S1352-2310(00)00403-9.9

Fameli K., Assimakopoulos V. (2015) Development of a road transport emission inventory for Greece and the Greater Athens Area: effects of important parameters. *Sci Total Environ* 505:770–786. doi:10.1016/j.scitotenv.2014.10.015

FAO/WHO (1999) Summary of Evaluations Performed by the Joint FAO/WHO Expert Committee on Food Additives Codex. http://www.inchem.org/documents/jecfa/jecval/jec_1260.htm Accessed 9 February 2014

First Daughter Directive (1999/30/EC), Commission of the European Communities Official, Journal of the European Communities, COM 423 final, 0164 Cod, 2003

Fourth Daughter Directive (2004/107/EC), Commission of the European Communities Official, Journal of the European Communities, COM 423 final, 0164 Cod, 2003

Gali K., Jiang Y., Yang F., Sun L., Ning Z. (2017) Redox characteristics of size-segregated PM from different public transport microenvironments in Hong Kong. *Air Qual Atmos Health* 39:1–12. doi:10.1007/s11869-017-0473-0.

Gerasopoulos E., Gratsea, M., Liakakou E., Lianou M., Psiloglou B., Kappos N., Kambezidis H., Mihalopoulos N. (2017) An Overview of Biomass Burning Impacts on Athens Air Quality and Analysis of Its Increasing Significance. *Perspectives on Atmospheric Sciences* (pp.1111-1116). doi:10.1007/978-3-319-35095-0_159.

Grass D., Ross J., Family F., Barbour J., Simpson H., Coulibaly D., Hernandez J, Chen Y, Slavkovich V, Lib Y, Graziano J, Santellab R, Brandt-Raufb P, Chillrud S (2010) Airborne particulate metals in the New York City subway: a pilot study to assess the potential for health impacts. *Environ Res* 110:1-11. doi: 10.1016/j.envres.2009.10.006.

Grivas G., Chaloulakou A., Kassomenos P. (2008) An overview of the PM₁₀ pollution problem, in the Metropolitan Area of Athens, Greece. Assessment of controlling factors and potential impact of long range transport. *Sci Total Environ* 389:165-177. doi:10.1016/j.scitotenv.2007.08.048.

Guo L., Hu Y., Hu Q., Lin J., Li C., Chen J., Li L., Fu H. (2014) Characteristics and chemical compositions of particulate matter collected at the selected metro stations of Shanghai, China. *Sci Total Environ* 496:443-452. doi:10.1016/j.scitotenv.2014.07.055

Hänninen O.O., Salonen RO, Koistinen K, Lanki T, Barregard L, Jantunen M. (2009) Population exposure to fine particles and estimated excess mortality in Finland from an East European wildfire episode. *J Expo Sci Environ Epidemiol.* 2009 May;19(4):414-22. doi: 10.1038/jes.2008.31.

Hildemann L.M., Markowski G.R., and Cass G.R. (1991) Chemical composition of emissions from urban sources of fine organic aerosol. *Environmental Science & Technology*, 25: 744–759

Hinds, W. C. (1999). *Aerosol technology : properties, behavior, and measurement of airborne particles*. 2nd ed. New York (N.Y.): Wiley.

IARC (2023) IARC Biennial Report 2022-2023.ISBN-13978-92-832-1108-2. doi: 10.1016/j.atmosenv.2009.03.044.

ICRP (1994a) Human Respiratory Tract Model for Radiological Protection, ICRP Publication 66. Pergamon Press, Oxford

ICRP (1994b) Dose Coefficients for intake of radionuclides by workers, ICRP Publication 68. Pergamon Press, Oxford

ICRP (2003) Human Basic Anatomical and Physiological Data for Use in Radiological Protection:Reference Values, ICRP Publication 89. Pergamon Press, Oxford

ICRP, (2003). Basic Anatomical and Physiological Data for Use in Radiological Protection Reference Values. ICRP Publication 89. *Ann. ICRP* 32 (3-4).

ICRP. (2012). Occupational intakes of radionuclides. *Ann. ICRP*. Publication in advanced Drafting. http://ani.sagepub.com/site/includefiles/upcoming_icrp_reports.xhtml.

ICRP, 2015. Occupational Intakes of Radionuclides: Part 1. ICRP Publication 130. *Ann. ICRP* 44(2).

IRIS, Integrated Risk Information System. EPA. <http://www.epa.gov/IRIS/> Accessed 18 January 2014

Jarup L. (2003) Hazards of heavy metal contamination. *British Medicine Bulletin*, 68:167-182. doi: 10.1093/bmb/ldg032.

Johansson C., Johansson A. (2003) Particulate matter in the underground of Stockholm. *Atmos Environ* 37:3–9. doi:10.1016/S1352-2310(02)00833-6.

Kalantzi O.I, Nezis I, Biskos G. (2021) The positive impact of the first-wave COVID-19 lockdown on urban air quality in Greece. *ISEE Conference Abstracts*, Volume 2021, Issue 1. doi: 10.1289/isee.2021.P-221.

Kam W., Cheung K., Daher N., Sioutas C. (2011) Particulate matter (PM) concentrations in underground and ground-level rail systems of the Los Angeles Metro. *Atmos Environ* 45:1506-1516. doi:10.1016/j.atmosenv.2010.12.049.

Kamani H., Hoseini M., Seyedsalehi M., Mahdavi Y., Jaafari J., Safari G. (2014) Concentration and characterization of airborne particles in Tehran's subway system. *Environ Sci Polluti R*, 21:7319-7328. doi:10.1007/s11356-014-2659-4.

Karanasiou A.A., Sitaras I.E., Siskos P.A., Eleftheriadis K. (2007) Size distribution and sources of trace metals and n-alkanes in the Athens urban aerosol during summer. *Atmospheric Environment* 41: 2368–2381.

Karlsson H., Nilsson L., Möller L. (2005) Subway particles are more genotoxic than street particles and induce oxidative stress in cultured human lung cells. *Chem Res Toxicol*, 18:19-23. doi: 10.1021/tx049723c.

Kim J., Magari S., Herrick R., Smith T., Christiani D. (2004) Comparison of Fine Particle Measurements from a Direct-Reading Instrument and a Gravimetric Sampling Method. *J Occup and Environ* 11:707-715. doi: 10.1080/15459620490515833.

Kim K., Kim Y., Roh Y., Lee C., Kim C. (2008) Spatial distribution of particulate matter (PM 10 and PM 2.5) in Seoul Metropolitan Subway stations. *J Hazard Mater* 154: 440-443. doi:10.1016/j.jhazmat.2007.10.042.

Kjellstrom T., Nordberg G..F (1978) A kinetic model of cadmium metabolism in the human being. *Environmental Research* 16: 248-269. doi:10.1016/0013-9351(78)90160-3.

Kopanakis, I., Mammi-Galani, E., Pentari, D. T. Glytsos, M. Lazaridis (2018) Ambient Particulate Matter Concentration Levels and their Origin During Dust Event Episodes in the Eastern Mediterranean, *Aerosol Science and Engineering*, doi: 10.1007/s41810-018-0023-7, pp 1–13.

Kousa, A., Oglesby, L., Koistinen, K., Künzli, N., Jantunen, M. (2002) Exposure chain of urban air PM_{2.5}—Associations between ambient fixed site, residential outdoor, indoor, workplace

and personal exposures in four European cities in the EXPOLIS-study. *Atmos. Environ.* 2002, 36, 3031–3039. doi: 10.1016/S1352-2310(02)00232-7.

Lazaridis M. (2011) *First Principles of Meteorology and Air Pollution*. Environmental Pollution Book 19, Springer. ISBN 978-94-007-0161-8. doi: 10.1007/978-94-007-0162-5.

Lazaridis M., Dzumbova L., Kopanakis I., Ondracek J., Glytsos T., Aleksandropoulou V., Voulgarakis A., Katsivela E., Mihalopoulos N., Eleftheriadis, K. PM₁₀ and PM_{2.5} Levels in the Eastern Mediterranean (Akrotiri Research Station, Crete, Greece). *Water Air Soil Pollut* **189**, 85–101 (2008). doi:10.1007/s11270-007-9558-y.

Lenz, T. (2010). Pharmacokinetic Drug Interactions With Physical Activity. *American Journal of Lifestyle Medicine*. 4. 226-229. doi: 10.1177/1559827610361565.

Liao C.M., Lin T.L., Chen S.C. A Weibull-PBPK model for assessing risk of arsenic-induced skin lesions in children. (2008) *Sci Total Environ.* 2008 Mar 25;392(2-3):203-17. doi: 10.1016/j.scitotenv.2007.12.017.

Lioy P. (1995) *Measurement Methods for Human Exposure Analysis*. Environmental Health Perspectives Vol. 103, Supplement 3: Human Tissue Monitoring and Specimen Banking (Apr., 1995), pp. 35-43. doi: 10.2307/3432558

Löndahl J., Möller W., Pagels JH., Kreyling W., Swietlicki E., Schmid O. (2014) Measurement techniques for respiratory tract deposition of airborne nanoparticles: a critical review. *J Aerosol Med Pulm Drug Deliv.* 2014 Aug;27(4):229-54. doi: 10.1089/jamp.2013.1044.

Maggs R. (2000) *A Review of Arsenic in Ambient Air in the UK*. Department of the Environment, Transport and the Regions Scottish Executive, The National Assembly for Wales. <http://uk-air.defra.gov.uk/assets/documents/reports/empire/arsenic00/arsenic.htm> Accessed 3 March 2014

Majid H., Madl P. (2011). Lung deposition predictions of airborne particles and the emergence of contemporary diseases Part-I. *theHealth*, Vol. 2, No. 2, 2011, p. 51-59.

Martins V., Minguillón M., Moreno T., Querol X., de Miguel E., Capdevila M., Centelles S., Lazaridis M. (2015a) Deposition of aerosol particles from a subway microenvironment in the human respiratory tract. *J Aerosol Sci* 90:103-113. doi:10.1016/j.jaerosci.2015.08.008.

Martins V., Moreno T., Minguillón M., Amato F., de Miguel E., Capdevila M., Querol X. (2015b) Exposure to airborne particulate matter in the subway system. *Sci Total Environ* 511:711–722. doi:10.1016/j.scitotenv.2014.12.013.

Martins V., Moreno T., Minguillón M., van Drooge B., Amato F., de Miguel E., Capdevila M., Centelles S., Querol X. (2016a) Origin of inorganic and organic components of PM_{2.5} in subway stations of Barcelona, Spain. *Environ Pollut* 208:125-136. doi:10.1016/j.envpol.2015.07.004.

Martins V., Moreno T., Mendes L., Eleftheriadis K., Diapouli E., Alves C., Duarte M., Miguel E., Capdevila M., Querol X., Minguillón M. (2016b) Factors controlling air quality in different European subway systems. *Environ Res* 146:35-46. doi:10.1016/j.envres.2015.12.007.

McGowan, J.A., Hider, P.N., Chacko, E. and Town, G.I. (2002). Particulate air pollution and hospital admissions in Christchurch, New Zealand. *Australian and New Zealand Journal of Public Health*, 26: 23-29. doi: 10.1111/j.1467-842X.2002.tb00266.x.

Moolgavkar S. Air pollution and hospital admissions for chronic obstructive pulmonary disease in three metropolitan areas in the United States. (2002) *Inhal Toxicol.* 2000;12 Suppl 4:75-90. doi: 10.1080/089583700750019512.

Morawska L., Salthammer T. (2003) Indoor environment: airborne particles and settled dust. WILEY VCH, Weinheim doi:10.1002/9783527610013

Moreno T., Martins V., Querol X., Jones T., BéruBé K., Minguillón M.C., Amato F., Capdevila M., Miguel E., Centelles S., Gibbons W. (2015) A new look at inhalable metalliferous airborne particles on rail subway platforms. *Sci Total Environ* 505:367-375. doi: 10.1016/j.scitotenv.2014.10.013.

Moreno T., Kelly F., Dunster C., Oliete A., Martins V., Reche C., Minguillón M., Amato F., Capdevila M., Miguel E., Querol X. (2017) Oxidative potential of subway PM_{2.5}. *Atmos Environ* 148:230-238. doi:10.1016/j.atmosenv.2016.10.045.

Mosqueron L., Momas I., Le Moullec Y. (2002) Personal exposure of Paris office workers to nitrogen dioxide and fine particles. *Occupational and Environmental Medicine* 2002;59:550-555. doi: 10.1136/oem.59.8.550.

Nerriera, E., Zmirou-Naviera, D., Blanchardb, O., Momas, I., Ladner, J., Le Moullec, Y., Personnaz, M.B., Lameloise, P., Delmas, V., Target, A., Desqueyroux, H. (2005) Can we use fixed ambient air monitors to estimate population long-term exposure to air pollutants? The case of spatial variability in the Genotox ER study. *Environmental Research* 97 (1), 32e42. doi:10.1016/j.envres.2004.07.009.

Nieuwenhuijsen M, Gómez-Perales J, Colville R (2007) Levels of particulate air pollution, its elemental composition, determinants, and health effects in metro systems. *Atmos Environ* 41:7995–8006. doi:10.1016/j.atmosenv.2007.08.002.

Papagiannakis E. (2015) User-friendly interface for ExDoM2 and model application for the dose estimation in Athens metro. Master thesis in the Schools of Chemical and Environmental Engineering (in Greek).

Pérez N., Pey J., Querol X., Alastuey A., López J.M., Viana (2008) Partitioning of major and trace components in PM₁₀–PM_{2.5}–PM₁ at an urban site in Southern Europe. *Atmospheric Environment*, 42: 1677-1691. doi:10.1016/j.atmosenv.2007.11.034

Perrino C., Catrambone M., Pietrodangelo A. (2008) Influence of atmospheric stability on the mass concentration and chemical composition of atmospheric particles: A case study in Rome, Italy. *Environment International* 34: 621-628. . doi:10.1016/j.envint.2007.12.006.

Perrino C., Marcovecchio F., Tofful L., Canepari S. (2015) Particulate matter concentration and chemical composition in the metro system of Rome, Italy. *Environ Sci Pollut Res Int* 22:9204-9214. doi: 10.1007/s11356-014-4019-9.

Pope C. A. (2000) Epidemiology of fine particulate air pollution and human health: biologic mechanisms and who's at risk? *3rd Environ Health Perspect.* 108: 713–723.

Pope A. III (2000) Review: Epidemiological Basis for Particulate Air Pollution Health Standards, *Aerosol Science & Technology*, 32:1, 4-14, DOI: 10.1080/027868200303885.

Pope C.A. 3rd, Burnett R.T., Thun M.J., Calle E.E, Krewski D., Ito K., Thurston G.D. (2002) Lung cancer, cardiopulmonary mortality, and long-term exposure to fine particulate air pollution. *JAMA.* 2002 Mar 6;287(9):1132-41. doi: 10.1001/jama.287.9.1132.

Pope C. 3rd, Dockery D. Health effects of fine particulate air pollution: lines that connect. (2006) *J Air Waste Manag Assoc.* 2006 Jun;56(6):709-42. doi:10.1080/10473289.2006.10464485.

Ramos C., Wolterbeek H., Almeida S. (2016) Air pollutant exposure and inhaled dose during urban commuting: a comparison between cycling and motorized modes. *Air Qual Atmos Health.* doi:10.1007/s11869-015-0389-5.

Rogula-Kozłowska W., Kozielska B., Klejnowski K. (2013) Hazardous Compounds in Urban Pm in the Central Part of Upper Silesia (Poland) in Winter. *Archives of Environmental Protection* 39: 53 – 65. doi:10.2478/aep-2013-0002.

Rückerl, R., Schneider, A., Breitner, S., Cyrus, J., Peters, A. (2011) Health effects of particulate air pollution: A review of epidemiological evidence. *Inhal Toxicol.* 2011 Aug;23(10):555-92. doi: 10.3109/08958378.2011.593587.

Salma I., Weidinger T., Maenhaut W. (2007) Time-resolved mass concentration, composition and sources of aerosol particles in a metropolitan underground railway station. *Atmos Environ* 41: 8391-8405. doi:10.1016/j.atmosenv.2007.06.017.

Samara C., Voutsas D. (2005) Size distribution of airborne particulate matter and associated heavy metals in the roadside environment. *Chemosphere* 59:1197–1206. doi: 10.1016/j.chemosphere.2004.11.061.

Sánchez-Soberón F., Mari M., Kumar V., Rovira J., Nadal M., Schuhmacher M. (2015) An approach to assess the particulate matter exposure for the population living around a cement plant: modelling indoor air and particle deposition in the respiratory tract. *Environ Res* 143:10–18. doi:10.1016/j.envres.2015.09.008

Schwartz C.E., Snidman N., Kagan J. (1999) Adolescent social anxiety as an outcome of inhibited temperament in childhood. *J Am Acad Child Adolesc Psychiatry.* 1999 Aug;38(8):1008-15. doi: 10.1097/00004583-199908000-00017.

See, W. and Balasubramanian, R. (2006) Physical Characteristics of Ultrafine Particles Emitted from Different Gas Cooking Methods. *Aerosol and Air Quality Research*, Vol. 6, No. 1, pp. 82-92, 2006

Sharma M, Maheshwari M, Morisawa S (2005) Dietary and inhalation intake of lead and estimation of blood lead levels in adults and children in Kanpur, India. *Risk Anal* 25: 1573-1588

Sharma M., Maheshwari M., Morisawa S. Dietary and inhalation intake of lead and estimation of blood lead levels in adults and children in Kanpur, India. (2005) *Risk Anal.* 2005 Dec;25(6):1573-88. doi: 10.1111/j.1539-6924.2005.00683.x.

Sicard P, Agathokleous E, De Marco A, Paoletti E, Calatayud V (2021) Urban population exposure to air pollution in Europe over the last decades. *Environ Sci Eur* **33**, 28 (2021). doi:10.1186/s12302-020-00450-2

Solomon Paul A. (2011) Special Issue of Atmospheric Environment for Air Pollution and Health: Bridging the Gap from Sources-to-Health Outcomes. *Atmospheric Environment* 45: 7537–7539

STASY (2017) <http://www.stasy.gr/index.php?id=342&L=title%3D%CE%9E%CE%95%CE%9E%CE%89%CE%9F%CE%83%CE>. Accessed 05 May 2017

Thomaidis N., Bakeas E., Siskos P. (2003) Characterization of lead, cadmium, arsenic and nickel in PM_{2.5} particles in the Athens atmosphere, Greece. *Chemosphere* 52:959–966

U.S. EPA (2011) *Exposure Factors Handbook 2011 Edition (Final)*. U.S. Environmental Protection Agency, Washington, DC, EPA/600/R-09/052F, 2011. <http://www.epa.gov/ncea/efh>. Accessed 15 January 2016

Varotsos C, Christodoulakis J, Kouremadas G.A, Fotaki E.F (2021) The Signature of the Coronavirus Lockdown in Air Pollution in Greece. *Water Air Soil Pollut* **232**, 119 (2021). doi:10.1007/s11270-021-05055-

Wang X and Gao H (2011) Exposure to fine particle mass and number concentrations in urban transportation environments of New York City. *TRANSPORT RES D-TR E Transport Res D-Tr E* 16:384-391. doi:10.1016/j.trd.2011.03.001

WHO (1993) Evaluation of certain food additives and contaminants, Forty-first report of Joint FAO/WHO Expert Committee on Food Additives. World Health Organization Technical Report Series, 837, 1–53.

WHO (1999) Hazard Prevention and Control in the Work Environment: Airborne Dust. WHO, Geneva - WHO/SDE/OEH/99.14. Available online at: http://www.who.int/occupational_health/publications/airdust/en/ Accessed 5 February 2014

WHO (2006) Inorganic and Organic Lead Compounds, World Health Organization, International agency for research on cancer Available online at: <http://www.inchem.org/documents/iarc/vol87/volume87.pdf> Accessed 24 January 2014

WHO (2007) Cadmium and cadmium compounds, World Health Organization, International agency for research on cancer. Available online at: <http://www.inchem.org/documents/iarc/vol58/mono58-2.html> Accessed 24 January 2014

WHO (2010) Ten chemicals of major public health concern, International Programme on Chemical Safety. Available online at: http://www.who.int/ipcs/assessment/public_health/chemicals_phc/en/ Accessed 24 January 2014

WHO (2020) Chronic obstructive pulmonary disease (COPD). Available online at: [https://www.who.int/news-room/fact-sheets/detail/chronic-obstructive-pulmonary-disease-\(copd\)](https://www.who.int/news-room/fact-sheets/detail/chronic-obstructive-pulmonary-disease-(copd))

Williams A., Jones J.M., Pourkashanian, M. (2012) Pollutants from the combustion of solid biomass fuels, *Progress in Energy and Combustion Science*, Volume 38, Issue 2, 2012, Pages 113-137, doi:10.1016/j.pecs.2011.10.001

Xu, H., Li, Y., Guinot, B., Wang, J., He, K., Ho, K. F., Cao, J., Shen, Z., Sun, J., Lei, Y., Gong, X., & Zhang, T. (2018). Personal exposure of PM_{2.5} emitted from solid fuels combustion for household heating and cooking in rural Guanzhong Plain, northwestern China. *Atmospheric Environment*, 185(Complete), 196–206. <https://doi.org/10.1016/j.atmosenv.2018.05.01>

Yang Y., Xu X. and Georgopoulos PG. (2010) A Bayesian population PBPK model for multiroute chloroform exposure. *J Exposure Sci Environ Epidemiol*, 20: 326-341

Ye W, Thangavel G, Pillarisetti A, Steenland K, Peel JL, Balakrishnan K, Jabbarzadeh S, Checkley W, Clasen T; HAPIN Investigators. (2022) Association between personal exposure to household air pollution and gestational blood pressure among women using solid cooking fuels in rural Tamil Nadu, India. *Environ Res*. 2022 May 15;208:112756. doi: 10.1016/j.envres.2022.112756.

Ypeka, 2006. National Reporting to the Fourteenth & Fifteenth Sessions of the Commission for sustainable development of the United Nations (UNCSD 14 – UNCSD 15), Greece. Hellenic Republic Ministry for the Environment, Physical Planning and Public Works. <http://www.ypeka.gr/LinkClick.aspx?fileticket=UFZ9SMfr7wQ%3D&tabid=552>. Accessed 15 January 2016

YPEKA (2015) Air pollution annual report 2015. Hellenic Ministry of Environment and Energy. <http://www.ypeka.gr/LinkClick.aspx?fileticket=81Y3zyY9w%2BU%3D&tabid=490&language=el-GR>. Accessed 15 January 2017

Zereini F., Alt F., Messerschmidt J., Wiseman C., Feldmann I., von Bohlen A., Müller J., Liebl K., Püttmann W. (2005) Concentration and Distribution of Heavy metals in Urban Airborne Particulate Matter in Frankfurt am Main, Germany. *Environ Sci Technol*. 39: 2983-2989

Appendix A

The following journal and conference articles were published or presented within the present thesis.

A1. Scientific Journals

Relative to the present thesis:

Mammi-Galani, E., Chalvatzaki, E. and Lazaridis, M. (2016). Personal Exposure and Dose of Inhaled Ambient Particulate Matter Bound Metals in Five European Cities. *Aerosol Air Quality Res.* 16: 1452-1463. doi:10.4209/aaqr.2015.09.0536

Mammi-Galani E., Eleftheriadis K., Mendes L. and Lazaridis M. (2017). Exposure and dose to particulate matter inside the subway system of Athens, Greece. *Air Quality Atmosphere & Health.* 10, 1015–1028. doi:10.1007/s11869-017-0490-z

Other:

Kopanakis I., Mammi-Galani E., Pentari D., Glytsos T., Lazaridis M. (2017). Ambient Particulate matter concentration levels and their origin during dust event episodes in the eastern Mediterranean. *Aerosol Science and Engineering,* 2: 61-73. doi:10.1007/s41810-018-0023-7

Chalvatzaki E., Chatoutsidou S.E., Mammi-Galani E., Almeida S.M, Gini M.I., Eleftheriadis K., Diapouli E., Lazaridis M. (2018) Estimation of the Personal Deposited Dose of Particulate Matter and Particle-Bound Metals Using Data from Selected European Cities. *Atmosphere* 9(7): 248. doi.org/10.3390/atmos9070248

A2. Conference presentations

Mammi-Galani E., Eleftheriadis K., Lazaridis, M., Particulate matter personal exposure in the Athens metro system. European Aerosol Conference, Milan, Italy, 6-11 September 2015.

Appendix B

Detailed figures of Chapter 4:

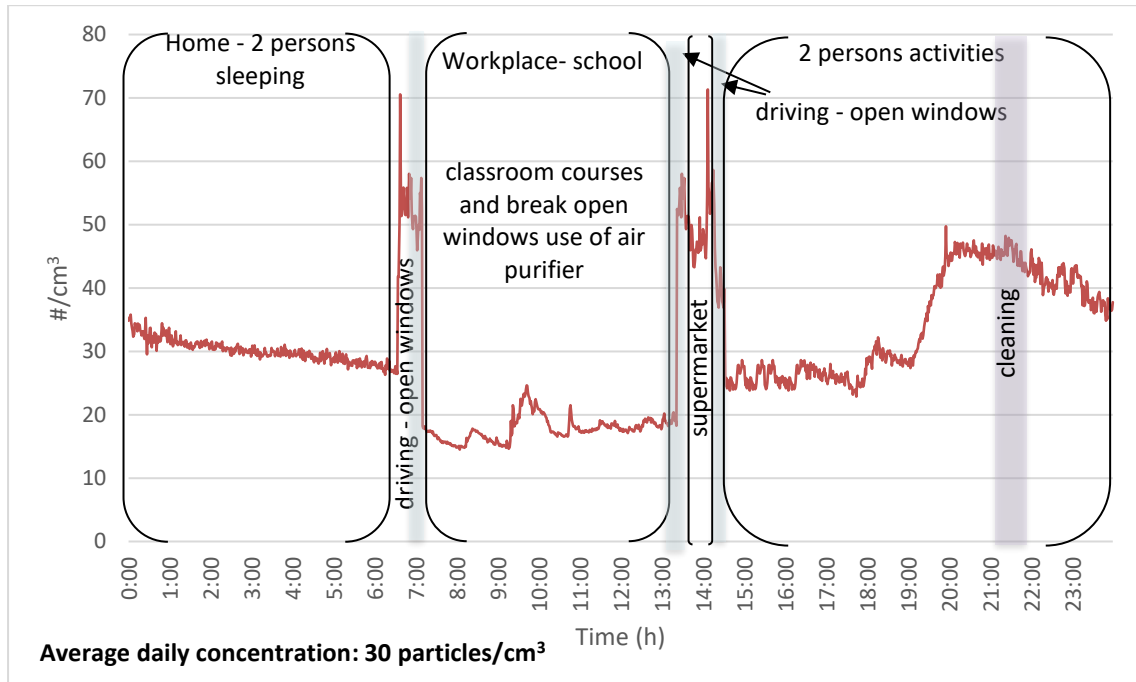


Figure B.1: Subject 1 daily exposure (number concentration) (day 1)

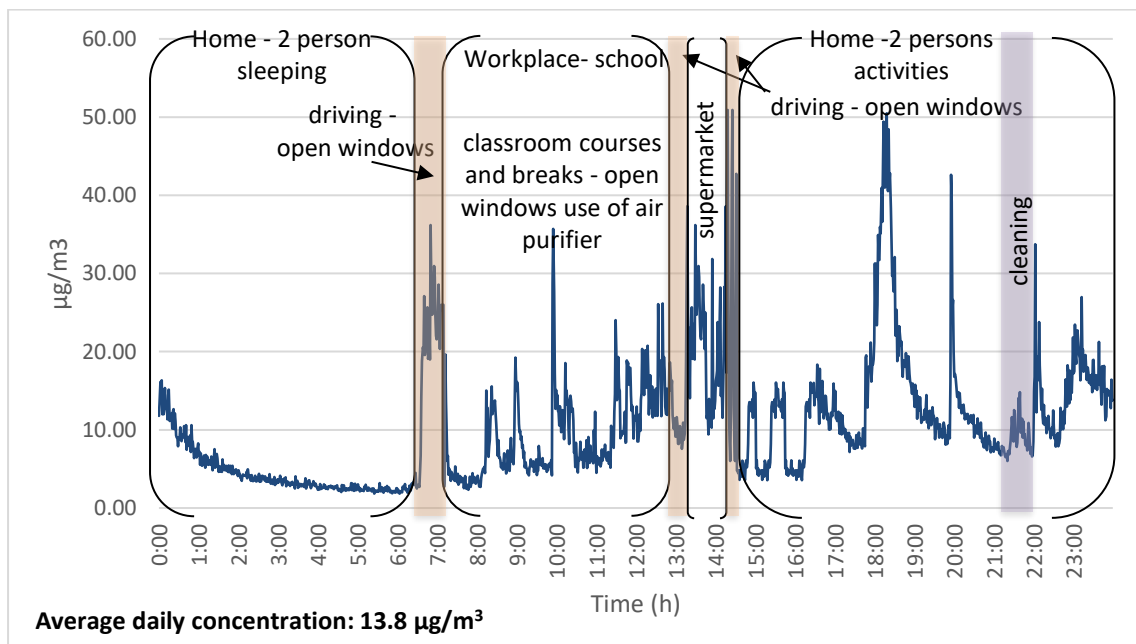


Figure B.2: Subject 1 daily exposure (mass concentration) (day 1).

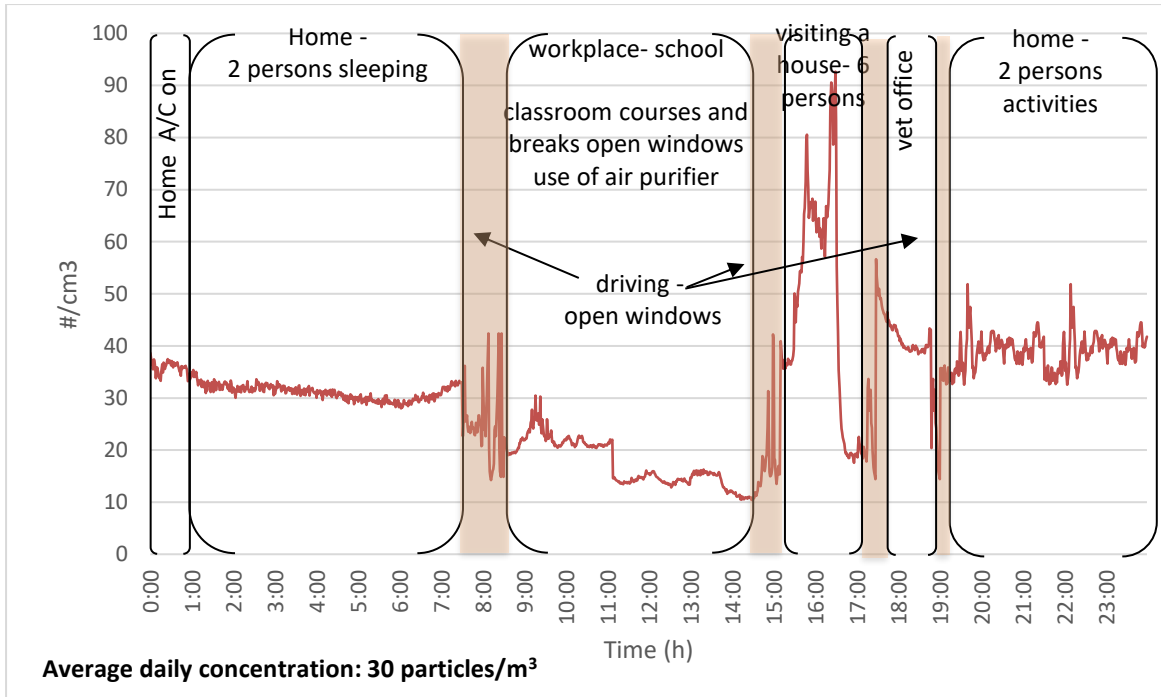


Figure B.3: Subject 1 daily exposure (number concentration) (day 2)

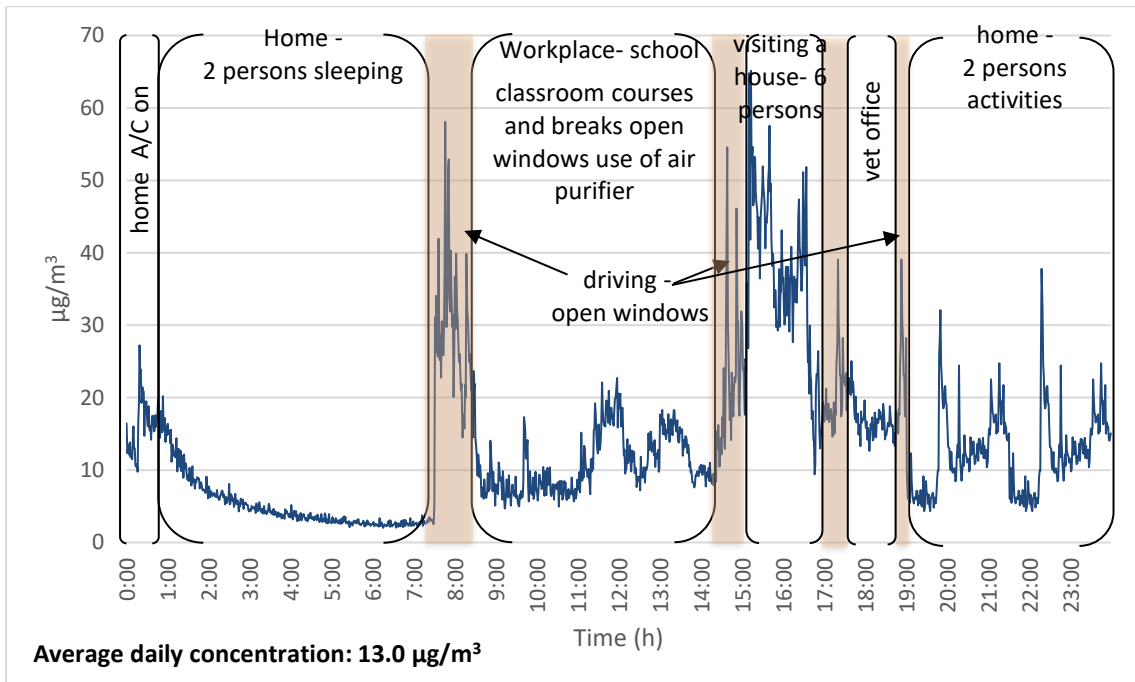


Figure B.4: Subject 1 daily exposure (mass concentration) (day 2).

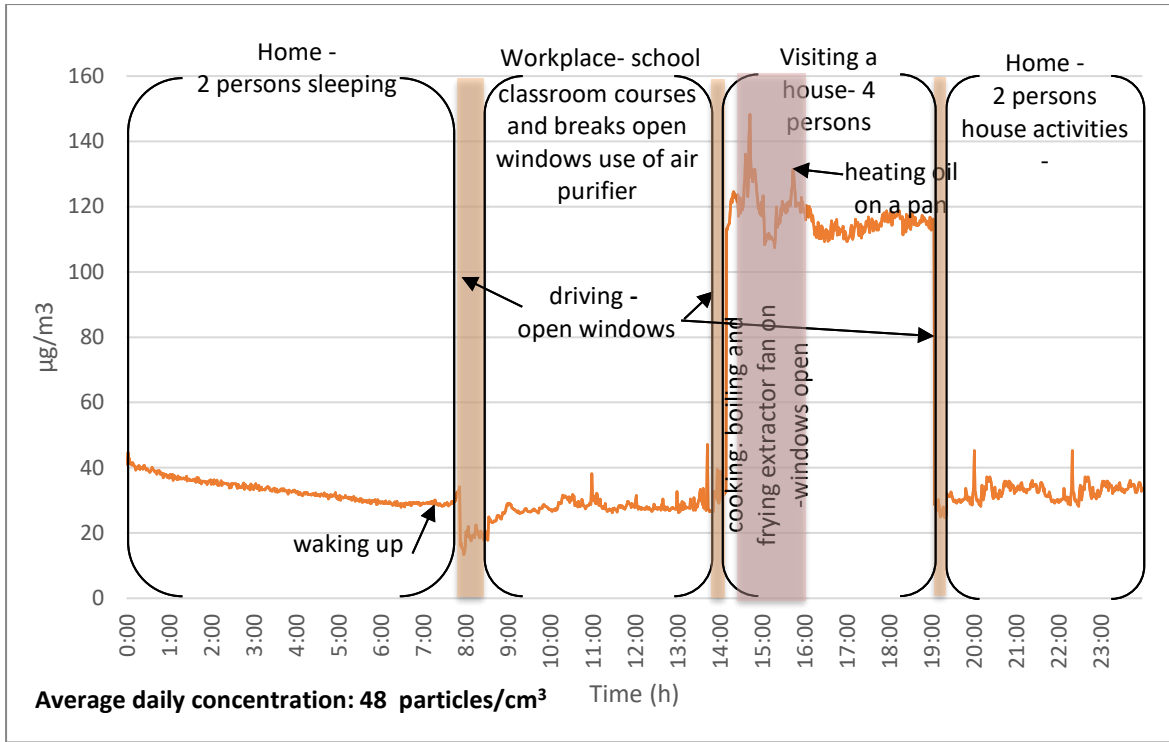


Figure B.5: Subject 1 daily exposure (number concentration) (day 3)

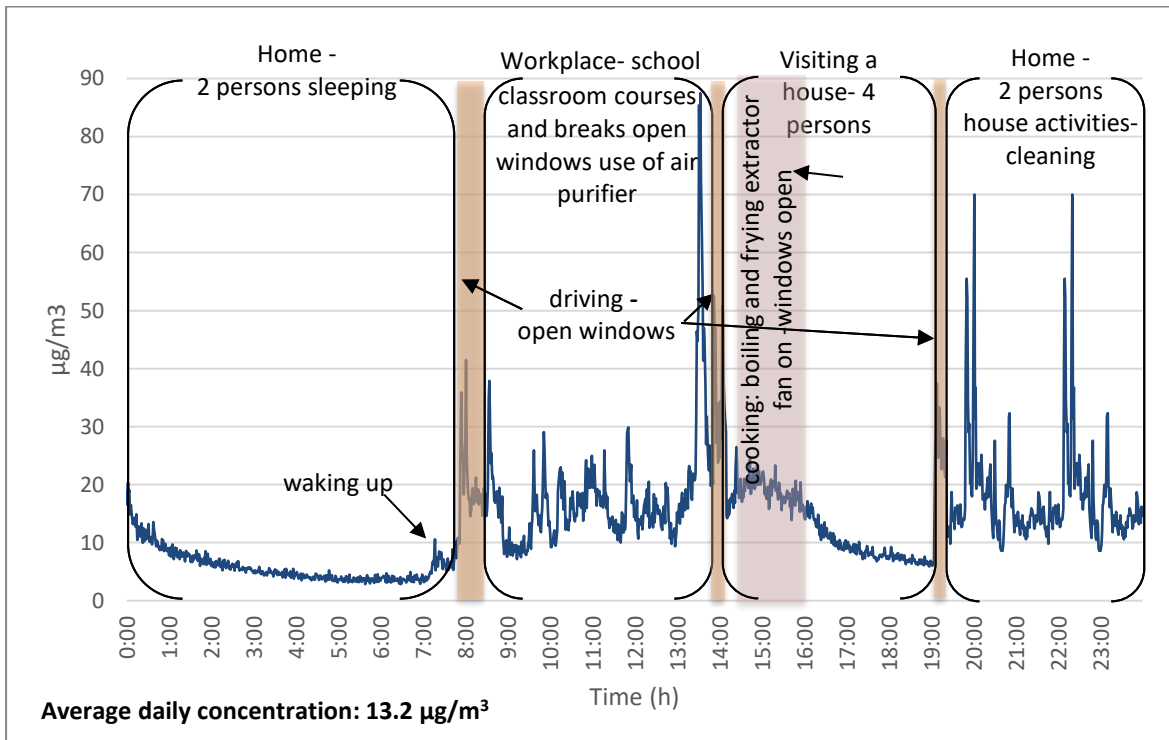


Figure B.6: Subject 1 daily exposure (mass concentration) (day 3).

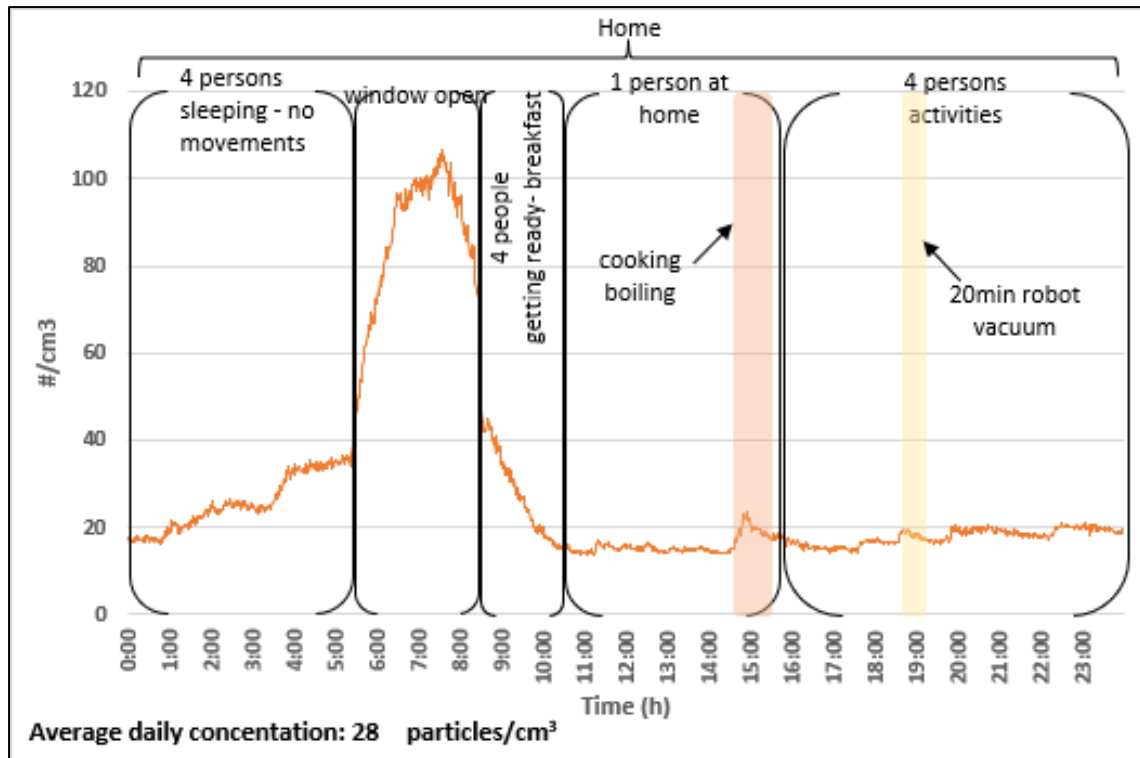


Figure B.7: Subject 2 daily exposure (number concentration) (day 1).

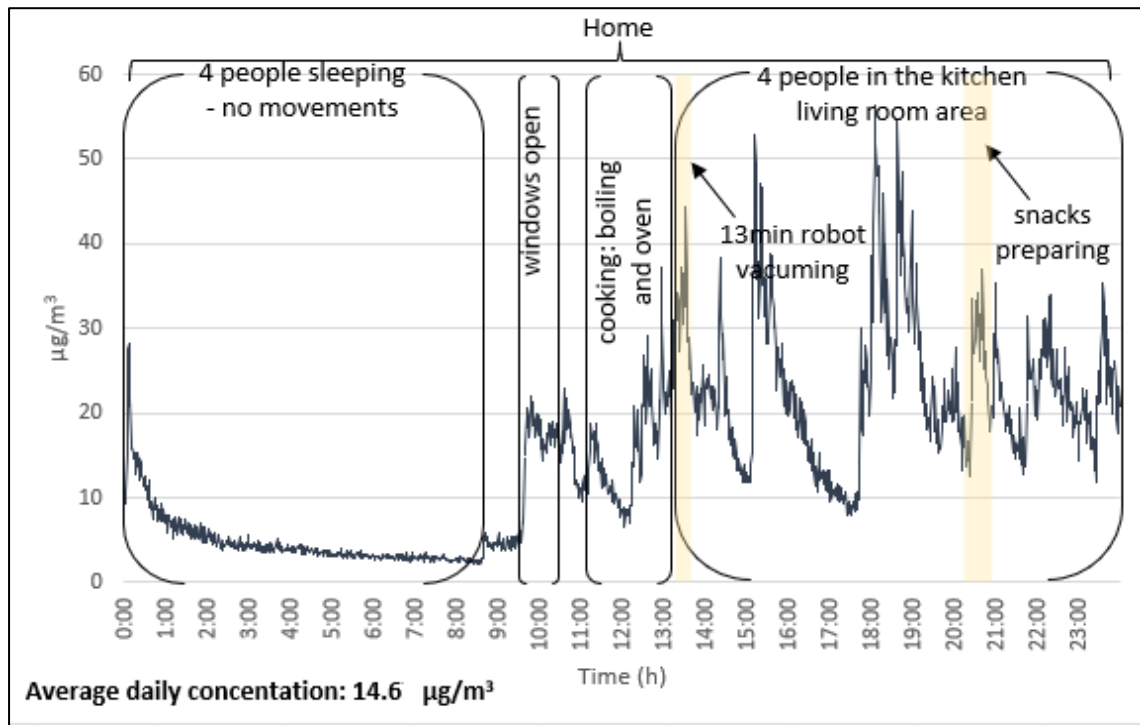


Figure B.8: Subject 2 daily exposure (mass concentration) (day 1).

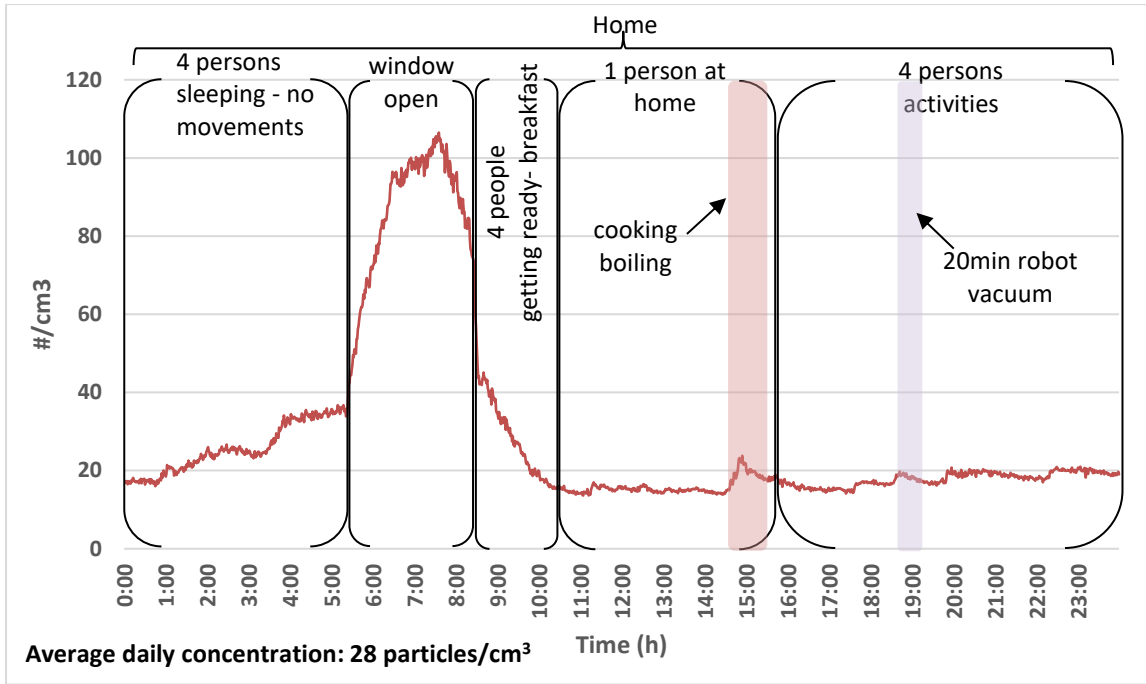


Figure B.9: Subject 2 daily exposure (number concentration) (day 2).

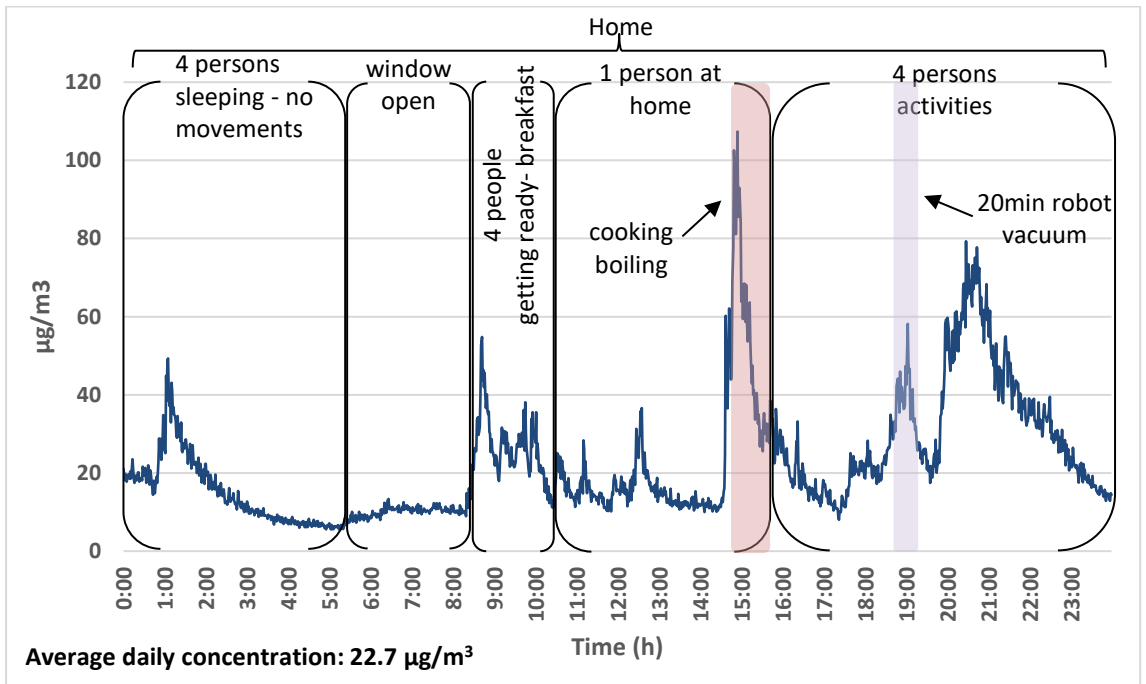


Figure B.10: Subject 2 daily exposure (mass concentration) (day 2).

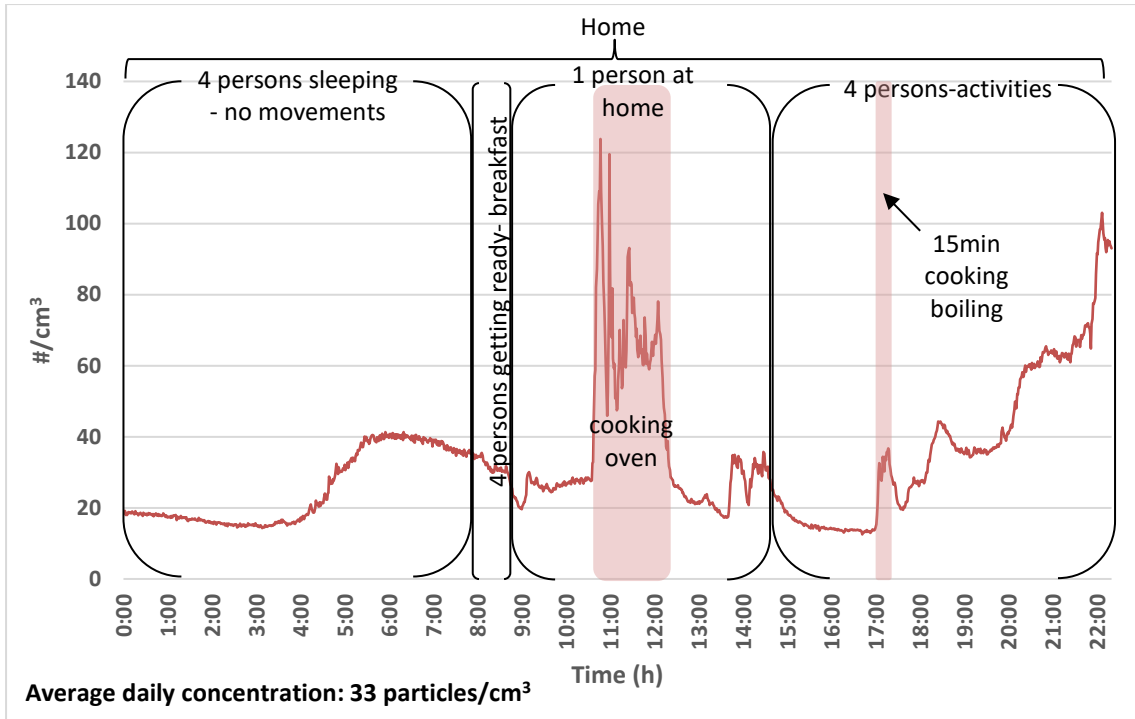


Figure B.11: Subject 2 daily exposure (number concentration) (day 3).

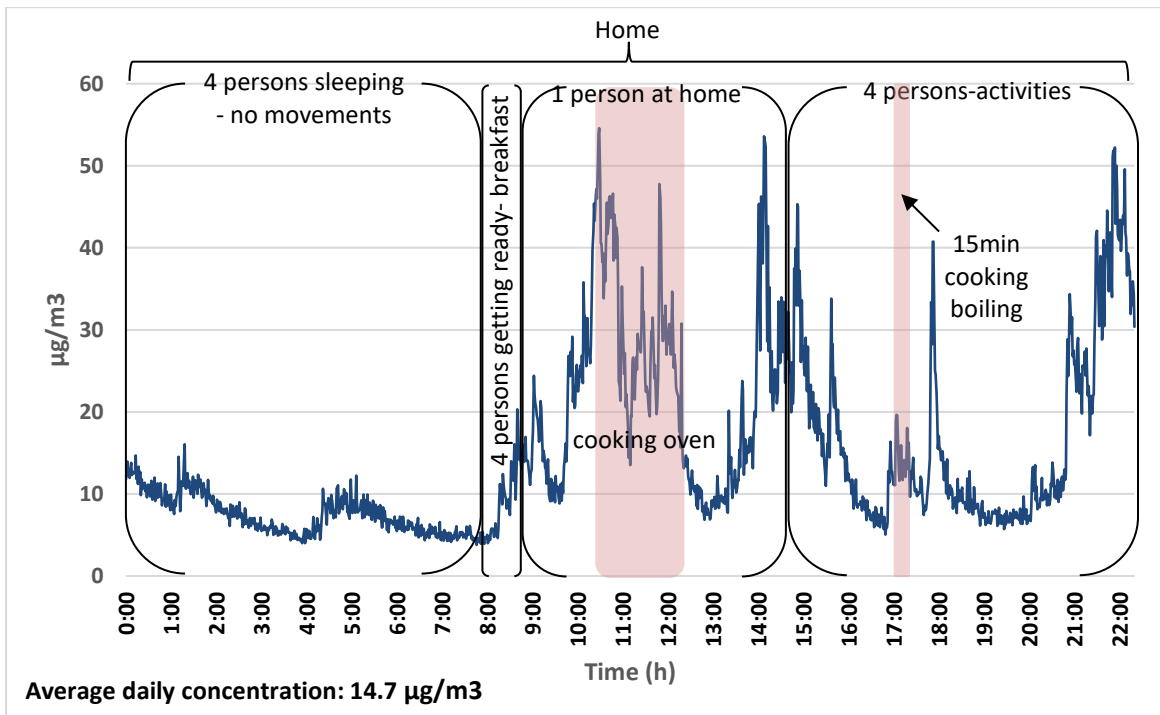


Figure B.12: Subject 2 daily exposure (mass concentration) (day 3).

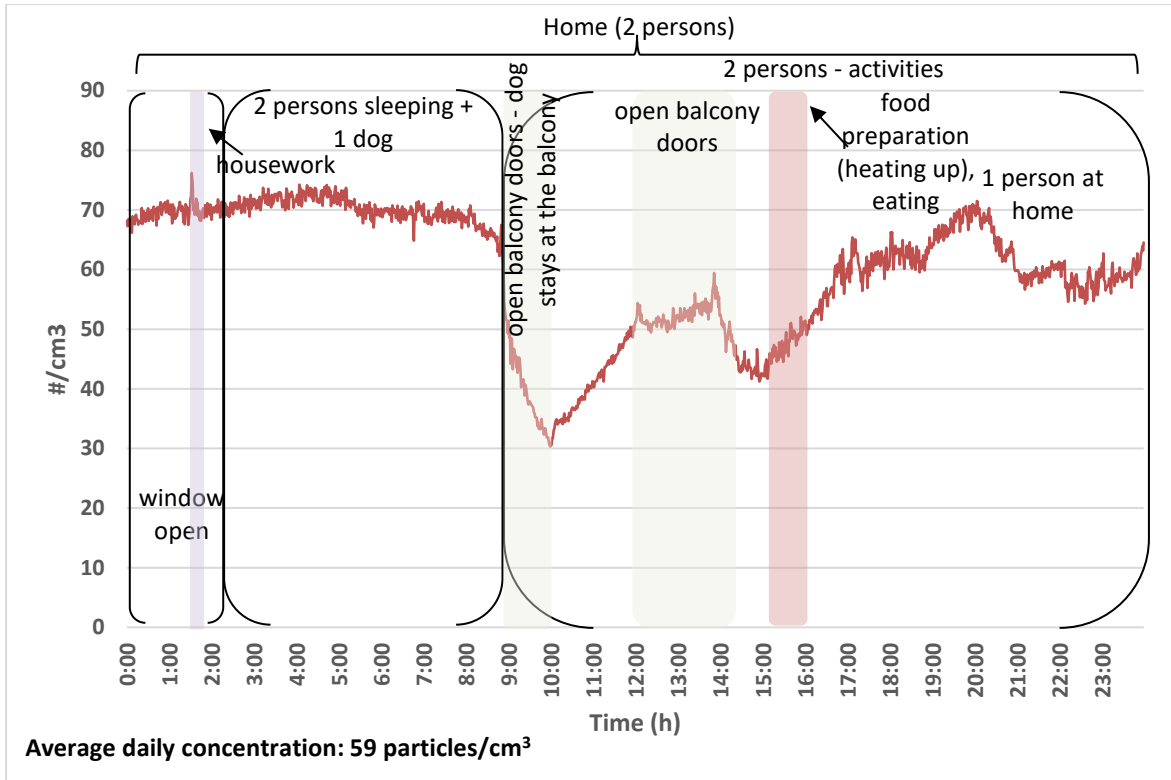


Figure B.13: Subject 3 daily exposure (number concentration) (day 1).

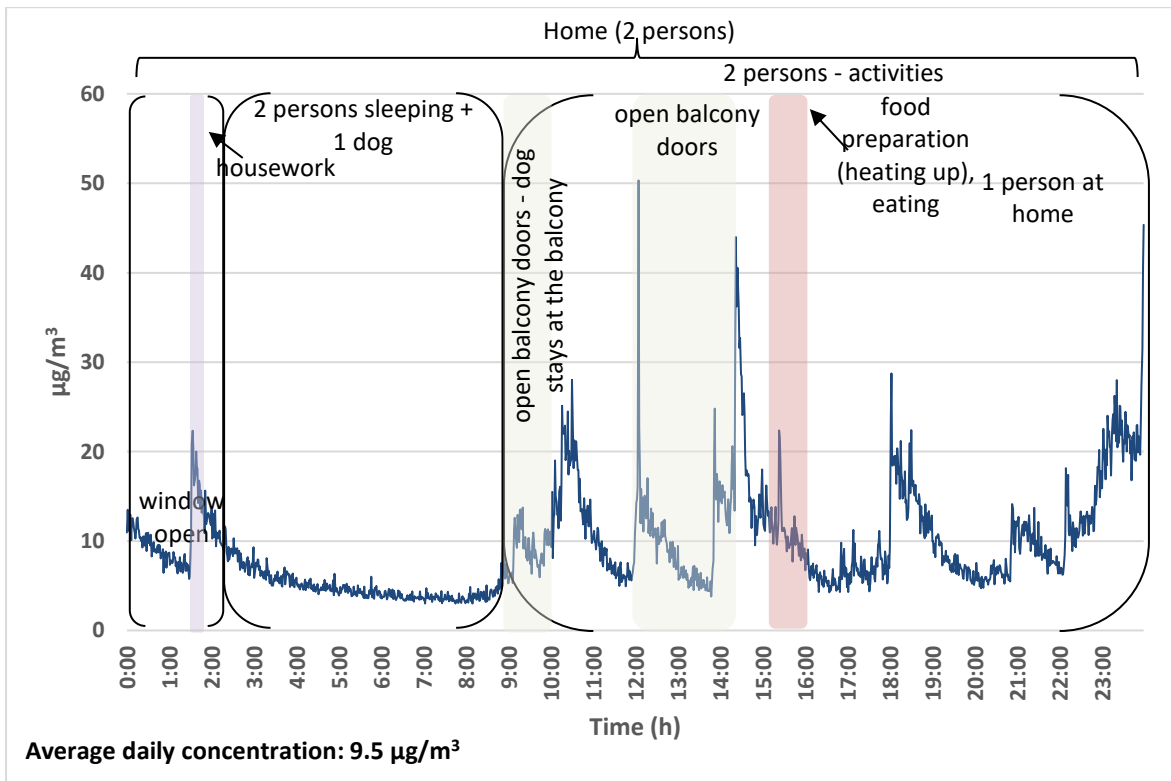


Figure B.14: Subject 3 daily exposure (mass concentration) (day 1).

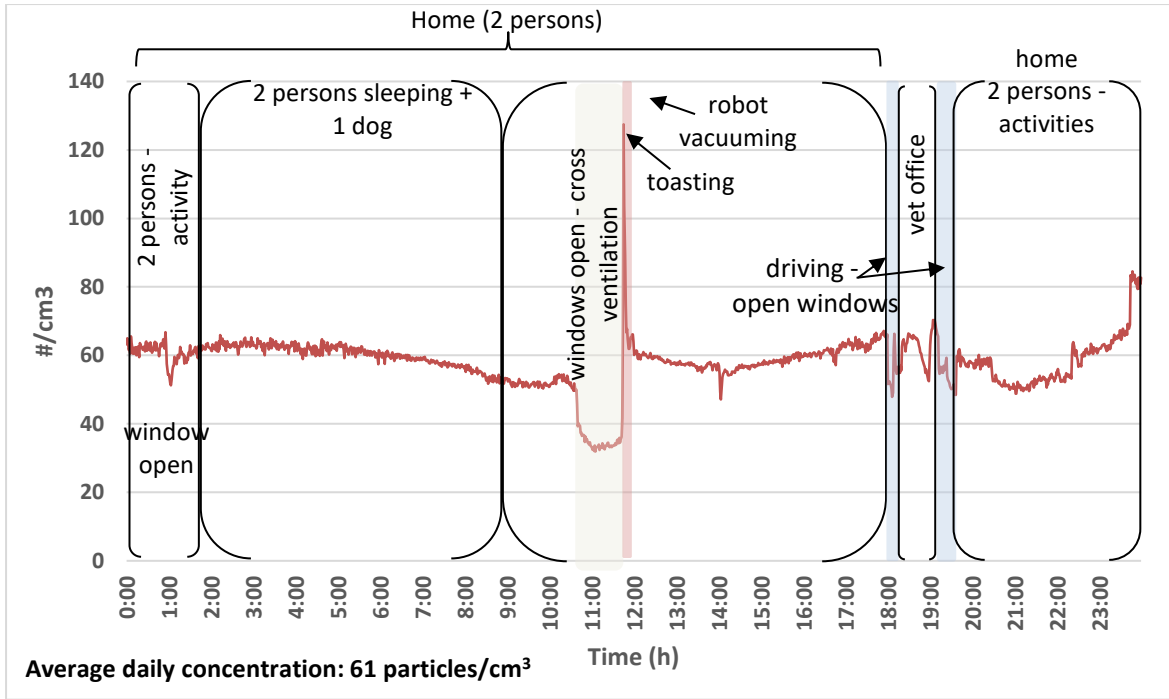


Figure B.15: Subject 3 daily exposure (number concentration) (day 2).

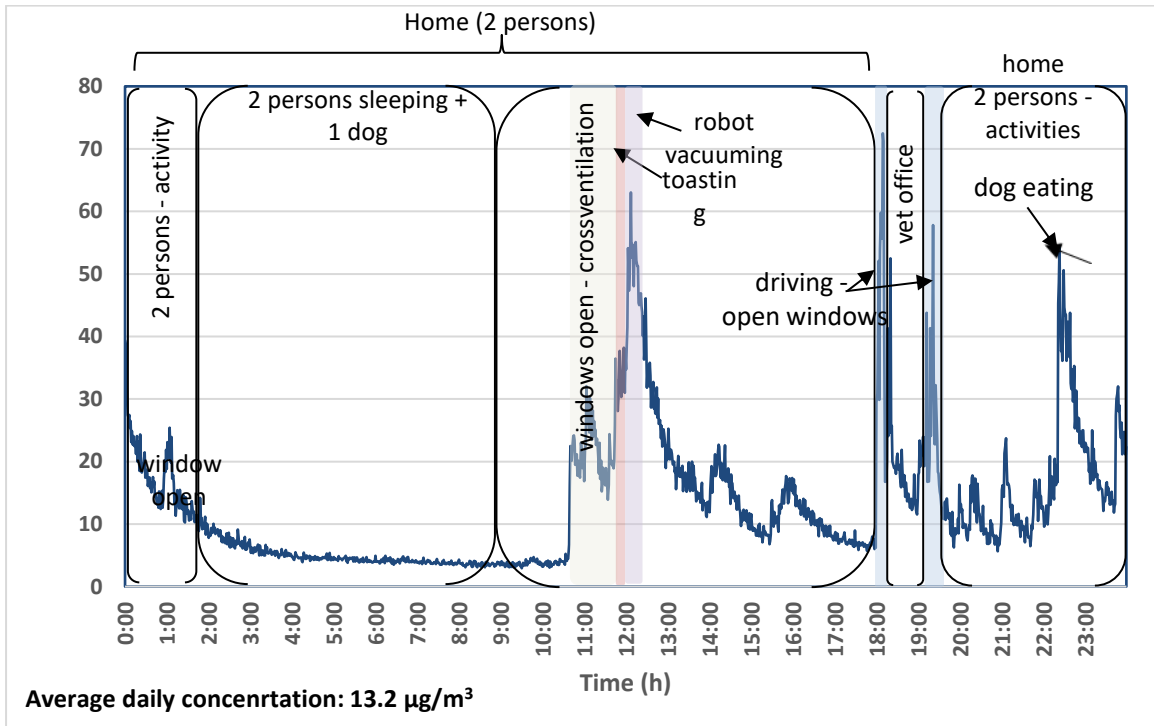


Figure B.16: Subject 3 daily exposure (mass concentration) (day 2).

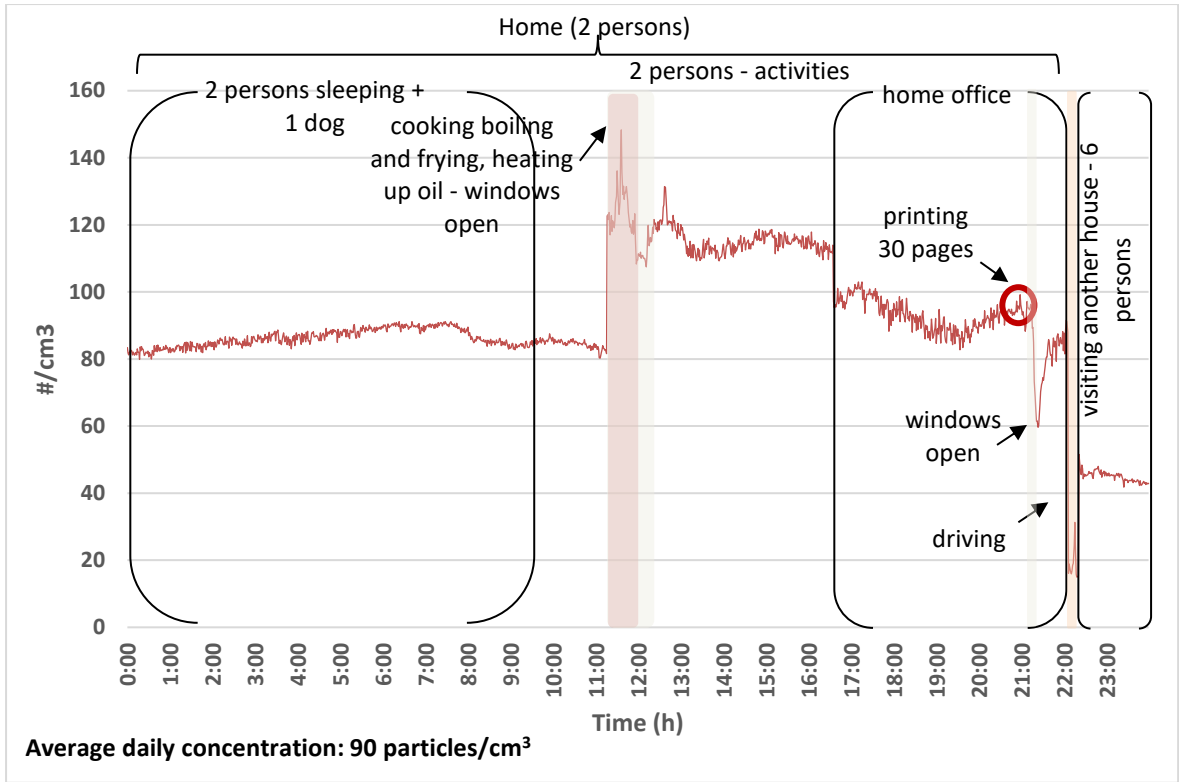


Figure B.17: Subject 3 daily exposure (number concentration) (day 3).

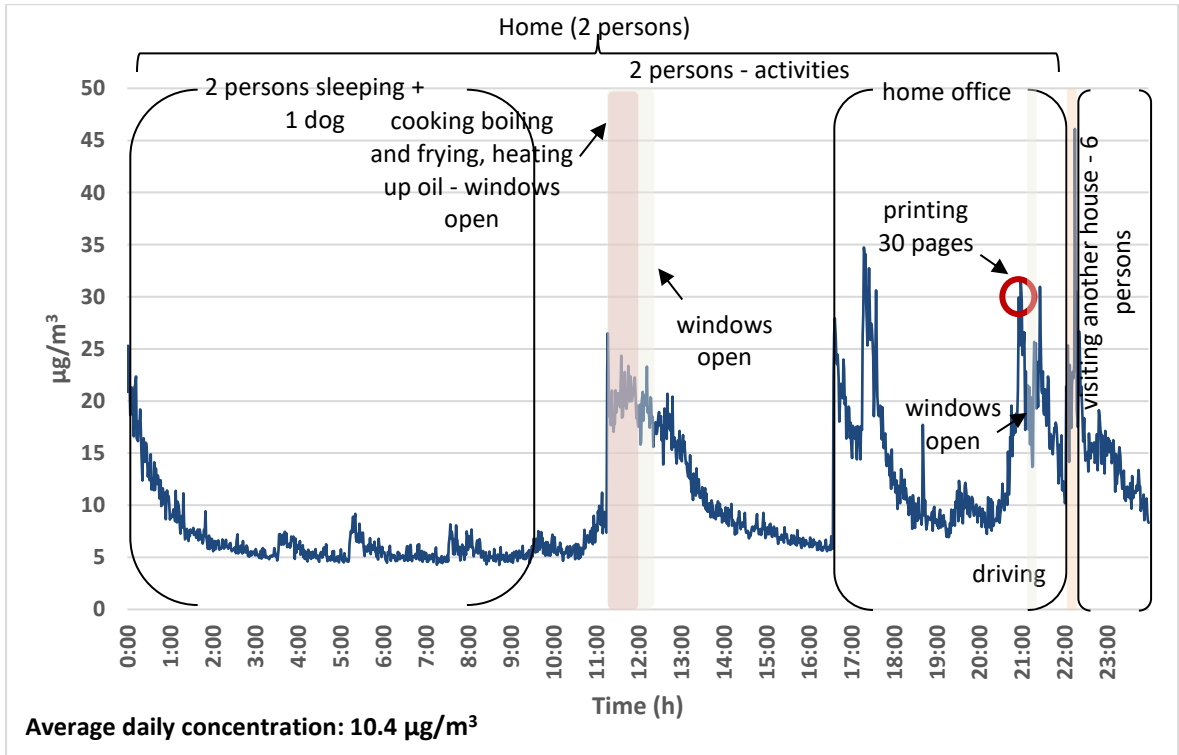


Figure B.18: Subject 3 daily exposure (mass concentration) (day 3).

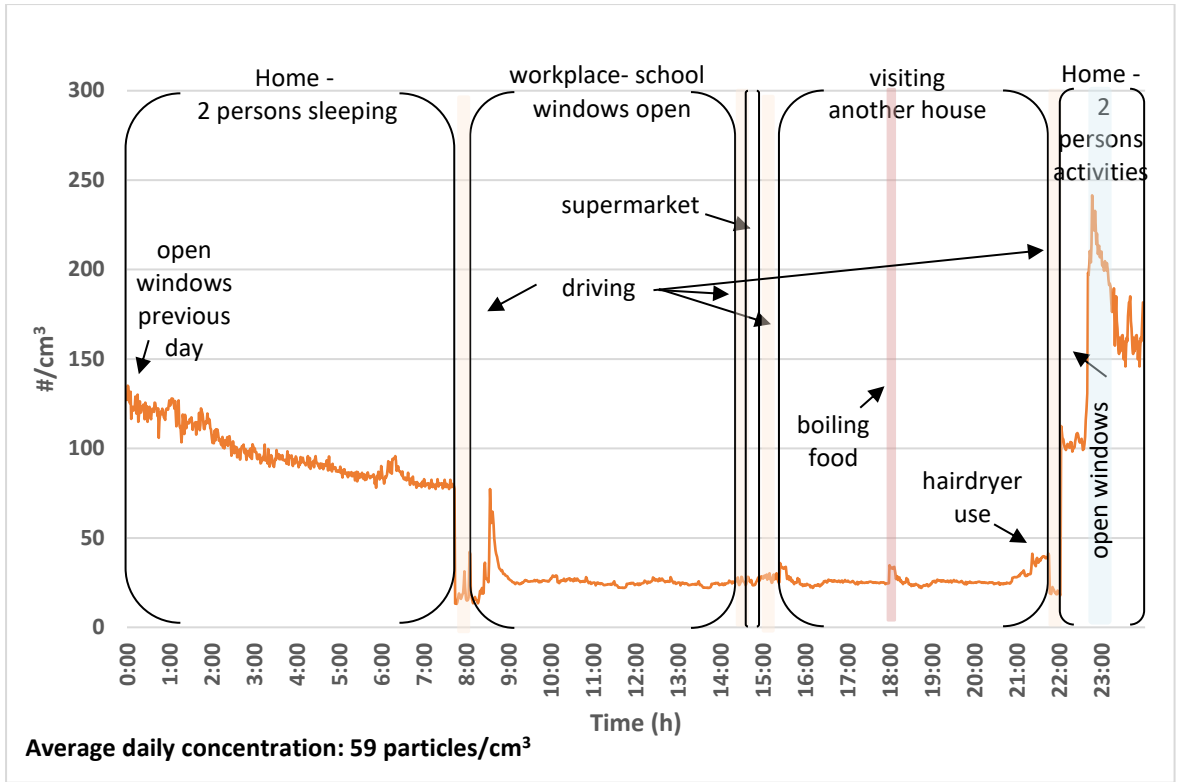


Figure B.19: Subject 4 daily exposure (number concentration) (day 1).

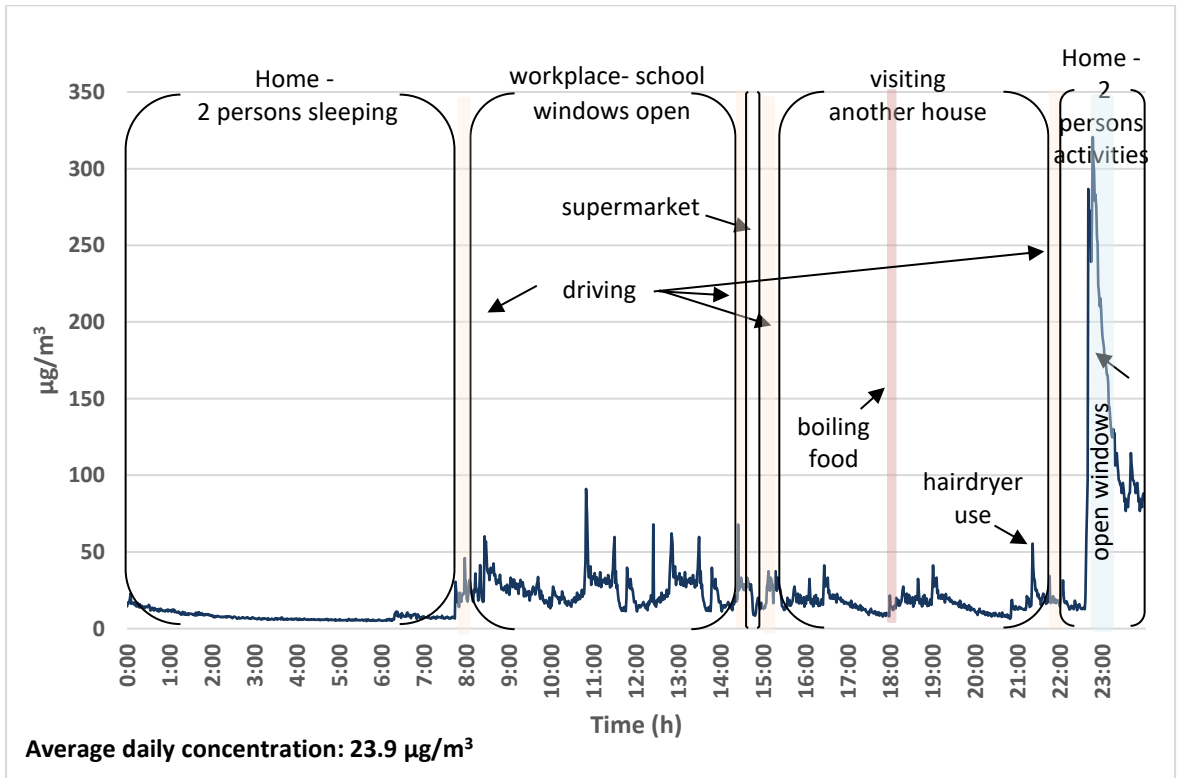


Figure B.20: Subject 4 daily exposure (mass concentration) (day 1).

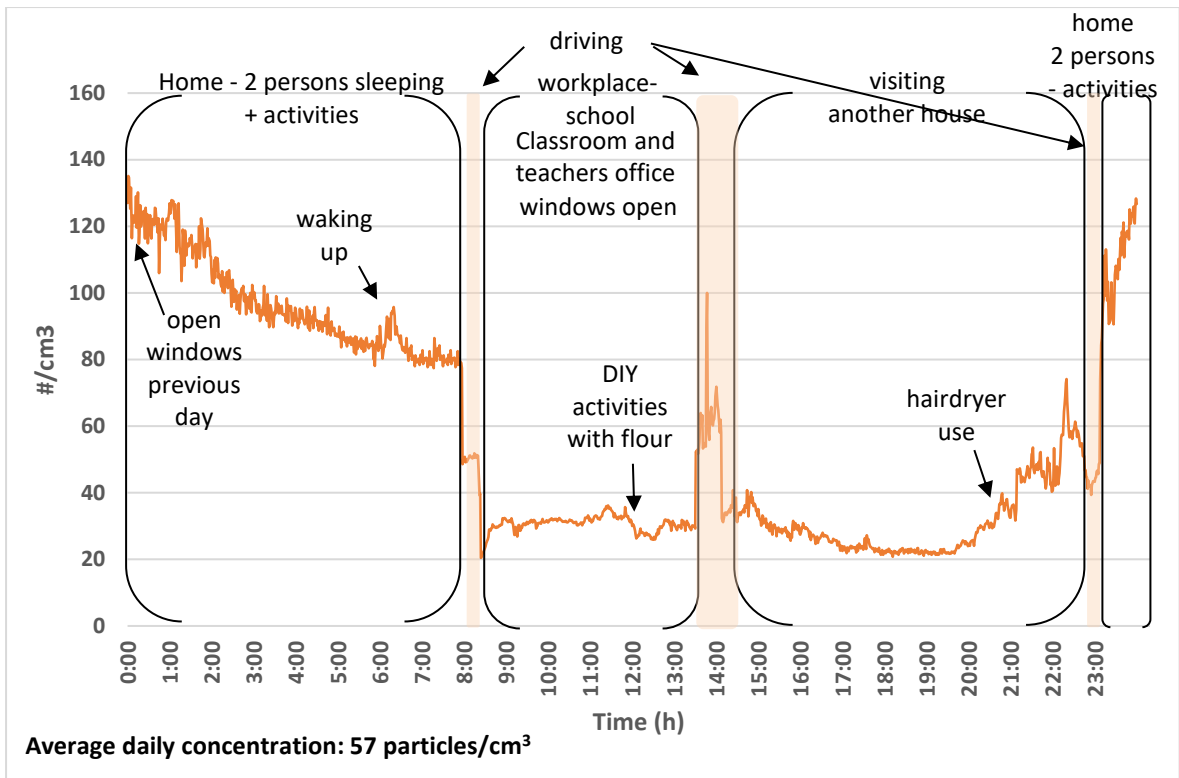


Figure B.21: Subject 4 daily exposure (number concentration) (day 2).

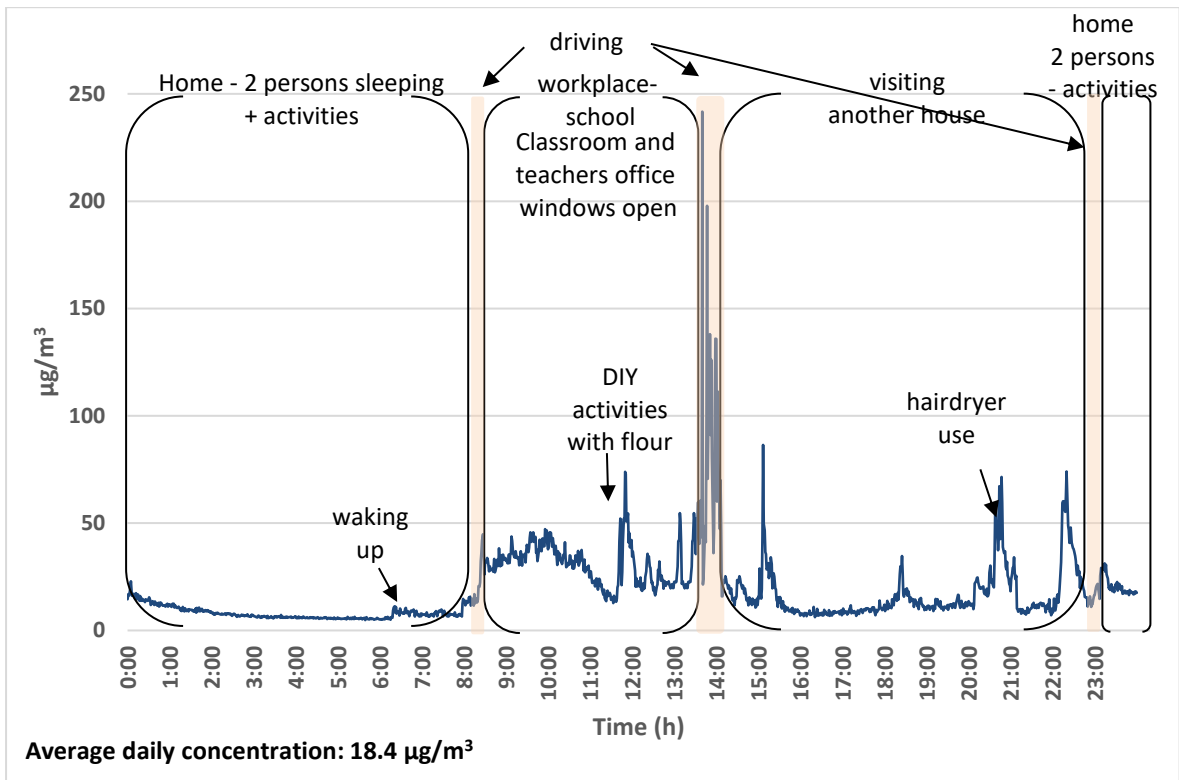


Figure B.22: Subject 4 daily exposure (mass concentration) (day 2).

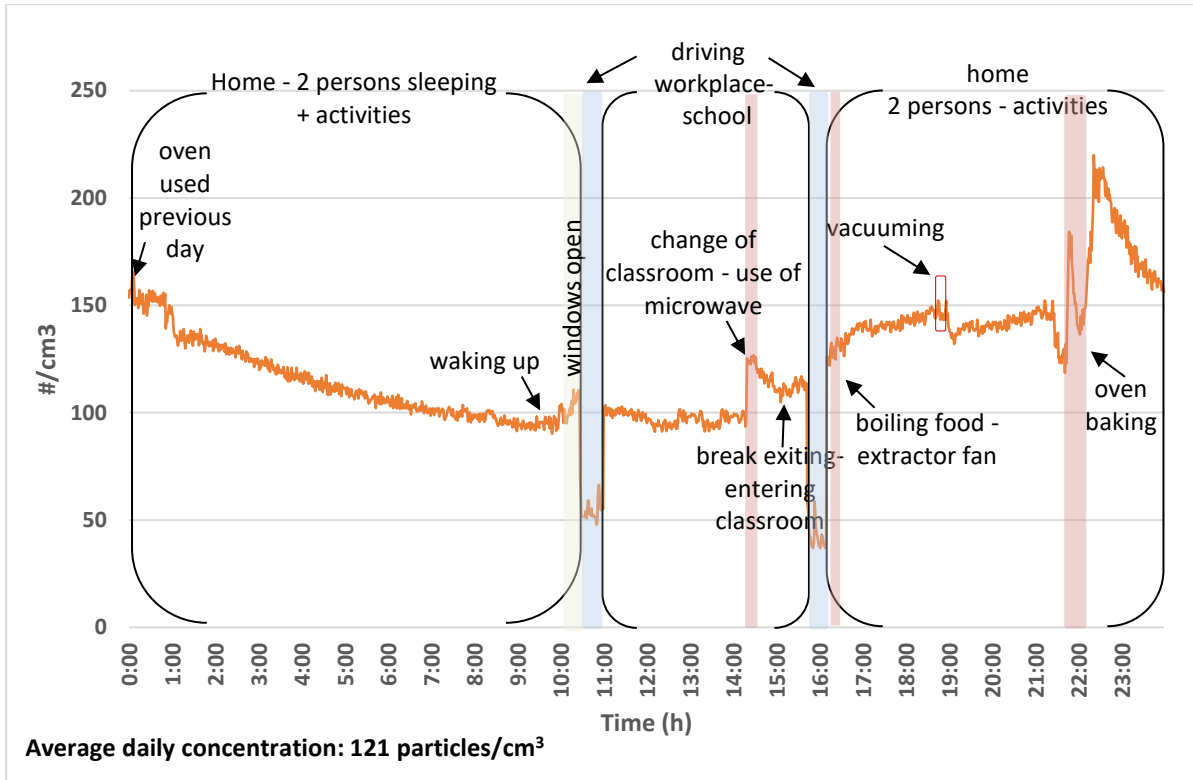


Figure B.23: Subject 4 daily exposure (number concentration) (day 3).

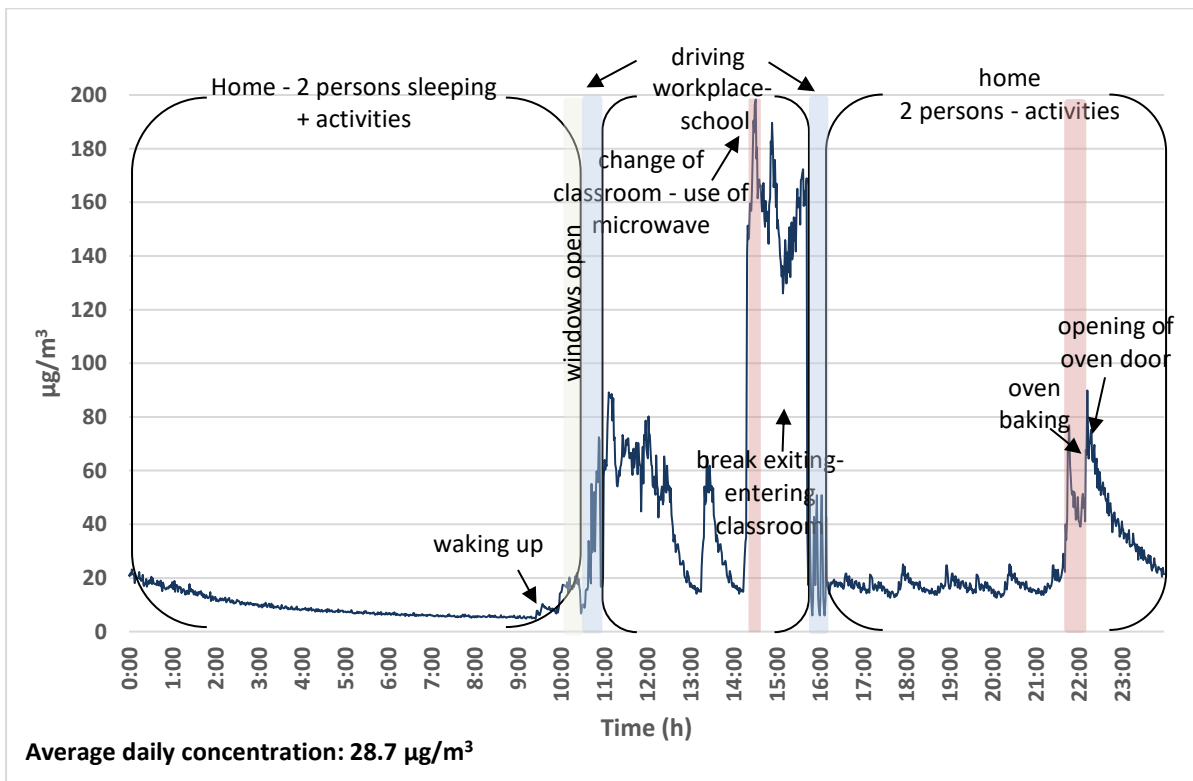


Figure B.24: Subject 4 daily exposure (mass concentration) (day 3).

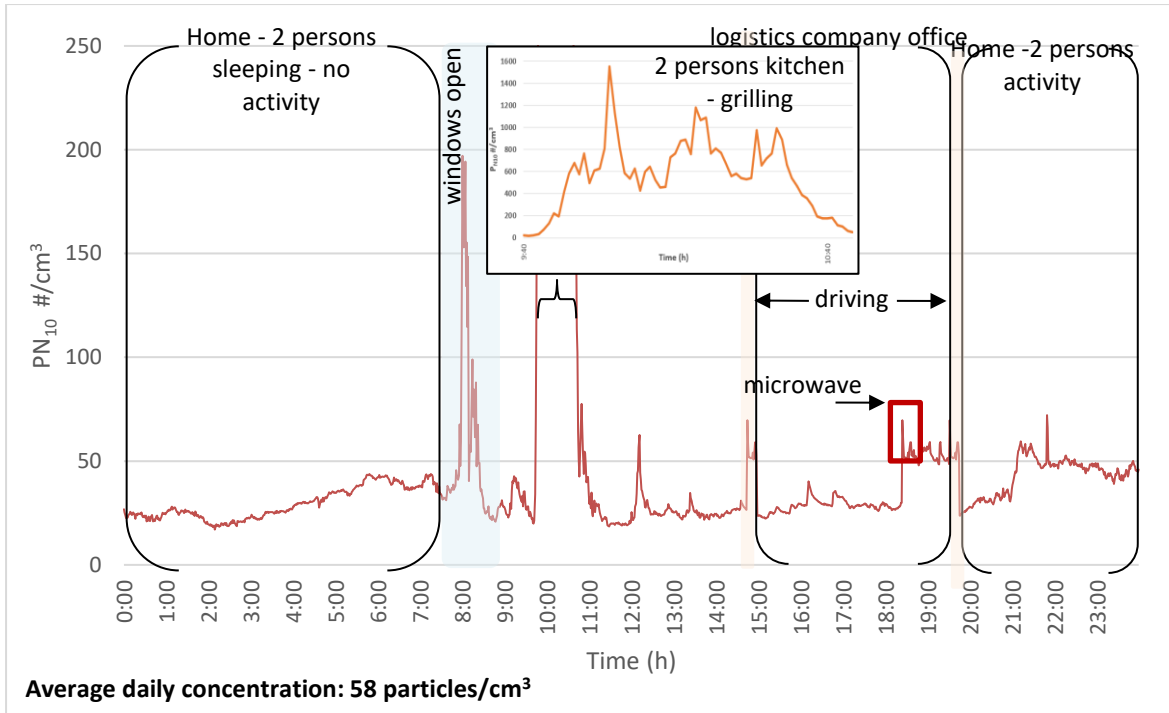


Figure B.25: Subject 5 daily exposure (number concentration) (day 1).

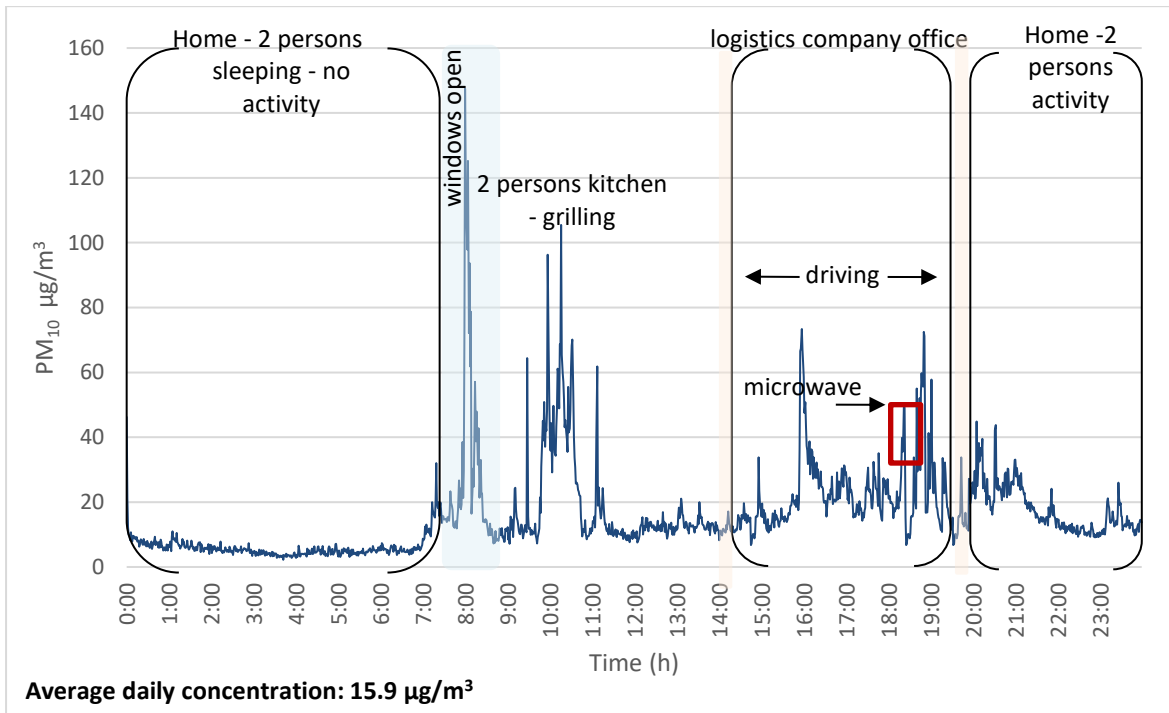


Figure B.26: Subject 5 daily exposure (mass concentration) (day 1).

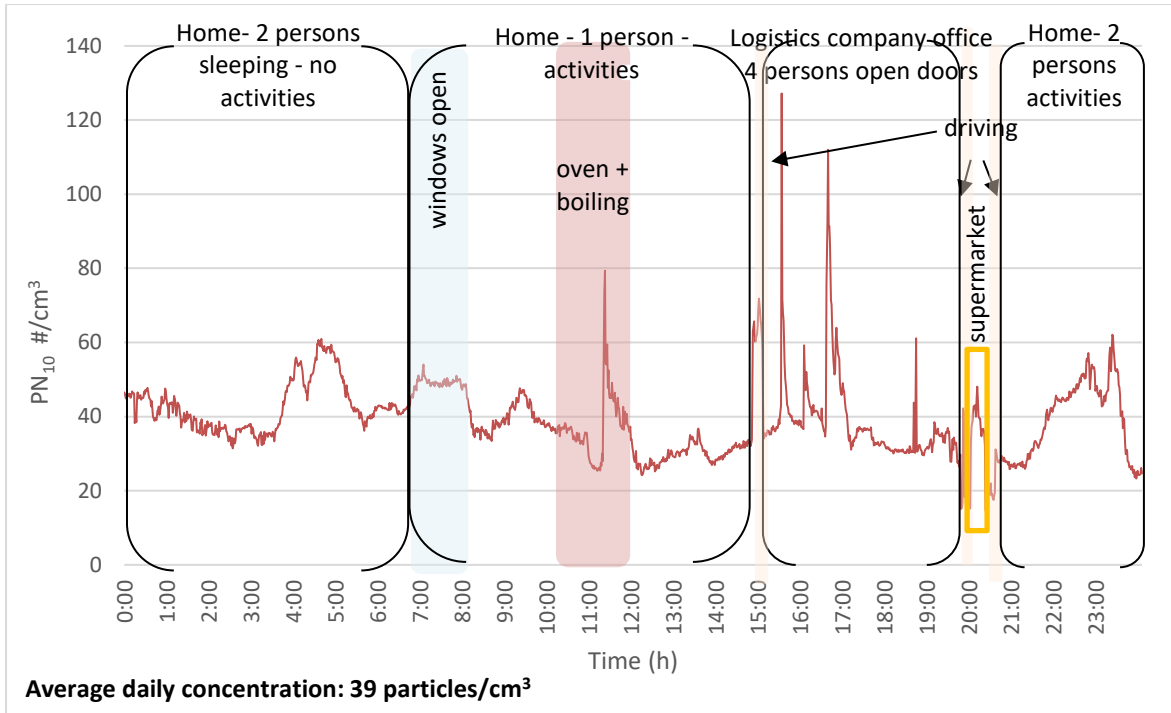


Figure B.27: Subject 5 daily exposure (number concentration) (day 2).

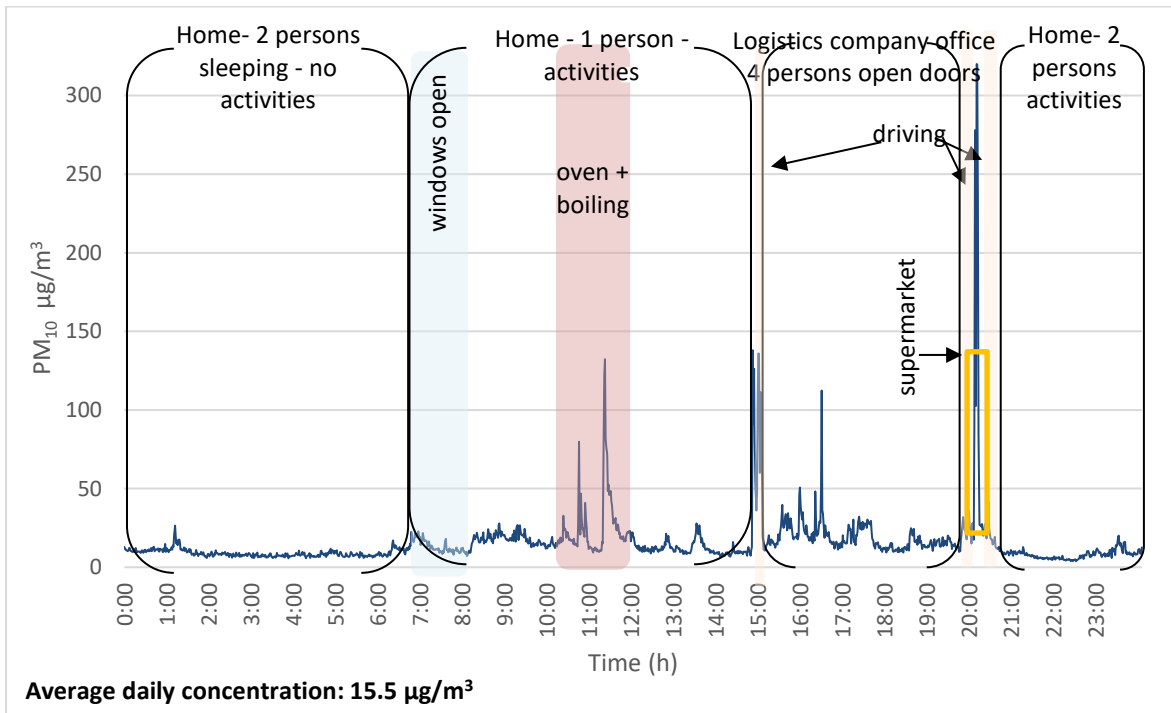


Figure B.28: Subject 5 daily exposure (mass concentration) (day 2).

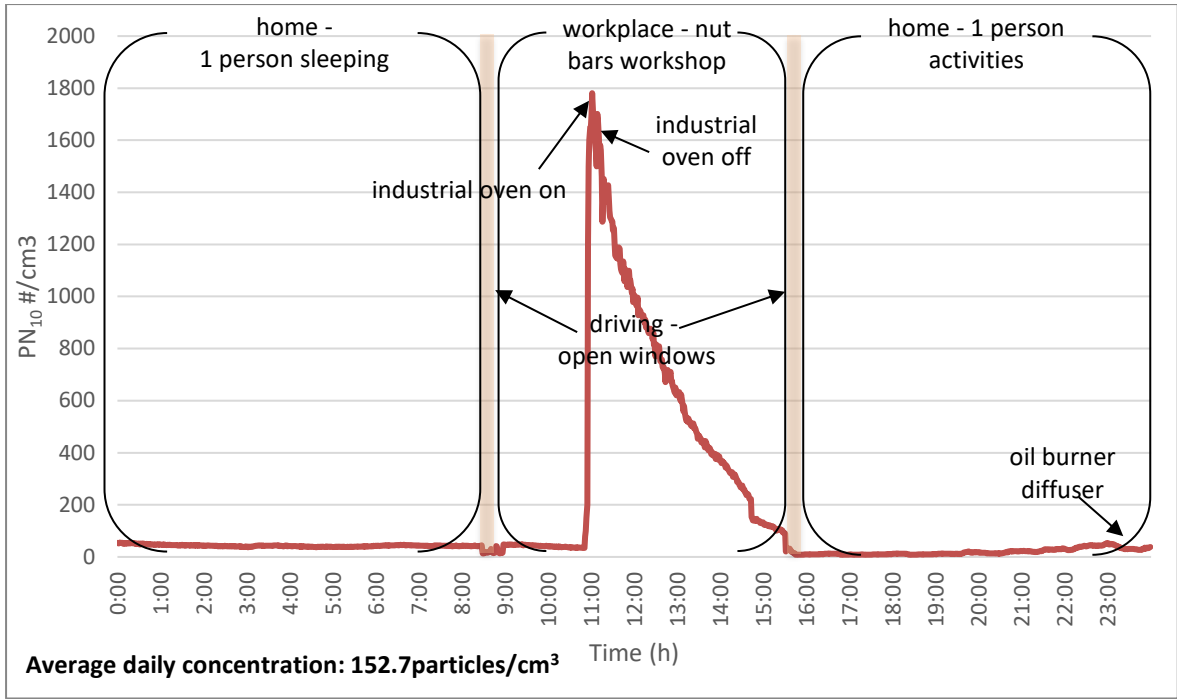


Figure B.29: Subject 6 daily exposure (number concentration) (day 1).

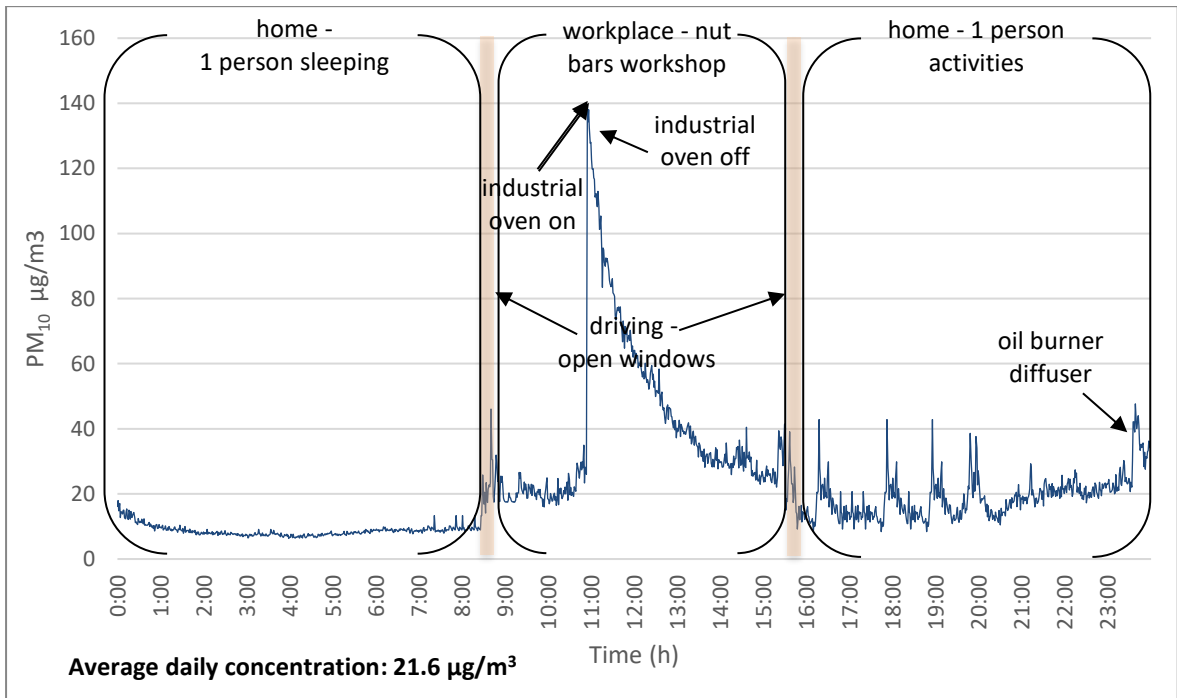


Figure B.30: Subject 6 daily exposure (mass concentration) (day 1).

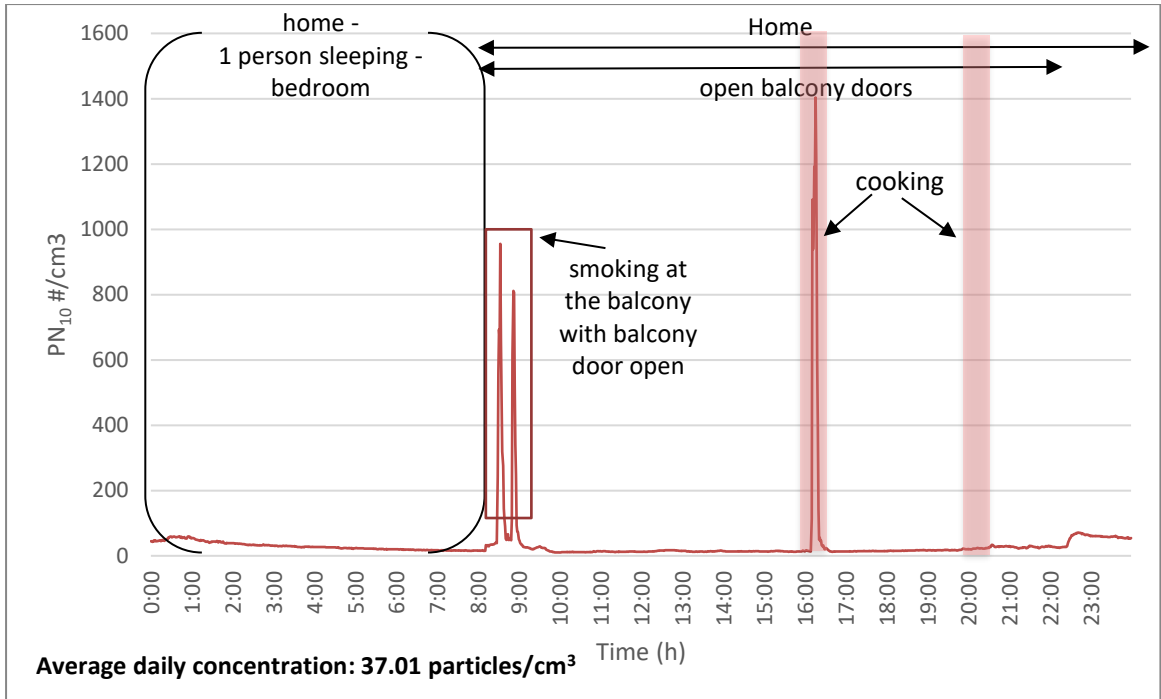


Figure B.31: Subject 6 daily exposure (number concentration) (day 2).

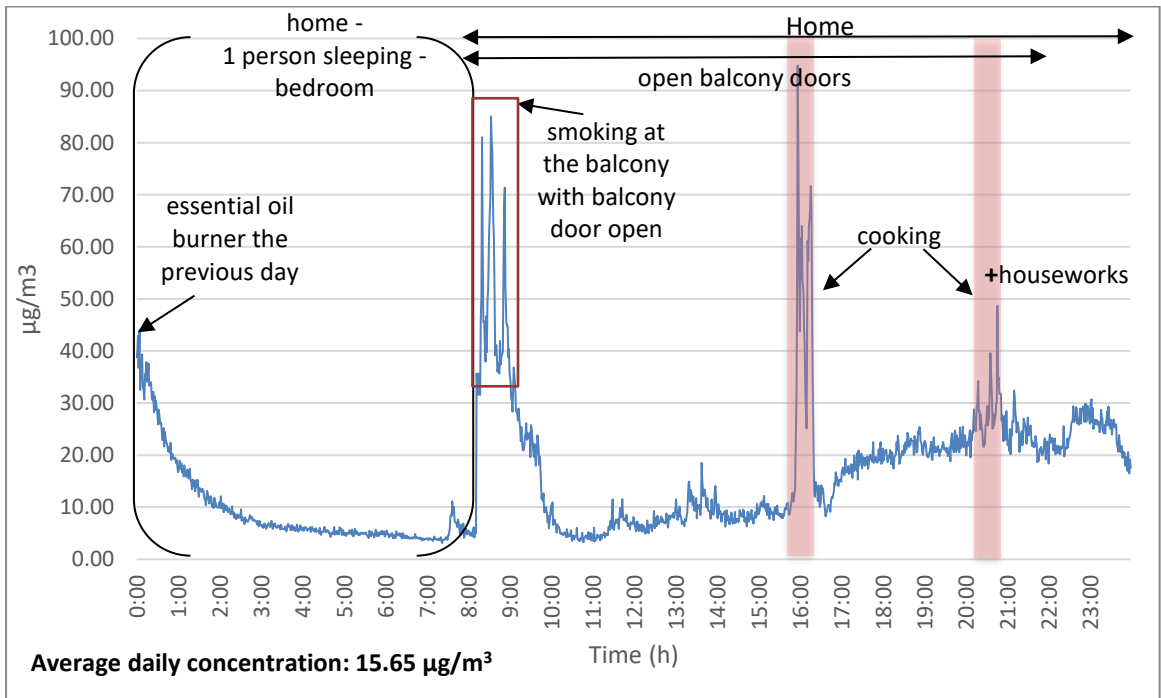


Figure B.32: Subject 6 daily exposure mass concentration) (day 2).

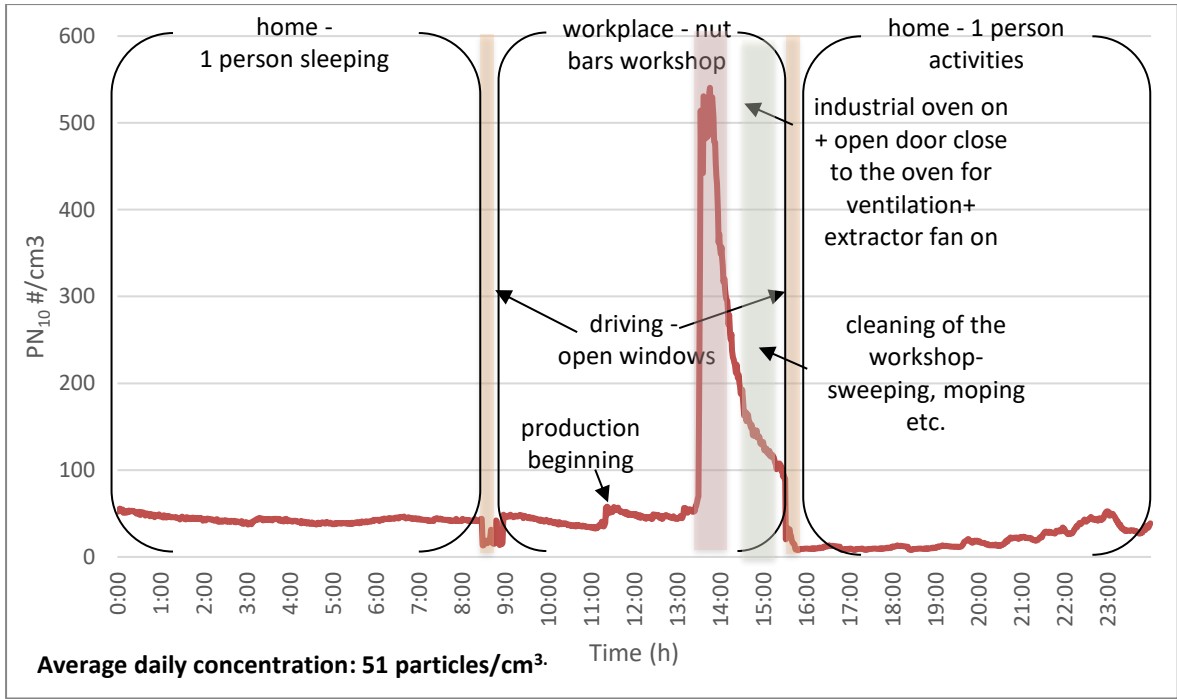


Figure B.33: Subject 6 daily exposure (number concentration) (day 3).

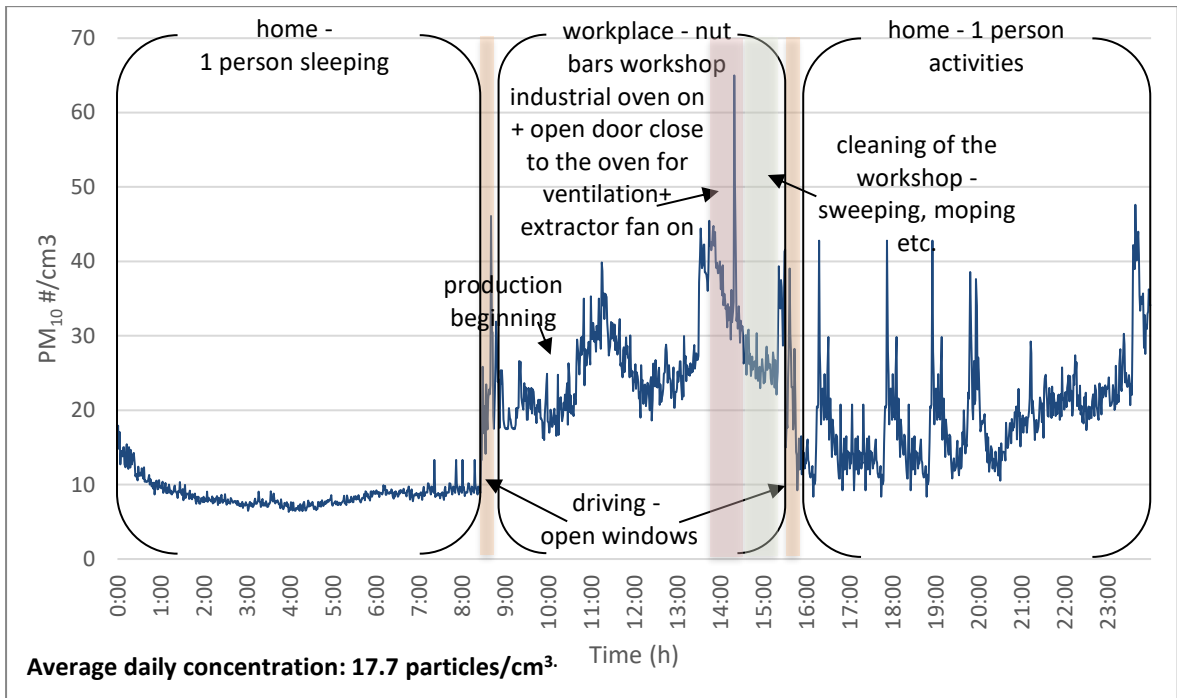


Figure B.34: Subject 6 daily exposure mass concentration) (day 3).

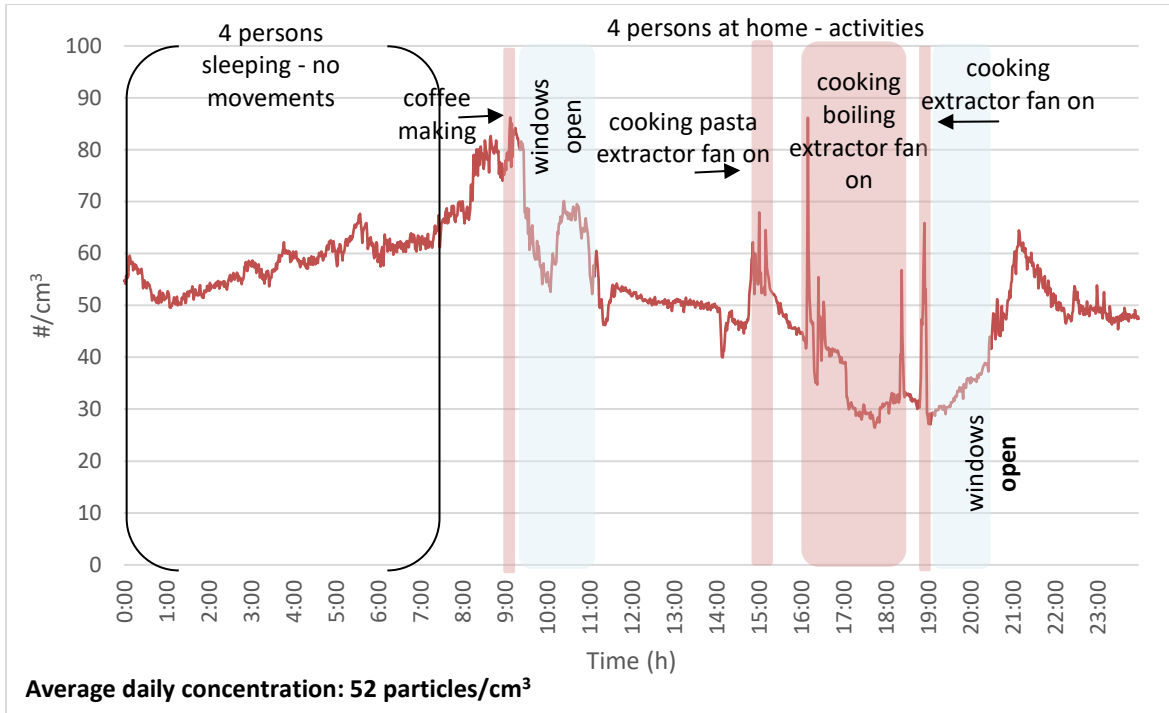


Figure B.35: Subject 7 daily exposure (number concentration) (day 1).

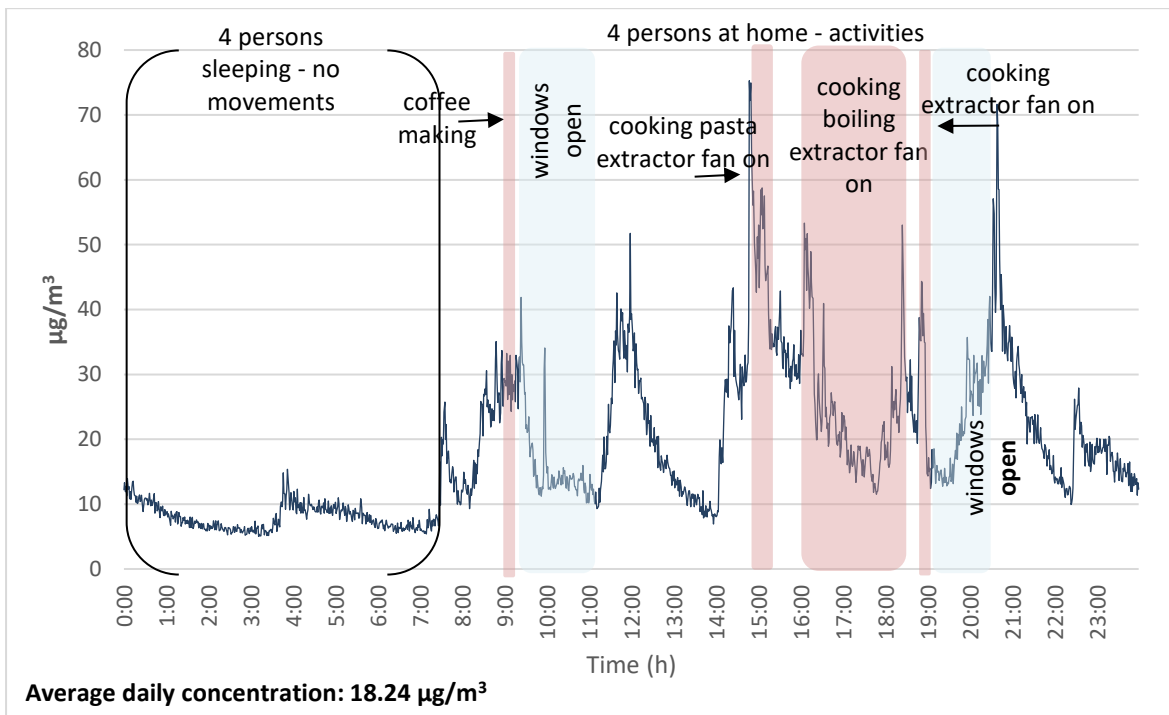


Figure B.36: Subject 7 daily exposure (mass concentration) (day 1).

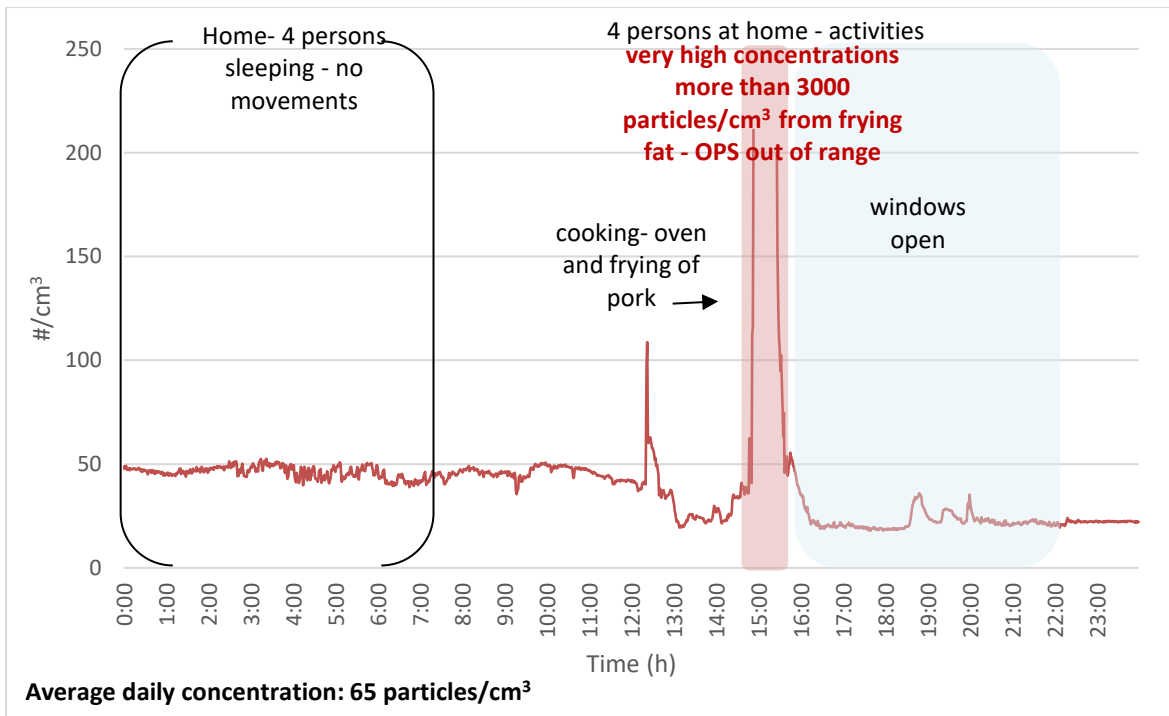


Figure B.37: Subject 7 daily exposure (number concentration) (day 2).

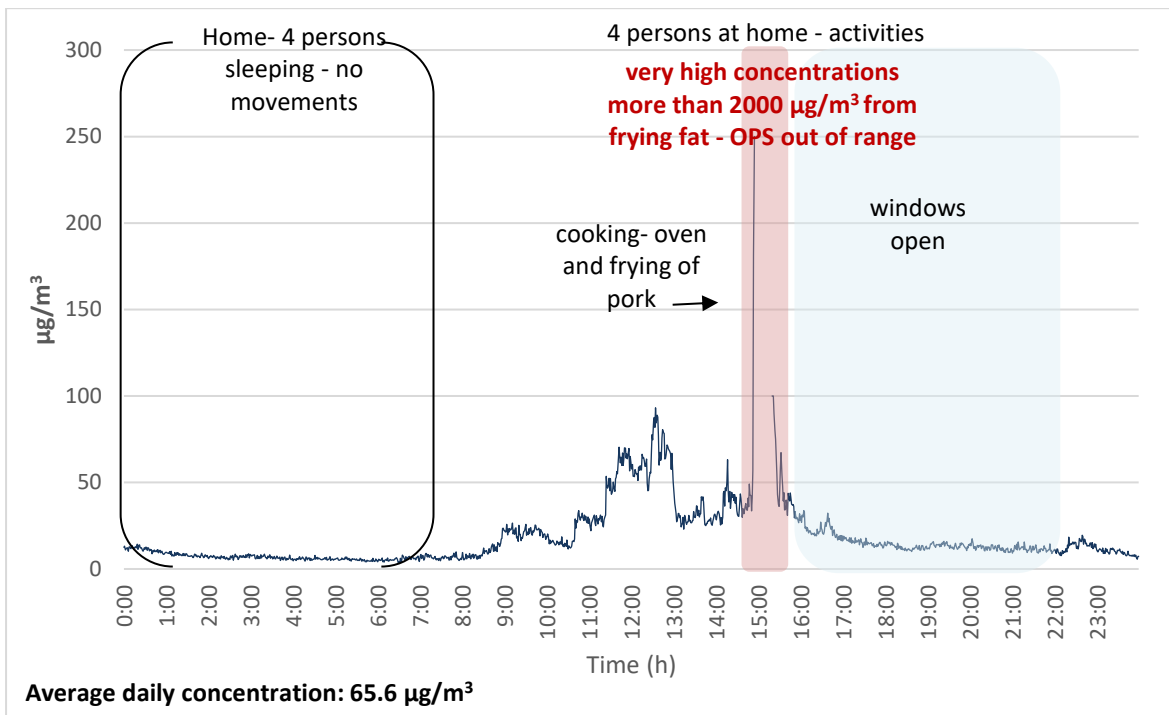


Figure B.38: Subject 7 daily exposure (mass concentration) (day 2).

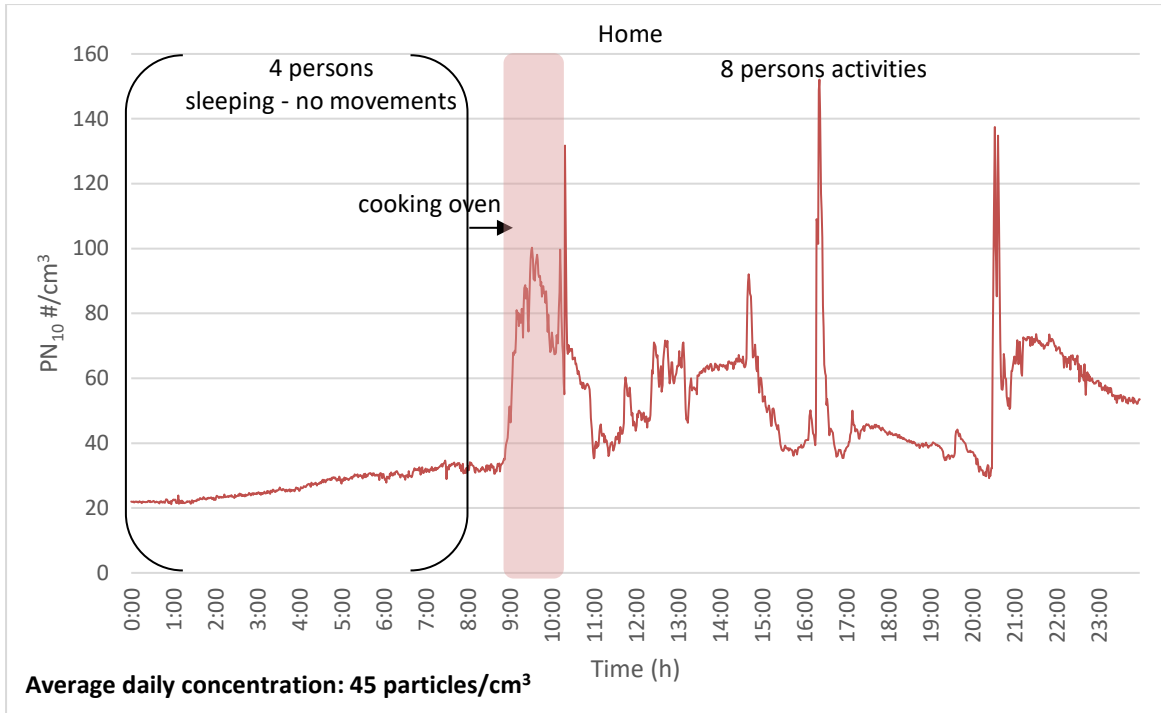


Figure B.39: Subject 7 daily exposure (number concentration) (day 3).

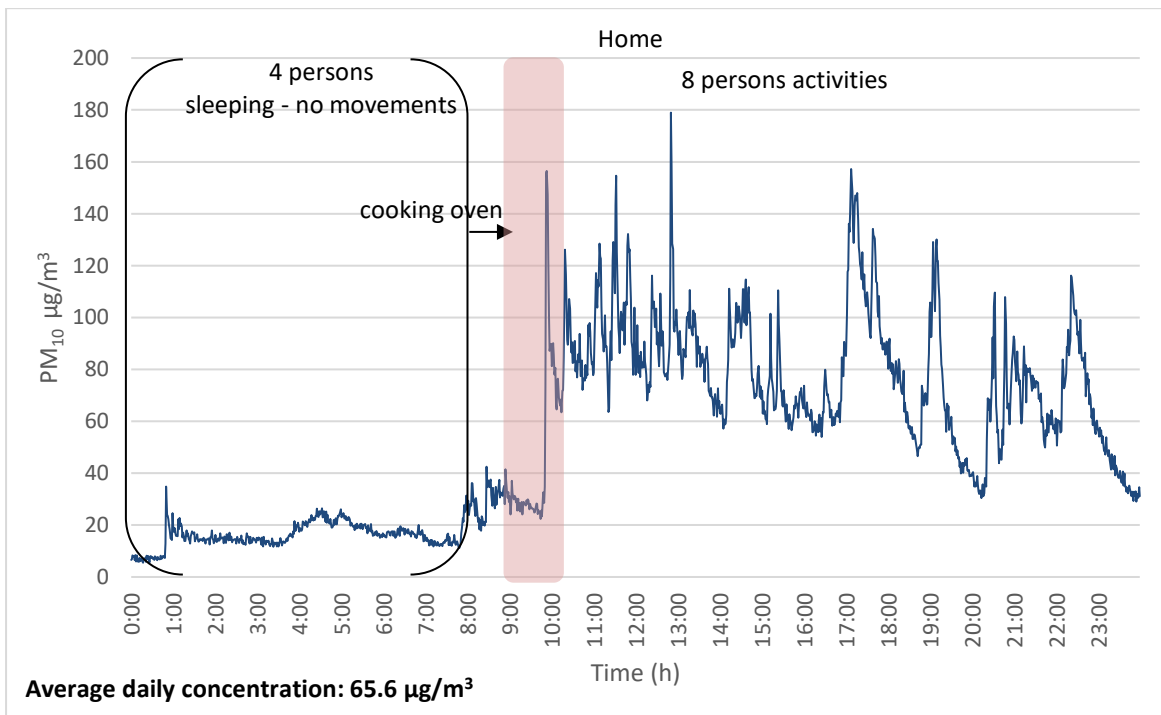


Figure B.40: Subject 7 daily exposure (mass concentration) (day 3).

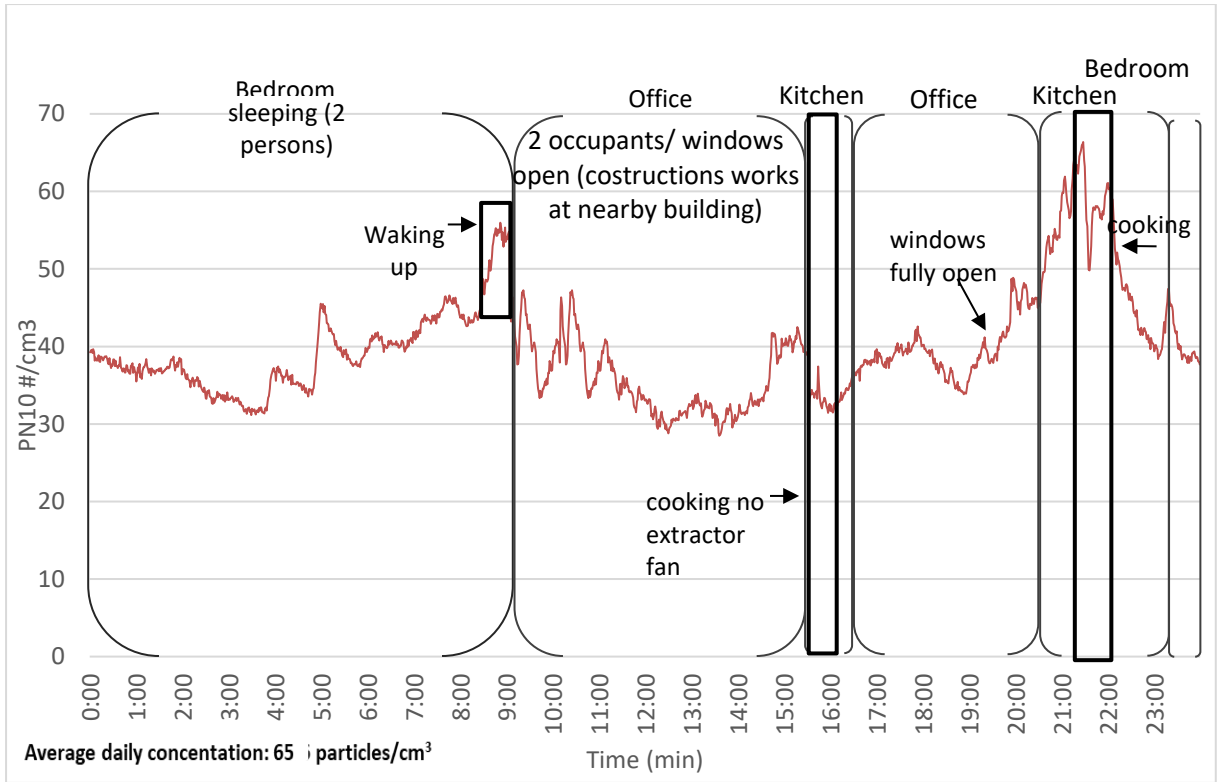


Figure B.41: Subject 8 daily exposure (number concentration) (day 1).

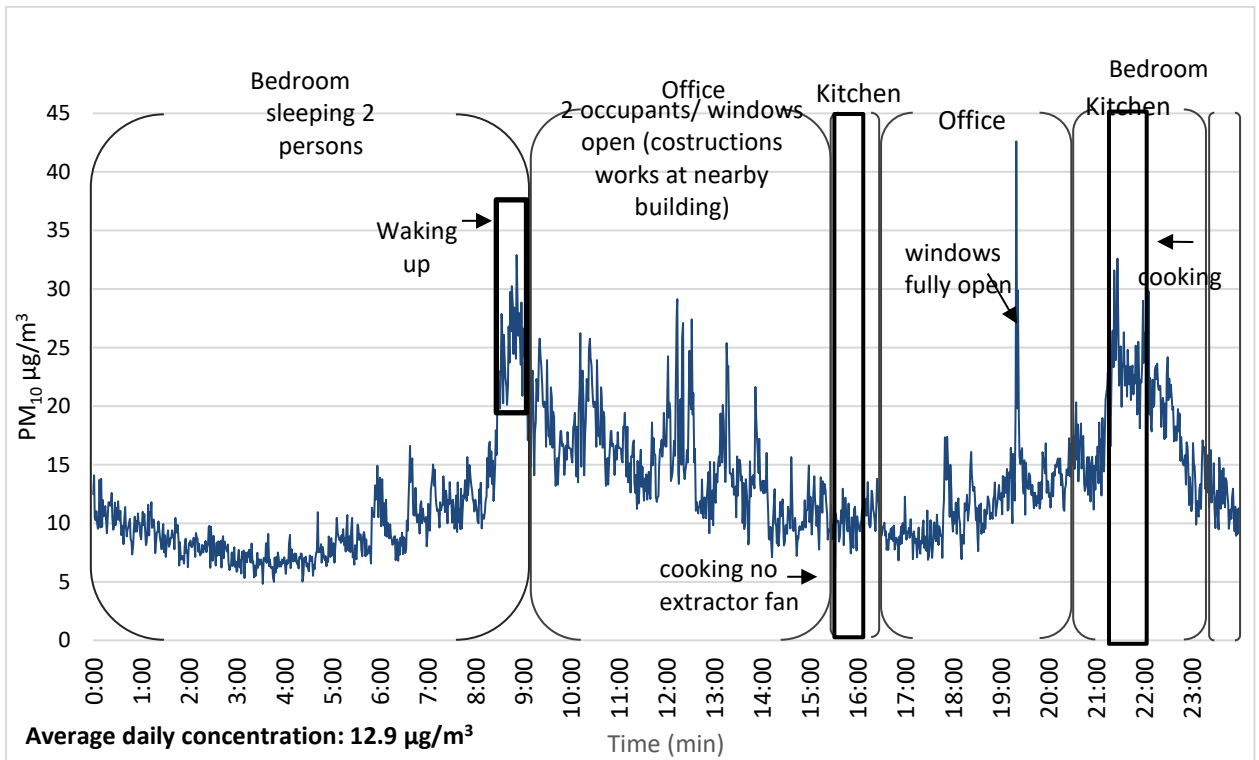


Figure B.42: Subject 8 daily exposure (mass concentration) (day 1).

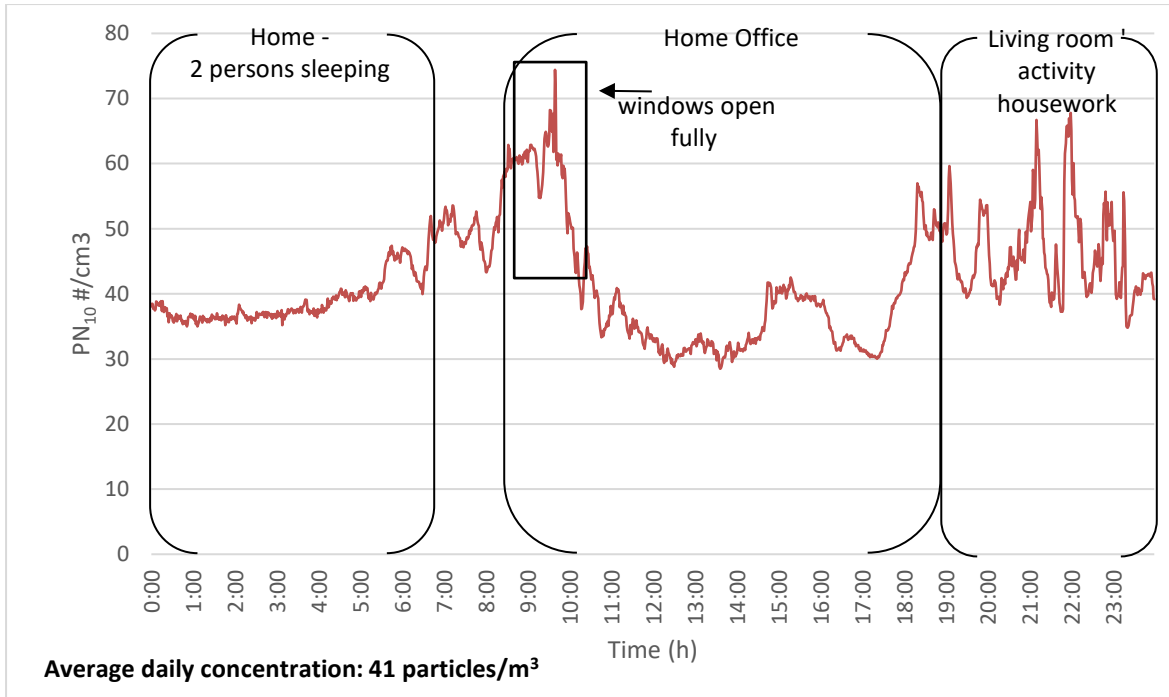


Figure B.43: Subject 8 daily exposure (number concentration) (day 2).

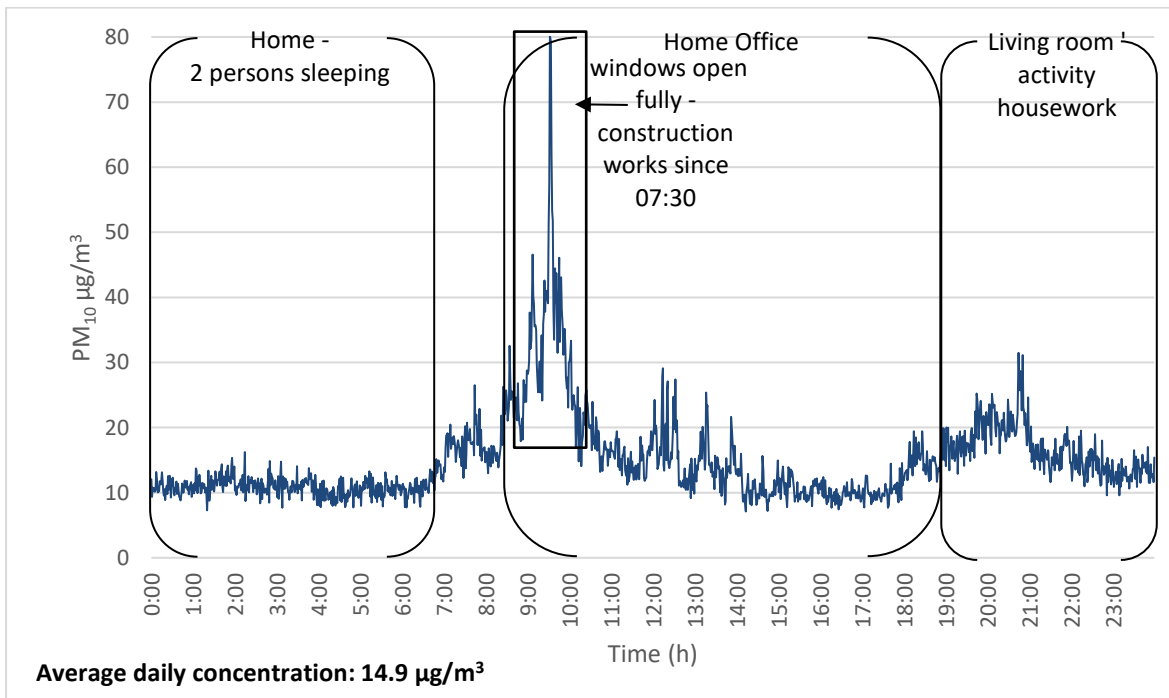


Figure B.44: Subject 8 daily exposure (mass concentration) (day 2).

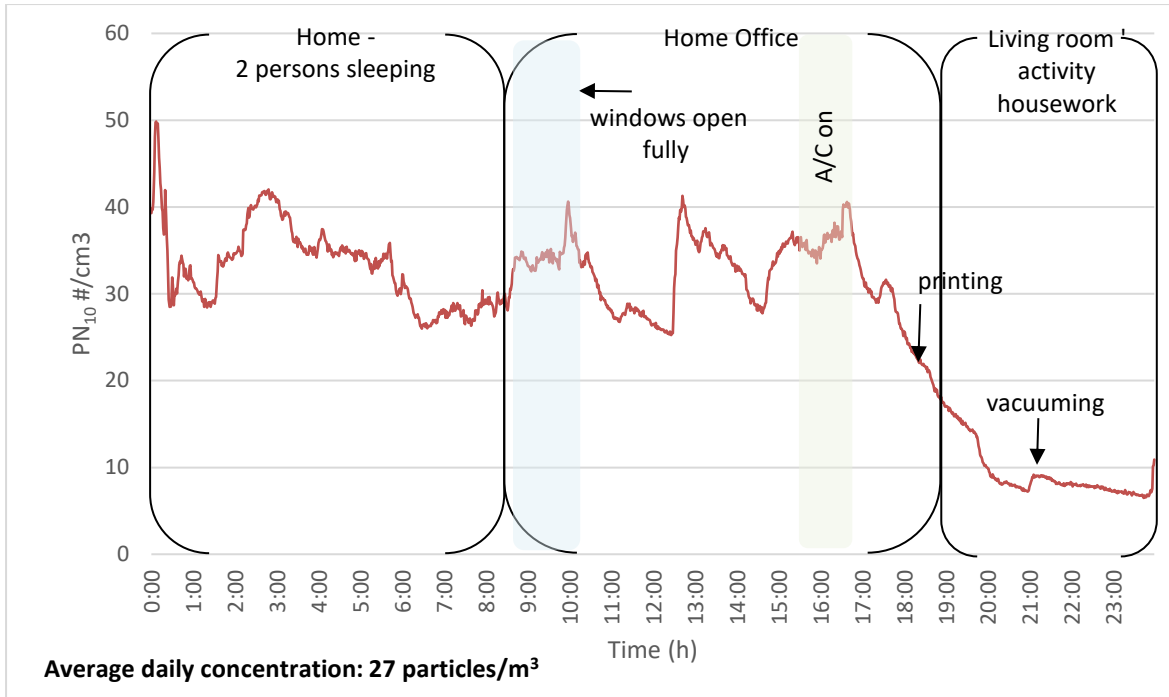


Figure B.45: Subject 8 daily exposure (number concentration) (day 3).

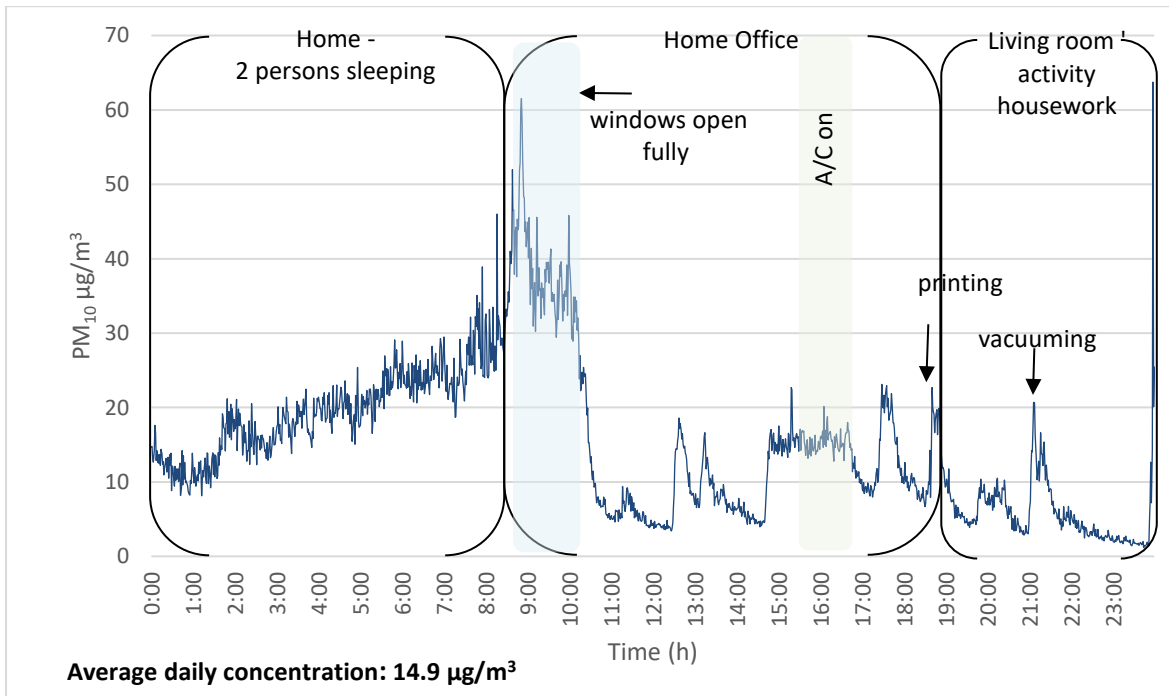


Figure B.46: Subject 8 daily exposure (mass concentration) (day 3).

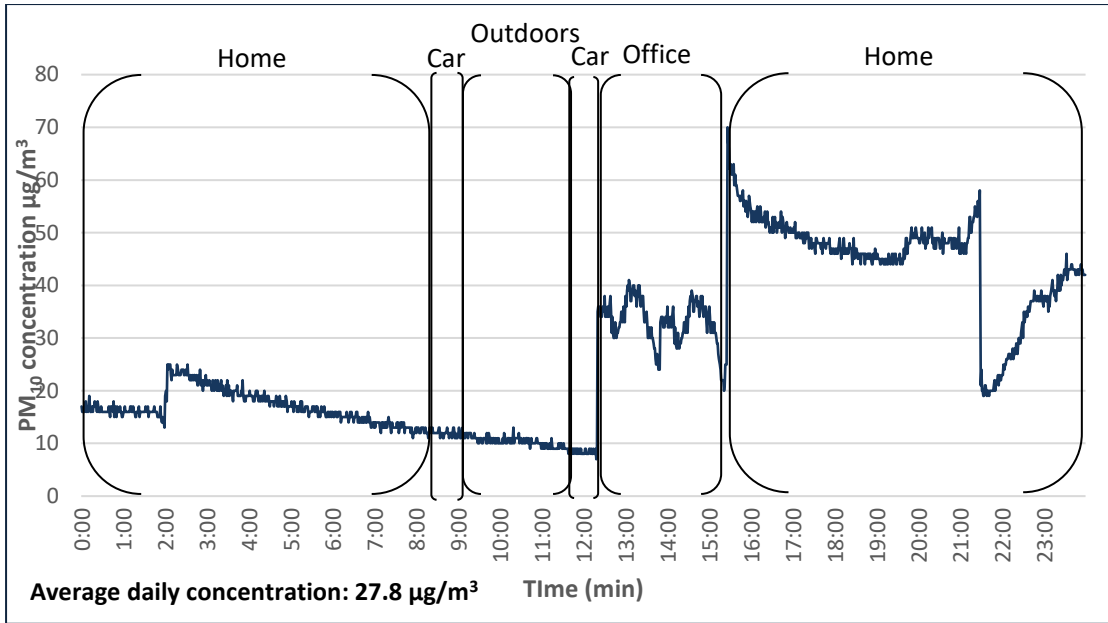


Figure B.47 : M1 daily exposure (day 1).

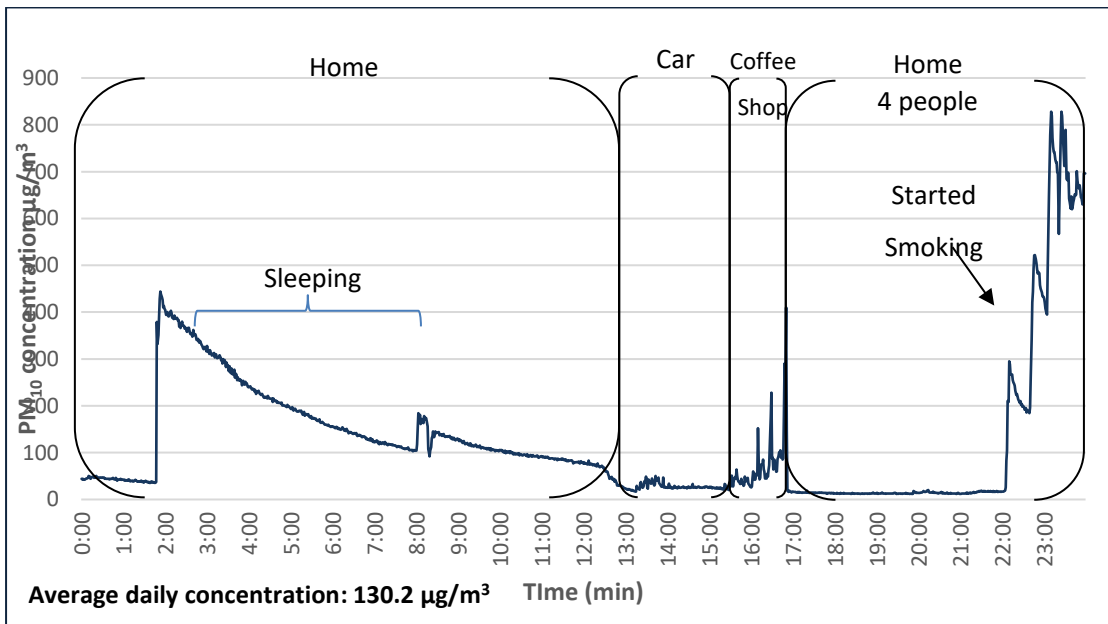


Figure B.48: M1 daily exposure (day 2)

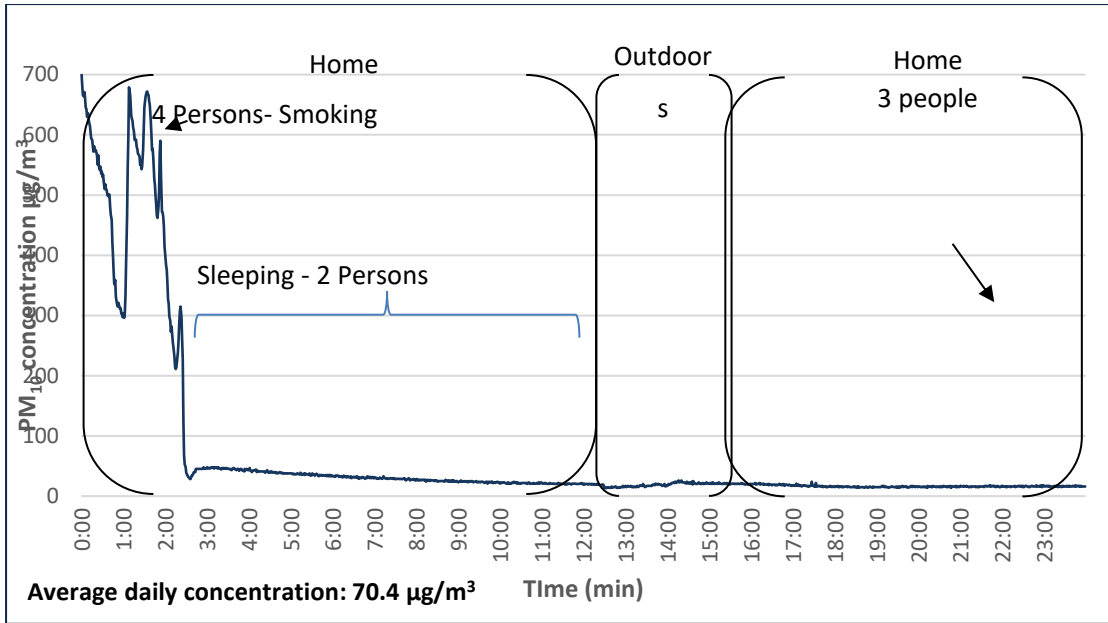


Figure B.49: M1 daily exposure (day 3)

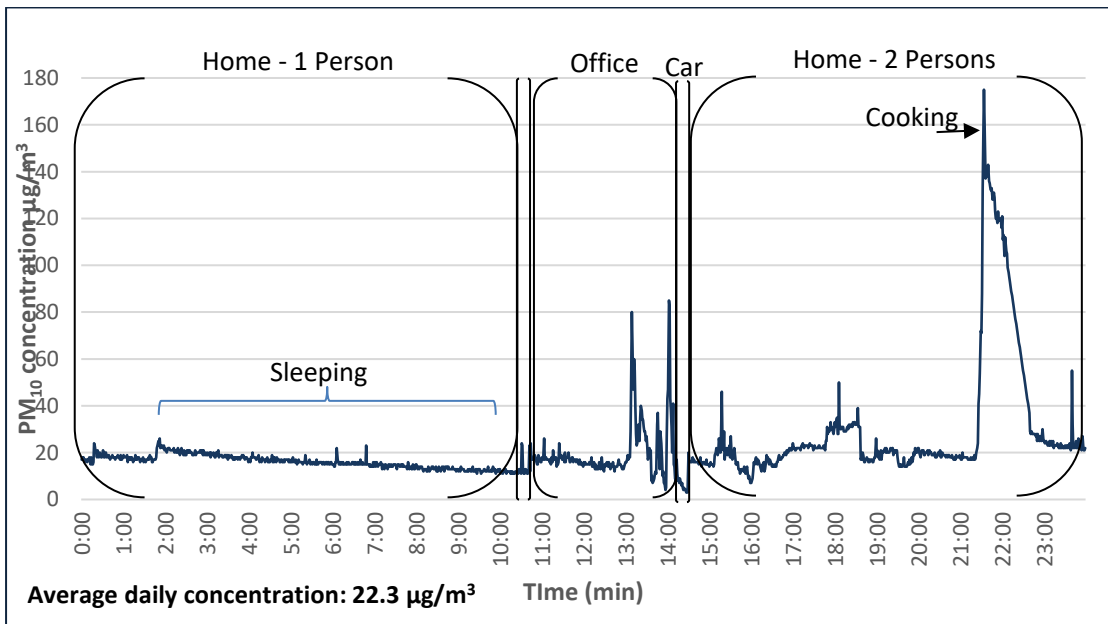


Figure B.50: M2 daily exposure (day 1)

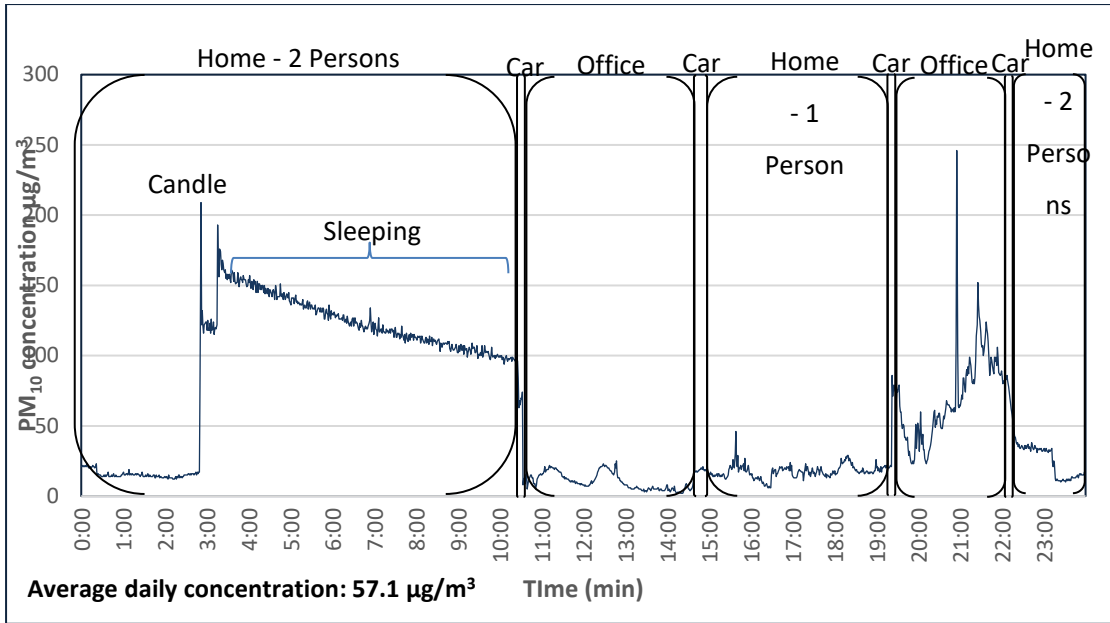


Figure B.51: M2 daily exposure (day 2)

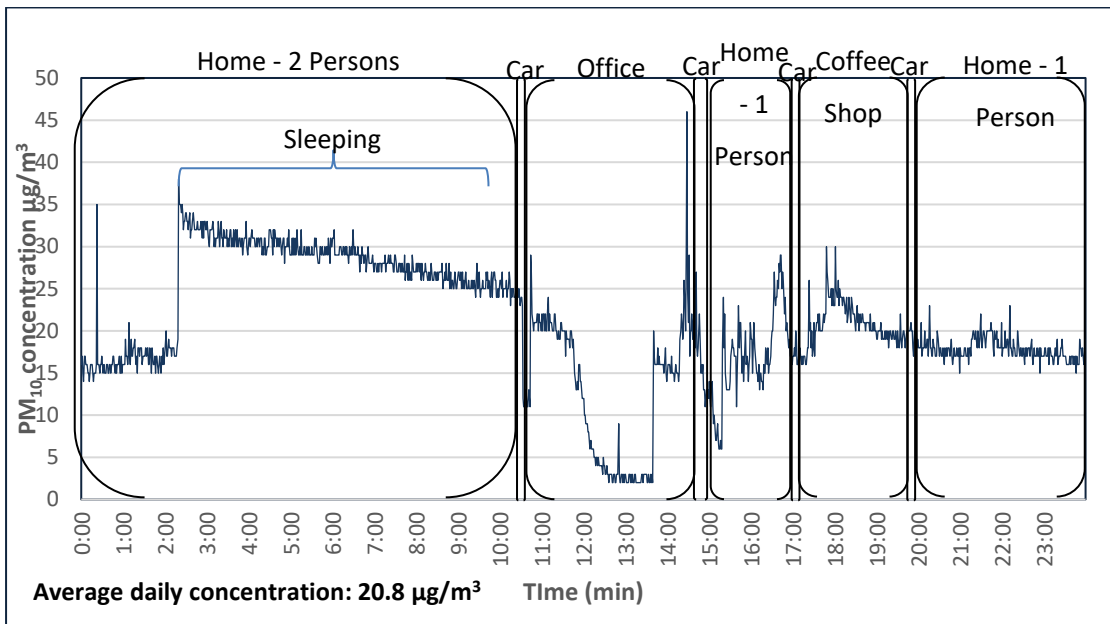


Figure B.52: M2 daily exposure (day 3)

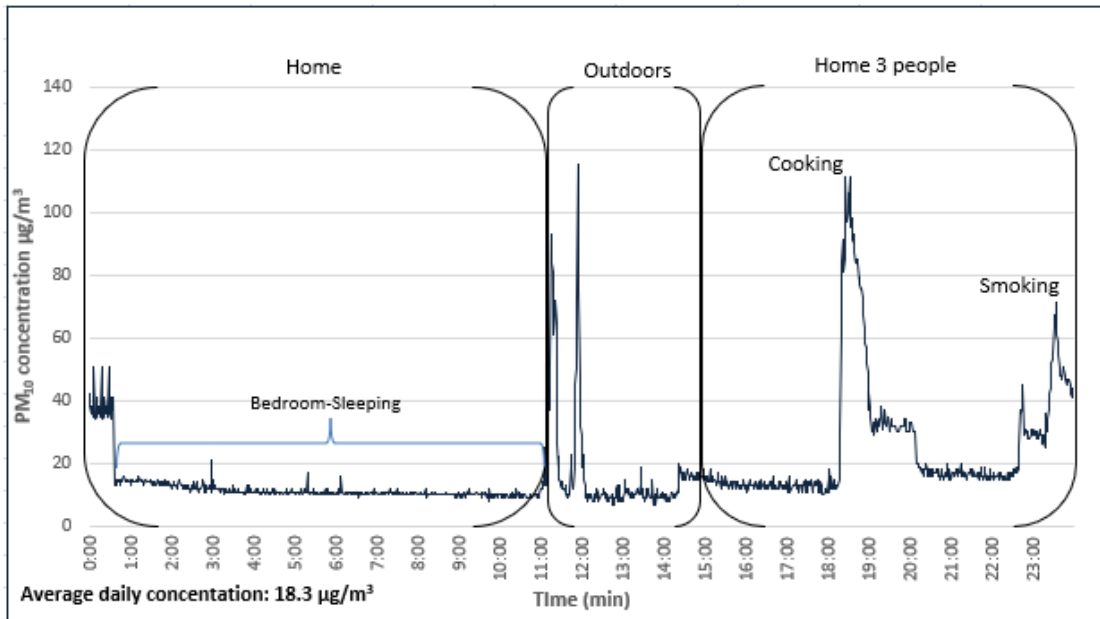


Figure B.53: M3 daily exposure (day 1)

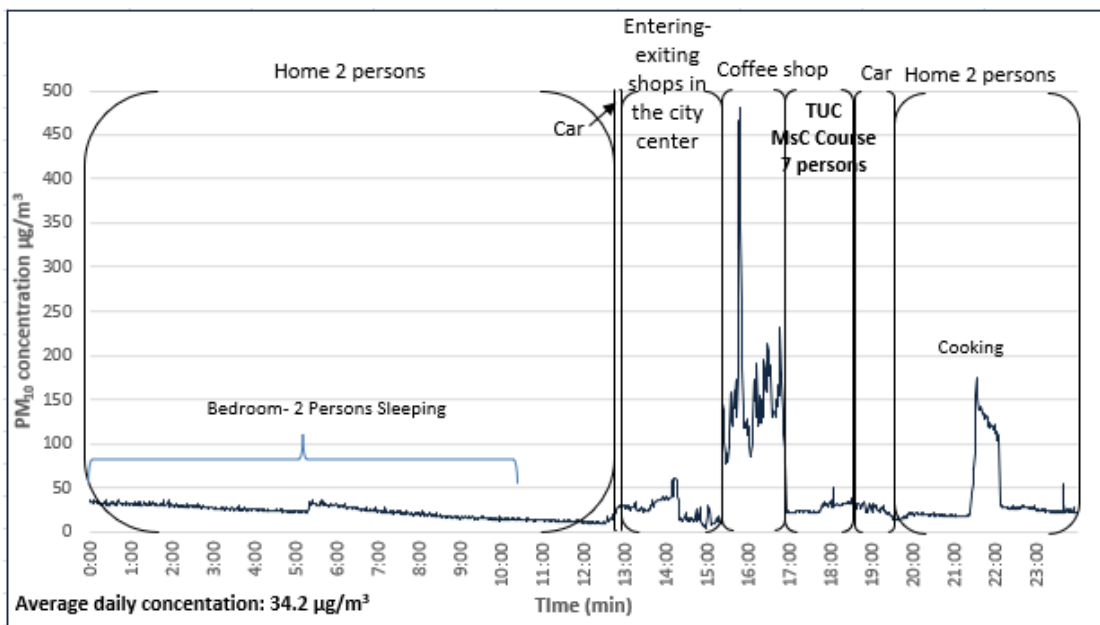


Figure B.54: M3 daily exposure (day 2)

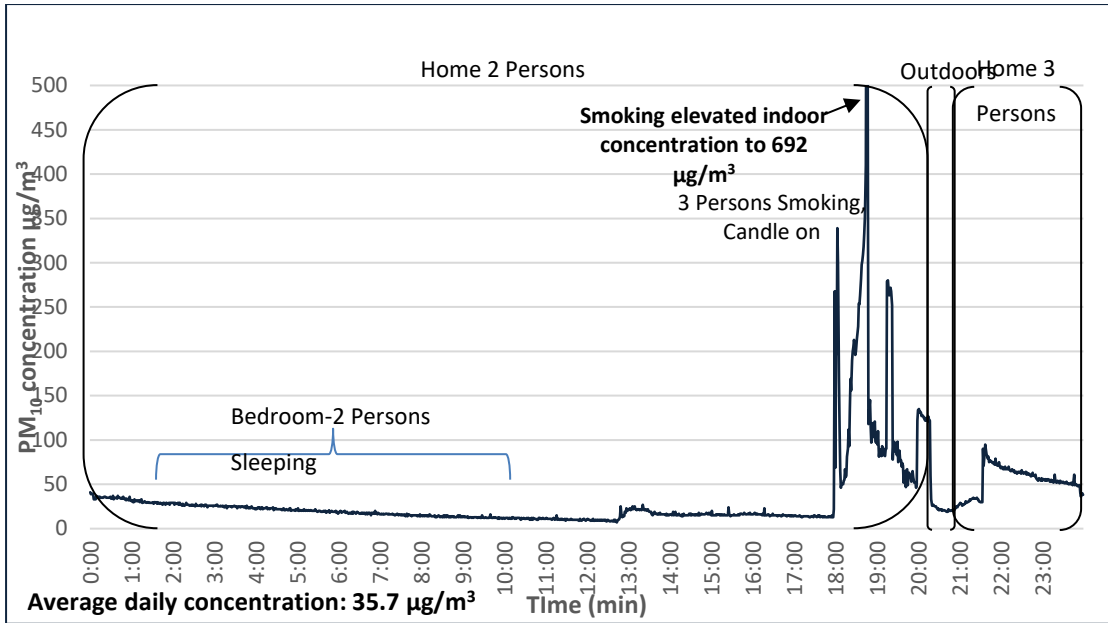


Figure B.55: M3 daily exposure (day 3)

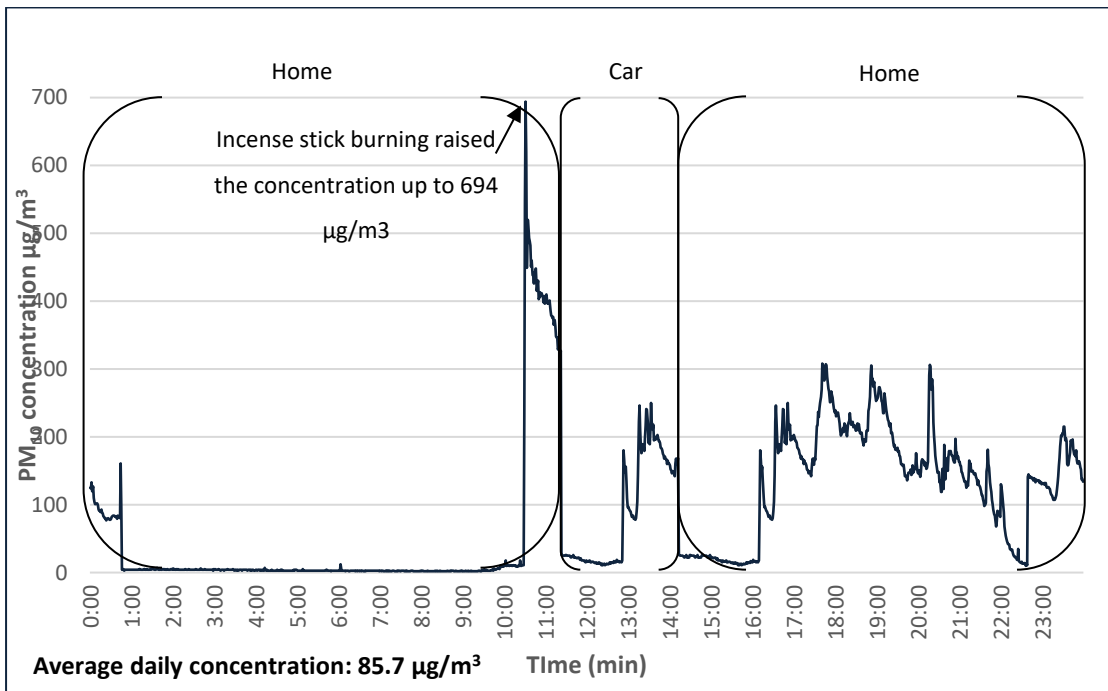


Figure B.56 : M4 daily exposure (day 1)

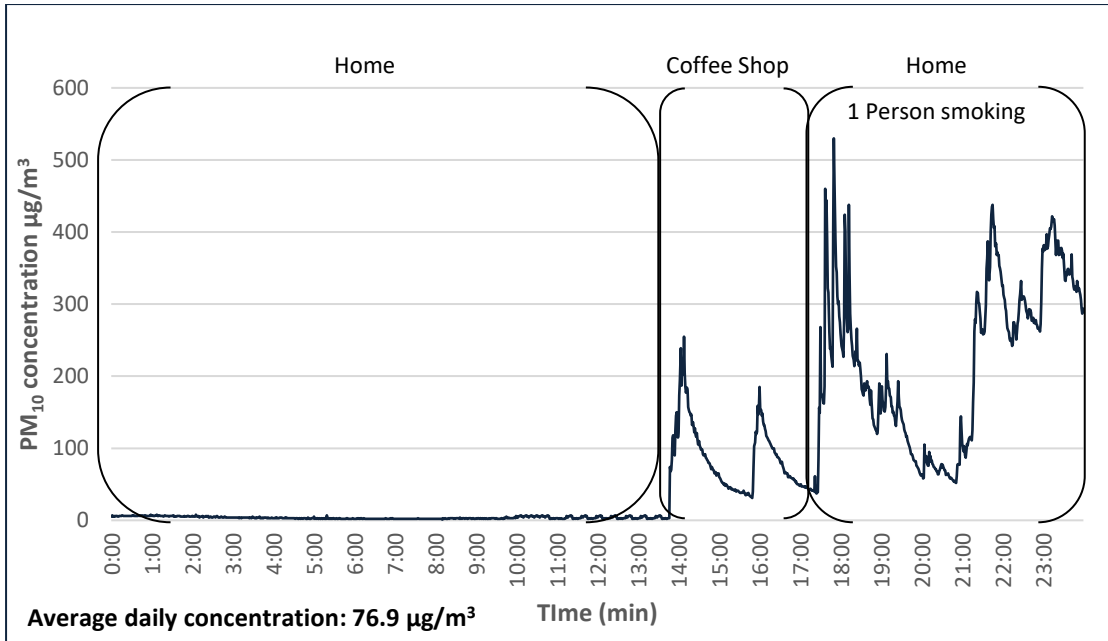


Figure B.57: M4 daily exposure (day 2)

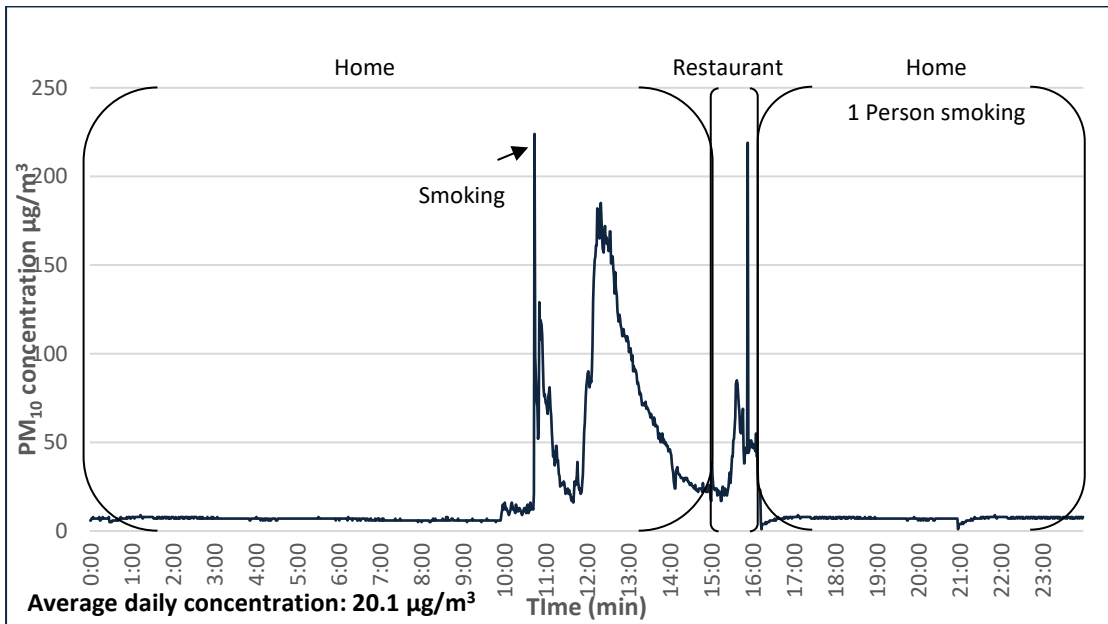


Figure B.58: M4 daily exposure (day 3)

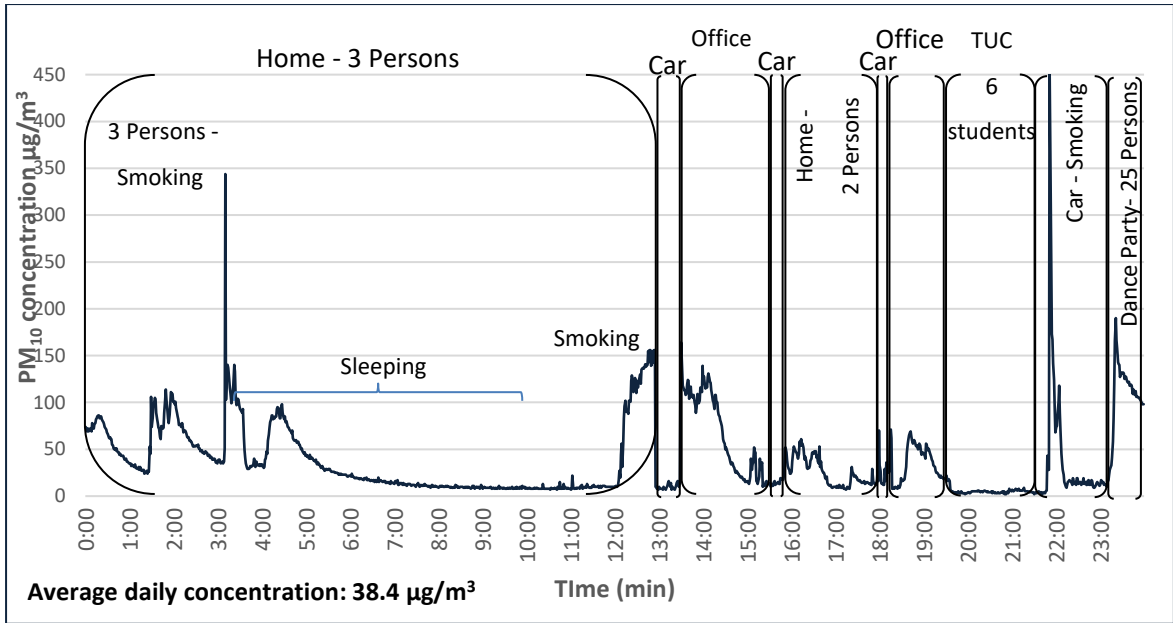


Figure B.59: M5 daily exposure (day 1).

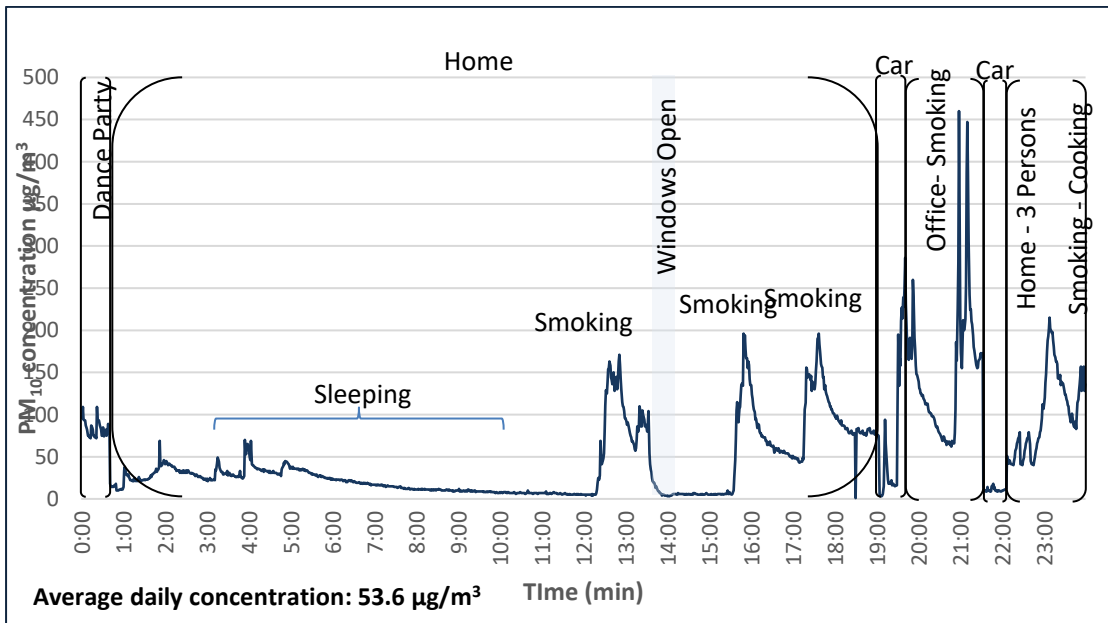


Figure B.60: M5 daily exposure (day 2).

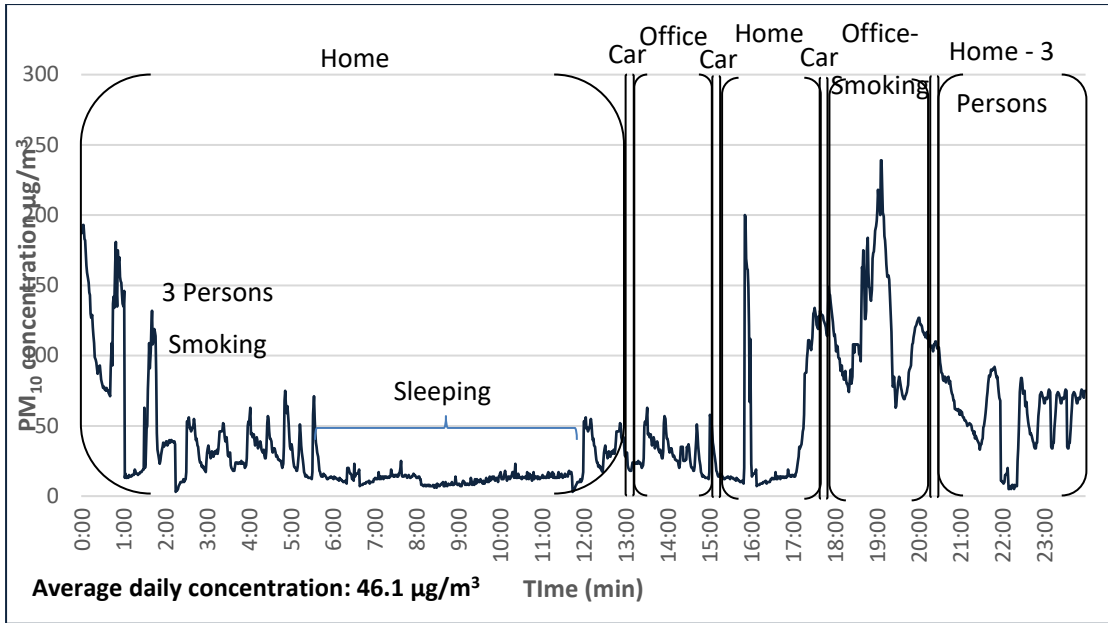


Figure B.61: M5 daily exposure (day 3).

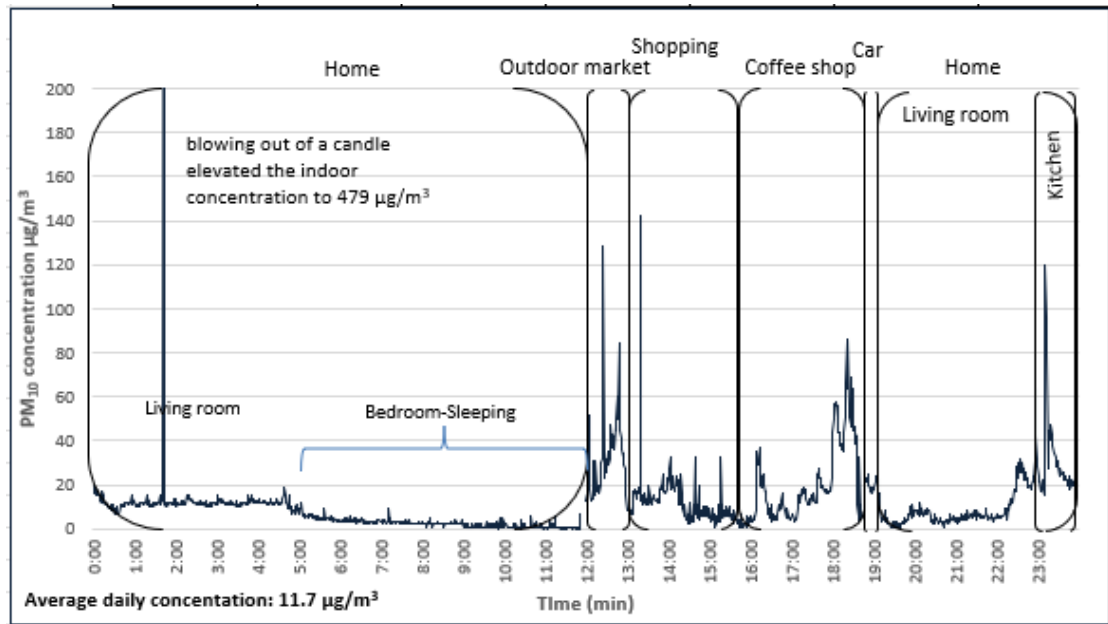


Figure B.62: M6 daily exposure (day 1).

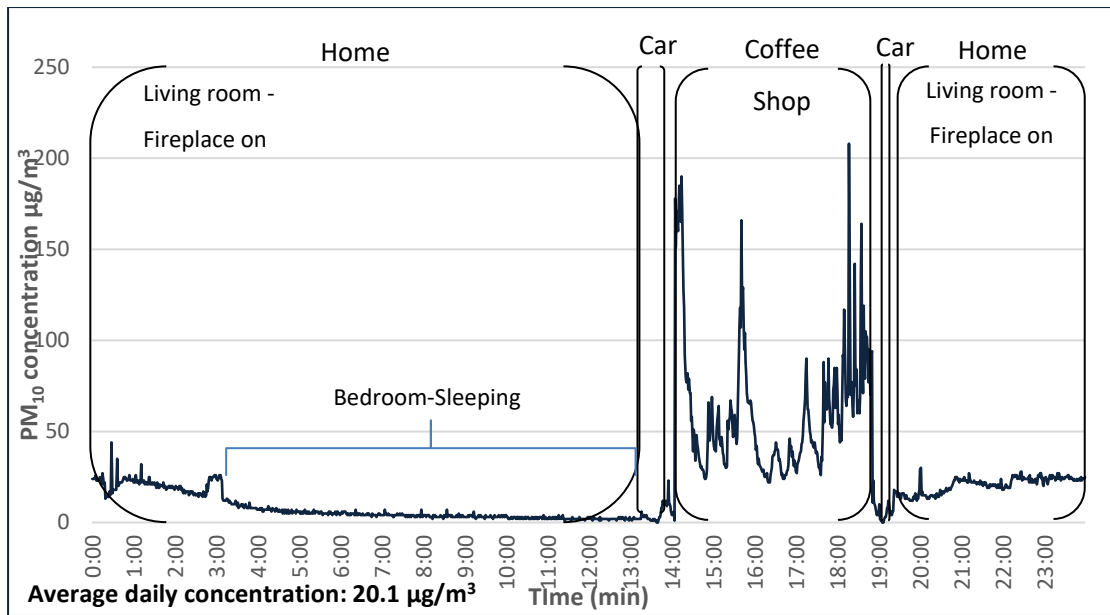


Figure B.63: M6 daily exposure (day 2).